U. S. ARMY
TRANSPORTATION RESEARCH COMMAND
FORT EUSTIS, VIRGINIA

TCREC Technical Report 61-15

RESULTS OF WIND TUNNEL TESTS OF A FULL SCALE, FUSELAGE MOUNTED, TIP TURBINE DRIVEN LIFT FAN

Volume 3

January 1961 - May 1961

Task 9R38-01-020-02
Contract DA 44-177-TC-584

March 1962

prepared by :

GENERAL ELECTRIC COMPANY
Flight Propulsion Laboratory Department
Cincinnati 15, Ohio

DISCLAIMER NOTICE

When Government drawings, specifications, or other data are used for any purpose other than in connection with a definitely related Government procurement operation, the United States Government thereby incurs no responsibility nor any obligation whatsoever; and the fact that the Government may have formulated, furnished, or in any way supplied the said drawings, specifications, or other data is not to be regarded by implication or otherwise as in any manner licensing the holder or any other person or corporation, or conveying any rights or permission, to manufacture, use, or sell any patented invention that may in any way be related thereto.

ASTIA AVAILABILITY NOTICE

Qualified requesters may obtain copies of this report from

Armed Services Technical Information Agency
Arlington Hall Station
Arlington 12, Virginia

This report has been released to the Office of Technical Services, U. S. Department of Commerce, Washington 25, D. C., for sale to the general public.

The information contained herein will not be used for advertising purposes.

The findings and recommendations contained in this report are those of the preparing agency and do not necessarily reflect the views of the Chief of Transportation or the Department of the Army.

HEADQUARTERS
U. S. ARMY TRANSPORTATION RESEARCH COMMAND
Fort Eustis, Virginia

FOREWORD

Publication of this report completes a three-volume contractor's report on the wind-tunnel tests of a tip-turbine-driven lift fan mounted in the fuselage of a large-scale model.

The U. S. Army Transportation Research Command, Fort Eustis, Virginia, extends its appreciation to the Ames Research Center, National Aeronautics and Space Administration, Moffett Field, California, for its major participation in building the model and in conducting the tests.

FOR THE COMMANDER:

L. A. Floro, Jr.
L. A. FLORO, JR.
Captain, TC
Actg Deputy Commander for
Plans and Programs

APPROVED BY:

John W. White
JOHN W. WHITE
USATRECOM Project Engineer

TCREC TECHNICAL REPORT 61-15

RESULTS OF WIND TUNNEL TESTS OF A FULL SCALE, FUSELAGE MOUNTED, TIP TURBINE DRIVEN LIFT FAN

VOLUME 3

MARCH 1962

Prepared By:
GENERAL ELECTRIC COMPANY
Flight Propulsion Laboratory Department
Cincinnati 15, Ohio

for
U. S. ARMY TRANSPORTATION RESEARCH COMMAND
FORT EUSTIS, VIRGINIA

AUTHOR: Z. J. PRZEDPELSKI

LIFT FAN PROJECT

GENERAL ELECTRIC COMPANY

TABLE OF CONTENTS

LIST OF ILLUSTRATIONS

LIST OF TABLES

Section I

SUMMARY

I. SUMMARY

Contract DA-44-177-TC-584 with the Army requires that, in addition to bi-monthly technical progress reports, comprehensive reports of major work phases be prepared and submitted to the contracting officer. Previous reports submitted under this requirement are:

- X353-5 Fan Design Report, May 30, 1960. (Proprietary)

- Fabrication, Test and Analysis of a Tip Turbine VTOL Propulsion System (Report of Phase I, Static Tests, Fuselage Mounted X353-5) TREC 60-42, August 31, 1960.

- Results of Wind Tunnel Tests of a Full Scale, Fuselage Mounted, Tip Turbine Driven Lift Fan (Report of Phase II Tests Volumes 1 and 2 of 3) TREC 61-15, January, 1961 and October 1961.

This is the required report for another major portion of Phase II contract work. It includes ground effect results for the full scale, fuselage mounted X353-5 lift fan obtained during a third test of 17 hours duration in the Ames 40 x 80 foot wind tunnel. The report includes:

- Modifications to test equipment (Section II)

- New instrumentation (Section III)

- Test procedures and results (Section IV)

- Analysis of test results, conclusions and discussion of any problems encountered (Section V)

- Hardware inspection results (Section VI)

- Program recommendations (Section VII)

The basic test data obtained for every test point is tabulated in Appendix A. A few items of summary:

Fan operating time	17 hours, 13 minutes
Data points recorded	427[a]
Range of variables tested -	
- Tunnel speed	0 to 80 knots
- Angle of attack	-4 to +18°
- Fan speed	0 to 2475 rpm
- Exit louver angle	-1° to +65°
- Wing flap angle	0°, 30°
- Tail position	0.4 b/2 above wing chord plane, and tail removed
- Tail configuration	no flap
- Tail incidence angle	0°
- J85 engine speed	0 to 16,500 rpm (100%)
- J85 turbine discharge bleed	6% of J85 inlet flow
- Tunnel temperature	58°F to 88°F

Analyses of the results is presented as a comparison of the performance in ground effect with that previously obtained out of ground effect. Emphasis is placed on the influence of fan performance changes on the overall system performance. A few items of performance conclusions are listed below:

AERODYNAMIC

1. The basic aircraft (fan o. .bited higher lift at low angles of attack, lower induced drag and higher downwash at the horizontal

[a] Does not include power off data points.

tail but essentially unchanged longitudinal stability characteristics.

2. Longitudinal stability margin with the fan operating was generally increased because of changed pressure distribution on the fuselage.

3. STOL performance was essentially unchanged from the results published in Volume 2.

4. The J85 engine encountered severe hot air reingestion because of the proximity of the inlet to the ground.

5. Lift loss (flow reduction) due to throttling the fan was very sensitive to height above ground. At $\beta = 0°$, constant fan rpm and near hover, following results were obtained:

h/d_F	% Reduction in Lift	% Reduction in Fan Flow
1.41	6	4
0.85	33	27

Based on scale model results at the lower heights the lift loss characteristic is very steep. At $h/d_F \approx 1.0$, a rough interpolation of full scale results indicates a lift loss of 15%.

6. Fan performance at high exit louver settings (35° to 40°) was essentially unchanged.

7. Downwash at the tail increased by $\approx 4°$ at $h/d_F = 1.41$.

8. Pitching moments (longitudinal trim requirements) in ground effect generally decreased at low velocity ratios because of reduced fan flow, but increased at high velocity ratios because of the tail downwash increase.

9. The fan flow decrease was accompanied by hub stall caused by a high static pressure ratio across the rotor (this phenomenon is not present when throttling with exit louvers).

10. Data scatter reduced the accuracy of the ground effect test results relative to those presented in Volume 1 and 2.

MECHANICAL

1. Cosine 2θ blade stress and stator stress increased as h/d_F was reduced.

2. There was a difference in mechanical performance of the rotor independent of ground proximity resulting from changing the torque band design (two piece). The vibratory stress in the torque band was reduced 40% which is the result of part of the torque load being transmitted through the carriers. The cosine 2θ mode was also generally lower.

3. Exit louver mounting pins were worn causing some inaccuracy in louver settings.

Section II

WIND-TUNNEL MODEL

II. WIND TUNNEL MODEL

AIRCRAFT MODEL

The aircraft configuration was the same as reported in Volume 2. The sketch in Figure 1 is repeated here for convenience.

TUNNEL MODIFICATIONS

The following are changes from the setup used during the tests described in Volumes 1 and 2.

1. A ground plane was installed above the tunnel floor to provide a smooth flat surface and a lower ground to fan discharge height (see Figure 2a).

2. The model was supported on variable height struts which provided adjustable ground to fan discharge height without disturbing the setup. Figure 2b shows the closest position to ground tested.

FAN MODIFICATIONS

The major change was the addition of a redesigned torque band and rotating seal.

A design change for the torque band to avoid cracking has resulted in two configurations: Design A, Figure 3a, used for this test is a two-piece approach which separates the seal and torque transmission functions of the component. The seal is made in 18 segments to remove an interaction with rotor axial vibration. The torque band is continuous but shortened in axial width to stay within the support length provided by the carrier side rails. Significant elements in the design include:

a. Each of the 18 seal segments provides both forward and aft seal surfaces in a single piece (Figure 3b).

b. Increase in seal stock thickness from 0.032 to 0.045.

c. Reduction in seal stock thickness to 0.020 in area beyond carrier support surface to reduce centrifugal loading.

d. Increase in torque-band thickness from 0.032 to 0.045 to maintain torque transmission cross-sectional area requirements.

Design B, Figure 3a, uses the original lightweight design philosophy but with reduced steady-state stress levels to accommodate the component vibratory loading. Stress reduction is accomplished through the use of thicker basic stock (0.045 vs. 0.032) with a thickness taper (0.045 to 0.020) across the band width. This design will be evaluated in a later program on rotor S/N No. 002 installed in the NASA fan-in-wing aircraft and tested in the 40 x 80 foot wind tunnel.

The only other changes were the replacement of all fastener hardware in the rotor assembly and replacement of 14 honeycomb seals in the front frame. The latter was necessary to reduce the cold radial clearance from 0.143 to 0.050.[a]

J85 ENGINE

The engine was the same as that used during the preceeding test period in the 40 x 80 foot wind tunnel.[b] A hot-parts inspection (turbine wheels, nozzle diaphragms and combustor) was performed and no wear or damage was noted prior to commencement of this test phase.

---

[a] Reduced clearance was desirable for the forthcoming wing installation which is more sensitive to leakage.

[b] J85-7 S/N 235-003.

Section III

TEST INSTRUMENTATION

Section III
TEST INSTRUMENTATION

III. TEST INSTRUMENTATION

The fan and tunnel instrumentation was essentially the same as reported in Volume 1 with the following exceptions:

1. A Pitot-static, combination pitch and yaw probe was installed in the test section located forward of the model and approximately 4 feet from the right wall in Figure 2b (not visible in the photograph). This probe was used to verify the calculated area reduction caused by ground plane installation, and to check for flow angularity in the test section.

2. Wing static pressures were not installed, however, fuselage static pressures, identical to those described in Volume 2, were installed and recorded.

Section IV

TEST PROCEDURES AND RESULTS

IV. TEST PROCEDURES AND RESULTS

Table I gives a summary of the test runs and the range of variable encompassed. Table II shows the breakdown of fan operating time as a function of fan speed and fan turbine inlet temperature. The testing reported herein was accomplished with Fan serial number 001 BU No. 4. (Table II includes all of the operating time on Fans S/N 001 and 002 through May, 1961).

The testing was conducted at two ground heights: 1.41 and 0.85 h/d_F[a] as compared with 2.98 h/d_F during the two previous wind tunnel tests. (See Figures 2 and 4 and Figure 7, Volume 1).

The test procedures were essentially the same as described in Volume 1, Section V. Negative values of angle of attack at the lower ground height were not tested since the proximity of engine inlet to the ground plane made this impossible. The ranges of other variables were essentially unchanged from ranges previously tested.

MEASUREMENT ACCURACIES

The inherent accuracy of the scale system to record lift, drag and moment is unchanged by the installation of the ground plane. The overall accuracy of the force measurements under conditions of low tunnel velocity and low exit louver angles was adversly affected by engine reingestion. (See discussion in Section V). The resulting fan speed fluctuation (+40 rpm at 1700 rpm) was equivalent to a thrust fluctuation of $\pm 5\%$.

The scale force measurement averages the variations since it consists of five separate readings for each data point. The recorded fan speed is obtained by visual averaging of the tachometer indication and is therefore subject to unknown reading error. During the test program effort

---

[a] Distance from the tunnel deck to the bottom of the fuselage divided by the blade tip diameter (62.5 inch). Corresponding values of h/d_F based on distance from wing chord plane to the tunnel deck were 1.83, 2.39, and 3.96.

TABLE I

SUMMARY OF TEST RUNS

Run No.	Date	V_P Knots	α Degree	N_F RPM	δ_f Degree	i_t Degree	β Degree	Ground Height h/d_F	Purpose of Run
1	5/3/61	40 - 60	-4 - +16	0		0 - Hi Pos.	90	1.41	Aircraft Power off Polar, Checkout Run
2	5/4/61	0	0	1170 - 1580	30	0 - Hi Pos.	0	1.41	Fan Mechanical Checkout
3	5/4/61	20	0	1150 - 1800	30	0 - Hi Pos.	0	1.41	Variable RPM at Low V_P
4	5/4/61	20 - 40	-4 - +16	1650 - 1790	30	0 - Hi Pos.	0 - 35	1.41	Polar at $\beta = 0°$; Some β Variation at $\alpha = 0°$
5	5/4/61	30 - 40	-4 - +18	1670 - 1760	30	0 - Hi Pos.	20 - 35	1.41	Polars with $\beta = 20°$ & $35°$
6	5/4/61	60	-4 - +12	1700 - 1750	30	0 - Hi Pos.	0 - 35	1.41	Polars with $\beta = 0°$, $20°$ & $35°$
7	5/5/61	60 - 80	-4 - +10	1700 - 1800	30	0 - Hi Pos.	0 - 40	1.41	Polars at $\beta = 0°$ and Variable β at $\alpha = 0°$
8	5/5/61	20 - 40	0	1200 - 2475	30	0 - Hi Pos.	0 - 40	1.41	Variable β at High Fan Speed
9	5/5/61	20 - 60	-4 - +16	0	30	0 - Hi Pos.	90	1.41	Power off Polar
10	5/8/61	20 - 30	-4 - +14	1650 - 1800	30	OFF	0 - 35	1.41	Polar at $\beta = 0°$; Some β Variation at $\alpha = 0°$
11	5/9/61	60	-4 - +14	0	30	OFF	90	1.41	Power off Polar
12	5/9/61	30 - 40	-4 - +14	1680 - 1750	30	OFF	0 - 40	1.41	Polars with $\beta = 0°$ & $35°$; Some β Variation
13	5/9/61	40 - 60	-4 - +14	1680 - 1740	30	OFF	0 - 40	1.41	Polars with $\beta = 0°$, $20°$ & $35°$
14	5/10/61	60	0 - +14	0	30	OFF	90	0.85	Power off Polar
15	5/10/61	20 - 30	0 - +12	1000 - 1750	30	OFF	0 - 35	0.85	Polars with $\beta = 0°$ & $35°$
16	5/11/61	30 - 60	0 - +12	1400 - 1725	30	OFF	0 - 35	0.85	Polars with $\beta = 0°$, $20°$ & $35°$
17	5/11/61	20 - 30	0 - +14	1690 - 1765	30	0 - Hi Pos.	0 - 40	0.85	Polars with $\beta = 0°$; Some β Variation
18	5/11/61	20 - 40	0 - +12	1170 - 1720	30	0 - Hi Pos.	0 - 40	0.85	Polars with $\beta = 0°$, $20°$ & $35°$; Some High Exit Louver Data
19	5/11/61	20 - 60	0 - +12	1360 - 2350	30	0 - Hi Pos.	0 - 40	0.85	Polars with $\beta = 0°$, $20°$ & $35°$; High Fan Speed Data; Mechanical Investigation
20	5/12/61	20 - 60	0 - +14	0	30	0 - Hi Pos.	90	0.85	Power off Polar

TABLE II

SUMMARY OF LIFT FAN OPERATING TIME

	Fan, S/N 001						S/N 002	Total
	B/U #1 Even.	B/U #2 Even.	B/U #2 Ames	B/U #3 Ames	B/U #4 Ames	Total	B/U #1 Even.	Both Fans
Speed Range								
0 - 24%	5:02	4:08				9:10	2:57	12:07
25 - 49	2:43	7:23	5:08	4:10	2:03	21:27	16:47	38:14
50 - 74	9:52	5:57	12:01	16:43	14:02	58:35	12:17	70:52
75 - 89	1:29	2:11	3:08	1:06	1:01	16:47	9:38	37:37
90 - 100				7:45	:07		11:12	
TOTAL HOURS	19:06	19:39	20:17	29:44	17:13	105:59	52:51	158:50
Temp. Range								
0 - 599°F	8:20	5:09				13:29	1:07	14:36
600 - 799	1:57	1:49		5:05	:53	9:44	1:39	11:23
800 - 899	7:49	7:05	:28	15:17	10:26	41:05	15:20	56:25
900 - 999	1:00	4:39	14:22	1:21	4:39	26:01	14:06	40:07
1000 - 1200		:57	5:27	8:01	1:15	15:40	20:39	36:19
TOTAL HOURS	19:06	19:39	20:17	29:44	17:13	105:59	52:51	158:50
DATA POINTS	71	66	348[a]	539[a]	427[a]	1451	554	2005

[a] Not including basic airplane data with fan off.

was made to obtain more than one reading at each condition where engine reingestion was present to compensate somewhat for this random error.

The model and fan vibrations may add dynamic loads to the static measurements and result in another source of data error. The scale system most likely does not respond to the predominantly one per revolution fan vibration, but is probably affected to some degree by the low frequency (3 to 5 cycles per second) model vibration. The level of model vibration was apparently not affected by the proximity of the ground and any error due to this phenomenon was also present in the previous out of ground effect tests in the tunnel.

The problem of exit louver repeatability had an adverse effect on accuracy. Six segments of the 24 fan exit louvers on the cold side of the fan had a tendency to loosen,[a] especially during the later runs. In the worst case this problem is estimated to have been an average of 2° less effective turning than indicated. At an exit louver setting 0° there was no effect on the lift and small effect on the drag. As the indicated exit louver angle is increased to 40°, the maximum error in fan lift was possible (the rate of change of fan lift with β at angles between 35° and 40° is $\approx$ 3 1/2% per degree). Horizontal thrust error is a function of exit louver angle and V_p and is more difficult to estimate; however, it is considerably less than the maximum lift error in absolute values (lbs.) of force.

Because of these conditions the data are not as accurate or as repeatable as obtained during the previous two wind tunnel tests. Point for point comparisons between two tests are always less accurate than comparison of average results and should be avoided with the data from this report;

[a] The indicated exit louver angle (measured from the actuation rod) was greater than the actual physical angle of these louvers, resulting in more lift and more drag than would be normally experienced.

however, the conclusions arrived at by comparing the average fan powered performance characteristics as represented by curves in Appendix B are accurate within $\pm$ 4% in lift and $\pm$ 4% or $\pm$ 150 lbs. in drag whichever is larger, and $\pm$ 8% or 1000 ft. lbs. in pitching moment whichever is larger.

TUNNEL CORRECTIONS

Tunnel wall corrections were not applied to either the powered or unpowered runs. (As the model is moved closer to the ground, wall correction becomes less significant.)

Since the model was supported by relatively un-streamlined support struts, strut tare corrections[a] were applied as follows:

High Position, 1.41 h/d_F

$\Delta C_L = 0.010$

$\Delta C_D = 0.117 - 0.0011\,\alpha$

$\Delta C_M = 0.079 - 0.00117\,\alpha$

Low Position, 0.85 h/d_F (Runs 14 & 15)

$\Delta C_L = 0.025$

$\Delta C_D = 0.078 - 0.0007\,\alpha$

$\Delta C_M = 0.044 - 0.0007\,\alpha$

Low Position, 0.85 h/d_F (Runs 16 to 20)

$\Delta C_L = 0.020$

$\Delta C_D = 0.078 - 0.0010\,\alpha$

$\Delta C_M = 0.038 - 0.0009\,\alpha$

---

[a] Provided by NASA.

The change after Run 15 was made to allow for some strut modifications accomplished between Runs 15 and 16.

All of the corrections are applied in the following manner: corrected quantity = uncorrected quantity minus delta quantity.

Results reported in Volumes 1 and 2 did not include any strut tare. Lift tare for the high struts used previously was insignificant. The drag and moment tares were estimated to be $\Delta C_D = 0.02$ and $\Delta C_M = 0.08$. To enable valid comparisons between results of Volume 1 and 2 and Volume 3, the following adjustments were made to the data:

1) Volume 3 drag results shown in Appendix B are increased by $\Delta C_D = 0.02$ above the value calculated in Appendix A.

2) Moment data from the previous tests are decreased by $\Delta C_M = 0.08$ when shown in comparison with Volume 3 results in Figure 9 and Figure 27a through c.

Standard tunnel q measurements were increased by about 3 1/2% to account for the blockage of the ground plane and resulting increase in test section velocity. All results are based on this corrected value. The Pitot-static combination angle probe mounted in the test section verified this correction.

Flow angularity corrections were not applied because the combination probe indicated less than 0.6° flow misalignment at 1.41 and 0.85 h/d_F.

Section V
ANALYSIS OF RESULTS

V. ANALYSIS OF RESULTS

A. BASIC AIRPLANE PERFORMANCE (FAN OFF)

Power-off-aircraft, tail-on and tail-off, polars are shown in Figures 5 to 8, and the comparison with out-of-ground-effect results are shown in Figure 9.

Stability - Power Off:

The static longitudinal stability, $\partial C_M/\partial C_L$, with power off was unaffected by ground proximity at $h/d_F = 0.85$ (see Figure 9). Data for 1.41 h/d_F indicate a reduction in stability at high angles of attack. This was inconsistent with expected results as it is normal for the rate of change of tail downwash angle with angle of attack ($\partial\epsilon/\partial\alpha$) to decrease in ground effect resulting in an increase in stability.

Lift - Power Off:

Normally the slope of the lift curve is increased due to the ground effect ($\partial C_L/\partial\alpha$ in ground effect = k $\partial C_L/\partial\alpha$ out of ground effect where k is a function of $h_{c/4}/b$ and aspect ratio). For the two ground heights tested $h_{c/4}/b$ was 0.35 and 0.27 and the corresponding k values 1.04 and 1.06[a]. This change is not apparent in the results; see Figure 9. There is, however, a definite increase in the value of C_L (above the C_L value for 2.98 h/d_F) at any given angle of attack up to stall ($\Delta C_L \approx 0.15$ and 0.25 at h/d_F of 1.41 and 0.85 respectively).

The $C_{L\ max}$ was slightly lower in ground effect. $C_{L\ max}$ was approximately 1.50, 1.41, and 1.45 for h/d_F of 2.98, 1.41 and 0.85 (see Figure 9). No significance should be attached to the indicated $C_{L\ max}$ at 0.85 h/d_F being higher than for 1.41 h/d_F; additional data

[a] Reference 2, p 4:10

would be required to establish the absolute values.

Drag-Power Off:

Induced drag is usually reduced in ground effect and for the values of $h_{c/4}/b$ tested, the ratio

$$\frac{\dfrac{\partial C_{Di}}{\partial C_L^2} \text{ (in ground effect)}}{\dfrac{\partial C_{Di}}{\partial C_L^2} \text{ (out of ground effect)}}$$

should be 0.85 and 0.80 for 1.41 and 0.85 h/d_F.[a] The actual reduction in C_{Di} is considerably more (50-80%). This may be due to tunnel effects and to the strut tare corrections being large relative to the airplane drag coefficients.

Pitching Moments and Tail Downwash - Power Off:

Tail downwash was higher at the lower h/d_F values (see Table III).

TABLE III (POWER OFF)

TAIL DOWNWASH RESULTS AS A FUNCTION OF GROUND PROXIMITY

h/d_F	Downwash Angle at $\alpha = 0°$ (deg.)	Downwash Angle at $\alpha = 8°$ (deg.)
2.98	1*	-
1.41	2	6
0.85	3	6

* estimated

This is not the normal trend as downwash is normally expected to be reduced significantly in the plane of the tail while in ground effect.[b] Previous test experience in the 40 x 80 foot tunnel in-

[a] Reference 2, p 2:66

[b] Reference 2, p 9:44

dicates that ground effect test results do not always agree with theory.

For this configuration the proximity to the ground of the large fuselage may be the overriding factor affecting downwash results.

B. FAN POWERED AIRCRAFT PERFORMANCE

Aircraft Power-On Characteristics:
The power-on, in-ground-effect data obtained during this phase of testing are shown in coefficient form (H_L, H_D, and H_M) as a function of V_P/V_{tip}, α and β in Figures 10 to 22.

In general there are two dominant factors which cause the ground effect performance to be different:

1. The fan is throttled severly at low β settings resulting in completely different throttling characteristics as a function of exit louver angle.

2. Basic aircraft characteristics are changed due to modified circulation patterns.

The first factor is predominant at low velocity ratio (low tunnel speeds) since most of the momentum changes in the system are direct contributions from the fan.

The second factor is predominant at higher velocity ratios (high tunnel speeds), for the following reasons: the momentum changes across the fan become a lesser part of the total system changes, and the fan tends to approach the out-of-ground-effect performance (Figures 23a to 23c) as velocity ratio is increased.

There was a third factor present during this particular test which would not be a problem in a flight installation. The exit louver linkage system developed excessive play and effectively deflected the fan efflux by a lesser angle than indicated. This did not apply to $\beta = 0°$ data but resulted in higher drag and lift readings at $\beta = 20°$, $35°$ and $40°$ (see Section II for details).

The above factors have to be considered when comparing aircraft characteristics in and out of ground effect. The following comparisons are based on the tail in the high position, $\delta_f = 30°$ data obtained during this phase of testing and comparable data as reported in Volume 2.

Lift - Power On:

Lift variations at $\alpha = 0°$ as a function of h/d_F, V_P/V_{tip} and β are shown in Figures 24a to 24c where lift is presented as a ratio of lift coefficient, H_L, at any given condition to the lift coefficient, H_{Looo}, at $\beta = 0°$, $V_P = 0$ and at $h/d_F = 2.98$.[a] The lift deficiency at low velocity ratio and $\beta = 0°$ and $20°$ is related to the fan flow deficiency for same conditions (see Figure 23a and 23b). Increasing velocity ratio brings the lift for the three different h/d_F values and $\beta = 0°$ closer together since the fan flow deficiency is decreased with velocity ratio and the positive ground effect on the wing is sufficient to offset it. At $\beta = 20°$ the flow deficiency is less and as velocity ratio increases the positive ground effect becomes the predominant factor and the result is an increase in lift. At $\beta = 35°$, at the lowest velocity ratios tested, flow and lift are essentially the same for 2.98 and 0.85 h/d_F. This does not mean that the fan operation was identical, actually the fan was throttled somewhat at $h/d_F = 0.85$ but the exit louver looseness offset this effect. At

[a] Comparisons are made using data obtained at $\approx$ 1700 rpm where H_{Looo} is 0.311. $h/d_F = 2.98$ is taken as equivalent to zero ground effect.

higher velocity ratios and $\beta = 35°$ the lift in ground effect was higher than could be attributed to 2° β error and indicates a positive ground effect.

The preceeding discussion was limited to lift values with $\alpha = 0°$. The maximum lift ratio values obtained where $\Delta C_L/\Delta\alpha = 0$ are shown in Figures 25a to 25c and have similar characteristics to those in Figures 24a to 24c indicating that the ground effect phenomena are not a function of angle of attack.

Drag - Power On:

Drag ratios as a function of β, V_P/V_{tip} and h/d_F at $\alpha = 0°$ are shown in Figures 26a to 26c. All the drag values are presented as a ratio of the drag coefficient, H_D, at any condition to the drag coefficient, $H_{D\ ref}$, at $\beta = 0°$, $V_P/V_{tip} = 0.20$ and $h/d_F = 2.98$ ($H_{D\ ref} = 0.178$); positive values of the ratio indicate drag and negative values thrust. This reference point was arbitrarily chosen for convenience.[a] The drag ratio at $\beta = 0°$ behaves similarily to the flow ratio. This is as expected since at $\beta = 0°$ there is a negligible amount of thrust from the fan and decreasing fan flow causes a proportional decrease in ram drag. At $\beta = 20°$ and 35° drag increases (thrust decreases) as the h/d_F value is reduced. This is caused by the lower fan flow (less net thrust) and the lower flow turning angle due to exit louver looseness.

Pitching Moments - Power On:

Pitching moments ratios as a function of β, V_P/V_{tip} and h/d_F are shown in Figures 27a to 27c. All of the moment values are presented as a ratio of pitching moment coefficient, H_M, at any condition to the moment coefficient, $H_{M\ ref}$, at $\beta = 0°$, $V_P/V_{tip} = 0.20$ and $h/d_F = 2.98$ ($H_{M\ ref} = 0.041$). This reference point was arbitrarily chosen for convenience.[a] Pitching moments in ground effect are generally lower at low V_P/V_{tip} due to fan flow reduction.

[a] H_D and H_M at $V_P/V_{tip} = 0$ are zero for $\beta = 0°$.

Some understanding is gained from fuselage static pressure data, Figure 28a to 28h, which show a definite decrease in pitch up moment (actually becoming a pitch down moment) contribution from the underside of the fuselage at 0.074 V_P/V_{tip}. For example, in Figure 28a the pressure coefficient aft of the fan produces no pitch up moment contribution at $h/d_F = 0.85$ while the pressure coefficient forward of the fan becomes more negative causing a pitch down moment.

At high velocity ratios another phenomenon takes over causing a pitching moment increase in ground effect, especially at $h/d_F = 1.41$. Fuselage underside static pressure data does not show this appreciable increase in pitch up moments; change in tail downwash in and out of ground effect is the predominant cause. At $\alpha = 0°$, $\delta_f = 30°$, $V_P/V_{tip} = 0.25$ the downwash, obtained from comparison of tail on with tail off data, is as shown in Table IV.

TABLE IV (POWER ON)

TAIL DOWNWASH ANGLE AS A FUNCTION OF GROUND PROXIMITY

h/d_F	Downwash Angle at $\beta = 0°$ (deg.)	Downwash Angle at $\beta = 35°$ (deg.)
2.98	2.5	0
1.41	5.0	4.5
0.85	3.0	3.5

Using the results at $\beta = 35°$ and 0.25 V_P/V_{tip} from Figure 26c, the H_M at 2.98 h/d_F is 1.67 ($H_{M\ ref}$) = 1.67 (0.041) = 0.068. At h/d_F of 1.41, H_M = 2.36 ($H_{M\ ref}$) = 2.36 (0.041) = 0.097. The difference

is $\Delta H_M = 0.029$ and converting[a] to C_M units gives:

$$\Delta C_M = \frac{0.4274\ (0.029)}{(V_P/V_{tip})^2} = 0.198$$

This is equivalent to $\approx 6.0^{\circ}$ tail downwash change while $\approx 4.5^{\circ}$ were measured by an independent method of comparing tail on and tail off data. Exact comparison is difficult since the fan flow and exit louver turning angle are not identical and the pitching moment data are subject to scatter, however, it can be concluded that the pitching moment reduction in ground effect at low velocity ratio is mainly due to fan flow reduction and a re-distribution of static pressures on the fuselage underside, while at high velocity ratios the increase is due to increase in tail downwash angle.

Pitch Trim Requirements During Transition - Power On:

Maximum pitch trim requirements for this configuration will have to be based on the out of ground effect results. The maximum trim requirement out of ground effect occurs at less than 50 knots (V_P/V_{tip} of 0.117 at N_F = 100%).[b] The pitching moments in ground effect are lower at velocity ratios below 0.117, and pitch control sufficient for trimming out of ground effect will be sufficient for in ground effect trim. There will be some longitudinal trim change when entering the ground effect, the magnitude and direction depending on flight speed (velocity ratio). It is possible that by changing the center of gravity to fan center location, a condition could exist where the in-ground-effect pitch trim requirements would be larger; each configuration considered should be evaluated to determine the trim requirements accurately.

---

[a] Volume 2, Table 7

[b] Volume 2, Appendix B

Static Longitudinal Stability and Tail Downwash - Power On:

Tail downwash results as a function of α, β and V_P/V_{tip} are shown in Figure 29a to 29f. The results were obtained by comparison of pitching moment data with the tail on (Figure 30a to 30h) and off (Figure 31a to 31f) and the previously determined relationship of ΔC_M versus i_t. The moment data are susceptible to error and non-repeatability and a variation of $\pm 2°$ in the downwash data is possible, however, the data show a trend toward a higher downwash as the height above ground is decreased; compare Figure 41, Volume 2 with Figure 29a and 29c. The same trend of increased downwash with decreased h/d_F was observed for the power off operation.

Longitudinal static stability margin increased at lower ground heights as shown in Figure 32a and 32b. This is caused mainly by the reduction in the de-stabilizing moment attributed to the fuselage, (tail off moment data are shown in Figure 31a to 31f). Power on stability with $\beta = 0°$ was considerably higher than the comparable power off value. At higher β settings the 2.98 and 1.41 h/d_F stability was reduced while 0.85 h/d_F stability increased above the power off value. The stability results are obtained from the average value of $\Delta C_M/\Delta C_L$ between $\alpha = -4°$ and $+10°$ (for $h/d_F = 0.85$ the lower limit was restricted to $\alpha = 0°$). The stability values were very sensitive to the range of α over which the value of $\Delta C_M/\Delta C_L$ was obtained because there was considerable scatter in the data.

Short Take-off Performance:

Short take-off performance is essentially as reported in Volume 2. Additional lift was found to be available in the velocity ratio and exit louver ranges where rotation is initiated (V_P/V_{tip} from 0.10 to 0.14 and $\beta = 35°$, see Figures 24c and 25c). This would allow a choice

of either:

1. Higher initial rate of rotation and a shorter horizontal distance for rotation (X_2).

2. Lower air speed at completion of ground run, and a shorter ground run distance (X_1).

The higher lift advantage, however, is offset by the lower thrust available in ground effect (see Figures 26b to 26c). This result supports the conclusion that part of the lift increase can be explained by the exit louver looseness resulting in higher lift readings at high indicated exit louver angles. Further, the higher lift is applicable only during the relatively short time when aircraft is close to the ground.

Using the ground effect data the improvement in take-off distance would be at most 50 feet relative to the results in Volume 2. The results in Volume 2 should be used since a change would be based on data with lower accuracy. In order to further refine the STOL analysis for optimum flight path and techniques, it would be necessary to have an understanding of the aircraft control response and also a suitable computer program to handle extensive trial solutions.

C. FAN AERODYNAMIC PERFORMANCE

Fan Flow and Pressure Coefficient:
The fan flow coefficient ratio is plotted as a function of velocity ratio for the three heights (see Figures 23a to 23c), and three exit louver settings (Φ_{000} is defined as the flow coefficient at $V_P = 0$, $\beta = 0°$, and $h/d_F = 2.98$).

Flow was reduced at $\beta = 0°$ and low velocity ratio because of proximity of the ground by a maximum of 27% at 0.85 h/d_F and 0.05 V_P/V_{tip}. At higher velocity ratios, the flow increased slightly above the $h/d_F = 2.98$ value for the $h/d_F = 1.41$ case. This may be caused by data scatter or a static pressure depression at the fan exit. The $\beta = 20°$ data are similar to $\beta = 0°$ results, however, the flow was not affected as much by ground proximity. The $\beta = 35°$ flow in ground effect was actually higher throughout which is again most likely β inaccuracy caused by the excessive tolerance in the exit louver system (at $\approx 35°$ β, a change of 1° β causes a change of 2% in flow coefficient).

It is significant that the flow coefficient at $V_P/V_{tip} = 0.075$ for $h/d_F = 0.85$ is slightly larger for $\beta = 35°$ than for $\beta = 0°$. This indicates that the ground presence is a more severe throttling influence than 35° of exit louver turning.

In addition to flow changes the pressure coefficient exhibited a trend not noted during static throttling at Evendale (see Figure 33a to 33f). The overall picture shows that during throttling with the exit louvers or the throttle plate the hub performance indicated by the pressure coefficient ($\Psi_{10.6}$) deteriorated only slightly; however, when throttling with the ground, the hub is essentially stalled at $h/d_F = 0.85$ and low velocity ratios, but the tip performance is slightly improved. This difference can be explained by examining the geometry of the two cases. Figure 34 shows probable flow conditions at the fan discharge for the configurations tested. The static build-up at the center of the fan in the vicinity of the hub (resulting from stagnation and the pressure gradient required to turn the flow) causes the hub region to stall, or nearly so. At 0.05 V_P/V_{tip} and $\beta = 0°$ two points at approximately the same fan speed and total lift were taken consecutively; while both of them indicated the same flow coefficient the pressure coefficient for one

point was 33% higher and the resulting calculated lift was different by ≈ 10% (see Figure 38). Either exit louver vectoring or high crossflow velocity restore original out-of-ground-effect fan performance. It has been pointed out that at low velocity ratios and low ground height, the flow coefficients are within 3% for $\beta = 0°$ and 35°; however, the pressure coefficient profile is quite different for the respective louver position. (Compare Figure 33d with 33f).

The very rapid decrease in flow coefficient, and lift at $\beta = 0°$, between V_P/V_{tip} 0.075 and 0.050 is an indication of fan stall (Figures 23a and 38). Some additional indications of stall were the high stator stresses and the large variation in rotor discharge pressure coefficient recorded under these conditions. (Fan speed variation observed under the same conditions of V_P/V_{tip} and β is not by itself an indication of discontinuous fan performance as the engine reingestion present could account for it.)

<u>Scale Model Ground Effect Test</u>:

In order to investigate ground effects further, a low speed 26 inch scale model fan was tested in the presence of a ground plane at $h/d_F = 0.81$. The flow decrease and pressure coefficient distribution in ground effect were similar to results obtained with full scale hardware at Ames, but the magnitude of change was not as pronounced. The flow reduction was 13% at $h/d_F = 0.81$ as compared with 27% for the full scale fan tested at the slightly higher h/d_F value of 0.85. The pressure coefficient distribution is shown in Figures 35a and 35b for $\beta = 0°$ and $h/d_F \sim \infty$ and 0.81 cases. For comparison see full scale results, Figures 33a and 33d.

A scale model test with a shallow inlet (wing installation) was conducted for comparison. The loss in flow was 10.5% and the pressure

coefficient profiles were affected less by the ground proximity than in the fuselage installation (see Figures 35c and 35d). The explanation for this difference is as follows. In the fan-in-fuselage configuration air accelerates over the bulletnose causing a low hub static pressure. The additional hub back pressure from the ground proximity causes the hub to stall in the full scale fan. In the scale model there was no evidence of stall but the performance was significantly reduced at the hub. On the other hand, the level of hub inlet static pressure was measured to be higher in the full scale wing installation[a] than in the fuselage installation, (a result also predicted by flux plots). This reduces the hub static pressure ratio the rotor must pump against and correspondingly in proximity of the ground, the scale model fan-in-wing showed less flow reduction.

The large difference in performance between the full scale and scale model hardware in ground effect could be the result of:

1. Better internal aerodynamics of the scale model fan because of cleaner blades, smoother bulletnose and bellmouth surfaces and closer clearances.

2. Differences in the "effective" h/d_F values between scale model and full scale tests. (For example, because of the J85 engine position).

3. Scale model results, for the fan-in-fuselage configuration, are based on internal measurements, not thrust readings.

In any event the scale model data show the correct trends, although, they are not representative enough to predict the magnitude of ground

[a] Reference 15

effects on full scale hardware.

Fan Power Absorption in Ground Effect:

Fan power absorption in ground effect was of interest, however most of the data in ground effect were obtained at $\approx$ 1700 rpm, and all of the data that exhibited lift deterioration were obtained with engine reingestion also present. The resulting randomly varying engine discharge conditions prevented a reasonable power estimate. Scale model data obtained at Evendale show that power absorption at constant fan speed drops in ground effect.

If fan speed is allowed to increase without restriction, then some of the lift lost because of ground effect can be recovered. This implies a nearly constant fan efficiency independent of fan throttling. As noted before the model data did not show the severe throttling at the hub which was evidenced on the full scale vehicle at 0.85 h/d_F, $\beta = 0^o$ and low velocity ratios. Because of this the model results in ground effect are optimistic. Table V shows the model results as a function of h/d_F for two configurations tested, and some full scale data for comparison. The discrepancy between the load cell, and the calculated thrust values for the fan-in-wing configuration (Table V) could be caused by some underside wing suction not accounted for in the thrust calculations.

Fan Thrust:

Fan thrust level and variations in thrust can be represented by the non-dimensional coefficients Φ and Ψ. Essentially Φ is proportional to weight flow while Ψ is proportional to jet velocity squared. The general thrust equation is $F = \rho A C_Z (V_{jet}) + A_{jet} (P_{s\ jet} - P_{amb})$. For all previous X353-5 testing the second term (plug thrust) was assumed to be so small to be negligible, as the discharge static

TABLE V

MODEL AND FULL SCALE THRUST RATIO COMPARISON ($\beta = 0°$)

	Constant Fan Speed Thrust Ratio, F/F_∞					Constant Power Thrust Ratio, F/F_∞				
h/d_F =	1.41	1.25	1.00	0.85	0.81	1.41	1.25	1.00	0.85	0.81
Fuselage (Scale Model)	-	-	-	-	0.88	-	-	-	-	0.94
Fuselage (Full Scale)	0.94*	-	-	0.67*	-	-	-	-	-	-
Wing (Scale Model)	-	0.97	0.96	-	0.92	-	1.0	1.0	-	0.97
Wing (Scale Model)	0.97*	0.94*	0.91*	0.90*	0.89*					

*Load Cell Measurements

pressure was nearly equal to ambient pressure, and the fan thrust was equal to the momentum thrust term. The fan flow reduction experienced during the ground effect testing is caused by the increase of back pressure ($P_{s\ jet}$) and the plug thrust therefore becomes significant. Using non-dimensional coefficients, a general expression for fan thrust under any condition is arrived at:

$$F = \rho\ A\ C_Z\ V_{jet}\ +\ A_{jet}\ (P_{s\ jet} - P_{s\ amb})$$

For this Fan

$A = A_{jet}$ and dividing by $\rho\ A\ (V_{tip})^2$ gives,

$$F/\rho\ A\ (V_{tip})^2 = C_Z/V_{tip}\quad V_{jet}/V_{tip} + \frac{P_{s\ jet} - P_{amb}}{\rho\ (V_{tip})^2}$$

By definition, $C_Z/V_{tip} = \Phi$

and for incompressible flow,

$$\Psi_t = \frac{P_{t\ jet} - P_{amb}}{\rho/2\ (V_{tip})^2}$$

$$\Psi_{s\ jet} = \frac{P_{s\ jet} - P_{amb}}{\rho/2\ (V_{tip})^2} = \frac{2\ (P_{s\ jet} - P_{amb}}{\rho\ (V_{tip})^2}$$

By definition, $P_{t\ jet} - P_{s\ jet} = \rho/2\ (V_{jet})^2$

dividing by $1/2\ \rho\ (V_{tip})^2$ gives,

$$\left(\frac{V_{jet}}{V_{tip}}\right) = \frac{P_{t\ jet} - P_{s\ jet}}{\rho/2\ (V_{tip})^2} = \frac{P_{t\ jet} - P_{amb}}{\rho/2\ (V_{tip})^2} = \frac{P_{s\ jet} - P_{amb}}{\rho/2\ (V_{tip})^2}$$

$$= \Psi_{t\ jet} - \Psi_{s\ jet}$$

In terms of the thrust coefficient,

$$F/\rho\ A\ (V_{tip})^2 = H_T = \Phi \sqrt{\Psi_{t\ jet} - \Psi_{s\ jet}} + \frac{\Psi_{s\ jet}}{2}$$

For incompressible flow, $C_Z = V_{jet}$,

$$\Psi_{t\ jet} - \Psi_{s\ jet} = V_{jet}/V_{tip} = C_Z/V_{tip} = \Phi$$

$$\Psi_{t\ jet} - \Psi_{s\ jet} = \Phi^2$$

and,

$$H_T = \Phi^2 + \frac{\Psi_{t\ jet} - \Phi^2}{2} = \frac{\Phi^2 + \Psi_{t\ jet}}{2}$$

where Φ is $\Phi_{10.3}$ and $\Psi_{t\ jet}$ is Ψ_{11}

Using this expression and the fan-in-fuselage throttling characteristics obtained during Evendale static tests[a], Figure 36 is obtained. Two solutions are used; one used the measured Ψ_{11} (stator discharge), the other the measured $\Psi_{10.6}$ (rotor discharge) and assumes a constant stator loss coefficient ($\Psi_{11} = 0.85\ \Psi_{10.6}$). The absolute value of H_T obtained either way is not the same as obtained from force measurements since they do not include the exit louver losses, discharge effective area reduction, nozzle losses, effects of compressibility nor the turbine flow contribution to thrust.

The relative thrust decrease as a function of flow coefficient decrease due to throttling shown in Figure 37 is a more accurate representation since the effects described above tend to cancel out in a comparison. Using the relationships in Figure 37 and the flow coefficient characteristics measured in the wind tunnel in ground effect, the thrust (lift) loss can be estimated. This together with actual measured lift loss is shown in Figure 38 for the $\beta = 0°$, $h/d_F = 0.85$ configuration. The explanation for the discrepancy between measured and calculated results cannot be definitely given without a more complete knowledge of fan internal characteristics when in ground effect (to include stator exit pressure measurements) together with a more complete static pressure survey of the aircraft.

Possible Sources of Discrepancy between Measured and Calculated Lift Loss:

Any one or all of the following conditions could contribute to the discrepancy between measured and calculated results:

1. The fan throttling characteristics Ψ vs. Φ are different in ground effect from results obtained at Evendale using the exit throttling system: The pressure coefficient, $\Psi_{10.6}$, was lower in the hub region for the ground effect case. The average value of $\Psi_{10.6}$ measured at Ames at 0.85 h/d_F, however, did not show

[a] Reference 11

any significant difference from the Evendale annular throttling plate results except at 0.05 velocity ratio. There are also considerable data obtained during scale model testing in Evendale which show the same characteristics.

2. There was hub stall at Ames when in ground effect: the stall evidence consisted of the very low and variable rotor discharge pressure near the hub. No direct indication of fan stall is available as the engine reingestion problem was present at the same time and the variations in fan speed and thrust can be attributed to that phenomenon without actually having had a stall problem. When stall is present the normal flow and pressure characteristics are discontinuous and pressure data obtained are questionable.

3. Indicated flow measurements are higher than actual: the flow coefficient, Φ, is obtained from eight wall static measurements approximately half way up in the deep inlet. If the low flow condition in the hub area, as evidenced by the low pressure coefficient measured at the fan rotor discharge, was reflected up stream, then the wall statics will indicate flow measurements higher than actual (a qualitative model is sketched below):

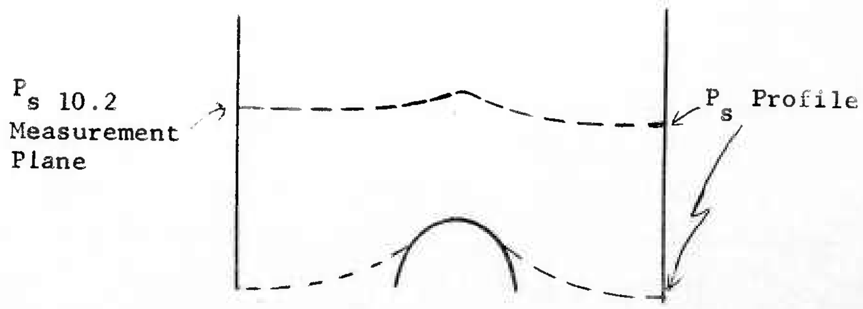

The magnitude of this error is small as the pressure measurement station is $\approx d_F/2$ above the rotor face and the pressure disturbance should be small that far up stream.

4. There is a more negative static pressure level on the underside of fuselage for the low h/d_F cases: within the limits of the sparse instrumentation this is not suspected. If anything, a less negative static pressure level on the underside of the fuselage is indicated for the lower h/d_F values. See Figure 28a to 28h.

5. Some of the lift loss is due to a change in pressure distribution on the wings: at a velocity ratio of 0.075 with $\alpha = 0°$ the total wing lift is about 9% of the total measured lift (C_L power off at $\alpha = 0°$ is 0.4 and interaction lift measured previously is 0.2). If all the interaction lift were lost in ground effect it would account for 3% of the lift discrepancy. If all the wing lift including interaction lift were lost, this together with the measured fan flow reduction would account for 80% of the lift loss measured at 0.075 V_P/V_{tip} and $\beta = 0°$. There were no static pressure measurement on the wings during this phase of test and no conclusive proof can be offered. It may be possible that some lift loss was present (like the disappearance of interaction lift), however, it is very unlikely that all wing lift was lost at low velocity ratios.

6. The fan efflux flow was not axial: in scale model tests at 0.81 h/d_F, flow angles of 15° from axial were measured in the fan discharge. This would decrease the vertical momentum by the cosine of the angle or 3.4%. The angles were measured at a distance of 3 inches below the stator discharge ($h/d_F = 0.12$); the angle leaving the stators is necessarily less than 15°, therefore, this effect is probably very small.

7. The assumption that the combined effect of exit louver losses, effective area changes and turbine to fan thrust ratio changes is the same in and out of ground effect is invalid: this may be true to some extent, however, none of these can be identified and evaluated separately.

In summary, it is apparent that the internal fan performance characteristics do not fully account for the change in measured lift in ground effect. It is believed that the two reasons for this are the lack of stage performance measurement Ψ_{11} (all fan performance estimates in ground effect are based on rotor discharge conditions and stator losses obtained under considerably different operating conditions) and a rotor stall condition with the inherent fluctuation of fan speed and internal pressures.

Engine Hot Air Reingestion and Ground Temperature:
Aircraft geometry is shown in Figures 2, 4 and 39. It can be seen that the engine is located at a very unfavorable position as far as hot air reingestion is concerned. The levels of reingestion are shown in Figure 40a to 43 for 1.41 and 0.85 h/d_F. At the lower height the engine was shielded (see Figure 4) and the results are not directly comparable with the 1.41 h/d_F results.

The maximum engine inlet temperature rise above ambient was 65°F and 45°F at h/d_F of 0.85 and 1.41 and occurred at low velocity ratios and $\beta = 0°$. All of the reingestion data were obtained at $\approx$ 1700 rpm on the fan and $\approx$ 950°F EGT. Assuming a constant value of $\frac{T_{inlet} - T_{amb}}{EGT - T_{amb}}$ the maximum inlet temperature rise is equivalent to 93°F and 64°F respectively at 1250°F EGT corresponding to J85-5 military rating.

In general the following reduced reingestion:

- increasing crossflow velocity

- increasing exit louver angle

- increasing angle of attack (for low exit louver position only).

The first two phenomena are obvious; the last was caused by angle of attack increases raising the engine inlet higher above the ground and removing it from the hottest part of the flow. However, at high louver positions, angle of attack increases, which increase the fan slipstream angle relative to the ground, caused reingestion to be more severe or, at best, unchanged.

The problems due to reingestion are twofold:

1. Loss in engine power and its effect on fan lift (Figure 44).

2. Unsteady fan speed making hover control difficult (fan speed variations were of the order of $\pm$ 40 rpm at 1700 rpm and constant engine throttle setting during the readings with severe reingestion. This is equivalent to over $\pm$ 5% in lift variation).

It is significant that no fan inlet reingestion was present even at the low ground height.

Temperature measurements were taken on the ground underneath the aircraft with a few thermocouples supplemented by many maximum reading thermometers. The thermocouple layout is shown in Figure 45 and results are shown in Figures 46a to 46e. The ground area

affected by hot gas flow extends over a considerable distance ahead and to the side of the fan.

No hot spots were found on the floor; maximum temperatures noted at 1700 rpm and 950°F EGT were around 160°F above ambient. This is equivalent to ≈ 215°F above ambient when extrapolated to 1250°F EGT using the parameter $\frac{T_{\ell} - T_{amb}}{EGT - T_{amb}}$ = constant. Temperature above the ground directly in the turbine slipstream was not measured, but thermocouples plugs located near the engine and rated at 600°F were charred; more data on this aspect of the environment is anticipated from the forthcoming fan-in-wing wind tunnel program

The conclusions that can be drawn from reingestion results are:

1. Engine inlets should be carefully located to prevent hot gas reingestion not only to minimize lift loss but also to prevent random lift variations and engine stall.

2. Ground surface temperatures will be moderate but objects above the ground (tires) and in the turbine slipstream may require shielding.

D. FAN MECHANICAL PERFORMANCE

Exit Louver Closure Transient:

Exit louvers were closed to 65° at ≈ 1300 rpm. At this condition the fan was shut down and the louvers closed all the way. It is estimated that the fan passed through 900 rpm with the louvers closed completely. There were no mechanical problems encountered during louver closure.

Rotor Vibratory Stresses:

In the 1750 rpm speed region where the majority of the ground effect testing was performed, there was little change in rotor vibratory stresses. At speeds over 2200 rpm and where the fan was throttled as a result of the $h/d_F = 0.85$ ground height, the rotor blade vibratory stresses, primarily the cosine 2θ mode, were effected. Since the fan throttling and hub stall were reduced by either closing the exit louvers or increasing the tunnel velocity, the rotor stresses correspondingly decreased; this effect is shown in Figure 47. Increasing the tunnel velocity to 40 knots or closing the exit louvers to 20° reduced the blade stress to the normal levels previously measured for a 2.98 h/d_F ground height. The 1.41 h/d_F ground height produced no changes in rotor blade stress at 2250 rpm as shown by the $\beta = 0°$ point in Figure 47.

Ground height had very little effect on the blade first flexural mode in the 1850 rpm speed region. 1850 rpm is the highest speed at which the first flexural mode is in resonance with a per revolution type of excitation.

A more complete study of the cosine 2θ mode stress as a function of crossflow velocity, exit louver angle, and acceleration or deceleration rates was made during this series of Ames tests. This study was made by accelerating the fan from 1200 to 2250 rpm at several different rates with 0°, 20°, 35° and 40° exit louver angles at 20, 40 and 60 knots tunnel velocity. The ground height was $h/d_F = 0.85$. The results of this study are shown in Figures 48, 49 and 50. In general, the faster the acceleration, the lower the cosine 2θ peak stress, however, two very fast accelerations, over 450 rpm/sec.[2], indicate that there is a maximum acceleration rate above which the stress begins to increase. For decelerations, the faster the deceleration, the higher the peak stress. This de-

celeration trend is not the same as the one found in Evendale tests[a] with the fan-in-wing configuration where the peak stress was highest for an average deceleration rate of 240 rpm/sec.[a] (i.e., for higher or lower deceleration rates the cosine 2θ peak stress was lower).

The cosine 2θ stress has been plotted in Figures 51 and 52 as a function of tunnel velocity and exit louver angle for instantaneous deceleration rates of 50 and 350 rpm/sec.[a] Extrapolating the 350 rpm/sec.[a] deceleration rate, $\beta = 40°$ data to 120 knots produces a stress of 22,000 psi, S.A. for this inlet and fan configuration. Peak cosine 2θ stress data obtained at 2.98 h/d_F in previous tests are plotted in Figure 53; these stresses are higher than those found during the ground effect test for approximately the same deceleration rate. The lower stresses experienced during the ground effect tests are attributed to a change in the torque band design which appears to have more damping in this mode of vibration.

The effect of hub stall at $\beta = 0°$ and low tunnel velocity can also be seen in Figure 47. At 20 knots the stress is higher than at 60 knots. With no ground effect, the stress increased as the tunnel velocity was increased, as can be seen in Figure 53.

Torque Band Stresses:

The new torque band design performed satisfactorily during this test. No cracks nor indications of imminent failure were found in the torque bands after the completion of the test.

Mechanically the new two piece seal and torque band behaved as expected. The torque band temperatures and the vibratory stresses resulting from the cosine nθ modes were lower. The torque band temperatures were reduced by 170°F at design rpm. The seal

---

[a] Reference 15, Section IV

temperatures were nearly as high as before but in the new design the seal does not carry the torque transmitting loads. The lower torque band temperatures, Figure 54, produces two beneficial effects. The steady state stresses in the torque band are lower which then permits more allowable vibratory stress, and the fatigue strength of the material at lower temperature is higher which also permits more allowable vibratory stress.

In the two piece design the torque band forward and aft edges are closer to the bucket carrier assembly making the torque band less sensitive to the bending stress of the $n\theta$ modes as shown in Figure 55.

<u>Stator Vane Stresses as a Function of Fan Height</u>:
The throttling of the fan and hub stall at a ground height of 0.85 h/d_F and for low tunnel velocities and with open louvers produced high stator vane stresses as shown in Figure 56. As the louvers were closed or the tunnel velocity was increased, the fan moved to a more unthrottled condition and the stator vane stresses decreased.

The stress, plotted in Figure 56 is for one vane which appears to be in resonance with the 36 rotor blades at 2320 rpm. This resonance is the torsional mode and it is the only resonance for this vane in the speed range above 1700 rpm that is sensitive to fan throttling. As the fan was accelerated through 2050 rpm with low tunnel velocity and open louvers this vane stress peaked at 20,000 psi, S.A. for less than half a second in the second flexural mode. A third vane whose stress also increases with fan throttling does not appear to be influenced by any particular resonance.

The second flexural mode responds to two slightly different exciting frequencies. When the stator vane sections on each side of the rear

frame support are vibrating in phase with one another, the second flexural mode frequency is slightly higher than when these vane sections are vibrating 180° out of phase with one another, this accounts for the wide variation in vane to vane stress noted in the testing.[a]

---

[a] After the airplane was removed from the wind tunnel, a stator vibration mode check was made showing the second flexural mode to respond to the 36 per rev blade passing frequency as follows:

	resonance speed
vane sections in phase	2000 to 2080 rpm
vane sections out of phase	1830 to 1950 rpm

Section VI

HARDWARE INSPECTION RESULTS

VI. HARDWARE INSPECTION RESULTS

A visual inspection of the vehicle was conducted after the ground effect test, with the following noted:

1. Rear Frame and Exit Louvers:
   Excessive pin wear was noted on several louvers due to insufficient engagement into the lever arm. All of the pins from both fans were removed and will be reworked to eliminate the tolerance between lever arm and pin and to increase depth of penetration.

2. J85 Engine and Fan Rotor:
   The inspection after test showed considerable engine damage and indicated that a small part (combustion liner igniter eyelet) had passed through the engine and the fan turbine. Subsequent investigation of the fan turbine showed no evidence of any damage (this is similar to the experience with Fan 001 which passed a J85-3 second stage turbine baffle with negligible fan turbine damage). The engine damage was, however, quite extensive and will require considerable parts replacement.

   The engine turbine was inspected by removing half of the turbine casing prior to the last 17 hour wind tunnel test and, therefore, the engine damage occurred during this final test period. It is very probable that re-installation of the igniter plug at this inspection damaged the eyelet where it passes into the liner resulting ultimately in failure of this part. This is not expected to be a repeatable problem.

SLIP RING COOLING

During previous X353-5 tests cooling air was provided to the strain gage slip ring. In this phase of testing this air was turned off for 35 minutes while the fan was operating at 1700 rpm. There was no in-

increase in slip ring bearing or fan bearing temperatures, however slip ring air temperature increased from 140°F to 210°F. There was no noticeable "noise" increase in the stress signals and the inspection of the slip ring after the test indicated normal brush wear. In view of these results it is believed feasible to operate the slip ring without cooling air for short periods (1/2 hour) in a flight test aircraft. Additional tests at higher fan speeds will be conducted in a later program.

Section VII

RECOMMENDATIONS

VII. RECOMMENDATIONS

The nature of the work under contract DA 44-177-TC-584 is such that specific individual recommendations are made in the regular and continuing working relationships between the contractor, TRECOM and NASA-Ames. Such recommendations are usually presented in correspondence and in the bi-monthly technical progress reports and are not restated here. Also in the body of this report, individual technical recommendations are incorporated in the technical discussions of which they are appropriately an inseparable part.

The intent of this part of the report is to summarize the major program recommendations relating to the continuation of the work. These are:

A. Complete, as planned, the program for wind tunnel testing of the fan-in-wing configuration, plus the associated inlet development and engineering analysis work as described in the January 4, 1961 contract amendment. This program will cover approximately 75 hours of testing, including inlet performance; fan mechanical performance (steady state and transient); effectiveness of thrust spoiling and vectoring for roll/yaw control; longitudinal and directional stability and static derivatives and trim control requirements; tail downwash; ground effects; and reingestion and circulation patterns.

B. Conduct wind tunnel scale model tests of a fan-in-wing configuration. Test several wing planforms, flap types, wing positions and fuselage shapes to allow a better understanding of lift, drag, moment and interaction phenomena observed in full scale tests, and to provide design data for fan powered VTOL aircraft.

C. Conduct full scale static tests of a fan-in-wing configuration to study reingestion patterns and to identify the optimum engine in-

let location.

D. Conduct full scale wind tunnel tests of a simulated Flight Research Vehicle by mid 1962 in order to provide advance data on this configuration for use in the detailed aircraft design. This should include lift, drag, moment and interaction studies; wing closures, stability and static derivatives and trim control requirements; static reingestion and circulation patterns and temperature surveys.

Section VIII

REFERENCES

VIII. REFERENCES

1. Aoyagi, K., Hickey, D.H., and deSavigny, R.A., Aerodynamic Characteristics of a Large-Scale Model with a High Disk-Loading Lifting Fan Mounted in the Fuselage, NASA Technical Note D-775.

2. Corning, Gerald, Supersonic and Subsonic Airplane Design, Second Edition, Edwards Brothers, Inc., Ann Arbor, Michigan, 1953.

3. Hickey, D.H., and Ellis, D.R., Wind-Tunnel Tests of a Semispan Wing with a Fan Rotating in the Plane of the Wing, NASA Technical Note D-88, October 1959.

4. Hoerner, S.F., Dr., Fluid-Dynamic Drag, Published by the Author, 1958, Library of Congress Catalog Card Number 57-13009.

5. *Kelly, M.W., Large-Scale Wind-Tunnel Studies of Several VTOL Types, Ames Research Center.

6. Kuhn, R.E., and Naeseth, R.L., Tunnel-Wall Effects Associated with VTOL-STOL Model Testing, NASA, Langley Research Center, Langley Field, Va., March 1959.

7. *Maki, R.L., and Hickey, D.H., Aerodynamics of Fan-in-Fuselage Model, Ames Research Center.

8. Pope, Alan, Wind-Tunnel Testing, Second Edition, John Wiley and Sons, Inc., New York, 1954.

9. *Spreemann, K.P., Induced Interference Effects on Jet and Burried Fan VTOL Configurations in Transition, Langley Research Center.

---

* From NASA Conference on V/STOL Aircraft (a compilation of papers presented), Langley Research Center, Langley Field, Virginia, November 17-18, 1960

10. Switzer, J.R., VTOL Wing-Fan Model Tests, General Electric Company, Flight Propulsion Laboratory Department, Cincinnati 15, Ohio, 1958, unclassified.

11. Theodorsen, Th., Dr., Theoretical Investigation of Ducted Propeller Aerodynamics, Volume 1, USA TRECOM Contract No. DA 44-177-TC-606, Project No. 9R 38-01-017-24, Republic Aviation Corporation, Farmingdale, New York, August 10, 1960, unclassified.

12. Joyce, J., Fabrication, Test and Analysis of a Tip-Turbine Lift-Fan VTOL Propulsion System for U.S. Army Transportation Research Command, Fort Eustis, Virginia, USA TRECOM Contract No. DA 44-177-TC-584, Project No. 9R 38-01-017-04, Technical Report TREC 60-42, General Electric Company, Flight Propulsion Laboratory Department, Cincinnati 15, Ohio, August 1960, unclassified.

13. Przedpelski, Z.J., Results of Wind Tunnel Tests of a Full Scale Fuselage Mounted, Tip Turbine Driven Lift Fan, USA TRECOM Contract No. DA 44-177-TC-584, Project No. 9R 38-01-020-02, Technical Report TREC 61-15, Volume 1, General Electric Company, Flight Propulsion Laboratory Department, Cincinnati 15, Ohio, January 1961, unclassified.

14. Przedpelski, Z.J., Results of Wind Tunnel Tests of a Full Scale Fuselage Mounted, Tip Turbine Driven Lift Fan, USA TRECOM Contract No. DA 44-177-TC-584, Task No. 9R 38-01-020-02, Technical Report TCREC 61-15, Volume 2, General Electric Company, Flight Propulsion Laboratory Department, Cincinnati 15, Ohio, April 1961, unclassified.

15. Heikkinen, A.H., Results of Static Tests of a Full Scale Wing Mounted, Tip Turbine Driven Lift Fan, USA TRECOM Contract No. DA 44-177-TC-584, Task No. 9R 38-01-020-02, Technical Report TCREC 62-21, General Electric Company, Flight Propulsion Laboratory Department, Cincinnati 15, Ohio, October 1961, unclassified.

APPENDIX A

TABLE A-1

DEFINITIONS AND SYMBOLS

a	Velocity of sound at fan inlet, ft/sec.
A_F	Fan exit area = 17.8 sq. ft.
AR	Wing aspect ratio, b^2/S_w = 5
b	Wing span = 35.36 ft.
c	Local wing chord, ft.
$\bar{c}$	Mean wing chord S_w/b = 7.07 ft.
C_D	Drag coefficient $D/q\ S_w$ (based on tunnel q)
C_{Di}	Induced drag coefficient, $C_L^2/\pi\ AR\ e$
C_{Do}	Drag coefficient at zero lift
C_{Dw}	Drag coefficient based on wetted area
c.g.	Center of gravity
C_L	Lift coefficient, $L/q\ S_w$ (based on tunnel q)
$\bar{C}_L$	Lift coefficient calculated from wing static pressure distribution $\frac{1}{2}\int_{-1}^{1}\frac{c_\ell c}{\bar{c}}\ d\left(\frac{y}{b/2}\right)$
$C_{L\ max}$	Maximum lift coefficient at $\Delta C_L/\Delta\alpha = 0$
C_{Lt}	Horizontal tail lift coefficient
C_ℓ	Rolling moment coefficient, Roll Force/q b S_w (based on tunnel q)
C_M	Pitching moment coefficient, $M/q\ S_w\ c_{mac}$ (based on tunnel q)
c_ℓ	Wing section lift coefficient
$\bar{C}_M$	Pitching moment coefficient calculated from wing static pressure distribution
ΔC_M	Change in moment coefficient due to change in tail incidence
c_{mac}	Mean aerodynamic chord $\int_{-b/2}^{b/2}\frac{c^2\ dy}{S_w}$ = 7.33 ft.
C_Z	Fan average axial (or through flow) velocity, ft/sec.
d	Diameter, ft.
D	Basic aircraft drag (fan off-holes covered), lbs.
D_{int}	Interaction drag, lbs.
D_R	Ram drag, lbs.
D_T	Total measured drag (fan on), lbs.
e	Oswald efficiency = 0.8 (assumed)
F	Total fan thrust, lbs.
F_{J85}	Thrust from J85 bleed gas
F_x	Horizontal component of fan thrust, $F\ [\sin(\alpha - \beta_v)]$ lbs.
F_y	Vertical component of fan thrust, $F\ [\cos(\beta_v - \alpha)]$ lbs.
g	Acceleration due to gravity = 32.2 ft/sec.^{2}
G.W.	Aircraft gross weight, lbs.
H_D	Drag coefficient, $D_T/\rho\ A_F\ (V_{tip})^2$ (based on fan q)
H_{DF}	Drag coefficient, $F_x/\rho\ A_F\ (V_{tip})^2$
H_{DN}	Drag coefficient, $H_{DF} - H_{DR}$
H_{DR}	Drag coefficient, $D_R/\rho\ A_F\ (V_{tip})^2$
$H_{C.W.}$	Coefficient, $G.W./\rho\ A_F\ (V_{tip})^2$
H_L	Lift coefficient, $L_T/\rho\ A_F\ (V_{tip})^2$ (based on fan q)
H_{LF}	Lift coefficient, $F_y/\rho\ A_F\ (V_{tip})^2$
H_M	Moment coefficient, $M_T/\rho\ A_F\ (V_{tip})^2\ l_t$ (based on fan q)
HP	Horsepower
H_T	Thrust coefficient, $F/\rho\ A_F\ (V_{tip})^2$
h	Height of the bottom of the fuselage above the ground, ft.
i_t	Tail incidence angle, degrees
L	Basic aircraft lift (fan off - holes covered), lbs.
L_{int}	Interaction lift, lbs.
l_{PRC}	Pitch reaction control moment arm = 25.5 ft.
L_T	Total measured lift (fan on), lbs.
l_t	Tail moment arm = 22 ft.
M	Basic aircraft pitching moment (tail off, power off), ft. lbs.
M_β	Pitching moment due to exit louver vectoring, ft. lbs.
$M_{D_R\ J85}$	Pitching moment due to J85 ram drag
M_{int}	Interaction pitching moment, ft. lbs.
M_{J85}	Pitching moment due to J85 bleed thrust, ft. lbs.
M_T	Total measured pitching moment (fan on), ft. lbs.
M_t	Pitching moment due to tail, ft. lbs.
N_F	Fan speed, RPM or % of design = 2640 RPM at 100%
N_{J85}	Engine speed, RPM or % of design = 16,500 RPM at 100%
P	Pressure, lbs/sq. in.
P/P	Fan rotor or fan stage pressure ratio
$P_{s\ell}$	Local static pressure, lbs/sq. in.
P_{to}	Tunnel total pressure, lbs/sq. in.
P_{so}	Tunnel static pressure, lbs/sq. in.
q	Tunnel dynamic pressure, lbs/sq. ft.
RC	Reaction control output, cycles/sec.
r/r_{fan}	Radius ratio, number of fan radii from fan centerline
S_t	Horizontal tail gross area = 50 sq. ft.
S_w	Wing gross area = 250 sq. ft.
T	Temperature, °R or °F
V_F	Tunnel or airplane velocity, Knots
V_{tip}	Fan blade tip speed = 720 ft/sec. or 426.6 knots at 2640 RPM
V_F/V_{tip}	Velocity ratio parameter (nondimensional)
V_{stall}	Airplane stall speed (fan off), Knots
W	Weight flow, lbs/sec.
y	Spanwise location from center line of the aircraft, ft.
ϕ	Flow coefficient - C_Z/V_{tip} (nondimensional)
α	Angle of attack, degrees
β	Indicated exit louver angle, degrees
β_V	Effective exit louver turning angle, degrees
δ	Pressure correction parameter, $P_{ambient}/14.696$
δ_f	Wing flap angle, degrees
ϵ	Tail downwash angle, degrees
η_R	Fraction of tunnel velocity head recovered by fan inlet (includes static loss)
θ	Temperature correction parameter, $T_{ambient}/518.7$
ρ	Mass density, slugs/cu. ft.
$\bar{\omega}$	Loss coefficient in per cent of fan inlet velocity head at the face of the rotor
Ψ	Aircraft yaw angle, or pressure coefficient = $\frac{2}{\gamma-1}\frac{(P/P)^{\gamma-1/\gamma} - 1}{(V_{tip}/a)^2}$ (nondimensional)

SUBSCRIPTS

c	Corrected
F	Denotes fan
f	Denotes flap or frontal area
P	Denotes airplane
s	Denotes static
t	Denotes total or tail
u	Uncorrected
w	Denotes wing or wetted area
10.1; 5.3; etc.	Denotes measurement plane identification

TABLE A-2 AMES TEST RESULTS

Point No. - Consecutive	Point No. - Per Run	Run No.	Tunnel Speed (V_p) - Knots	Tunnel Dynamic Pressure (q) - Lbs/sq.ft.	Fan Speed (N_p) - RPM	Tunnel Temp. °F	Angle of Attack (α) - degrees	Exit Louver Angle (β) - degrees	Horizontal Tail Incidence Angle (i_t) - degrees	Reaction Control Setting (RC) - CPS	Wing Flap Angle (δ_p) - degrees	Engine Speed (N_{J85}) - RPM	Exhaust Gas Temp. (EGT) - °F	Total Lift (L_T) - Lbs.	Total Drag (D_T) - Lbs.	Total Pitch Moment (M_T) - Ft. Lbs.	Lift Coefficient (C_L)	Drag Coefficient (C_D)	Pitch Moment Coefficient (C_M)	Lift To Drag Ratio (L_T/D_T)	Barometer In. Hg.	Velocity Ratio (V_p/V_{tip})	Lift Coefficient (H_L)	Drag Coefficient (H_D)	Pitch Moment Coefficient (H_M)	Yaw Angle (ψ) - Degrees
1	1	3	20	1.39	1150	72	0	0	0	OFF	30	12,000	926	1239	290	1377	3.555	0.7175	0.6196	4.969	30.12	0.109	0.2971	0.0600	0.0172	0
2	2			1.41	1240							12,500		1519	280	1431	4.299	0.6773	0.6328	6.362		0.103	0.3173	0.0500	0.0156	
3	3			1.37	1400	73						13,400	917	1860	305	1705	5.421	0.7735	0.7580	7.021		0.094	0.3343	0.0477	0.0156	
4	4			1.33	1560	74						14,250		2204	274	1993	6.619	0.7071	0.8966	9.375		0.081	0.3012	0.0322	0.0136	
5	5				1710							14,850	981	2568	260	1776	7.713	0.6650	0.8078	11.615		0.074	0.2925	0.0252	0.0102	
6	6				1800	75						15,100	993	2895	286	1714	8.697	0.7432	0.7822	11.716		0.069	0.2913	0.0249	0.0087	
7	1	4	20	1.39	1700	75	-4	0	0	OFF	30	15,600	951	2465	101	2353	7.084	0.1692	0.9979	41.912	30.12	0.076	0.2846	0.0068	0.0134	0
8	2			1.29	1670	76	-2							2412	179	1782	7.469	0.4358	0.8304	17.160		0.074	0.2896	0.0169	0.0107	
9	3			1.33	1650	77	0							2314	215	1528	6.949	0.5296	0.7060	13.140		0.076	0.2840	0.0216	0.0096	
10	4			1.27	1750		2					15,700		2892	381	770	9.0991	1.0852	0.4123	8.394		0.070	0.3093	0.0369	0.0047	
11	5			1.37		78	4						922	2886	513	1391	8.416	1.3852	0.6380	6.083		0.073	0.3139	0.0517	0.0079	
12	6				1760	79	6							2941	668	1443	8.577	1.8400	0.6612	4.667		0.073	0.3186	0.0684	0.0082	
13	7				1750		8							3005	720	897	8.764	1.9940	0.4458	4.400			0.3256	0.0741	0.0055	
14	8			1.39	1745	80	10					15,600	917	3118	938	1899	8.963	2.5933	0.8356	3.460		0.074	0.3437	0.0994	0.0107	
15	9				1740		12					15,500		3122	1022	2065	8.974	2.8372	0.9041	3.167		0.074	0.3492	0.1104	0.0117	
16	10		30	3.17	1720	81	-4							2733	607	3638	3.439	0.6445	0.7004	5.351		0.113	0.3106	0.0582	0.0211	
17	11			3.11	1730	82	-2						913	2871	680	2972	3.683	0.7554	0.5980	4.888		0.111	0.3238	0.0664	0.0175	
18	12				1740		0							3062	778	3589	3.928	0.8836	0.7087	4.457		0.111	0.3418	0.0769	0.0205	
19	13			3.09	1745		2							3201	889	2459	4.134	1.0360	0.5156	4.000			0.3597	0.0901	0.0149	
20	14			3.17	1755		4							3484	1035	2723	4.386	1.1934	0.5525	3.684		0.112	0.3850	0.1048	0.0162	
21	15						6						905	3564	1161	2848	4.487	1.3546	0.5765	3.320			0.3939	0.1189	0.0169	
22	16	4	30	3.17	1755	82	8	0	0	OFF	30	15,500	905	3594	1266	2347	4.525	1.4893	0.4926	3.045	30.12	0.112	0.3972	0.1307	0.0144	
23	17			3.31		83	10							3946	1468	2820	4.759	1.6680	0.5558	2.859		0.114	0.4358	0.1528	0.0170	
24	18				1750		12						901	3946	1584	2905	4.759	1.8104	0.5724	2.634			0.4358	0.1658	0.0175	
25	19			3.17	1740		0						905	3223	825	3180	4.057	0.9240	0.6264	4.401		0.112	0.3599	0.0820	0.0185	
26	20				1760		0	20						2973	-202	7750	3.741	-.3719	1.4131	10.087		0.111	0.3250	-0.0323	0.0409	
27	21			3.25	1785		0	35					892	2716	-825	9716	3.333	-1.1324	1.7104	-2.952		0.111	0.2905	-0.0987	0.0496	
28	22		40	5.62	1730		-4	0					917	3153	1082	5819	2.234	0.6487	0.6393	3.459		0.151	0.3568	0.1036	0.0340	
29	23				1740	84	-2							3439	1178	5323	2.438	0.7192	0.5935	3.403		0.150	0.3852	0.1136	0.0312	
30	24				1750		0						901	3692	1282	4919	2.618	0.7955	0.5566	3.303		0.149	0.4087	0.1242	0.0289	
31	25				1760		2							4074	1408	4353	2.890	0.8873	0.5041	3.268		0.148	0.4457	0.1368	0.0259	
32	26				1765		4							4247	1515	4092	3.013	0.9657	0.4811	3.130		0.148	0.4621	0.1481	0.0246	
33	27						6							4619	1678	4365	3.278	1.0839	0.5101	3.033			0.5028	0.1663	0.0261	
34	28						8						896	4723	1778	3765	3.352	1.1573	0.4541	2.905			0.5141	0.1775	0.0232	
35	29				1760		10							4796	1878	3925	3.404	1.2307	0.4721	2.744		0.148	0.5250	0.1898	0.0242	

TABLE A-2 AMES TEST RESULTS (Continued)

Point No. - Consecutive	Point No. - Per Run	Run No.	Tunnel Speed (V_p) - Knots	Tunnel Dynamic Pressure (q) - Lbs/sq.ft.	Fan Speed (N_F) - RPM	Tunnel Temp. °F	Angle of Attack (α) - degrees	Exit Louver Angle (β) - degrees	Horizontal Tail Incidence Angle (i_t) - degrees	Reaction Control Setting (RC) - CPS	Wing Flap Angle (δ_F) - degrees	Engine Speed (N_{J85}) - RPM	Exhaust Gas Temp. (EGT) - °F	Total Lift (L_T) - Lbs.	Total Drag (D_T) - Lbs.	Total Pitch Moment (M_T) - Ft. Lbs.	Lift Coefficient (C_L)	Drag Coefficient (C_D)	Pitch Moment Coefficient (C_M)	Lift To Drag Ratio (L_T/D_T)	Barometer In. Hg.	Velocity Ratio (V_p/V_{tip})	Lift Coefficient (H_L)	Drag Coefficient (H_D)	Pitch Moment Coefficient (H_M)	Yaw Angle (ψ) - Degree
36	30		40			83	0							3756	1300	5139	2.663	0.8083	0.5780	3.307			0.4107	0.1247	0.0297	
37	31			5.70	1770			20				15,000	892	3750	216	9940	2.622	0.0346	1.0306	76.103			0.4044	0.0053	0.0529	
38	32			5.62	1780			35						3277	-480	11119	2.322	-.4586	1.1587	-5.085		.147	0.3504	-0.0692	0.0582	
39	33		20	1.48	1750			0						2886	513	1398	7.790	1.2695	0.5946	6.144		.076	0.3184	0.0519	0.0081	
40	34			1.46	1720			20					922	2613	-433	5508	7.149	-1.3033	2.1376	-5.493		.077	0.3002	-0.0547	0.0299	
41	35			1.54	1790			35					896	2333	-1129	8013	6.050	-3.0495	2.9186	-1.987		.079	0.2677	-0.2677	0.0430	
42	1	5	30	3.13	1750	64	-4	35	0	OFF	30	14,350	850	2324	-1001	10290	2.960	-1.4006	1.8683	-2.120	30.15	.109	0.2465	-0.1167	0.0518	0
43	2				1755	65	-2						854	2552	-918	9428	3.251	-1.2924	1.7204	-2.524		.108	0.2653	-0.1055	0.0468	
44	3			3.19		66	0							2764	-824	10031	3.456	-1.1502	1.7949	-3.013		.110	0.2937	-0.0977	0.0508	
45	4			3.17			2					14,400	858	2913	-763	9819	3.666	-1.0776	1.7717	-3.411			0.3115	-0.0916	0.0501	
46	5				1760	67	4							3071	-696	10042	3.865	-.9908	1.8125	-3.911		.110	0.3265	-0.0837	0.0510	
47	6			3.15			6							3221	-609	9838	4.080	-.8837	1.7906	-4.628		.109	0.3404	-0.0737	0.0498	
48	7			3.17			8							3446	-496	9951	4.338	-.7341	1.8017	-5.924		.110	0.3665	-0.0602	0.0507	
49	8	5	30	3.15	1760	68	10	35	0	OFF	30	14,400	858	3549	-405	9612	4.497	-.6203	1.7561	-7.265	30.15	.109	0.3752	-0.0518	0.0488	
50	9			3.13			12							3710	-297	9744	4.731	-.4834	1.7923	-9.809		.109	0.3934	-0.0402	0.0496	
51	10				1750	69	14						862	3749	-149	9678	4.845	-.2920	1.7832	-16.63		.109	0.4073	0.0245	0.0499	
52	11			3.19			16							3874	36	9436	4.848	-.0543	1.7124	-89.53		.110	0.4144	-0.0046	0.0487	
53	12			3.17		70	18							3875	158	8645	4.880	0.1022	1.5888	47.86			0.4171	0.0087	0.0452	
54	13		40	5.62	1735		-4							2566	-570	10940	1.816	-.5271	1.1365	-3.465		.149	0.2816	-0.0817	0.0587	
55	14				1740		-2							2862	-506	11096	2.027	-.4793	1.1540	-4.250		.148	0.3113	-0.0736	0.0590	
56	15				1745	71	0					14,350		3185	-444	10955	2.257	-.4330	1.1427	-5.235		.148	0.3462	-0.0664	0.0584	
57	16			5.66			2						871	3563	-388	11200	2.508	-.3890	1.1613	-6.473		.148	0.3873	-0.0601	0.0597	
58	17			5.70	1740		4							3849	-315	11364	2.691	-.3337	1.1718	-8.095		.149	0.4207	-0.0522	0.0610	
59	18			5.88			6							4094	-262	11396	2.925	-.2982	1.2007	-9.841		.147	0.4458	-0.0454	0.0609	
60	19			5.62		72	8							4387	-131	11237	3.112	-.2014	1.1797	-15.50		.148	0.4793	-0.0310	0.0605	
61	20						10							4675	-25	11190	3.317	-.1238	1.1775	-26.88		.149	0.5144	-0.0192	0.0608	
62	21				1745		12							4834	99	11074	3.431	-.0333	1.1687	-103.2		.148	0.5263	-0.0051	0.0597	
63	22			5.48	1730		14							4663	385	9198	3.394	0.1794	1.0117	18.97		.148	0.5213	0.0276	0.0518	
64	23			5.66	1720		-4	20					862	3206	61	10584	2.256	-.0783	1.0946	-28.94		.150	0.3555	-0.0123	0.0575	
65	24			5.64	1710		-2							3400	130	10061	2.401	-.0270	1.0500	-89.30		.151	0.3824	-0.0043	0.0557	
66	25			5.62	1700	73	0							3629	218	9954	2.573	0.0382	1.0067	67.69		.151	0.4142	-0.0061	0.0540	
67	26						2							3899	335	9212	2.765	0.1236	0.9759	22.45			0.4451	-0.0199	0.0523	
68	27			5.58	1690		4						875	4100	417	8587	2.929	0.1863	0.9236	15.77		.152	0.4772	0.0304	0.0501	
69	28			5.66	1680		6							4369	529	8050	3.078	0.2635	0.8623	11.72		.154	0.5147	0.0041	0.0480	

TABLE A-2 AMES TEST RESULTS (Continued)

Point No. - Consecutive	Point No. - Per Run	Run No.	Tunnel Speed (V_p) - Knots	Tunnel Dynamic Pressure (q) - Lbs/sq.ft.	Fan Speed (N_F) - RPM	Tunnel Temp. °F	Angle of Attack (α) - degrees	Exit Louver Angle (β) - degrees	Horizontal Tail Incidence Angle (i_t) - degrees	Reaction Control Setting (RC) - CPS	Wing Flap Angle (δ_F) - degrees	Engine Speed (N_{J85}) - RPM	Exhaust Gas Temp. (EGT) - °F	Total Lift (L_T) - Lbs.	Total Drag (D_T) - Lbs.	Total Pitch Moment (M_T) - Ft. Lbs.	Lift Coefficient (C_L)	Drag Coefficient (C_D)	Pitch Moment Coefficient (C_M)	Lift To Drag Ratio (L_T/D_T)	Barometer In. Hg.	Velocity Ratio (V_p/V_{tip})	Lift Coefficient (H_L)	Drag Coefficient (H_D)	Pitch Moment Coefficient (H_M)	Yaw Angle (ψ) - Degrees
70	29			5.62			8							4555	625	8522	3.232	0.3366	0.9161	9.630		0.152	0.5266	0.0548	0.0497	
71	30						10							4692	730	7842	3.330	0.4136	0.8525	8.075			0.5426	0.0674	0.0463	
72	31			5.64	1670	74	12							4948	882	8402	3.4999	0.5217	0.9063	6.726		0.153	0.5775	0.0861	0.0498	
73	32			5.50	1680		14						880	5054	1045	8446	3.666	0.6584	0.9338	5.583		0.151	0.5878	0.1056	0.0499	
74	1	6	60	12.71	1725	75	-4	0	0	OFF	30	15,500	888	4440	2085	12561	1.387	0.5348	0.6135	2.613	30.15	0.224	0.4906	0.1891	0.0273	0
75	2			12.69	1710									5309	2123	9957	1.663	0.5547	0.5072	3.017		0.227	0.6012	0.2005	0.0611	
76	3			12.65	1700	75	4							6328	2260	8010	1.991	0.6020	0.4293	3.324		0.226	0.7168	0.2167	0.0515	
77	4			12.73	1710		6							6986	2554	7885	2.185	0.6921	0.4242	3.172		0.227	0.7929	0.2511	0.0513	
78	5			13.32	1720		8							7746	2818	7343	2.316	0.7380	0.3894	3.152		0.230	0.8582	0.2735	0.0481	
79	6			12.71			10							8071	2884	6878	2.530	0.8016	0.3863	3.169		0.222	0.8788	0.2784	0.0447	
80	7			12.67	1750		12							8381	3110	6081	2.636	0.8780	0.3553	3.013		0.222	0.9132	0.3042	0.0410	
81	8						14							8704	3325	5783	2.738	0.9481	0.3449	2.898		0.222	0.9434	0.3267	0.0396	
82	9				1700		-4	20				15,400	850	3893	1049	15000	1.219	0.2098	0.7202	5.859		0 227	0.4400	0.0757	0.0866	
83	10			12.87			0							5206	1255	13854	1.608	0.2731	0.6664	5.926		0.229	0.5938	0.1008	0.0820	
84	11						4						846	6552	1356	13868	2.026	0.3088	0.6718	6.593		0.230	0.7514	0.1145	0.0830	
85	12						6							7150	1506	12704	2.212	0.3577	0.6249	6.213			0.8204	0.1327	0.0772	
86	13			12.67	1710	76	8					15,300		7508	1619	11951	2.360	0.4029	0.6034	5.883		0.227	0.8541	0.1458	0.0727	
87	14			12.46	1730		10							7566	1784	12130	2.419	0.4667	0.6222	5.204		0.221	0.8319	0.1605	0.0713	
88	15				1750		12							7880	2162	11917	2.520	0.5903	0.6153	4.286		0.218	0.8472	0.1985	0.0689	
89	16			12.67	1710		-4	35						3061	281	16525	0.956	-.0327	0.7860	-29.565		0.227	0.3456	-0.0118	0.0946	
90	17						0							4364	387	15799	1.368	0.0052	0.7594	266.057			0.4946	0.0019	0.0914	
91	18						4							5694	559	13761	1.788	0.0639	0.6765	28.141		0.228	0.6505	0.0232	0.0820	
92	19			12.79			6							6268	684	14323	1.950	0.1035	0.6973	18.937		0.229	0.7169	0.0381	0.0854	
93	20			12.81	1720		8						854	6900	808	13645	2.145	0.1441	0.6699	14.952		0.223	0.7491	0.0503	0.0779	
94	21			12.61		77	10							6794	1055	11399	2.145	0.2287	0.5843	9.425		0.224	0.7586	0.0809	0.0688	
95	1	7	60	12.56	1750	72	0	0	0	OFF	30	15,500	884	5285	2201	10241	1.673	0.5840	0.5239	2.882	30.20	0.225	0.5943	0.2075	0.0620	0
96	2			12.68	1800	73		20					854	5474	1142	15799	1.717	0.2433	0.7589	7.099		0.220	0.5821	0.0825	0.0857	
97	3			12.86		75		35				14,500	858	4663	362	16024	1.440	-.0044	0.7589	-329.42		0.222	0.4976	-0.0015	0.0873	
98	4			12.68		76		40					862	3952	166	17513	1.237	-.0646	0.8327	-19.288		0.221	0.4232	-0.0221	0.0949	
99	5		80	22.58	1700	78		0				14,250	837	8069	3639	18109	1.419	0.5276	0.5166	2.709		0.303	0.9161	0.3406	0.1111	
100	6							20					846	7196	2408	17953	1.265	0.3096	0.5129	4.118			0.8167	0.1999	0.1103	
101	7					79		35						5967	1529	17926	1.047	0.1539	0.5122	6.870		0.304	0.6786	0.0998	0.1106	
102	8			22.66		80		40					854	5589	1337	16279	0.977	0.1190	0.4710	8.290		0.305	0.6374	0.0776	0.1023	
103	9			22.48		81	-4	0					846	6207	3390	19622	1.094	0.4818	0.5515	2.292		0.304	0.7091	0.3123	0.1191	

TABLE A-2 AMES TEST RESULTS (Continued)

Point No. - Consecutive	Point No. - Per Run	Run No.	Tunnel Speed (V_p) - Knots	Tunnel Dynamic Pressure (q) - Lbs/sq.ft.	Fan Speed (N_F) - RPM	Tunnel Temp. °F	Angle of Attack (α) - degrees	Exit Louver Angle (β) - degrees	Horizontal Tail Incidence Angle (i_t) - degrees	Reaction Control Setting (RC) - CPS	Wing Flap Angle (δ_F) - degrees	Engine Speed (N_{J85}) - RPM	Exhaust Gas Temp. (EGT) - °F	Total Lift (L_T) - Lbs.	Total Drag (D_T) - Lbs.	Total Pitch Moment (M_T) - Ft. Lbs.	Lift Coefficient (C_L)	Drag Coefficient (C_D)	Pitch Moment Coefficient (C_M)	Lift To Drag Ratio (L_T/D_T)	Barometer In. Hg.	Velocity Ratio (V_p/V_{tip})	Lift Coefficient (H_L)	Drag Coefficient (H_D)	Pitch Moment Coefficient (H_M)	Yaw Angle (ψ) - Degrees
104	10	7	80	22.79	1700	81	0	0	0	OFF	30	14,250	846	8215	3494	17544	1.432	0.4963	0.4991	2.906		0.306	0.9398	0.2257	0.1091	
105	11			22.48		82	4							9776	3722	14389	1.730	0.5497	0.4331	3.165		0.304	1.1243	0.3572	0.0937	
106	12			22.50			6						820	10869	3848	12820	1.922	0.5737	0.3971	3.368			1.2491	0.3729	0.0860	
107	13			22.42		83	8						829	11547	3988	10625	2.050	0.6033	0.3472	3.415			1.3323	0.3921	0.0752	
108	1	8	20	1.37	1700	74	0	10	0	OFF	30	14,750	812	2550	-116	2925	7.435	-.4557	1.2439	-16.339	30.20	0.074	0.2893	-0.0177	0.0161	0
109	2			1.27	2230	76		10				16,000		4380	-384	4852	13.785	-1.3264	2.1638	-10400		0.055	0.2885	-0.0278	0.0151	
110	3			1.78	1200	71		20				12,000	829	1535	-39	3565	3.439	-.2046	1.1719	-16.856		0.119	0.3408	-0.0203	0.0387	
111	4			1.37	1400							13,500		1784	-245	4524	5.199	-.8323	1.8811	-6.258		0.090	0.2958	-0.0473	0.0356	
112	5				1480			35						1704	-757	5971	4.965	-2.3272	2.4573	-2.138		0.085	0.2532	-0.1187	0.0417	
113	6			1.55	1600	72						14,000		2034	-893	6947	5.239	-2.4215	2.5248	-2.168		0.084	0.2616	-0.1209	0.0420	
114	7			1.37	1450			20						2047	-316	4198	5.967	-1.0396	1.7513	-5.749		0.087	0.3192	-0.0556	0.0312	
115	8			1.35	1600	73							998	2333	-482	5343	6.903	-1.5451	2.2388	-4.474		0.078	0.2982	-0.0667	0.0322	
116	9			1.47	2260	74						16,000	1141	4568	-1163	8444	12.420	-3.2816	3.2137	-3.788		0.058	0.2957	-0.0781	0.0255	
117	10				2250	75		35					1027	3713	-1983	11319	10.093	-5.5129	4.2809	-1.833		0.059	0.2502	-0.1367	0.0353	
118	11			1.39	2310			40						3459	-2283	12311	9.944	-6.6839	4.9122	-1.489		0.056	0.2165	-0.1455	0.0356	
119	12			1.52	2475	76		35				16,100	1149	4475	-2478	13107	11.766	-6.6381	4.7847	-1.774		0.054	0.2446	-0.1380	0.0331	
120	13			1.27	2400	77		20				16,300	1222	3073	-1443	5839	9.669	-4.6619	2.5879	-2.076		0.051	0.1779	-0.0858	0.0159	
121	14			1.43	1220	71		35				12,000		1258	-407	3880	3.509	-1.2555	1.5597	-2.803		0.105	0.2738	-0.0980	0.0405	
122	15			.86	2300			0				16,200	1065	4641	275	1863	21.576	1.1621	1.2613	18.576		0.044	0.2864	-0.0154	0.0056	
123	16			1.35	2475	72						16,600	1099	5704	390	1372	16.891	1.0386	0.6334	16.273		0.051	0.3061	-0.0188	0.0038	
124	17		40	5.62	2250	74						16,300		5257	1135	7305	3.732	0.6908	0.7883	5.416		0.114	0.3420	-0.0634	0.0235	
125	1	9	20	1.39	0	62	-4	90	0	OFF	30	0	N/A	111	87	-621	0.309	0.1290	-.1694	2.477		N/A	N/A	N/A	N/A	0
126	2						0							222	85	-485	0.629	0.1276	-.1116	5.006						
127	3						4							355	87	-734	1.012	0.1378	-.2045	7.416						
128	4						6							425	93	-756	1.213	0.1572	-.2108	7.779						
129	5						8							487	102	-798	1.391	0.1853	-.2246	7.562						
130	6					61	10							488	126	-704	1.394	0.2566	-.1852	5.473						
131	7						12							471	151	-655	1.345	0.3307	-.1636	4.098						
132	8						14							439	174	-908	1.253	0.3991	-.2607	3.165						
133	9			1.35			16							435	196	-892	1.279	0.4813	-.2624	2.678						
134	10		40	5.62			-4							264	357	-1106	0.178	0.1327	-.0332	1.416						
135	11			5.70		60	0							823	345	-1503	0.568	0.1251	-.0649	4.616						
136	12						4							1395	361	-2252	0.969	0.1407	-.1318	6.956						
137	13			5.62			6							1594	352	-2326	1.125	0.1401	-.1397	8.096						

TABLE A-2 AMES TEST RESULTS (Continued)

Point No. - Consecutive	Point No. - Per Run	Run No.	Tunnel Speed (V_p) - Knots	Tunnel Dynamic Pressure (q) - Lbs/sq.ft.	Fan Speed (N_p) - RPM	Tunnel Temp. °F	Angle of Attack (α) - degrees	Exit Louver Angle (β) - degrees	Horizontal Tail Incidence Angle (i_t) - degrees	Reaction Control Setting (RC) - CPS	Wing Flap Angle (δ_F) - degrees	Engine Speed (N_{J85}) - RPM	Exhaust Gas Temp. (EGT) - °F	Total Lift (L_T) - Lbs.	Total Drag (D_T) - Lbs.	Total Pitch Moment (M_T) - Ft. Lbs.	Lift Coefficient (C_L)	Drag Coefficient (C_D)	Pitch Moment Coefficient (C_M)	Lift To Drag Ratio (L_T/D_T)	Barometer In. Hg.	Velocity Ratio (V_p/V_{tip})	Lift Coefficient (H_L)	Drag Coefficient (H_D)	Pitch Moment Coefficient (H_M)	Yaw Angle (ψ) - Degrees
138	14	9	40	5.62	0	60	8	90	0	OFF	30	0	N/A	1832	383	-2420	1.294	0.1644	-.1463	7.931	30.20	N/A	N/A	N/A	N/A	0
139	15						10							1927	426	-2541	1.362	0.1972	-.1557	6.955						
140	16			5.56			12							1927	499	-2314	1.376	0.2552	-.1337	5.432						
141	17			5.62			14							1879	631	-2827	1.327	0.3475	-.1787	3.848						
142	18			5.56			16							1867	728	-2750	1.333	0.4243	-.1717	3.165						
143	19		60	12.65			-4							587	806	-2153	0.176	0.1335	-.0187	1.391						
144	20			12.69			0							1700	749	-3410	0.526	0.1191	-.0676	4.500						
145	21						4							2971	753	-4428	0.926	0.1248	-.1066	7.507						
146	22						6							3576	805	-5042	1.117	0.1433	-.1306	7.864						
147	23						8							4096	853	-5352	1.281	0.1607	-.1416	8.036						
148	24						10							4504	950	-5410	1.410	0.1934	-.1416	7.339						
149	25			12.61			12							4465	1098	-5471	1.406	0.2445	-.1434	5.793						
150	26			12.57			14							4357	1342	-6683	1.376	0.3254	-.1943	4.260						
151	27			12.65			16							4068	1625	-7284	1.276	0.4144	-.2160	3.104						
152	1	10	20	1.35	1700	68	-4	0	OFF	OFF	30	14,750	964	2623	104	935	7.762	0.1867	0.4522	41.617	30.24	0.073	0.2922	0.0070	0.0057	0
153	2					69	-2						989	2724	206	844	8.061	0.4912	0.4176	16.432		0.074	0.3057	0.0186	0.0053	
154	3			1.29		70	0						964	2898	336	1183	8.976	0.9249	0.5795	9.716		0.072	0.3265	0.0336	0.0070	
155	4				1800	71	2						939	3007	432	622	9.314	1.2247	0.3446	7.613		0.070	0.3205	0.0421	0.0039	
156	5			1.37	1700	72	4					14,500	913	2833	600	1256	8.262	1.6392	0.5841	5.046		0.074	0.3197	0.0634	0.0075	
157	6			1.41		73	6						913	2813	677	1241	7.970	1.8102	0.5665	4.409		0.075	0.3185	0.0723	0.0075	
158	7			1.45		74	8					14,250	909	2824	778	1409	7.780	2.0380	0.6187	3.823		0.077	0.3196	0.0837	0.0085	
159	8			1.44	1725		10					14,500	922	2974	900	2191	8.251	2.3940	0.9212	3.451		0.076	0.3332	0.0967	0.0124	
160	9			1.35		75	12						968	2991	989	2188	8.852	2.8266	0.9777	3.135		0.073	0.3351	0.1070	0.0123	
161	10			1.37		76	14						1044	2997	1105	2056	8.740	3.1247	0.9148	2.800		0.074	0.3401	0.1216	0.0119	
162	11			1.44	1700	77	0						1027	2800	415	1409	7.768	1.0358	0.6130	7.509		0.077	0.3191	0.0426	0.0084	
163	12			1.41		78		20				14,750	1023	2617	-485	5747	7.414	-1.4929	2.3031	-4.973		0.076	0.2984	-0.0601	0.0309	
164	13			1.49	1650	79		35				14,250	909	2144	-939	7160	5.746	-2.6378	2.7015	-2.182		0.079	0.2530	-0.1162	0.0396	
165	14		30	3.17	1700	80	-4	0				14,800	1023	2785	457	1575	3.504	0.4931	0.3454	7.127		0.114	0.3187	0.0448	0.0105	
166	15				1675		-2					14,750	985	2761	597	2055	3.474	0.6341	0.4304	5.494		0.115	0.3216	0.0587	0.0133	
167	16				1650	81	0					14,500	989	2684	645	2462	3.629	0.6969	0.5028	5.222		0.116	0.3418	0.0656	0.0158	
168	1	11	60	12.67	0	71	-4	90	OFF	OFF	30	0	N/A	930	708	-9594	0.284	0.1021	-.3390	2.875	30.05	N/A	N/A	N/A	N/A	
169	2			12.63			0							1867	718	-4932	0.581	0.1104	-.1341	5.356						
170	3			12.88			4							2973	755	-4275	0.913	0.1219	-.0973	7.576						
171	4			12.80			6							3508	768	-3781	1.086	0.1296	-.0750	8.459						
172	5			12.72			8							3822	810	-3664	1.192	0.1465	-.0686	8.203						

TABLE A-2 AMES TEST RESULTS (Continued)

Point No. - Consecutive	Point No. - Per Run	Run No.	Tunnel Speed (V_p) - Knots	Tunnel Dynamic Pressure (q) - Lbs/sq.ft.	Fan Speed (N_F) - RPM	Tunnel Temp. °F	Angle of Attack (α) - degrees	Exit Louver Angle (β) - degrees	Horizontal Tail Incidence Angle (i_t) - degrees	Reaction Control Setting (RC) - CPS	Wing Flap Angle (δ_F) - degrees	Engine Speed (N_{J85}) - RPM	Exhaust Gas Temp. (EGT) - °F	Total Lift (L_T) - Lbs.	Total Drag (D_T) - Lbs.	Total Pitch Moment (M_T) - Ft. Lbs.	Lift Coefficient (C_L)	Drag Coefficient (C_D)	Pitch Moment Coefficient (C_M)	Lift To Drag Ratio (L_T/D_T)	Barometer In. Hg.	Velocity Ratio (V_p/V_{tip})	Lift Coefficient (H_L)	Drag Coefficient (H_D)	Pitch Moment Coefficient (H_M)	Yaw Angle (ψ) - Degrees
173	6	11	60	12.57	0	71	10	90	OFF	OFF	30	0	N/A	4285	877	-2784	1.354	0.1731	-.0298	7.878	30.05	N/A	N/A	N/A	N/A	
174	7			12.67			12							4382	1084	-2633	1.373	0.2384	-.0200	5.802						
175	8			12.61			14							4215	1285	-1928	1.327	0.3060	-.0124	4.369						
176	1	12	30	3.27	1710	71	-4	0	OFF	OFF	30	14,800		2935	497	1766	3.580	0.4866	0.3689	7.379	30.05	0.114	0.3279	0.0446	0.0113	0
177	2			3.13	1720	72	-2							2966	534	2180	3.780	0.5632	0.4567	6.730		0.111	0.3252	0.0485	0.0131	
178	3			3.00	1750	73	0					14,700		3212	691	2590	4.273	0.8043	0.5501	5.324		0.107	0.3409	0.0642	0.0146	
179	4			3.11	1720	74	+2					14,500		3256	859	2758	4.178	0.9900	0.5654	4.230		0.111	0.3621	0.0858	0.0163	
180	5			3.09	1730		+4							3416	1032	1697	4.412	1.2233	0.3835	3.615		0.110	0.3762	0.1043	0.0109	
181	6			3.31		75	6					14,550		3631	1208	1848	4.378	1.3494	0.3909	3.252		0.114	0.4003	0.1234	0.0119	
182	7			3.32	1720		8							3667	1262	3345	4.531	1.4546	0.6538	3.122		0.114	0.4099	0.1316	0.0197	
183	8			3.19		76	10							3561	1318	2672	4.455	1.5465	0.5480	2.887		0.113	0.3980	0.1382	0.0163	
184	9			3.11	1710		12							3593	1394	2753	4.611	1.6891	0.5765	2.736		0.112	0.4061	0.1488	0.0169	
185	10				1700	77	14							3630	1508	2366	4.659	1.8379	0.5109	2.540		0.112	0.4067	0.1604	0.0149	
186	11			3.17	1710	78	0	0				14,700		3146	719	1927	3.960	0.7903	0.4108	5.023		0.113	0.3577	0.0714	0.0124	
187	12			3.19	1680		0	20				14,500		2994	-145	6761	3.744	-.2988	1.2356	-12.564		0.116	0.3521	-.0281	0.0387	
188	13			3.17	1700		0	35				14,400		2619	-734	7862	3.295	-1.0432	1.4323	-3.168		0.115	0.3045	-.0964	0.0441	
189	14			3.15	1710	79	0	40				14,300		2532	-864	8228	3.205	-1.2141	1.5044	-2.648		0.113	0.2879	-.1091	0.0450	
190	15			3.17	1730		-4	35				14,400		2319	-897	7928	2.916	-1.2533	1.4391	-2.335		0.112	0.2578	-.1108	0.0424	
191	16				1695		-2					14,300		2424	-787	7373	3.049	-1.1123	1.3459	-2.750		0.115	0.2822	-.1030	0.0415	
192	17			3.27			0							2669	-702	7527	3.255	-.9757	1.3351	-3.346		0.116	0.3077	-.0922	0.0420	
193	18			3.25			+2							2807	-637	7934	3.445	-.8988	1.4137	-3.844		0.116	0.3273	-.0854	0.0447	
194	19			3.21			4							2951	-586	8505	3.667	-.8428	1.5297	-4.363		0.115	0.3423	-.0787	0.0476	
195	20			3.17	1690		6							3091	-494	8479	3.890	-.7337	1.5459	-5.316		0.114	0.3606	-.0680	0.0477	
196	21				1695	81	8							3243	-415	8753	4.082	-.6319	1.5954	-6.476		0.114	0.3764	-.0583	0.0490	
197	22			3.21	1690		10							3414	-312	8801	4.244	-.4948	1.5871	-8.598		0.115	0.3970	-.0463	0.0494	
198	23			3.17	1695		12							3532	-223	9354	4.447	-.3852	1.7037	-11.570		0.115	0.4110	-.0356	0.0524	
199	24						14	35						3581	- 73	9059	4.509	-.1937	1.6552	-23.326		0.115	0.4167	-.0179	0.0509	
200	25		40	5.70	1720	82	-4	0				14,800		3321	975	3333	2.321	0.5628	0.3933	4.141		0.151	0.3731	0.0905	0.0211	
201	26			5.62	1725		-2							3569	1050	3679	2.530	0.6281	0.4338	4.044		0.151	0.4035	0.1002	0.0230	
202	27			5.60	1740		0							3700	1078	2661	2.633	0.6530	0.3383	4.047		0.149	0.4088	0.1014	0.0175	
203	28			5.64	1720		+2					14,600		3861	1218	3330	2.728	0.7490	0.4036	3.656		0.151	0.4368	0.1199	0.0215	
204	29			5.56			4							4143	1331	2517	2.971	0.8450	0.3308	3.528		0.150	0.4701	0.1337	0.0174	
205	30			5.66	1710		6							4416	1544	3914	3.111	0.9808	0.4636	3.182		0.151	0.5008	0.1579	0.0249	
206	31			5.60	1720		8							4508	1655	3926	3.210	1.0739	0.4712	2.998		0.151	0.5113	0.1711	0.0250	
207	32			5.78		83	10							4822	1828	4799	3.327	1.1591	0.5441	2.879		0.153	0.5470	0.1906	0.0298	

TABLE A-2 AMES TEST RESULTS (Continued)

Point No. - Consecutive	Point No. - Per Run	Run No.	Tunnel Speed (V_p) - Knots	Tunnel Dynamic Pressure (q) - Lbs/sq.ft.	Fan Speed (N_F) - RPM	Tunnel Temp. °F	Angle of Attack (α) - degrees	Exit Louver Angle (β) - degrees	Horizontal Tail Incidence Angle (i_t) - degrees	Reaction Control Setting (RC) - CPS	Wing Flap Angle (δ_F) - degrees	Engine Speed (N_{J85}) - RPM	Exhaust Gas Temp. (EGT) - °F	Total Lift (L_T) - Lbs.	Total Drag (D_T) - Lbs.	Total Pitch Moment (M_T) - Ft. Lbs.	Lift Coefficient (C_L)	Drag Coefficient (C_D)	Pitch Moment Coefficient (C_M)	Lift To Drag Ratio (L_T/D_T)	Barometer In. Hg.	Velocity Ratio (V_p/V_{tip})	Lift Coefficient (H_L)	Drag Coefficient (H_D)	Pitch Moment Coefficient (H_M)	Yaw Angle (ψ) - Degrees
208	33	12	40	5.76	1720	83	12	0	OFF	OFF	30	14,600	N/A	4959	1990	4659	3.434	1.2781	0.5348	2.694	30.05	0.153	0.5624	0.2093	0.0292	0
209	34			5.58	1710		14					14,500		5099	2111	5180	3.645	1.4117	0.6024	2.589		0.151	0.5852	0.2266	0.0322	
210	1	13	40	5.54	1690	83	0	0	OFF	OFF	30	14,700		3523	1018	2620	2.534	0.6180	0.3371	4.116		0.152	0.4090	0.0997	0.0181	
211	2			5.62	1680			20				14,500		3659	242	7426	2.594	0.0552	0.8001	47.143		0.154	0.4292	0.0091	0.0441	
212	3			5.70	1700			35				14,400		3198	-374	9094	2.234	-.3795	0.9496	-5.914		0.153	0.3687	-.0626	0.0522	
213	4			5.58	1720			40						2695	-551	9076	1.922	-.5120	0.9666	-3.773		0.150	0.3049	-.0812	0.0511	
214	5			5.74	1700		-4	35				14,500		2552	-505	8384	1.768	-.4733	0.8713	-3.757		0.153	0.2922	-.0782	0.0480	
215	6			5.68	1720		0							3165	-382	8718	2.219	-.3860	0.9166	-5.774		0.153	0.3625	-.0631	0.0499	
216	7			5.62	1715		+4							3751	-289	10101	2.660	-.3183	1.0646	-8.388		0.151	0.4276	-.0512	0.0570	
217	8				1710		6							4012	-211	10284	2.846	-.2606	1.0848	-10.958		0.152	0.4599	-.0421	0.0584	
218	9				1715		8					14,450		4278	-107	10443	3.035	-.1844	1.1026	-16.516		0.151	0.4879	-.0296	0.0590	
219	10				1710	84	10							4521	- 6	10923	3.208	-.1103	1.1516	-29.181		0.152	0.5198	-.0179	0.0621	
220	11			5.64	1725		12							4635	143	10866	3.277	-.0024	1.1448	-1380.2		0.151	0.5240	-.0004	0.0610	
221	12			5.62	1740		-4	20				14,550		3289	30	8187	2.331	-.1000	0.8692	-23.398		0.149	0.3649	-.0157	0.0453	
222	13			5.56	1710		0					14,500		3645	211	7767	2.612	0.0348	0.8413	75.357		0.152	0.4237	0.0056	0.0455	
223	14				1690		4							3964	405	7251	2.842	0.1788	0.7955	15.953		0.153	0.4666	0.0294	0.0435	
224	15			5.64	1680		6							4239	523	8143	2.996	0.2605	0.8741	11.540		0.156	0.5113	0.0445	0.0497	
225	16			5.70	1710		8					14,600		4569	638	8378	3.196	0.3395	0.8907	9.444		0.153	0.5254	0.0558	0.0488	
226	17			5.62	1700		10							4747	717	8154	3.369	0.4043	0.8827	8.356		0.152	0.5458	0.0655	0.0476	
227	18			5.66	1720		12							4991	866	8402	3.517	0.5082	0.9035	6.940		0.152	0.5676	0.0820	0.0486	
228	19			5.50		85	14							5140	1023	9194	3.728	0.6424	1.0080	5.819		0.148	0.5726	0.0987	0.0516	
229	20		60	12.71	1700		-4	0				14,500		4631	2077	6445	1.447	0.5323	0.3509	2.738		0.230	0.5381	0.1979	0.0435	
230	21			12.69	1680		0							5408	2152	6197	1.695	0.5613	0.3455	3.037		0.234	0.6523	0.2160	0.0443	
231	22			12.44	1710		4					14,600		6392	2290	6500	2.045	0.6237	0.3690	3.295		0.225	0.7271	0.2218	0.0437	
232	23			12.65	1730		6					14,650		6940	2572	6924	2.184	0.7029	0.3849	3.122		0.224	0.7717	0.2484	0.0453	
233	24			12.69	1700		8					14,600		7446	2675	7087	2.337	0.7350	0.3934	3.193		0.230	0.8674	0.2728	0.0486	
234	25			12.59			10					14,500		7908	2793	7977	2.502	0.7814	0.4367	3.215		0.229	0.9215	0.2878	0.0536	
235	26				1720		12							8047	2977	8419	2.547	0.8420	0.4583	3.036		0.226	0.9112	0.3012	0.0546	
236	27			12.65			14					14,450		7822	3327	6065	2.463	0.9504	0.3575	2.602		0.230	0.9111	0.3516	0.0440	
237	28				1710		0					14,650		5390	2110	6829	1.694	0.5502	0.3736	3.098		0	0.6266	0.2035	0.0460	
238	29			12.79	1720	84		20				14,500		5453	1132	10916	1.695	0.2370	0.5448	7.195		0.228	0.6194	0.0866	0.0663	
239	30			12.59	1705			35						4432	375	11886	1.398	0.0021	0.5942	657.323		0.227	0.5095	0.0008	0.0716	
240	31			12.65	1715			40						3961	259	12178	1.242	-.0351	0.6043	-35.681		0.227	0.4490	-.0127	0.0728	
241	1	14	60	12.68	0	70	0	90						2043	567	-4464	0.619	0.1009	0.1481	6.390	30.14					

TABLE A-2 AMES TEST RESULTS (Continued)

Point No. - Consecutive	Point No. - Per Run	Run No.	Tunnel Speed (V_p) - Knots	Tunnel Dynamic Pressure (q) - Lbs/sq.ft.	Fan Speed (N_F) - RPM	Tunnel Temp. °F	Angle of Attack (α) - degrees	Exit Louver Angle (β) - degrees	Horizontal Tail Incidence Angle (i_t) - degrees	Reaction Control Setting (RC) - CPS	Wing Flap Angle (δ_F) - degrees	Engine Speed (N_{J85}) - RPM	Exhaust Gas Temp. (EGT) - °F	Total Lift (L_T) - Lbs.	Total Drag (D_T) - Lbs.	Total Pitch Moment (M_T) - Ft. Lbs.	Lift Coefficient (C_L)	Drag Coefficient (C_D)	Pitch Moment Coefficient (C_M)	Lift To Drag Ratio (L_T/D_T)	Barometer In. Hg.	Velocity Ratio (V_p/V_{tip})	Lift Coefficient (H_L)	Drag Coefficient (H_D)	Pitch Moment Coefficient (H_M)	Yaw Angle (ψ) - Degrees
242	2	14	60	12.60	0	70	2	90						2534	575	-4008	0.779	0.1059	-.1282	7.593	30.14					0
243	3			12.64			4							3012	598	-3574	0.928	0.1140	-.1075	8.358						
244	4			12.60			6							3446	622	-2935	1.069	0.1237	-.0789	8.847						
245	5			12.68			8							4001	677	-2455	1.237	0.1412	-.0561	8.941						
246	6			12.64			10							4398	769	-1874	1.367	0.1724	-.0299	8.075						
247	7			12.66			12							4322	989	-1913	1.341	0.2429	-.0300	5.622						
248	8			12.68			14							4235	1234	-2377	1.311	0.3211	-.0485	4.161						
249	1	15	20	1.37	1120	67	0	0				11,750		1105	234	485	3.201	0.6052	0.2373	5.331	30.15	0.112	0.2830	0.0535	0.0070	
250	2			1.39	1260							12,500		1275	232	374	3.644	0.5896	0.1908	6.223		0.101	0.2585	0.0418	0.0045	
251	3				1395	68						13,500		1509	246	545	4.317	0.6299	0.2578	6.894		0.091	0.2495	0.0364	0.0050	
252	4				1570							14,500		1820	229	324	5.212	0.5810	0.1713	9.015		0.080	0.2354	0.0262	0.0026	
253	5				1710							14,700		2056	243	307	5.892	0.6213	0.1644	9.523		0.074	0.2272	0.0240	0.0021	
254	6		30	3.29	1700	70								2557	569	1598	3.084	0.6138	0.3091	5.065		0.115	0.2855	0.0568	0.0095	
255	7			3.09	1750	71	2							2717	656	1682	3.492	0.7726	0.3424	4.552		0.108	0.2840	0.0628	0.0093	
256	8			3.15	1690	72	4					14,500		2666	793	1532	3.360	0.9318	0.3122	3.633		0.113	0.3018	0.0837	0.0093	
257	9			3.09	1700		6							2969	925	2077	3.818	1.1236	0.4149	3.421		0.112	0.3333	0.0981	0.0121	
258	10			3.17			8							3089	1061	2413	3.873	1.2664	0.4649	3.078		0.113	0.3473	0.1136	0.0139	
259	11			3.13	1705		10							3144	1167	2116	3.993	1.4204	0.4200	2.829		0.112	0.3511	0.1249	0.0123	
260	12			3.21		73	12					14,450		3310	1327	2258	4.100	1.5840	0.4363	2.604		0.114	0.3729	0.1441	0.0132	
261	13			3.17	1715		0	35				14,400		2495	-711	7952	3.123	-.9752	1.4130	-3.228		0.112	0.2757	-.0861	0.0415	
262	14				1720	74	2							2596	-616	7642	3.251	-.8539	1.3609	-3.836		0.112	0.2843	-.0747	0.0396	
263	15			3.15			4							2713	-518	7422	3.420	-.7330	1.3326	-4.700		0.112	0.2986	-.0640	0.0387	
264	16			3.21	1710		6							2867	-412	7292	3.548	-.5872	1.2879	-6.084		0.113	0.3177	-.0526	0.0384	
265	17			3.19	1705		8							3012	-284	7209	3.752	-.4285	1.2828	-8.814		0.114	0.3394	-.0388	0.0386	
266	18			3.17	1695		10							3086	-173	7039	3.869	-.2893	1.2627	-13.460		0.112	0.3432	-.0257	0.0373	
267	19			3.15	1690	75	12					14,350		3198	- 68	7294	4.036	-.1559	1.3161	-26.040		0.114	0.3656	-.0141	0.0397	
268	1	16	30	3.15	1700	64	0	0				14,750		2524	583	1755	3.185	0.6623	0.3421	4.839	30.24	0.112	0.2801	0.0582	0.0100	
269	2			3.17	1725	66		20						2854	-117	4993	3.581	-.2256	0.8975	-15.961		0.113	0.3184	-.0201	0.0266	
270	3			3.19	1700			35				14,500		2563	-692	7986	3.194	-.9457	1.4041	-3.398		0.113	0.2860	-.0847	0.0419	
271	4		40	5.58	1725	69		0				15,000		3324	1000	3452	2.363	0.6388	0.3756	3.730		0.150	0.3724	0.1007	0.0197	
272	5			5.62	1700	70	2					14,750		3472	1107	3147	2.451	0.7119	0.3454	3.471		0.151	0.3899	0.1132	0.0183	
273	6			5.64		71	4							3730	1208	3412	2.625	0.7827	0.3718	3.380		0.151	0.4198	0.1252	0.0198	
274	7			5.60			6							3917	1331	4266	2.778	0.8787	0.4591	3.184		0.150	0.4413	0.1396	0.0243	
275	8			5.70		72	8							4224	1527	4126	2.944	1.0016	0.4402	2.960		0.152	0.4770	0.1623	0.0238	

TABLE A-2 AMES TEST RESULTS (Continued)

Point No. - Consecutive	Point No. - Per Run	Run No.	Tunnel Speed (V_p) - Knots	Tunnel Dynamic Pressure (q) - Lbs/sq.ft.	Fan Speed (N_p) - RPM	Tunnel Temp. °F	Angle of Attack (α) - degrees	Exit Louver Angle (β) - degrees	Horizontal Tail Incidence Angle (i_t) - degrees	Reaction Control Setting (RC) - CPS	Wing Flap Angle (δ_p) - degrees	Engine Speed (N_{J85}) - RPM	Exhaust Gas Temp. (EGT) - °F	Total Lift (L_T) - Lbs.	Total Drag (D_T) - Lbs.	Total Pitch Moment (M_T) - Ft. Lbs.	Lift Coefficient (C_L)	Drag Coefficient (C_D)	Pitch Moment Coefficient (C_M)	Lift To Drag Ratio (L_T/D_T)	Barometer In. Hg.	Velocity Ratio (V_p/V_{tip})	Lift Coefficient (H_L)	Drag Coefficient (H_D)	Pitch Moment Coefficient (H_M)	Yaw Angle (ψ) - Degrees
276	9	16	40	5.62	1700	72	10	0				14,500		4221	1625	4303	2.984	1.0886	0.4649	2.760	30.24	0.151	0.4772	0.1741	0.0248	0
277	10			5.52		73	12							4324	1758	4097	3.113	1.2079	0.4538	2.594		0.150	0.4893	0.1899	0.0238	
278	11			5.72		74	0	20						3373	339	5886	2.339	0.1591	0.5996	14.829		0.153	0.3821	0.0260	0.0326	
279	12			5.62			2							3536	398	6050	2.497	0.2073	0.6273	12.142		0.151	0.4004	0.0332	0.0335	
280	13			5.54			4							3722	470	6173	2.667	0.2654	0.6496	10.128		0.150	0.4214	0.0419	0.0342	
281	14					75	6							3874	562	6705	2.777	0.3338	0.7039	8.380		0.152	0.4400	0.0529	0.0371	
282	15			5.64			8							4041	707	7919	2.846	0.4314	0.8114	6.643		0.152	0.4593	0.0696	0.0436	
283	16				1680		10							4358	825	6697	3.071	0.5171	0.6949	5.977			0.4956	0.0835	0.0374	
284	17			5.62	1700	76	12							4566	922	7317	3.230	0.5902	0.7592	5.506		0.152	0.5206	0.0951	0.0408	
285	18						0	35						3163	-365	9011	2.231	-.3378	0.9130	-6.665			0.3596	-.0544	0.0490	
286	19					77	2							3348	-278	9234	2.363	-.2739	0.9364	-8.701		0.152	0.3814	-.0442	0.0503	
287	20						4							3529	-206	9294	2.492	-.2206	0.9441	-11.385			0.4022	-.0356	0.0507	
288	21						6							3777	- 93	9000	2.668	-.1382	0.9173	-19.453			0.4306	-.0223	0.0493	
289	22					78	8							3985	19	9227	2.816	-.0565	0.9412	-50.221		0.152	0.4557	-.0091	0.0507	
290	23			5.58			10							4145	123	9288	2.951	0.0202	0.9553	147.290		0.151	0.4744	0.0032	0.0511	
291	24			5.66			12							4473	225	9546	3.141	0.1142	0.9692	27.678		0.153	0.5131	0.0187	0.0527	
292	25			5.60			0	0				15,000		3181	979	3235	2.252	0.6213	0.3533	3.657		0.152	0.3639	0.1004	0.0190	
293	26			5.62				20				14,500		3348	270	6319	2.363	0.1142	0.6516	20.872		0.152	0.3829	0.0185	0.0352	
294	27			5.72		80		35						3119	-320	9290	2.161	-.3018	0.9243	-7.228		0.154	0.3576	-.0499	0.0509	
295	28			5.58				40						2903	-518	9352	2.061	-.4493	0.9526	-4.631		0.152	0.3326	-.0725	0.ø512	
296	29		60	12.65	1400	81		35				13,500		4341	556	9216	1.353	0.0978	0.4356	14.034		0.277	0.7312	0.0529	0.0784	
297	30			12.85	1405	82		20						4843	1154	7763	1.488	0.2812	0.3677	5.361		0.280	0.8187	0.1547	0.0674	
298	31			12.49	1400			0						4618	1675	4419	1.459	0.4584	0.2311	3.226		0.276	0.7806	0.2452	0.0412	
299	32			12.79	1700							14,500		5621	1932	-2578	1.738	0.5262	-.0720	3.341		0.230	0.6457	0.1955	-.0089	
300	33			12.89				20						5377	1183	8614	1.649	0.2891	0.4027	5.772		0.231	0.6180	0.1083	0.0503	
301	34			12.77		83		35						5049	361	11389	1.562	0.0351	0.5247	45.086		0.230	0.5809	0.0131	0.0650	
302	35			12.69	1710			40						4617	126	11929	1.435	-.0383	0.5510	-38.014		0.229	0.5299	-.0141	0.0678	
303	36			12.65	1690	84	2	35						5563	426	11146	1.739	0.0587	0.5206	29.965		0.229	0.6415	0.0217	0.0640	
304	37						4							6050	524	11636	1.893	0.0917	0.5436	20.864			0.6984	0.0338	0.0668	
305	38				1700		6							6509	615	11654	2.038	0.1225	0.5462	16.806			0.7519	0.0452	0.0671	
306	39						8							6959	762	12099	2.180	0.1709	0.5671	12.872			0.8042	0.0630	0.0697	
307	40			12.55	1725		10							7257	959	11827	2.293	0.2377	0.5613	9.732		0.228	0.8393	0.0870	0.0684	
308	41			12.44			12							7182	1409	11077	2.289	0.3871	0.5347	5.966		0.227	0.8313	0.1406	0.0647	
309	42			12.65	1700	85	0	20						5478	1131	8807	1.712	0.2796	0.4179	6.195		0.230	0.6333	0.1034	0.0515	

TABLE A-2 AMES TEST RESULTS (Continued)

Point No. - Consecutive	Point No. - Per Run	Run No.	Tunnel Speed (V_p) - Knots	Tunnel Dynamic Pressure (q) - Lbs/sq.ft.	Fan Speed (N_F) - RPM	Tunnel Temp. °F	Angle of Attack (α) - degrees	Exit Louver Angle (β) - degrees	Horizontal Tail Incidence Angle (i_t) - degrees	Reaction Control Setting (RC) - CPS	Wing Flap Angle (δ_F) - degrees	Engine Speed (N_{J85}) - RPM	Exhaust Gas Temp. (EGT) - °F	Total Lift (L_T) - Lbs.	Total Drag (D_T) - Lbs.	Total Pitch Moment (M_T) - Ft. Lbs.	Lift Coefficient (C_L)	Drag Coefficient (C_D)	Pitch Moment Coefficient (C_M)	Lift To Drag Ratio (L_T/D_T)	Barometer In. Hg.	Velocity Ratio (V_p/V_{tip})	Lift Coefficient (H_L)	Drag Coefficient (H_D)	Pitch Moment Coefficient (H_M)	Yaw Angle (ψ) - Degrees
310	43	16	60	12.69	1700	86	2	20				14,500		5965	1221	9119	1.860	0.3089	0.4320	6.087	30.24	0.230	0.6917	0.1149	0.0535	0
311	44			12.65			4							6340	1309	9267	1.985	0.3399	0.4414	5.898		0.230	0.7362	0.1260	0.0545	
312	45						6							6865	1416	9292	2.151	0.3757	0.4442	5.777			0.7978	0.1393	0.0549	
313	46				1690		8							7335	1538	9833	2.299	0.4163	0.4694	5.571			0.8527	0.1544	0.0580	
314	47				1680		10							7672	1704	10419	2.406	0.4708	0.4965	5.153			0.8923	0.1746	0.0613	
315	48				1700		12					14,600		7786	1983	10430	2.442	0.5610	0.4987	4.388			0.9057	0.2081	0.0616	
316	49				1710	87	0	0				14,750		5253	1893	5807	1.641	0.5206	0.2885	3.191		0.230	0.6102	0.1936	0.0357	
317	50			12.89	1705		2							5796	1993	6395	1.779	0.5425	0.3105	3.316		0.232	0.6742	0.2056	0.0392	
318	51			12.81	1700	88	4							6418	2070	6357	1.984	0.5724	0.3124	3.501		0.232	0.7487	0.2160	0.0393	
319	52			12.69	1710		6							7003	2215	7998	2.187	0.6262	0.3373	3.525		0.231	0.8174	0.2341	0.0482	
320	53			12.65			8							7324	2322	7336	2.296	0.6642	0.3617	3.487		0.230	0.8559	0.2476	0.0449	
321	54			12.53	1700		10							7448	2462	8212	2.358	0.7180	0.4046	3.312		0.229	0.8699	0.2649	0.0497	
322	55			12.75	1715		12							7767	2704	8997	2.417	0.7823	0.4339	3.115		0.231	0.9073	0.2937	0.0542	
323	56			12.63	1405		0					13,500		4846	1706	5146	1.515	0.4623	0.2603	3.320		0.279	0.8305	0.2534	0.0475	
324	57			12.77	1400		2							5273	1785	5485	1.632	0.4831	0.2730	3.419		0.281	0.9050	0.2679	0.0504	
325	58			12.65		87	4							5774	1815	5635	1.806	0.4999	0.2847	3.652		0.279	0.9901	0.2741	0.0520	
326	59			12.69			6							6374	1901	5832	1.989	0.5272	0.2942	3.811		0.280	1.094	0.2899	0.0539	
327	60			12.63	1395		8							6710	1977	7034	2.105	0.5561	0.3491	3.821		0.279	1.152	0.3044	0.0636	
328	61			12.65	1400		10							6683	2098	7665	2.093	0.5954	0.3777	3.549		0.279	1.147	0.3264	0.0690	
329	62			12.69	1450	86	12							6821	2324	4462	2.130	0.6665	0.2407	3.226			1.168	0.3654	0.0439	
330	63			12.61	1400	87	0	20						4784	1116	7989	1.498	0.2760	0.3837	5.498		0.279	0.8184	0.1508	0.0698	
331	64			12.69	1405		2							5265	1208	8151	1.640	0.3048	0.3903	5.445		0.280	0.9017	0.1676	0.0715	
332	65			12.85	1400		4							5806	1273	8547	1.787	0.3223	0.4046	5.608		0.282	0.9987	0.1801	0.0753	
333	66				1405		6							6216	1360	8132	1.915	0.3513	0.3887	5.507			1.070	0.1963	0.0724	
334	67			12.83			8							6733	1456	7951	2.079	0.3839	0.3834	5.467		0.281	1.156	0.2135	0.0710	
335	68			12.65	1440		10							6722	1675	7675	2.106	0.4616	0.3781	4.604		0.279	1.155	0.2531	0.0690	
336	69			12.89	1425		12							6681	2122	7086	2.053	0.5925	0.3488	3.499		0.282	1.147	0.3311	0.0649	
337	70			12.65	1400		0	35						4210	576	8756	1.311	0.1041	0.4157	12.784		0.279	0.7187	0.0571	0.0759	
338	71						2							4788	622	9189	1.494	0.1207	0.4362	12.546			0.8190	0.0662	0.0796	
339	72						4							5266	678	9310	1.645	0.1404	0.4432	11.861			0.9018	0.0770	0.0809	
340	73						6							5827	793	8918	1.823	0.1788	0.4281	10.308			0.9994	0.0980	0.0782	
341	74				1410		8							6240	873	8967	1.953	0.2060	0.4320	9.576			1.071	0.1129	0.0789	
342	75			12.55	1440	88	10							6334	1150	9144	1.999	0.2985	0.4446	6.762		0.279	1.089	0.1626	0.0807	
343	76			12.44	1445		12							5957	1553	7865	1.895	0.4334	0.3938	4.420		0.277	1.023	0.2341	0.0708	

TABLE A-2 AMES TEST RESULTS (Continued)

Point No. - Consecutive	Point No. - Per Run	Run No.	Tunnel Speed (V_p) - Knots	Tunnel Dynamic Pressure (q) - Lbs/sq.ft.	Fan Speed (N_F) - RPM	Tunnel Temp. °F	Angle of Attack (α) - degrees	Exit Louver Angle (β) - degrees	Horizontal Tail Incidence Angle (i_t) - degrees	Reaction Control Setting (RC) - CPS	Wing Flap Angle (δ_F) - degrees	Engine Speed (N_{J85}) - RPM	Exhaust Gas Temp. (EGT) - °F	Total Lift (L_T) - Lbs.	Total Drag (D_T) - Lbs.	Total Pitch Moment (M_T) - Ft. Lbs.	Lift Coefficient (C_L)	Drag Coefficient (C_D)	Pitch Moment Coefficient (C_M)	Lift To Drag Ratio (L_T/D_T)	Barometer In. Hg.	Velocity Ratio (V_p/V_{tp})	Lift Coefficient (H_L)	Drag Coefficient (H_D)	Pitch Moment Coefficient (H_M)	Yaw Angle (ψ) - Degrees
344	77	16	60	12.65	1400	88	0	40				13,500		3831	487	7882	1.191	0.0760	0.3780	15.941	30.24	0.280	0.6539	0.0417	0.0691	0
345	1	17	20	1.39	1700	73	0	0				14,800		2108	297	912	5.491	0.6985	0.3632	7.890	30.26	0.079	0.2382	0.0306	0.0052	0
346	2			1.35	1690	74	2					14,600		2253	405	671	5.988	1.0040	0.2838	5.984		0.078	0.2580	0.0436	0.0040	
347	3			1.37			4					14,500		2241	511	1009	6.037	1.3071	0.4137	4.634		0.078	0.2565	0.0558	0.0058	
348	4			1.39	1700	75	6							2310	607	44	6.352	1.6025	0.0599	3.977		0.077	0.2648	0.0669	0.0008	
349	5			1.43	1710		8					14,550		2531	776	217	6.685	1.9856	0.1235	3.377		0.078	0.2836	0.0844	0.0017	
350	6			1.39		76	10							2582	850	1037	7.202	2.3096	0.4427	3.127		0.076	0.2935	0.0942	0.0060	
351	7			1.35	1690		12					14,600		2557	904	717	7.286	2.5169	0.3282	2.903		0.076	0.2940	0.1016	0.0044	
352	8			1.39	1710	75	0					14,800		2114	289	1412	5.580	0.6876	0.5484	8.145		0.078	0.2410	0.0300	0.0078	
353	9			1.31	1690	76	0	20						2235	-376	3864	6.146	-1.1152	1.4923	-5.528		0.078	0.2609	-.0470	0.0210	
354	10			1.43	1720			35				14,600		2078	-937	6311	5.377	-2.5118	2.2742	-2.149		0.078	0.2315	-.1079	0.0326	
355	11			1.39	1705			40				14,500		1836	-1068	7303	4.658	-2.7990	2.5764	-1.671		0.080	0.2081	-.1246	0.9383	
356	12		30	3.21	1695	82		0				15,000		2604	624	2621	2.931	0.6291	0.4432	4.690		0.121	0.3006	0.0652	0.0150	
357	13			3.17	1765		2							2808	760	2183	3.217	0.8001	0.3831	4.046		0.115	0.2994	0.0750	0.0118	
358	14			3.15	1730		4					14,700		2924	865	2153	3.410	0.9407	0.3861	3.646		0.116	0.3195	0.0886	0.0119	
359	15			3.17	1700	81	6					14,650		3004	973	2231	3.493	1.0660	0.3994	3.296		0.118	0.3401	0.1042	0.0128	
360	16			3.09	1705		8							3082	1088	1411	3.627	1.2176	0.2730	2.996		0.117	0.3491	0.1177	0.0086	
361	17			3.17	1700		10							3311	1267	1937	3.819	1.4010	0.3533	2.740		0.119	0.3767	0.1387	0.0115	
362	18			3.09	1705		12							3298	1338	1142	3.942	1.5412	0.2360	2.570		0.117	0.3761	0.1475	0.0074	
363	19			3.09	1700		14							3355	1429	1101	3.986	1.6423	0.2300	2.439		0.117	0.3844	0.1588	0.0073	
364	20			3.15			0					14,900		2538	593	2655	2.923	0.6095	0.4579	4.828		0.119	0.2902	0.0612	0.0150	
365	21			3.21				20				14,750		2808	-25	5708	3.083	-.1056	0.8985	-29.375		0.122	0.3198	-.0100	0.0309	
366	22			3.04	1690			35				14,500		2438	-642	8658	2.807	-.8223	1.4075	-3.437		0.120	0.2823	-.0817	0.0470	
367	23			3.21	1695			40						2310	-786	9132	2.583	-.9636	1.4417	-2.701		0.121	0.2656	-.0982	0.0492	
368	24			3.15	1710			35						2451	-638	8691	2.805	-.8134	1.4048	-3.473		0.119	0.2773	-.0797	0.0461	
369	25				1720	82	2							2625	-557	8228	2.971	-.7108	1.3190	-4.209		0.119	0.2955	-.0699	0.0435	
370	26			3.21	1710		4							2731	-451	8362	3.040	-.5793	1.3199	-5.282		0.120	0.3077	-.0578	0.0443	
371	27			3.19	1705		6							2950	-345	7503	3.276	-.4575	1.1872	-7.205		0.121	0.3346	-.0459	0.0402	
372	28			3.11	1695		8	35				14,500		3032	-236	6666	3.435	-.3389	1.0816	-10.194		0.121	0.3504	-.0337	0.0365	
373	29			3.35	1710		10					14,550		3368	-109	6936	3.535	-.1830	1.0457	-19.420		0.124	0.3793	-.0188	0.0372	
374	30			3.17			12					14,600		3452	-23	6839	3.959	-.0925	1.1243	-43.013		0.119	0.3895	-.0085	0.0367	
375	1	18	40	5.64	1705	83	0	0				14,900		3375	1075	4633	2.143	0.6111	0.4431	3.540	30.26	0.161	0.3873	0.1117	0.0264	
376	2			5.62	1690		2					14,750		3464	1151	4092	2.211	0.6654	0.3993	3.353		0.161	0.4020	0.1222	0.0239	
377	3			5.60	1695		4					14,700		3742	1242	3989	2.406	0.7312	0.3944	3.318		0.160	0.4298	0.1317	0.0232	
378	4			5.66	1700		6							3992	1419	3955	2.527	0.8333	0.3876	3.056		0.161	0.4570	0.1519	0.0231	

TABLE A-2 AMES TEST RESULTS (Continued)

Point No. - Consecutive	Point No. - Per Run	Run No.	Tunnel Speed (V_p) - Knots	Tunnel Dynamic Pressure (q) - Lbs/sq.ft.	Fan Speed (N_F) - RPM	Tunnel Temp. °F	Angle of Attack (α) - degree	Exit Louver Angle (β) - degrees	Horizontal Tail Incidence Angle (i_t) - degrees	Reaction Control Setting (RC) - CPS	Wing Flap Angle (δ_F) - degrees	Engine Speed (N_{J85}) - RPM	Exhaust Gas Temp. (EGT) - °F	Total Lift (L_T) - Lbs.	Total Drag (D_T) - Lbs.	Total Pitch Moment (M_T) - Ft. Lbs.	Lift Coefficient (C_L)	Drag Coefficient (C_D)	Pitch Moment Coefficient (C_M)	Lift To Drag Ratio (L_T/D_T)	Barometer In. Hg.	Velocity Ratio (V_p/V_{tip})	Lift Coefficient (H_L)	Drag Coefficient (H_D)	Pitch Moment Coefficient (H_M)	Yaw Angle (ψ) - Degrees
379	5	18	40	5.60	1705	84	8	0				14,700		4244	1524	3607	2.727	0.9164	0.3637	2.997	30.26	0.159	0.4820	0.1633	0.0212	0
380	6			5.62	1710		10							4371	1667	2741	2.856	1.0287	0.2930	2.795		0.158	0.5002	0.1810	0.0169	
381	7			5.58	1720		12							4566	1809	2902	3.014	1.1360	0.3118	2.671		0.156	0.5140	0.1945	0.0175	
382	8			5.64	1695		0					14,850		3264	1082	3876	2.099	0.6246	0.3813	3.393		0.160	0.3792	0.1139	0.0227	
383	9			5.62	1700			20				14,600		3353	366	7741	2.157	0.1597	0.7238	13.637		0.160	0.3855	0.0297	0.0429	
384	10			5.58	1705			35						3147	-338	10809	2.050	-.3004	1.0082	-6.893		0.158	0.3595	-.0515	0.0586	
385	11			5.60	1710			40				14,550		2880	-538	11082	1.872	-.4314	1.0310	-4.385		0.158	0.3266	-.0741	0.0597	
386	12			5.64	1700			35				14,500		3148	-292	10536	2.021	-.2673	0.9699	-7.635		0.160	0.3638	-.0469	0.0579	
387	13				1695		2							3410	-201	10299	2.169	-.2051	0.9419	-10.677		0.160	0.3922	-.0358	0.0564	
388	14			5.62	1700		4							3678	-101	9609	2.357	-.1393	0.8887	-17.066		0.161	0.4255	-.0239	0.0532	
389	15			5.60			6							3881	-14	9247	2.512	-.0811	0.8666	-31.213		0.159	0.4465	-.0133	0.0510	
390	16			5.66	1695		8							4245	114	8725	2.688	0.0027	0.8045	992.98		0.162	0.4918	0.0017	0.0487	
391	17			5.58	1690		10							4446	222	8245	2.839	0.0748	0.7704	38.242		0.161	0.5187	0.0149	0.0465	
392	18			5.62			12							4785	343	7570	3.057	0.1546	0.7130	19.907		0.161	0.5581	0.0294	0.0430	
393	19			5.58	1700		0	20				14,600		3377	362	7420	2.198	0.1598	0.7029	13.883		0.158	0.3860	0.0292	0.0409	
394	20				1695		2							3566	444	7560	2.303	0.2133	0.7117	10.894		0.160	0.4125	0.0394	0.0422	
395	21				1690		4							3777	520	6927	2.437	0.2642	0.6563	9.298		0.160	0.4372	0.0486	0.0390	
396	22			5.72	1685		6							4111	666	6585	2.574	0.3482	0.6337	7.449		0.164	0.4848	0.0669	0.0395	
397	23			5.54	1705		8					14,700		4340	724	6257	2.798	0.4001	0.5995	7.043		0.159	0.4940	0.0718	0.0350	
398	24			5.60	1700		10							4552	865	5883	2.926	0.4919	0.5665	5.990		0.160	0.5242	0.0892	0.0335	
399	25			5.64			12							4871	1000	5383	3.078	0.5699	0.5158	5.435		0.161	0.5618	0.1052	0.0310	
400	26		20	1.45	1170		0	35				12,000		1191	-276	4251	2.487	-.6591	1.2590	-3.805		0.128	0.2851	-.0733	0.0476	
401	27			1.31	1190			40						1024	-397	4264	2.508	-1.0582	1.4745	-2.389		0.117	0.2407	-.0999	0.0468	
402	28			1.47	1230			45						878	-440	4223	1.931	-1.0558	1.3182	-1.848		0.120	0.1945	-.1047	0.0439	
403	29			1.43	1255			50						719	-450	4192	1.642	-1.1185	1.3604	-1.486		0.115	0.1513	-.1016	0.0415	
404	30			1.37	1290			55						451	-449	4188	1.080	-1.1731	1.4314	-.938		0.108	0.0882	-.0944	0.0386	
405	31			1.27	1325			60						425	-377	-3725	1.308	-1.2561	-1.5501	-1.057		0.093	0.0793	-.0761	-.0313	
406	32			1.49	1340			65				11,900		197	-281	2958	0.438	-.7315	0.9766	-.626		0.107	0.0354	-.0579	0.0260	
407	1	19	60	12.80	1405	65	0	0				13,400		4925	1912	7972	1.386	0.4679	0.3485	3.005		0.286	0.7922	0.2709	0.0656	
408	2			12.70	1400	66	2							5424	1917	7998	1.573	0.4870	0.3603	3.271	30.28	0.282	0.8796	0.2750	0.0666	
409	3			12.68	1395	67	4							6037	1964	7345	1.753	0.5028	0.3359	3.526		0.285	0.9963	0.2885	0.0630	
410	4						6							6751	2011	7170	1.963	0.5186	0.3307	3.823		0.284	1.1084	0.2954	0.0616	
411	5				1390	68	8							7221	2106	5975	2.094	0.5467	0.2839	3.868		0.284	1.1801	0.3107	0.0526	
412	6			12.64	1410		10					13,300		7168	2158	4340	2.123	0.5771	0.2240	3.713		0.277	1.1381	0.3113	0.0395	

TABLE A-2 AMES TEST RESULTS (Continued)

Point No. - Consecutive	Point No. - Per Run	Run No.	Tunnel Speed (V_p) - Knots	Tunnel Dynamic Pressure (q) - Lbs/sq.ft.	Fan Speed (N_F) - RPM	Tunnel Temp. °F	Angle of Attack (α) - degrees	Exit Louver Angle (β) - degrees	Horizontal Tail Incidence Angle (i_t) - degrees	Reaction Control Setting (RC) - CPS	Wing Flap Angle (δ_F) - degrees	Engine Speed (N_{J85}) - RPM	Exhaust Gas Temp. (EGT) - °F	Total Lift (L_T) - Lbs.	Total Drag (D_T) - Lbs.	Total Pitch Moment (M_T) - Ft. Lbs.	Lift Coefficient (C_L)	Drag Coefficient (C_D)	Pitch Moment Coefficient (C_M)	Lift To Drag Ratio (L_T/D_T)	Barometer In. Hg.	Velocity Ratio (V_p/V_{tip})	Lift Coefficient (H_L)	Drag Coefficient (H_D)	Pitch Moment Coefficient (H_M)	Yaw Angle (ψ) - Degrees
413	7	19	60	12.64	1385	68	12	0				13,000		7000	2484	2517	2.076	0.6777	0.1516	3.092	30.28	0.285	1.1768	0.3861	0.0281	0
414	8				1405		0	20				13,400		4796	1268	11177	1.377	0.2914	0.4822	4.795		0.282	0.7693	0.1660	0.0890	
415	9				1410	69	2					13,450		5728	1321	11142	1.656	0.3105	0.4846	5.397		0.282	0.9228	0.1760	0.0893	
416	10				1405		4							6077	1393	9768	1.747	0.3309	0.4290	5.338		0.283	0.9794	0.1888	0.0794	
417	11			12.80	1410		6					13,500		6781	1490	8384	1.937	0.3580	0.3735	5.466		0.284	1.0938	0.2051	0.0696	
418	12				1360		8					13,000		7072	1552	6942	2.021	0.3779	0.3185	5.401		0.294	1.2266	0.2324	0.0636	
419	13			12.54			10							6818	1858	5556	2.008	0.4846	0.2724	4.184		0.288	1.1655	0.2838	0.0520	
420	14				1390	70	12							6909	2166	4228	2.044	0.5811	0.2211	3.552		0.286	1.1668	0.3338	0.0414	
421	15			12.64	1395		0	35				13,350		4305	678	12223	1.226	0.1182	0.5206	10.538		0.287	0.7076	0.0720	0.0993	
422	16						2							4949	704	11274	1.407	0.1270	0.4834	11.236		0.288	0.8152	0.0774	0.0925	
423	17				1400		4					13,400		5604	758	10628	1.596	0.1446	0.4598	11.177		0.288	0.8731	0.0826	0.0830	
424	18			12.58	1405		6							6264	841	9335	1.793	0.1714	0.4120	10.577		0.285	1.0201	0.1011	0.0772	
425	19			12.48	1420		8							6654	972	8076	1.923	0.2138	0.3669	9.087		0.279	1.0319	0.1179	0.0648	
426	20			12.64	1405	71	10	35				13,200		6620	1374	5192	1.920	0.3346	0.2546	5.797		0.285	1.0884	0.1924	0.0474	
427	21			12.58	1405		12							6375	1694	5109	1.875	0.4374	0.2559	4.331		0.281	1.0329	0.2432	0.0463	
428	22		40	5.62	2270		0	0				16,600		4722	1118	3392	3.036	0.6456	0.3375	4.734		0.118	0.2963	0.0637	0.0109	
429	23			5.74	2230	72		20				16,000		4874	30	9840	2.943	-.0598	0.8540	-49.578		0.124	0.3176	-.0054	0.0305	
430	24			5.62	2300			35				15,250		4781	-1144	14685	3.162	-.8394	1.3714	-3.791		0.115	0.2927	-.0772	0.0422	
431	25			5.68	2330			40						4506	-1481	16291	2.994	-1.0686	1.5246	-2.820		0.113	0.2688	-.0956	0.0455	
432	26		20	1.39	2310			35				16,600		3705	-1920	9844	9.994	-5.2672	3.6677	-1.901		0.057	0.2287	-.1204	0.0279	
433	27			1.51	2330			40				15,250		3430	-2182	10750	8.397	-5.4326	3.6369	-1.549		0.059	0.2044	-.1321	0.0295	
434	28			1.16	2270			20				16,600		4514	-914	5619	15.282	-3.1763	2.6364	-4.817		0.052	0.2839	-.0590	0.0163	
435	29			1.39	2250	76		0						3451	271	940	10.281	0.7310	0.4206	14.093		0.056	0.2227	0.0158	0.0030	
436	30			1.23	2320			0						3749	256	2062	12.272	0.7613	0.9604	16.145		0.051	0.2257	0.0140	0.0059	
437	31			1.47	1200	75		20				12,300		1333	-6	2753	3.116	-.0921	0.9217	-34.049		0.118	0.3020	-.0079	0.0296	
438	32			1.88	1210			35				12,200		1151	-252	10455	2.215	-.5673	2.8077	-3.939		0.128	0.2561	-.0647	0.1079	
439	33				1420							13,400		1709	-446	5820	3.189	-.9156	1.5290	-3.505		0.111	0.2763	-.0785	0.0440	
440	34			1.51	1380			20				13,500		1639	-92	3064	3.836	-.2945	1.0215	-13.096		0.102	0.2091	-.0156	0.0185	
441	35				1605							14,500		2094	-279	3701	4.822	-.7231	1.2054	-6.696		0.088	0.2643	-.0391	0.0219	
442	36			1.64				35				15,300		1930	-700	6069	4.131	-1.5834	1.8186	-2.621		0.092	0.2462	-.0938	0.0360	
443	37			1.68	1755							15,700		2241	-866	6874	4.577	-1.8544	1.9618	-2.479		0.086	0.2360	-.0950	0.0336	
444	38			1.33	1745			20				15,000		2388	-392	3669	5.876	-1.0459	1.2740	-5.338		0.079	0.2550	-.0448	0.0183	
445	39		60	12.43	2320							16,500		7147	983	15034	2.297	0.2406	0.7028	9.627		0.164	0.4328	0.0452	0.0441	
446	40			13.56	2260	76		35				16,300		6934	-57	19925	1.884	-.0936	0.7843	-20.327		0.182	0.4380	-.0205	0.0605	

TABLE A-2 AMES TEST RESULTS (Continued)

Point No. - Consecutive	Point No. - Per Run	Run No.	Tunnel Speed (V_p) - Knots	Tunnel Dynamic Pressure (q) - Lbs/sq.ft.	Fan Speed (N_F) - RPM	Tunnel Temp. °F	Angle of Attack (α) - degrees	Exit Louver Angle (β) - degrees	Horizontal Tail Incidence Angle (i_t) - degrees	Reaction Control Setting (RC) - CPS	Wing Flap Angle (δ_F) - degrees	Engine Speed (N_{J85}) - RPM	Exhaust Gas Temp. (EGT) - °F	Total Lift (L_T) - Lbs.	Total Drag (D_T) - Lbs.	Total Pitch Moment (M_T) - Ft. Lbs.	Lift Coefficient (C_L)	Drag Coefficient (C_D)	Pitch Moment Coefficient (C_M)	Lift To Drag Ratio (L_T/D_T)	Barometer In. Hg.	Velocity Ratio (V_p/V_{tip})	Lift Coefficient (H_L)	Drag Coefficient (H_D)	Pitch Moment Coefficient (H_M)	Yaw Angle (ψ) - Degrees
447	41	19	60	12.19	2350	76	0	35				15,900		6498	-689	21512	1.923	-.2840	0.9153	-6.841	30.28	0.167	0.3830	-.0551	0.0605	0
448	42			10.55	2260			0				16,650		5954	1955	8581	2.122	0.6252	0.4591	3.425		0.159	0.3760	0.1115	0.0270	
449	43			12.48	1710							14,600		5463	2015	3535	1.630	0.5308	0.3898	3.110		0.232	0.6160	0.2021	0.0487	
450	44			12.64			2							5993	2098	7572	1.770	0.5507	0.3484	3.251		0.233	0.6722	0.2105	0.0437	
451	45			12.54	1715		4					14,650		6709	2224	7463	1.983	0.5899	0.3455	3.395		0.232	0.7431	0.2227	0.0428	
452	46				1695		6							7280	2325	7479	2.156	0.6231	0.3484	3.493		0.234	0.8206	0.2387	0.0438	
453	47			12.54	1695		8	0				14,650		7589	2468	6876	2.261	0.6717	0.3271	3.395		0.234	0.9544	0.2589	0.0456	
454	48			12.64	1690		10							8128	2691	5488	2.385	0.7282	0.2685	3.303		0.236	0.9300	0.2851	0.0345	
455	49			12.27	1700		12							8308	2858	3969	2.486	0.7961	0.2121	3.148		0.233	0.9456	0.3045	0.0264	
456	50			12.64	1705	77	0	20				14,600		5691	1258	11817	1.648	0.2906	0.5104	5.738		0.235	0.6378	0.1146	0.0654	
457	51			12.74	1695		2					14,550		6304	1354	11476	1.801	0.3150	0.4920	5.779		0.239	0.7195	0.1282	0.0650	
458	52				1690		4							6868	1449	10453	1.968	0.3454	0.4544	5.755		0.239	0.7846	0.1399	0.0599	
459	53				1715		6					14,600		8269	1546	11273	2.384	0.3774	0.4905	6.369		0.234	0.9143	0.1467	0.0622	
460	54			12.64	1705		8							7941	1657	9199	2.305	0.4152	0.4127	5.600		0.235	0.8880	0.1619	0.0525	
461	55			12.19	1710		10					14,650		8301	1852	8094	2.409	0.4739	0.3701	5.125		0.233	0.9598	0.1916	0.0484	
462	56			12.03	1715		12							7923	2026	7842	2.418	0.5574	0.3780	4.374		0.229	0.8861	0.2060	0.0457	
463	57			12.66	1710		0	35				14,600		5275	425	14994	1.488	0.0435	0.6229	34.659		0.238	0.5908	0.0202	0.0818	
464	58				1705		2							5974	528	13227	1.693	0.0754	0.5572	22.719		0.237	0.6659	0.0324	0.0724	
465	59			12.64	1710		4							6470	587	13514	1.851	0.0958	0.5749	19.538		0.235	0.7175	0.0396	0.0737	
466	60			12.54			6							6974	702	12502	2.006	0.1319	0.5389	15.356		0.235	0.7791	0.0537	0.0691	
467	61			12.64	1720		8							7568	868	11971	2.163	0.1803	0.5162	12.103		0.234	0.8265	0.0712	0.0651	
468	62			12.31			10					14,500		7689	1161	9494	2.270	0.2778	0.4328	8.224		0.233	0.8601	0.1074	0.0541	
469	63			12.27	1690		12					14,450		6809	1624	6153	2.037	0.4246	0.3024	4.844		0.233	0.7739	0.1630	0.0378	
470	64			12.64	1700		0	40				14,500		4742	277	15077	1.354	0.0023	0.6342	600.253		0.237	0.5336	0.0035	0.0827	
471	1	20	20	1.37		59	0							218	79	-440	0.554	0.1299	-.1198	4.417	30.26					
472	2			1.39			2							305	85	-448	0.738	0.1352	-.1120	5.606						
473	3			1.42			4							363	87	-450	0.882	0.1421	-.1110	6.344						
474	4						6							449	87	-800	1.124	0.1497	-.2347	7.644						
475	5						8							500	97	-659	1.262	0.1787	-.1852	7.174						
476	6						10							528	116	-788	1.334	0.2294	-.2288	5.901						
477	7						12							477	147	-981	1.244	0.3234	-.3057	3.907						
478	8		40	5.56		60	0							986	313	-1273	0.641	0.1317	-.0784	5.016						
479	9			5.62			2							1272	322	-1458	0.809	0.1338	-.0898	6.195						
480	10			5.64										1544	333	-1758	0.978	0.1412	-.1134	7.067						
481	11			5.66										1833	348	-1865	1.155	0.1511	-.1197	7.777						

TABLE A-2 AMES TEST RESULTS (Continued)

Point No. - Consecutive	Point No. - Per Run	Run No.	Tunnel Speed (V_p) - Knots	Tunnel Dynamic Pressure (q) - Lbs/sq.ft.	Fan Speed (N_F) - RPM	Tunnel Temp. °F	Angle of Attack (α) - degrees	Exit Louver Angle (β) - degrees	Horizontal Tail Incidence Angle (i_t) - degrees	Reaction Control Setting (RC) - CPS	Wing Flap Angle (δ_F) - degrees	Engine Speed (N_{J85}) - RPM	Exhaust Gas Temp. (EGT) - °F	Total Lift (L_T) - Lbs.	Total Drag (D_T) - Lbs.	Total Pitch Moment (M_T) - Ft. Lbs.	Lift Coefficient (C_L)	Drag Coefficient (C_D)	Pitch Moment Coefficient (C_M)	Lift To Drag Ratio (L_T/D_T)	Barometer In. Hg.	Velocity Ratio (V_p/V_{tip})	Lift Coefficient (H_L)	Drag Coefficient (H_D)	Pitch Moment Coefficient (H_M)	Yaw Angle (ψ) - Degrees
482	12	20	40	5.66		61								2099	374	-2589	1.326	0.1697	-.1812	7.927	30.26					
483	13													2251	437	-2448	1.432	0.2139	-.1685	6.788						
484	14			5.58										2188	522	-3179	1.422	0.2780	-.2370	5.187						
485	15			5.48										2076	615	-3675	1.364	0.3460	-.2837	4.000						
486	16		60	12.65										2276	727	-2121	0.646	0.1349	-.0467	4.941						
487	17			12.79		62								2872	739	-2030	0.806	0.1367	-.0713	6.048						
488	18			12.83										3555	742	-3537	0.998	0.1385	-.0966	7.352						
489	19			12.77										4024	787	-4209	1.132	0.1533	-.1210	7.514						
490	20			12.69		63								4593	828	-4810	1.298	0.1676	-.1431	7.864						
491	21			12.61										5093	938	-5378	1.457	0.2041	-.1658	7.239						
492	22			12.51										4776	1192	-6718	1.391	0.2861	-.2220	4.931						
493	23			12.65		64								4880	1424	-7677	1.421	0.3564	-.2586	4.042						

APPENDIX B

APPENDIX B

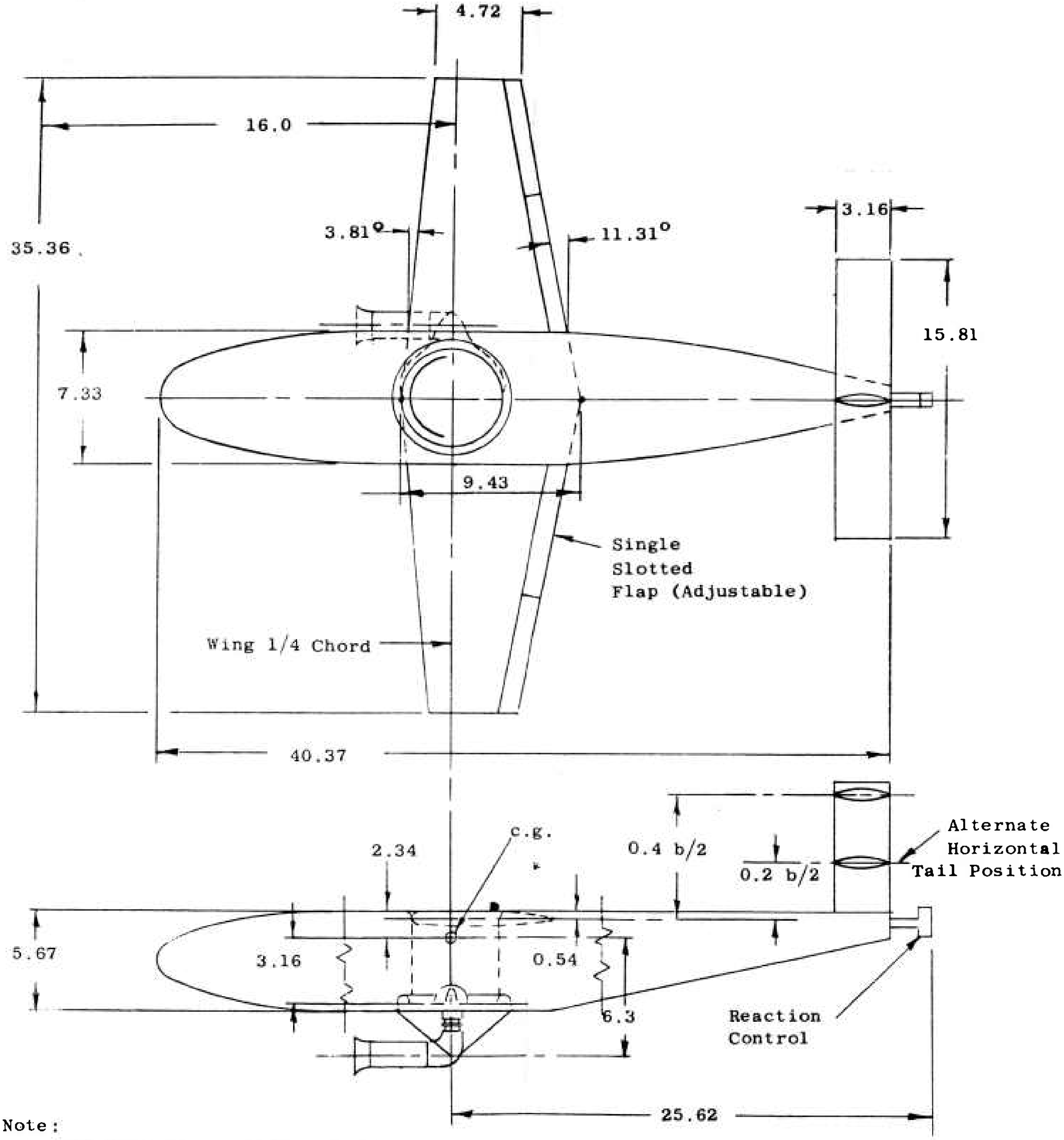

Note:
All Dimensions In Feet Unless Otherwise Specified.

FIGURE 1. SKETCH OF NASA FULL-SCALE AIRCRAFT MODEL

ernate
izontal
osition

GEOMETRIC DATA

WING

Area	250 Sq. Ft.
Aspect Ratio	5
Taper Ratio	0.5
Mean Aero. Chord	7.33 Ft.
Airfoil Section	NASA 63-210
Wing Loading	28 PSF.

HORIZONTAL TAIL

Area	50 Sq. Ft.
Aspect Ratio	5
Taper Ratio	1.0
Airfoil Section	NASA 63 A 012

VERTICAL TAIL

Area	25 Sq. Ft.
Aspect Ratio	2.5
Taper Ratio	1.0
Airfoil Section	NASA 63 A 015

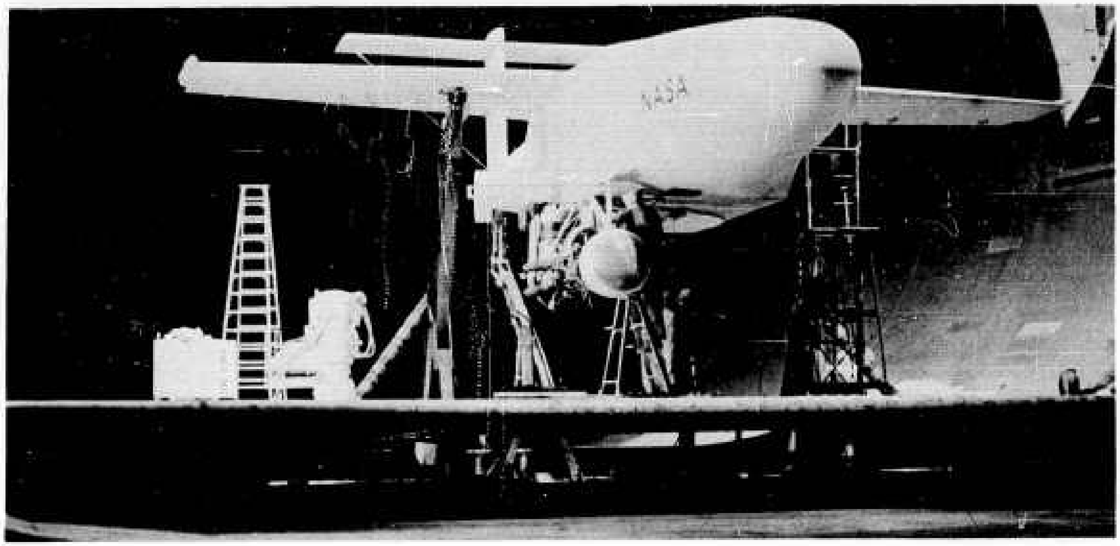

FIGURE 2a WIND TUNNEL INSTALLATION, $h/d_F = 1.41$

FIGURE 2b WIND TUNNEL INSTALLATION, $L/d_F = 0.85$

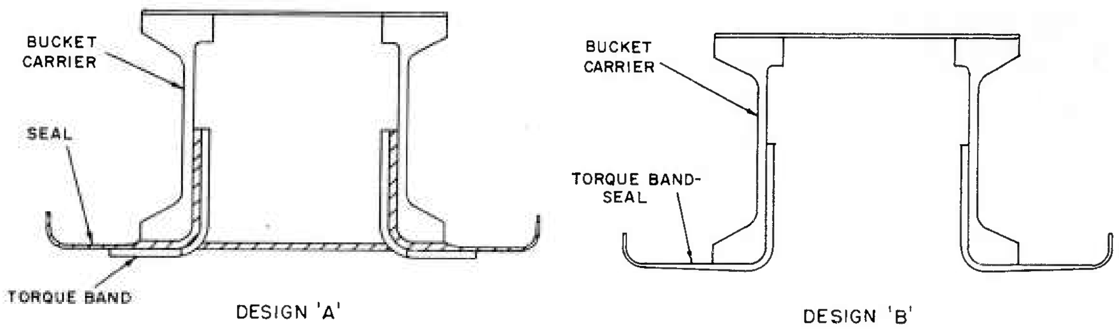

FIGURE 3a TORQUE BAND/SEAL DESIGN CONFIGURATIONS

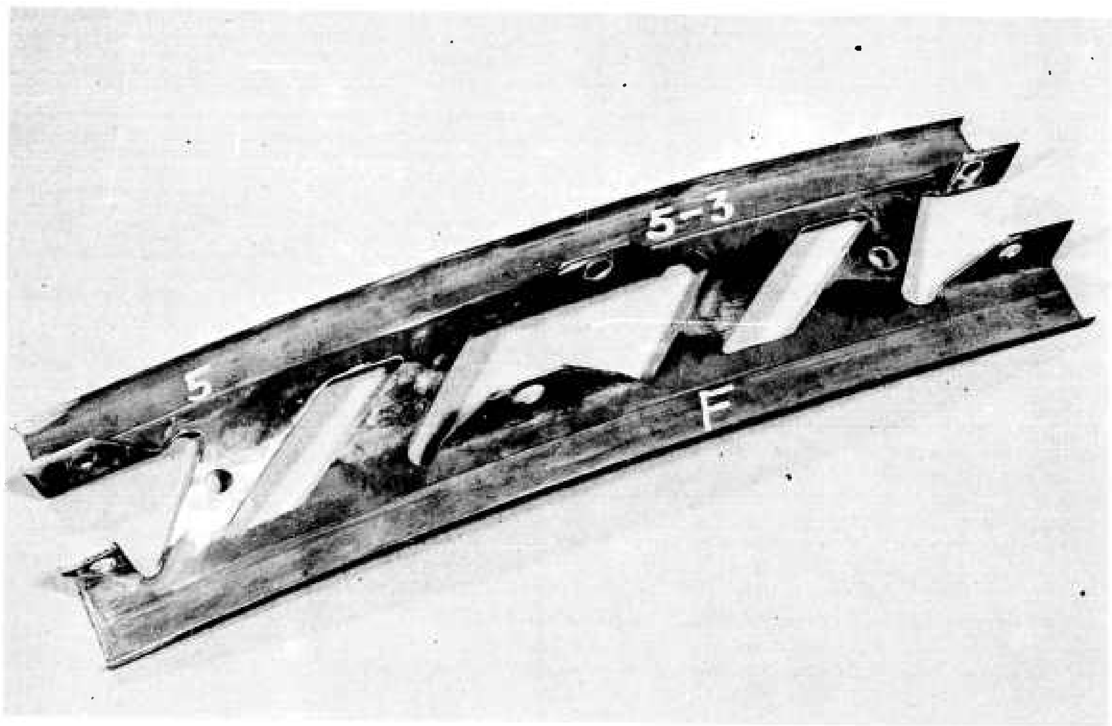

FIGURE 3b ROTATING SEAL SEGMENT (DESIGN 'A')

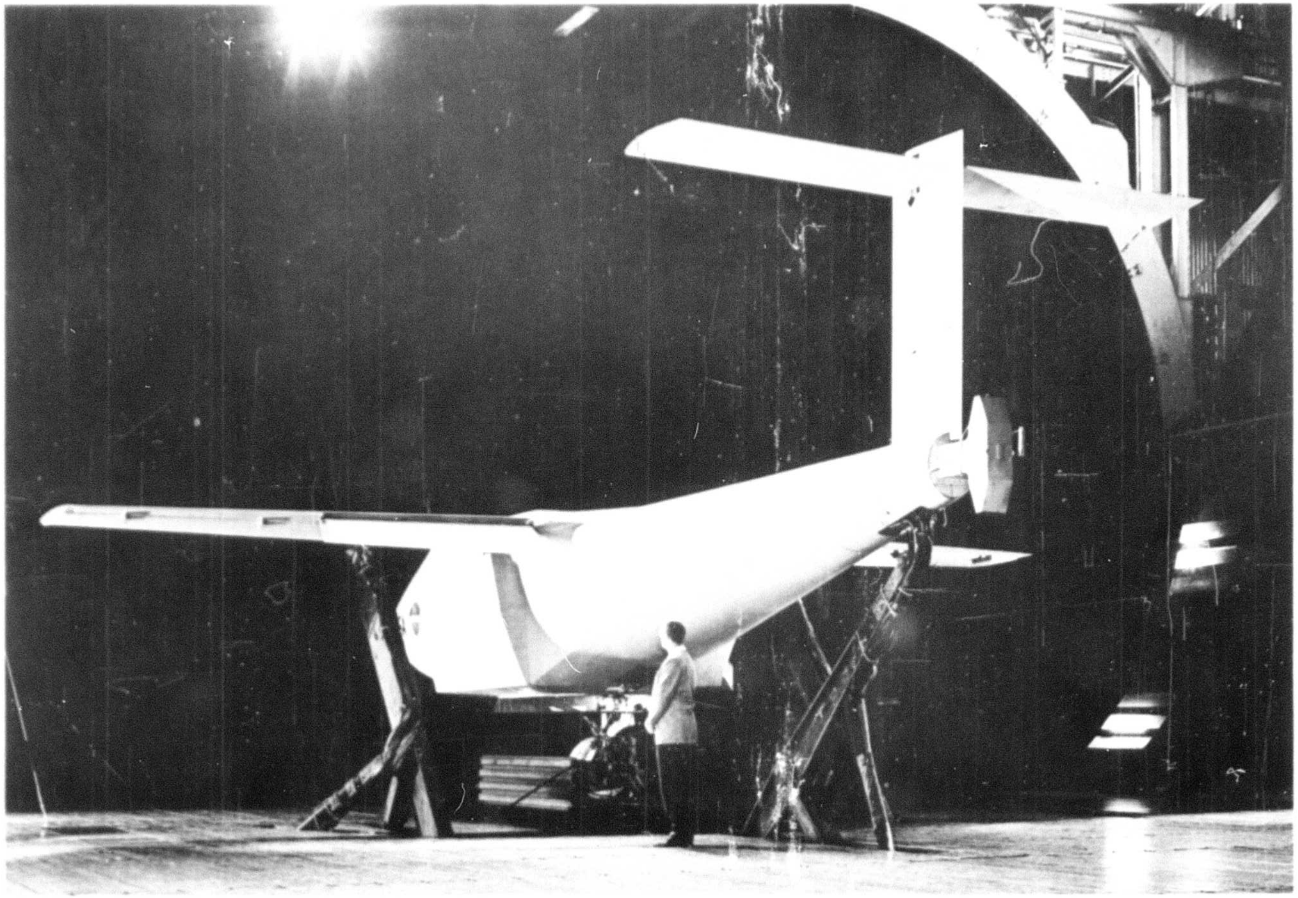

FIGURE 4 WIND TUNNEL INSTALLATION, $h/d_F = 0.85$

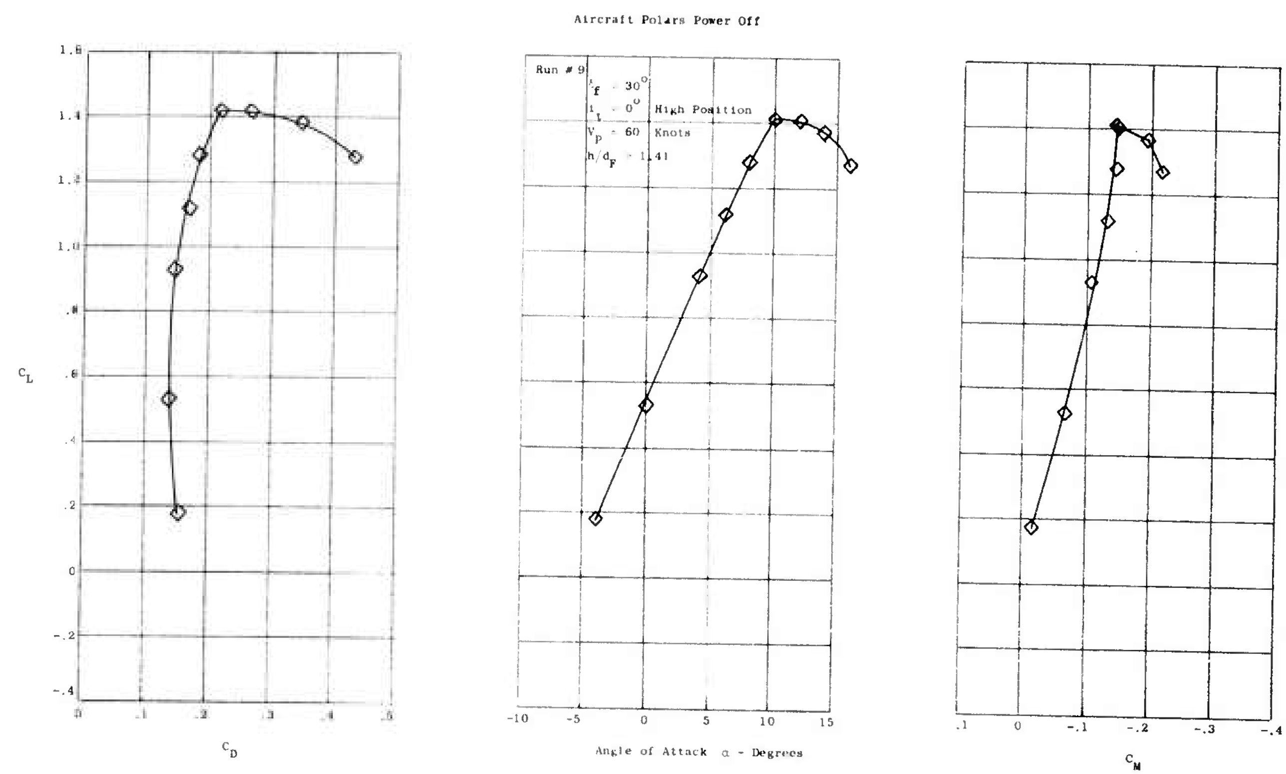

Figure 5. Unpowered A/C Performance (Run 9)

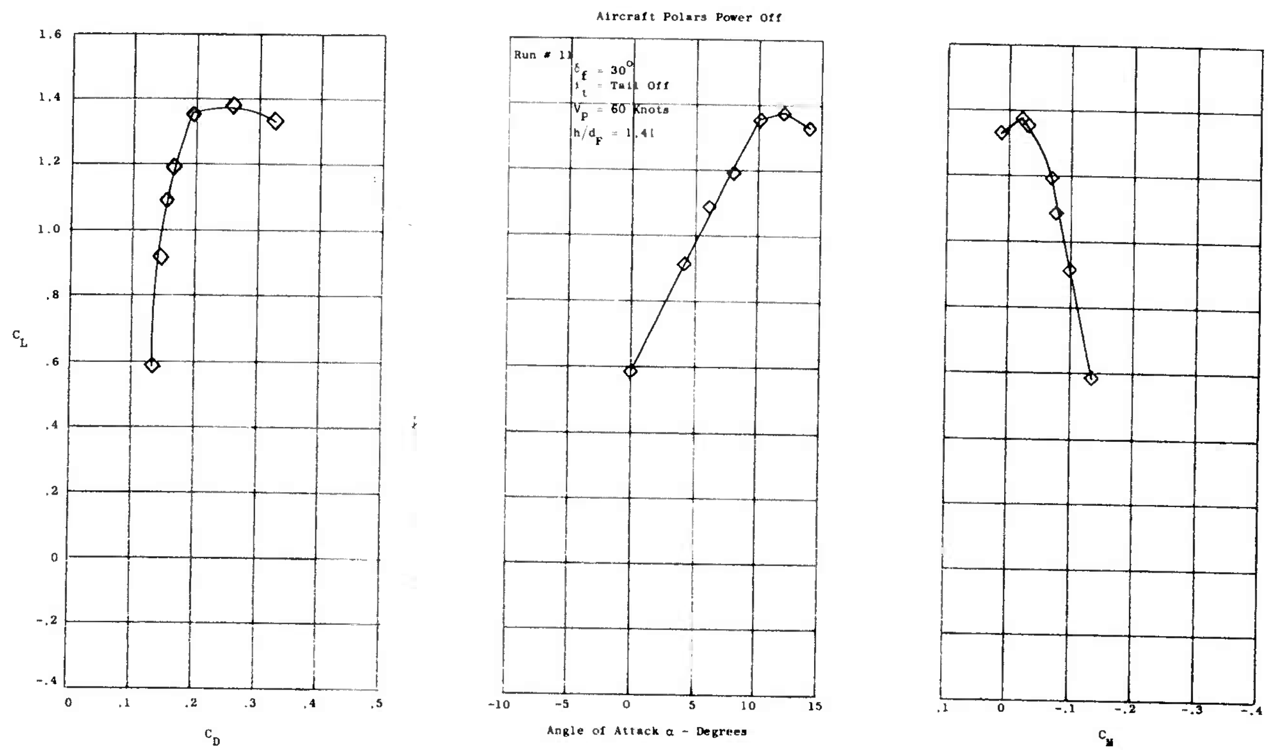

Figure 6. Unpowered A/C Performance (Run 11)

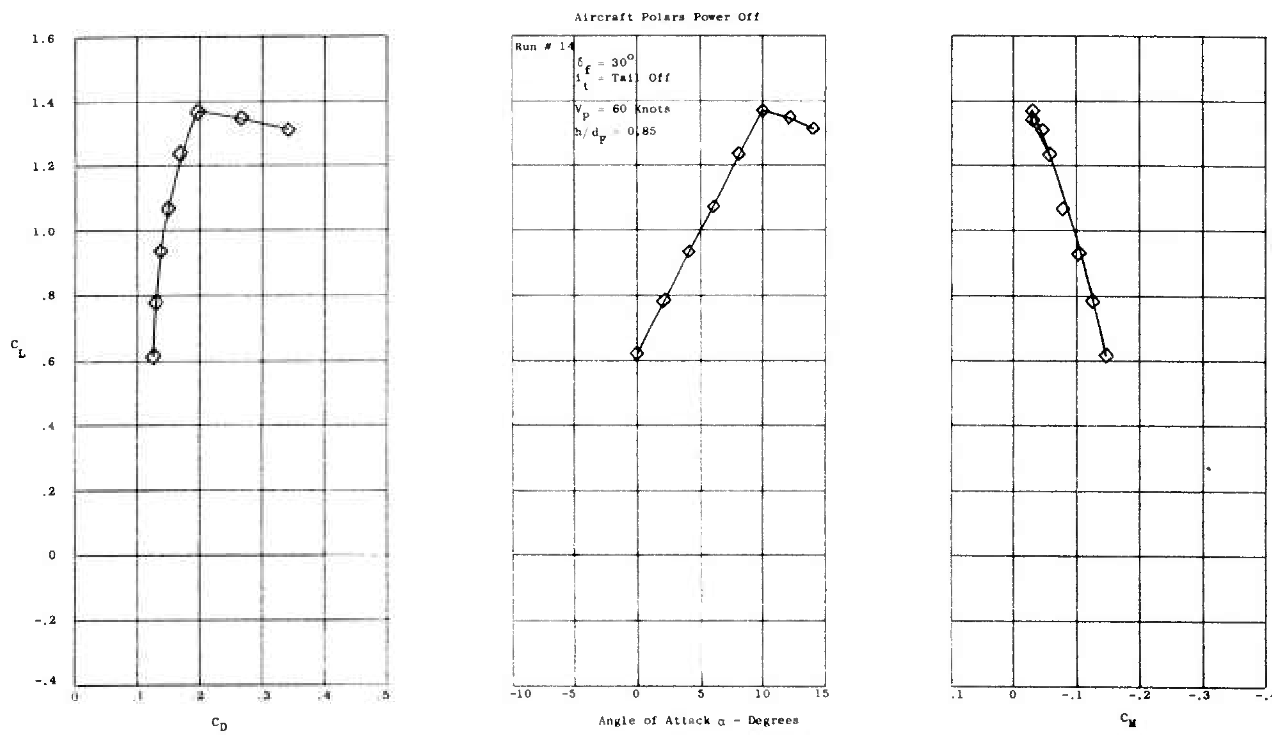

Figure 7. Unpowered A/C Performance (Run 14)

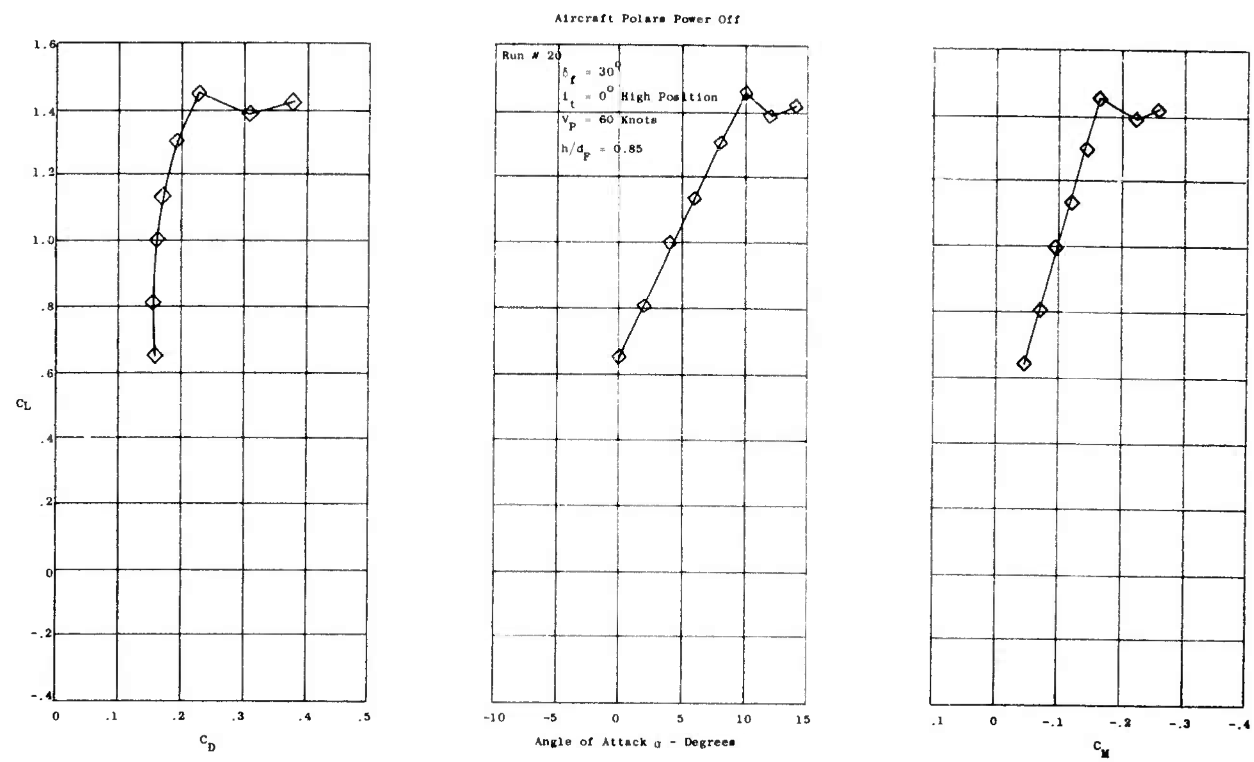

Figure 8. Unpowered A/C Performance (Run 20)

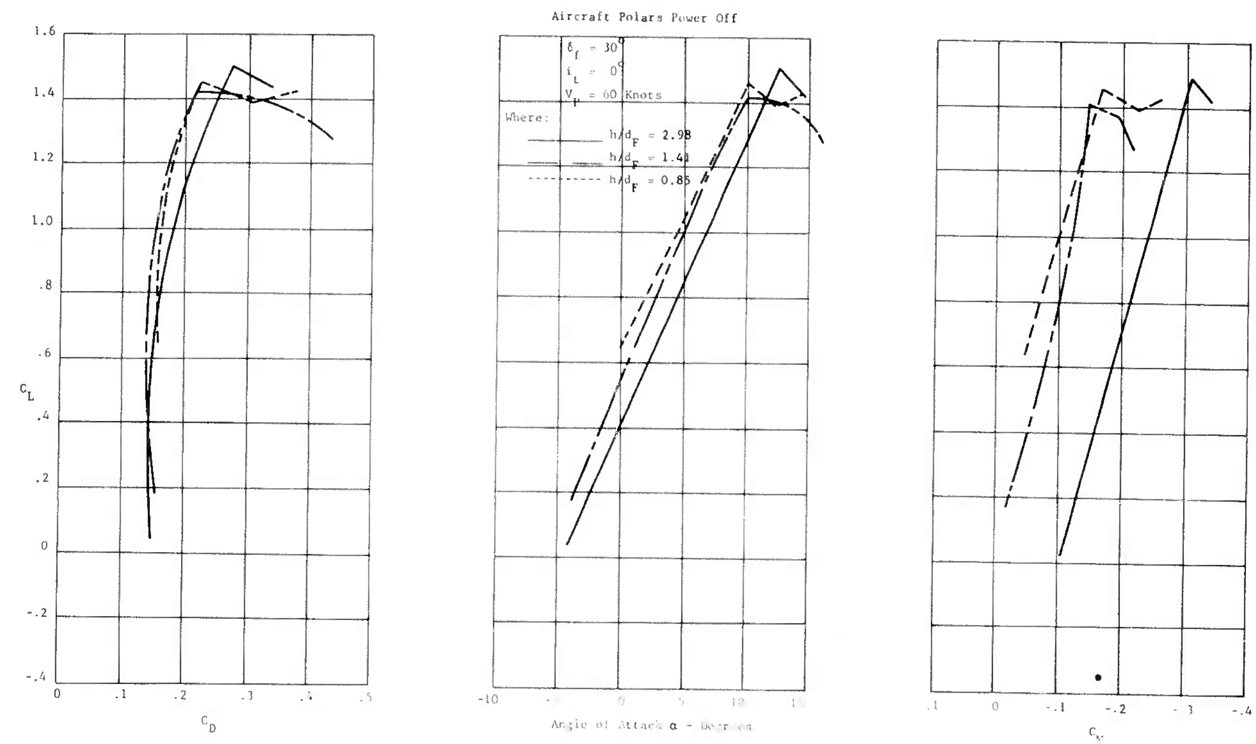

Figure 9. Comparison Of The Unpowered

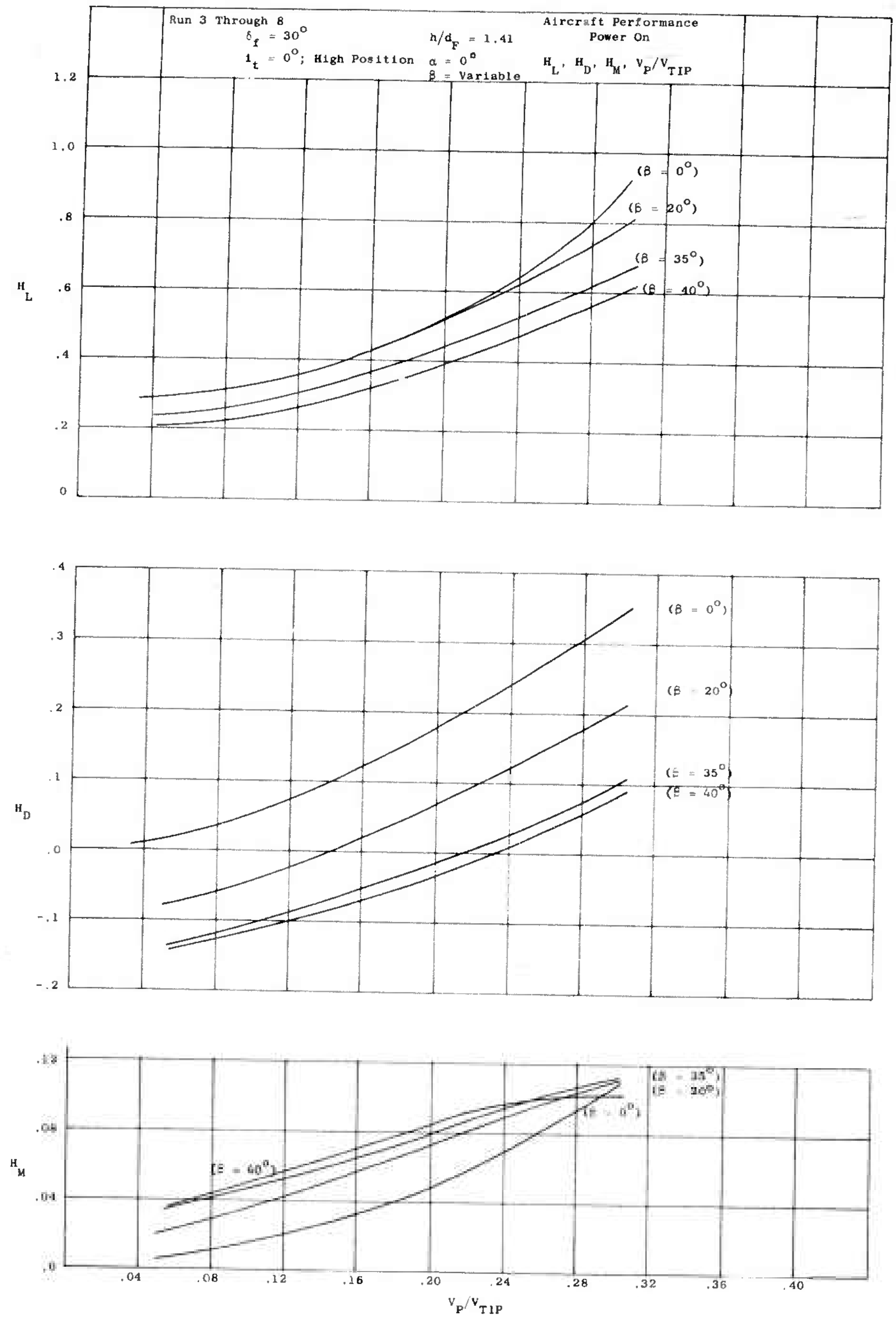

Figure 10. Fan Powered A/C Performance Runs 3 Through 8

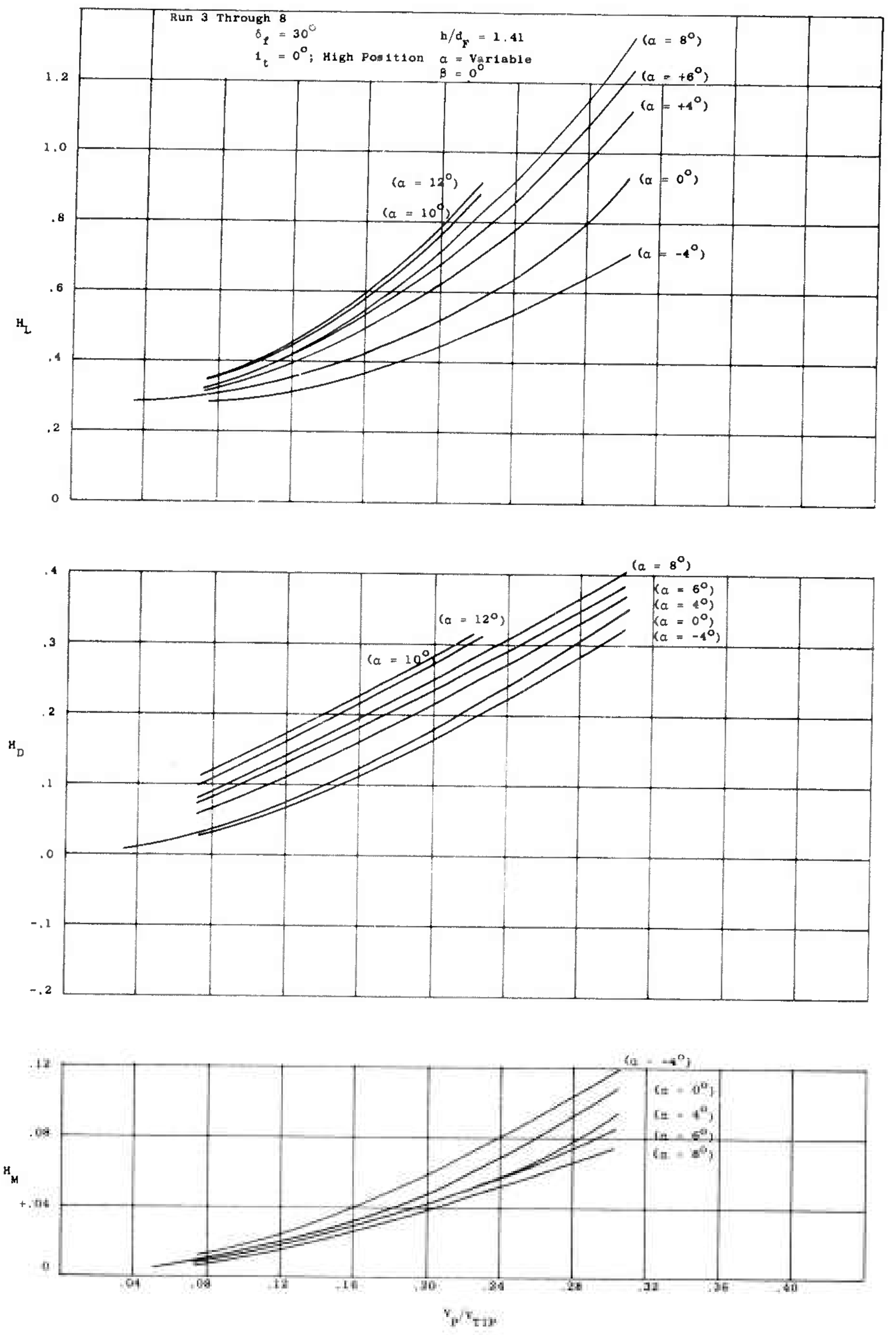

Figure 11. Fan Powered A/C Performance Runs 3 Through 8

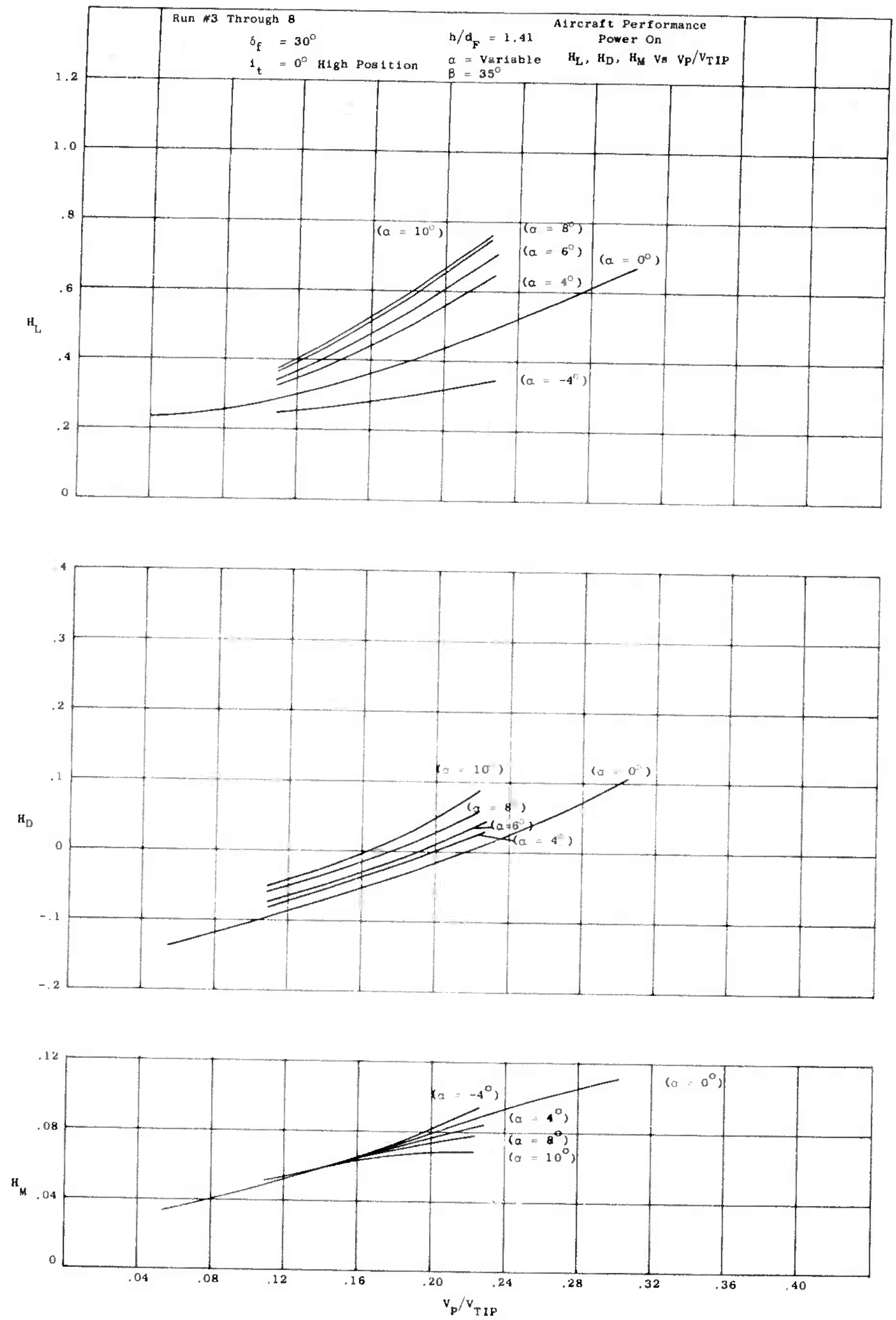

Figure 12. Fan Powered A/C Performance Runs 3 through 8

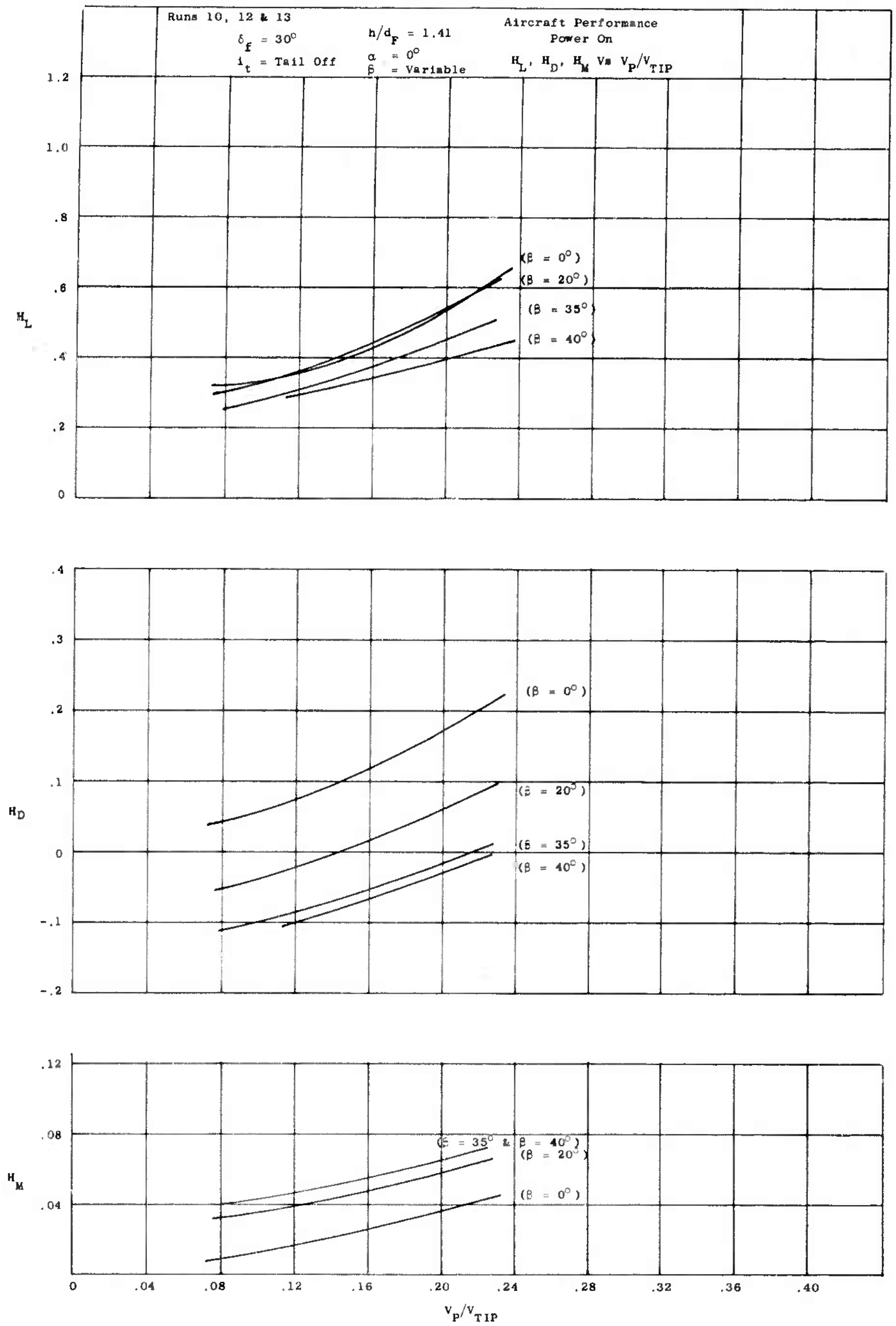

Figure 13. Fan Powered A/C Performance Runs 10, 12 & 13

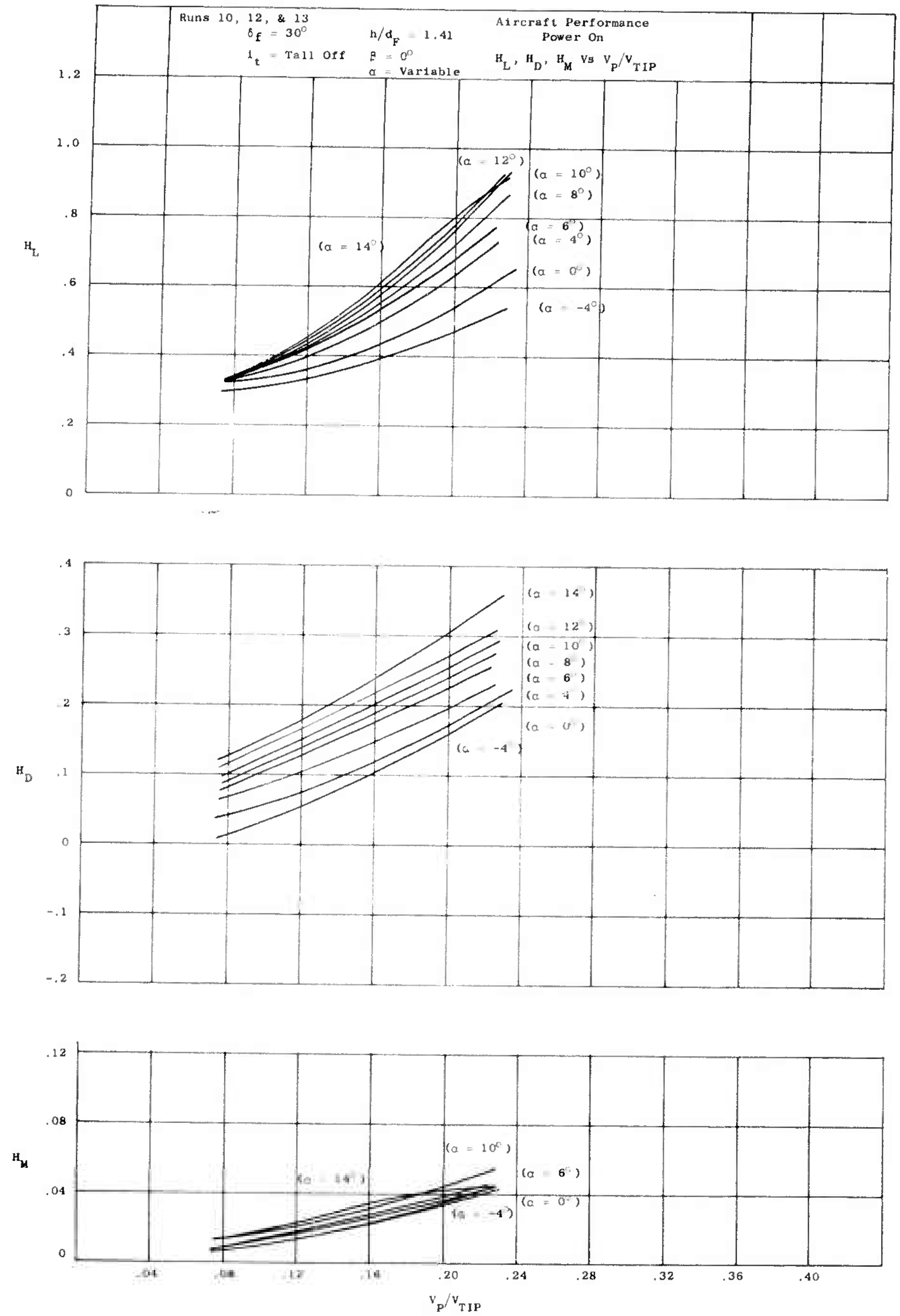

Figure 14. Fan Powered A/C Performance Runs 10, 12 & 13

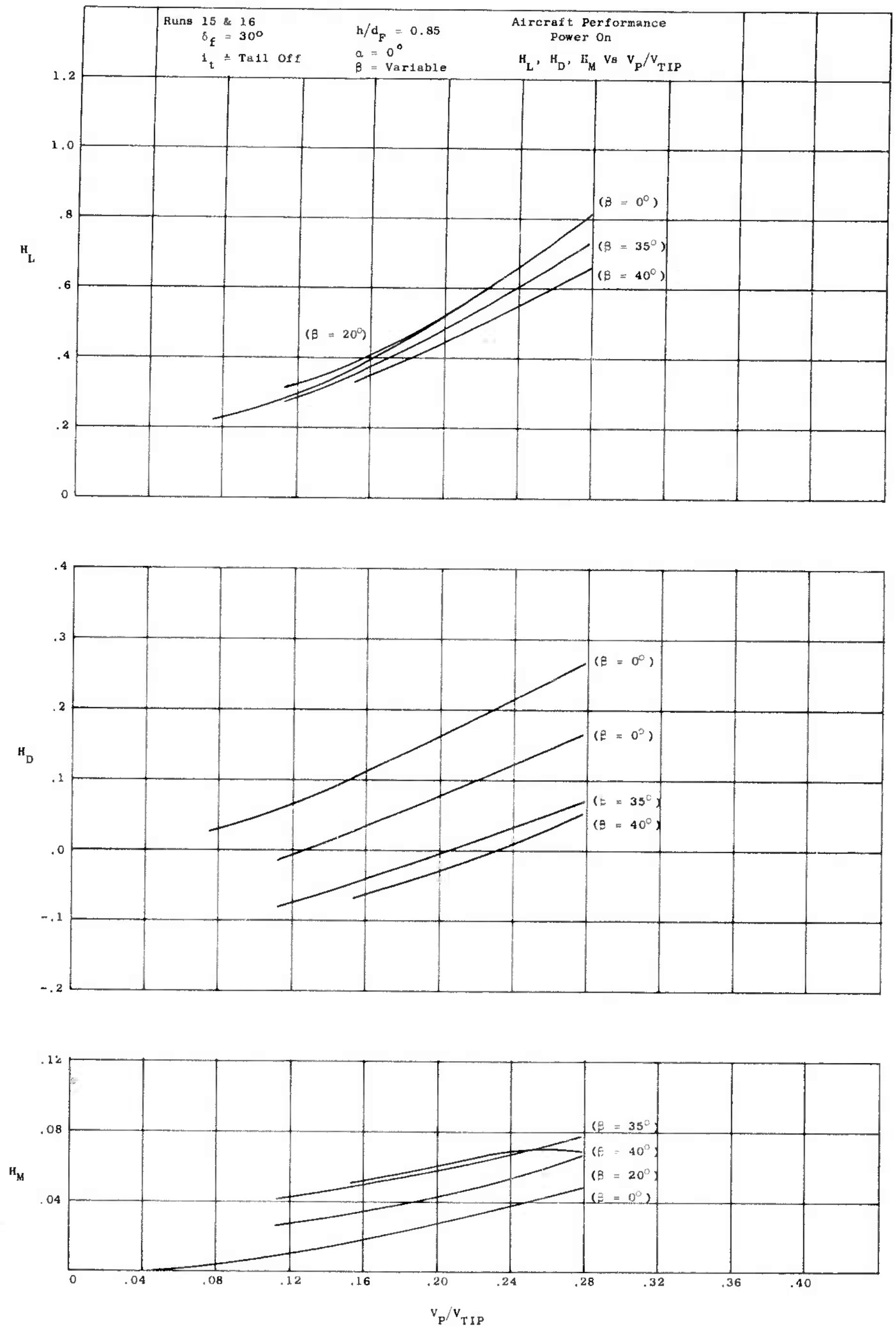

Figure 15. Fan Powered Aircraft Performance Runs 15 & 16

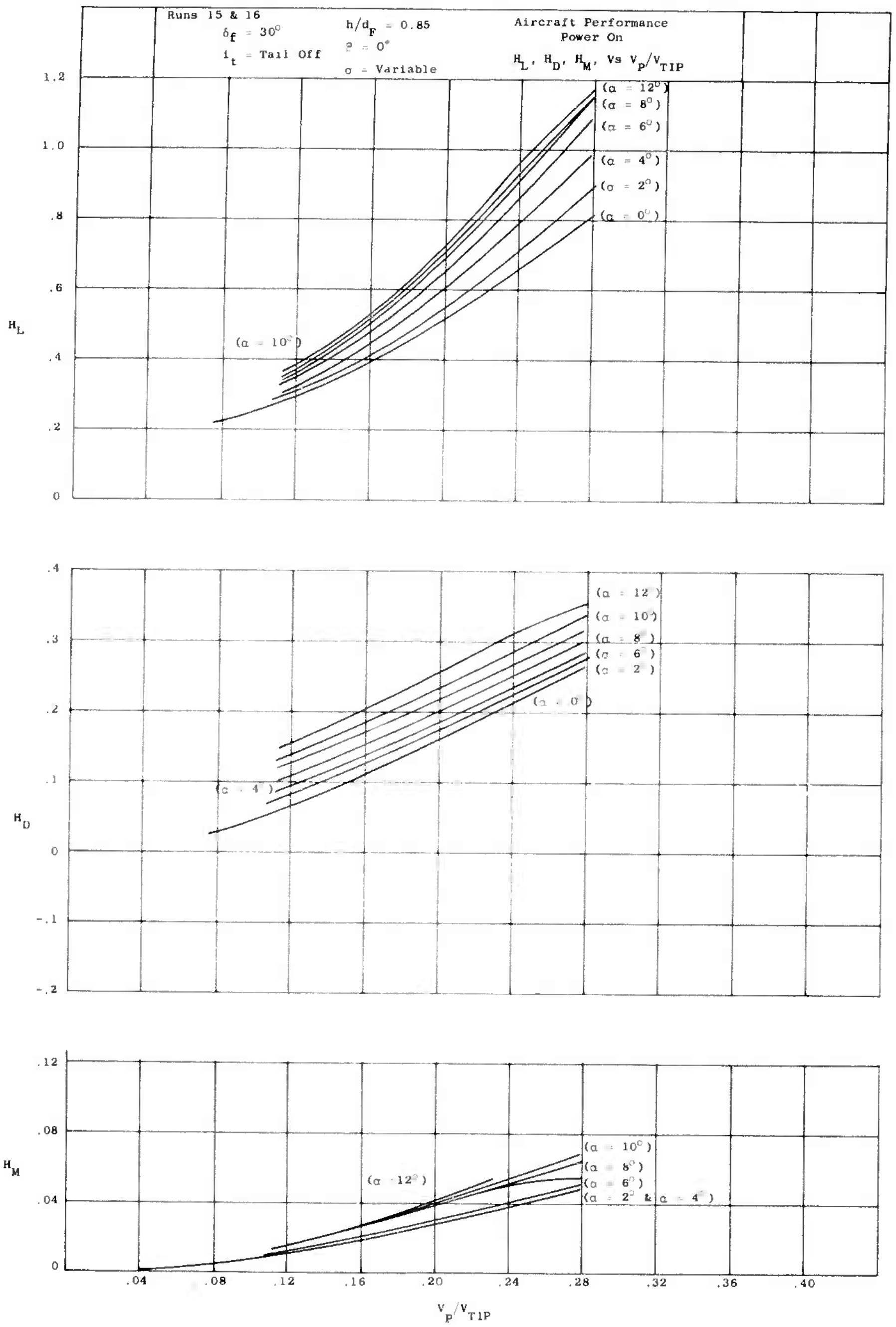

Figure 16. Fan Powered A/C Performance Runs 15 & 16

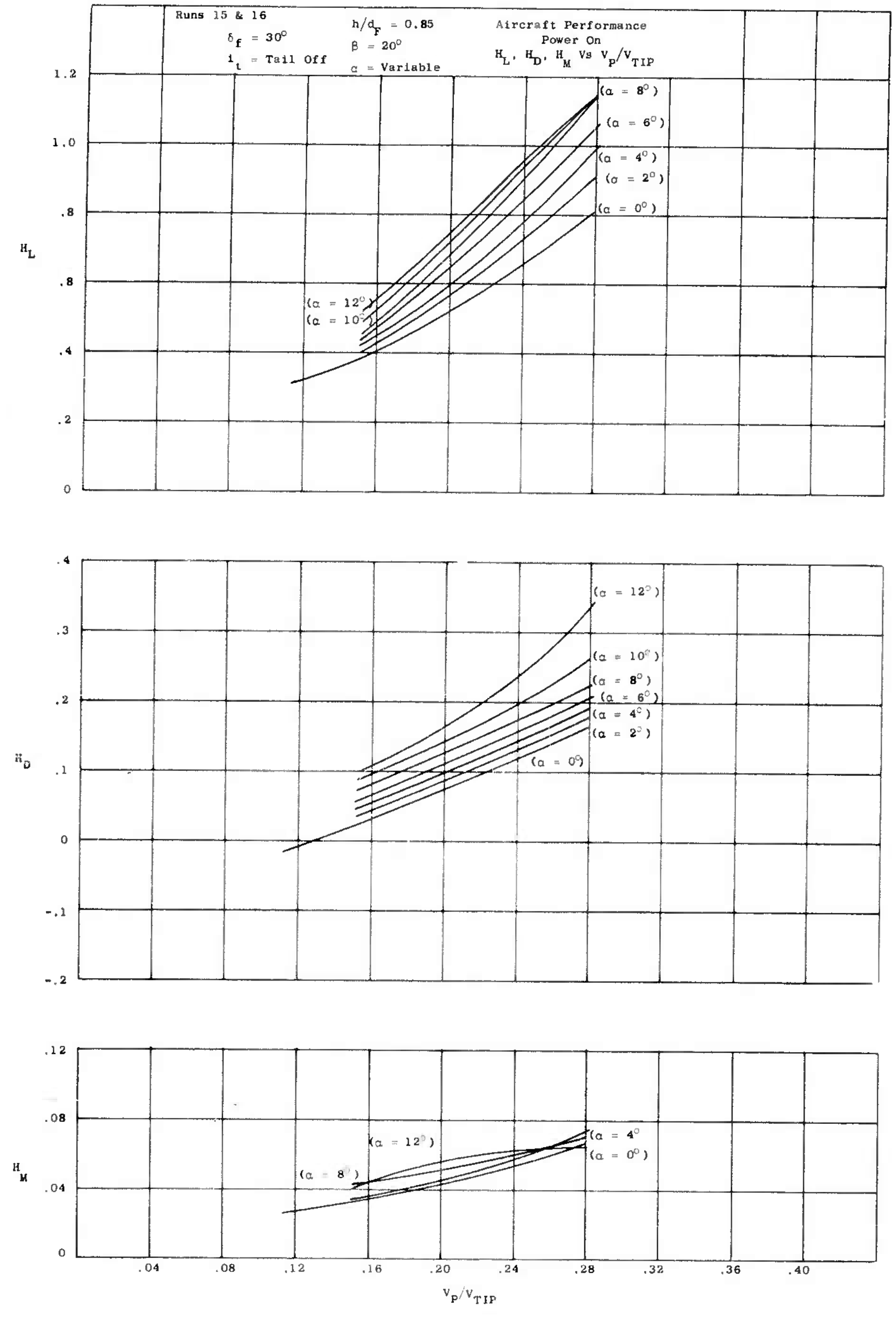

Figure 17. Fan Powered A/C Performance Runs 15 & 16

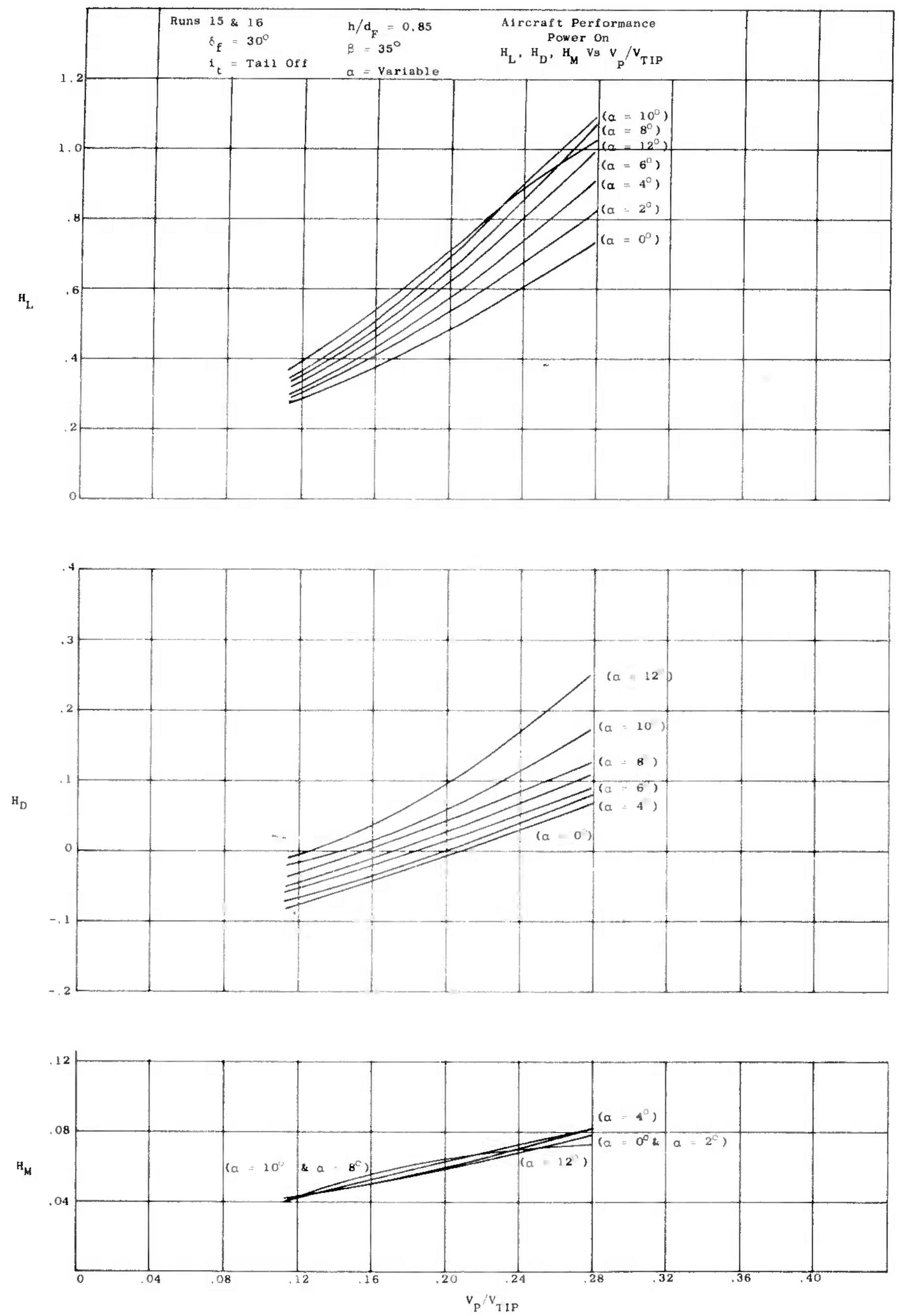

Figure 18. Fan Powered A/C Performance Runs 15 & 16

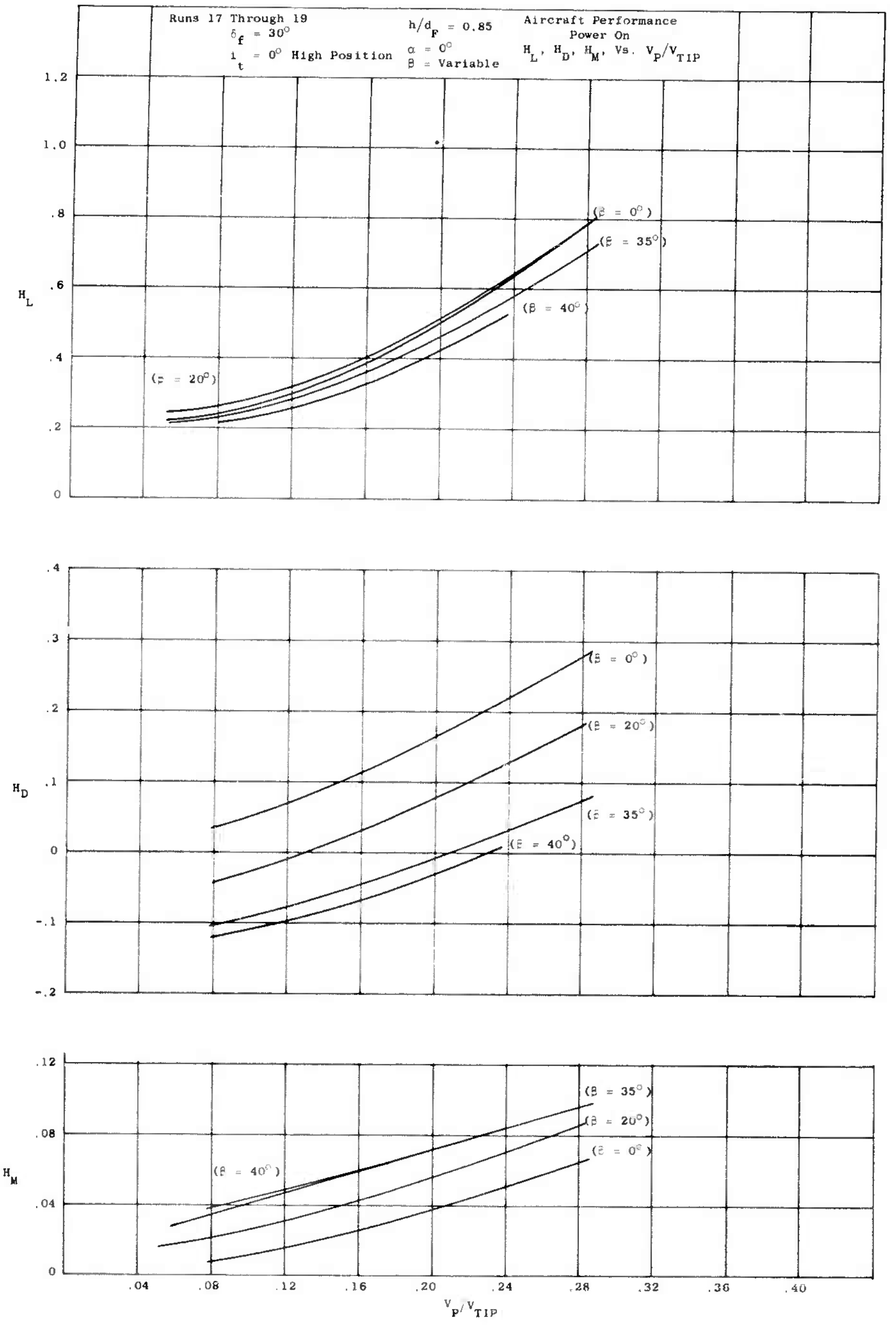

Figure 19. Fan Powered A/C Performance Runs 17 to 19

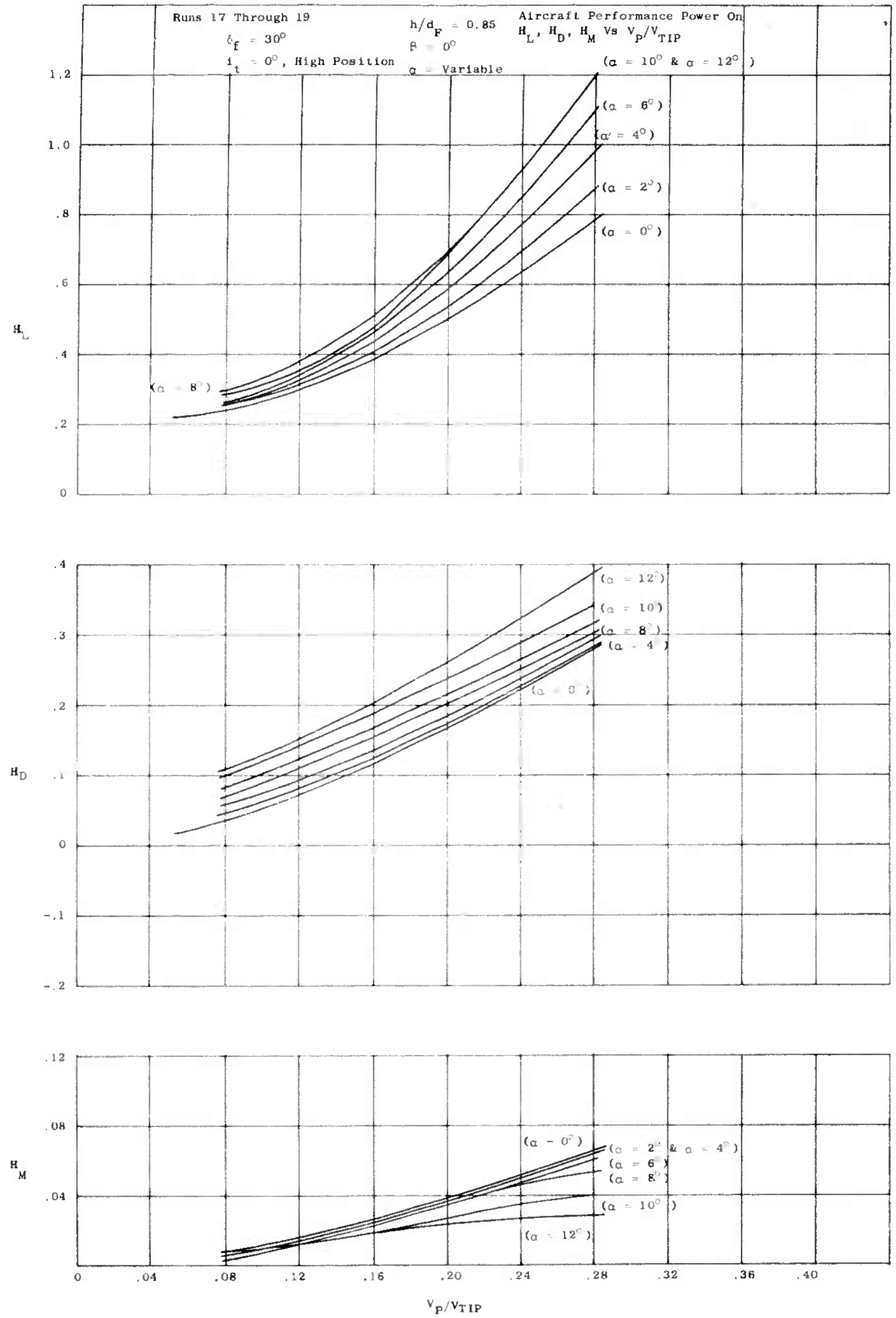

Figure 20. Fan Powered A/C Performance Runs 17 to 19

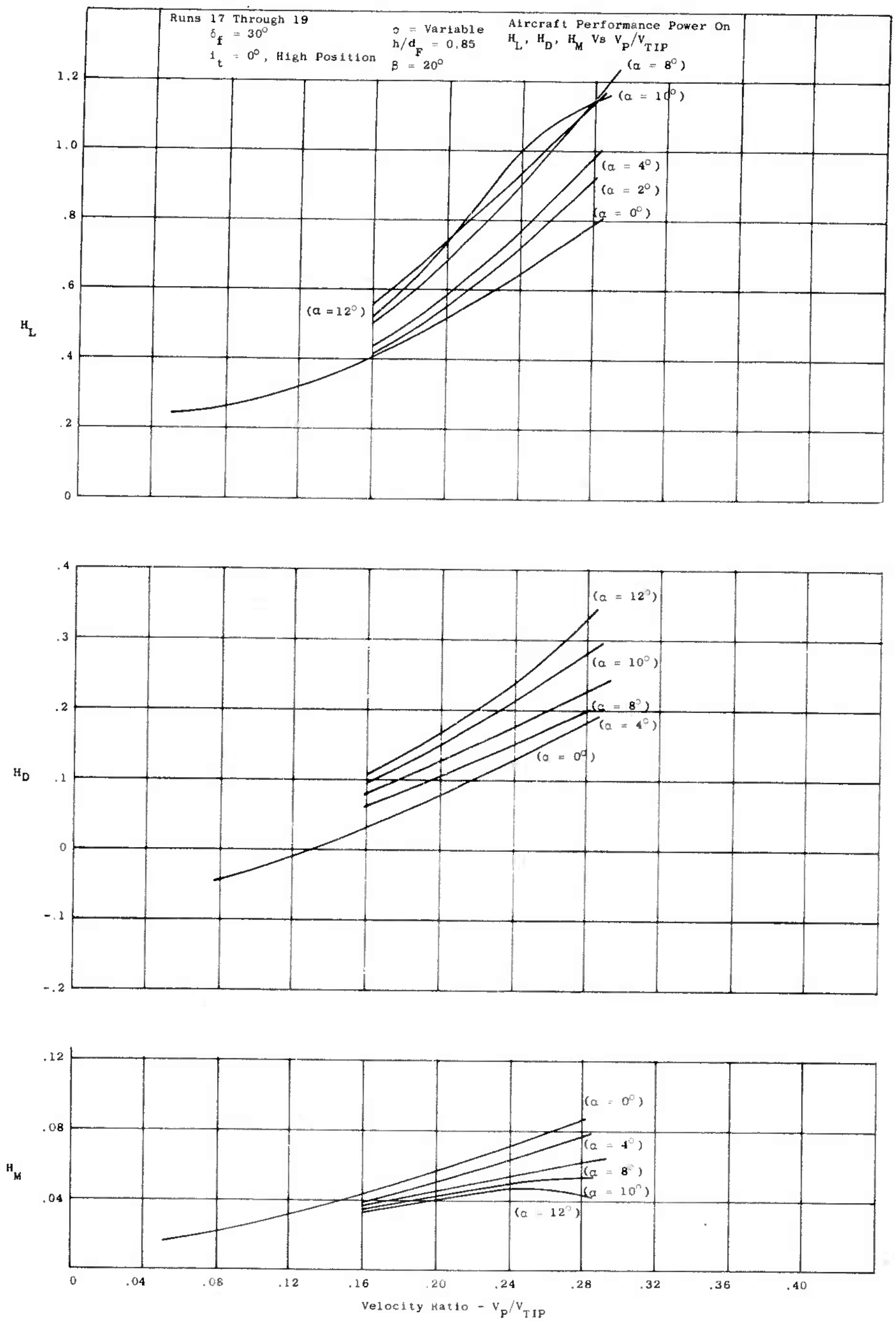

Figure 21. Fan Powered A/C Performance Runs 17 to 19

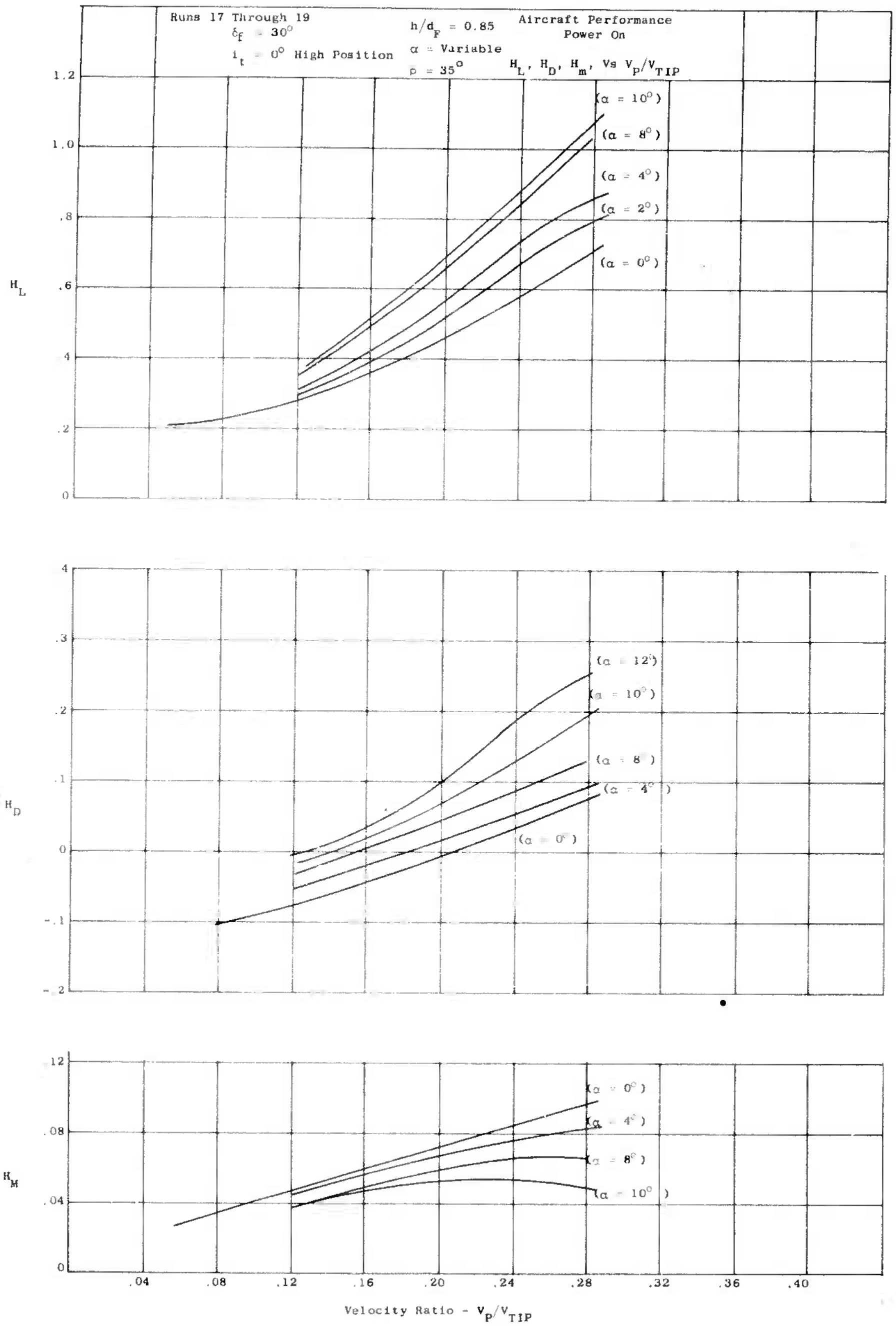

Figure 22. Fan Powered A/C Performance Runs 17 to 19

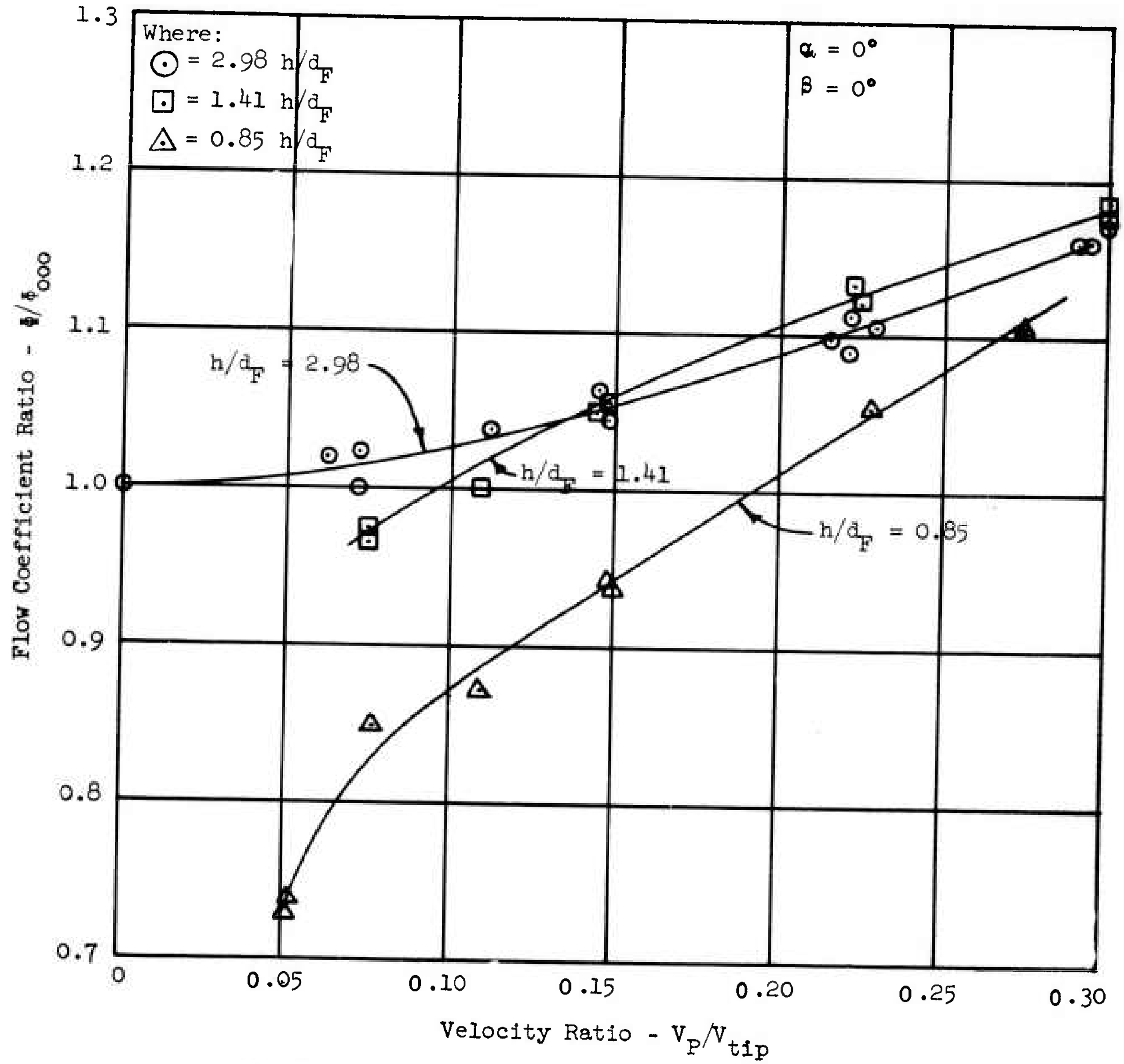

FIGURE 23a - FLOW COEFFICIENT RATIO VERSUS VELOCITY RATIO

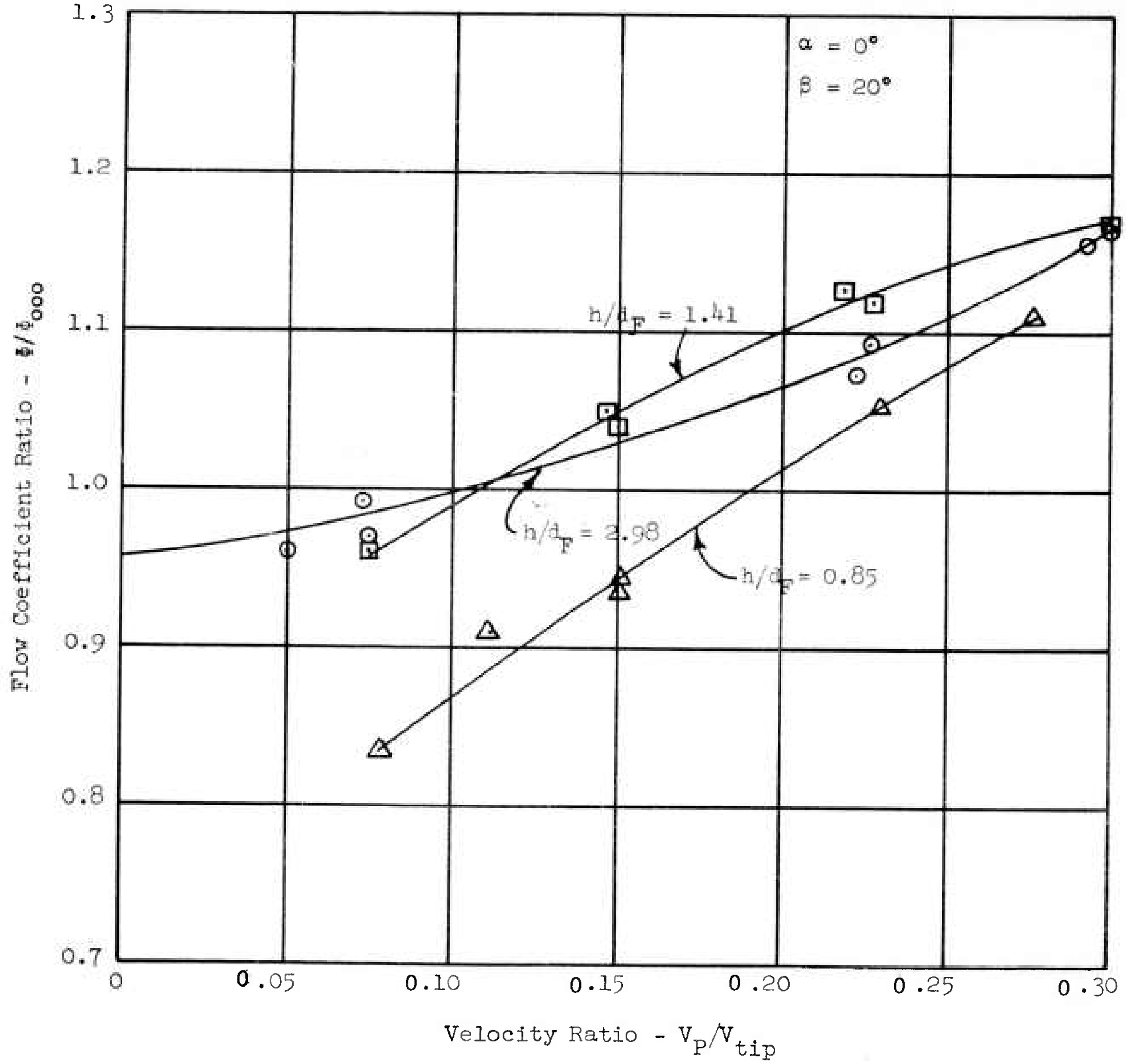

FIGURE 23b - FLOW COEFFICIENT RATIO VERSUS VELOCITY RATIO

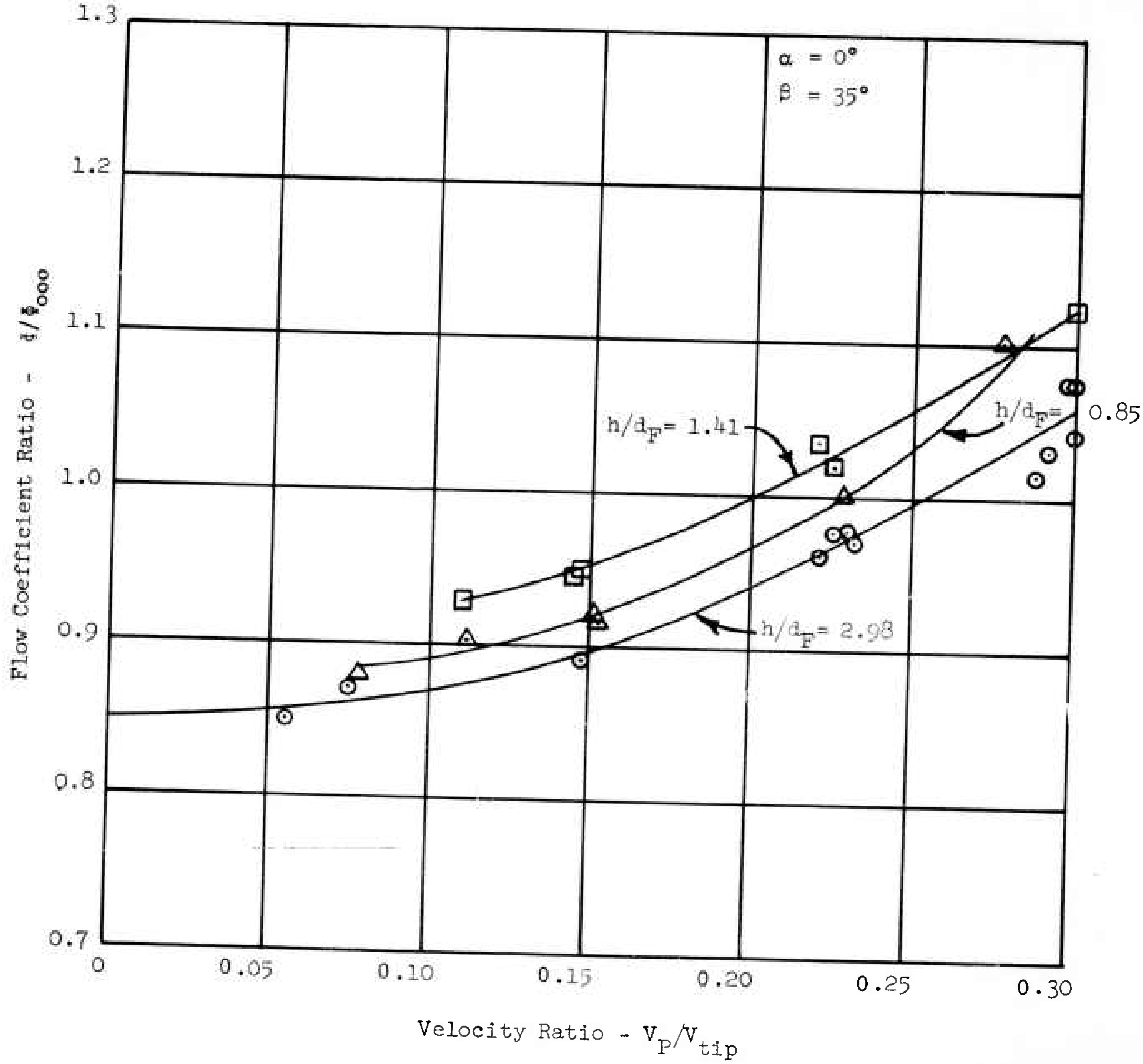

FIGURE 23c - FLOW COEFFICIENT RATIO VERSUS VELOCITY RATIO

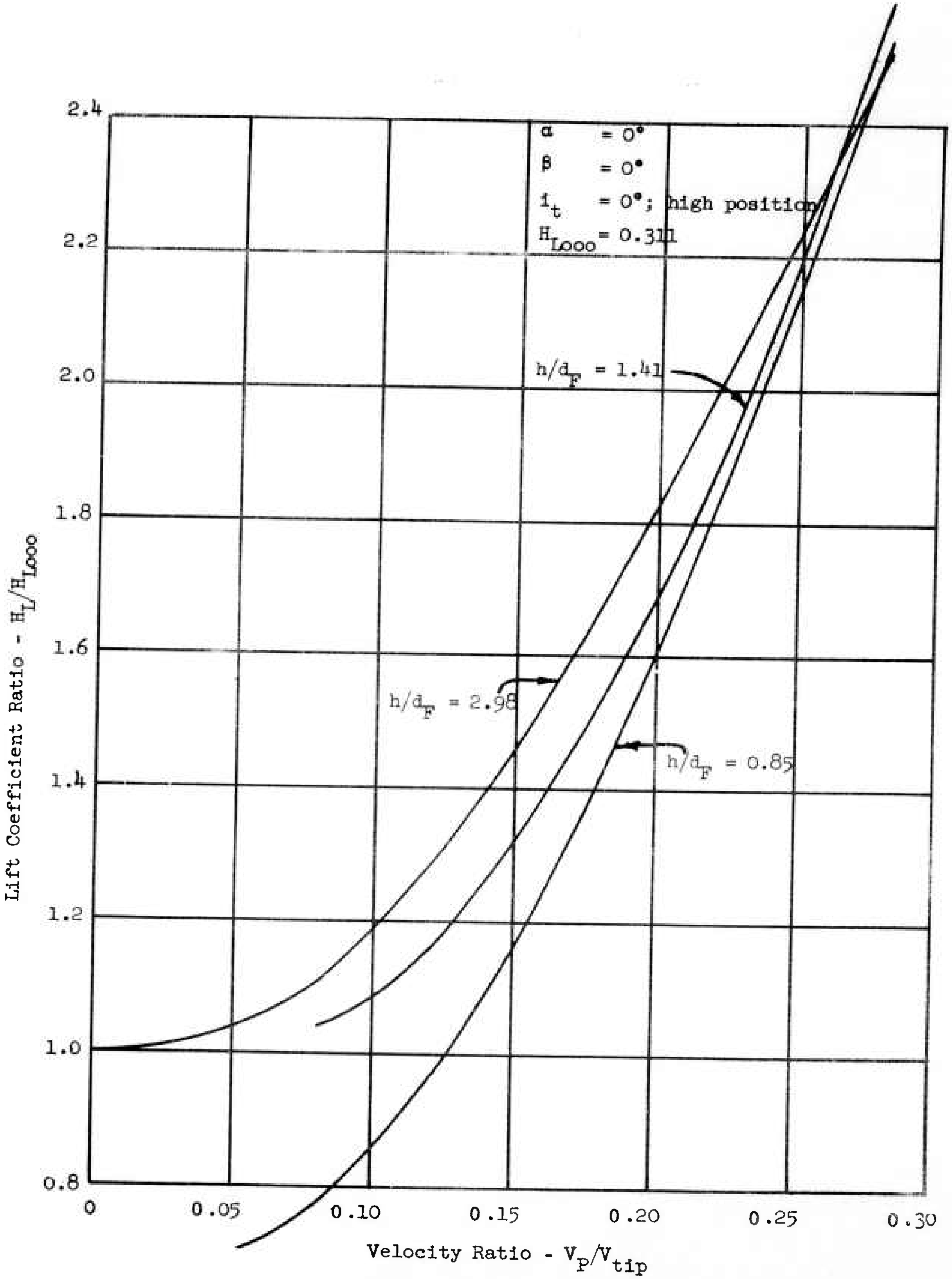

FIGURE 24a - LIFT COEFFICIENT RATIO VERSUS VELOCITY RATIO

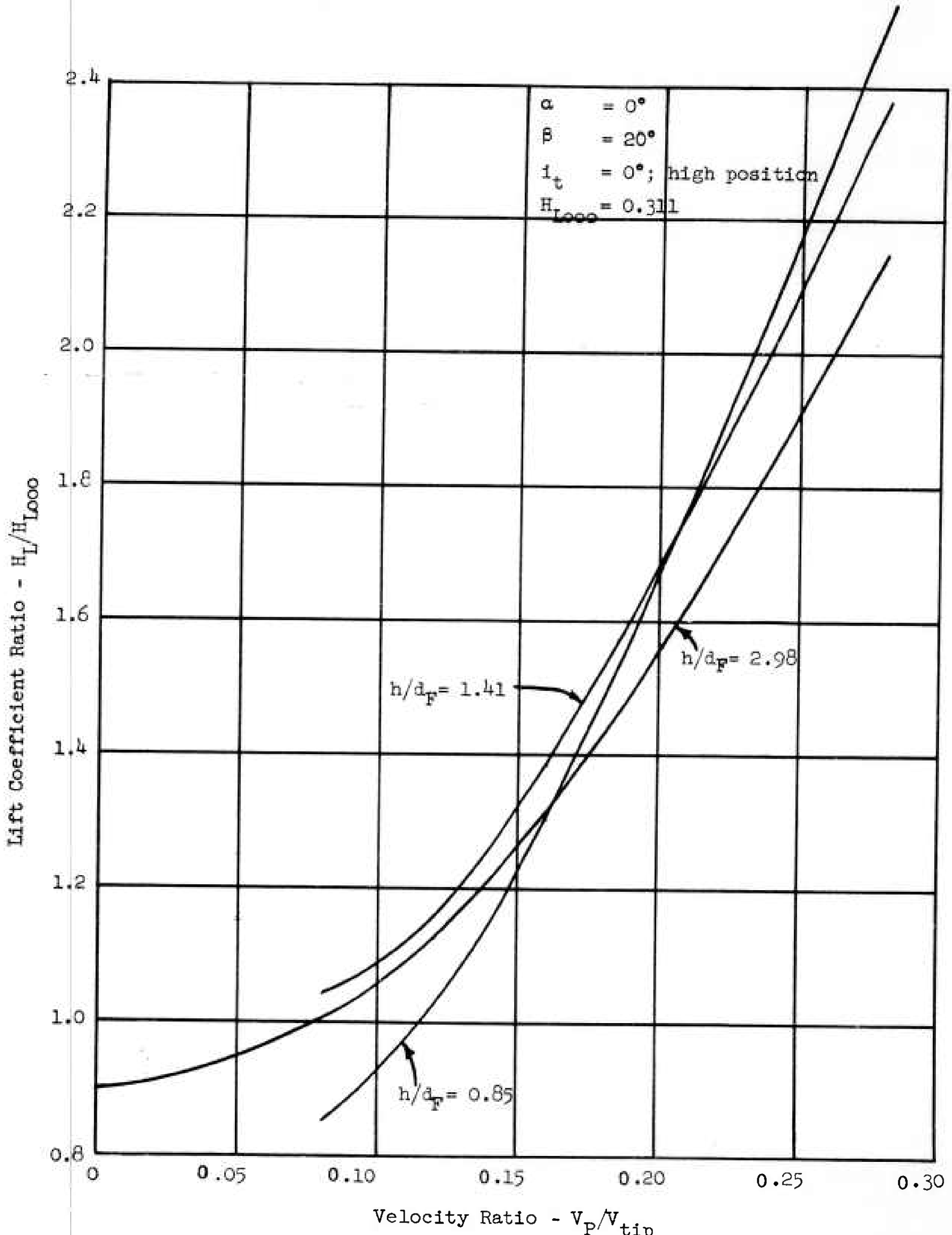

FIGURE 24b - LIFT COEFFICIENT RATIO VERSUS VELOCITY RATIO

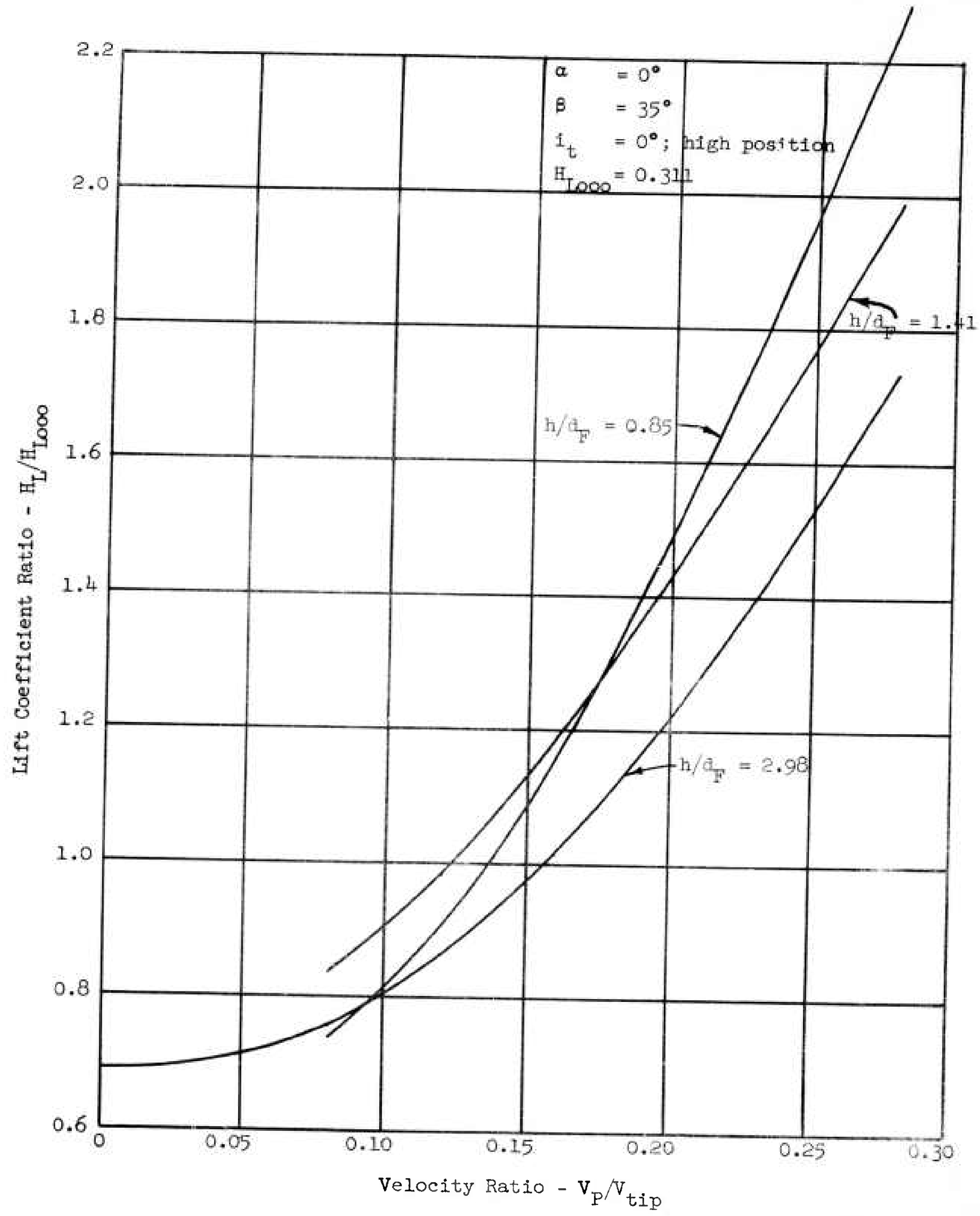

FIGURE 24c - LIFT COEFFICIENT RATIO VERSUS VELOCITY RATIO

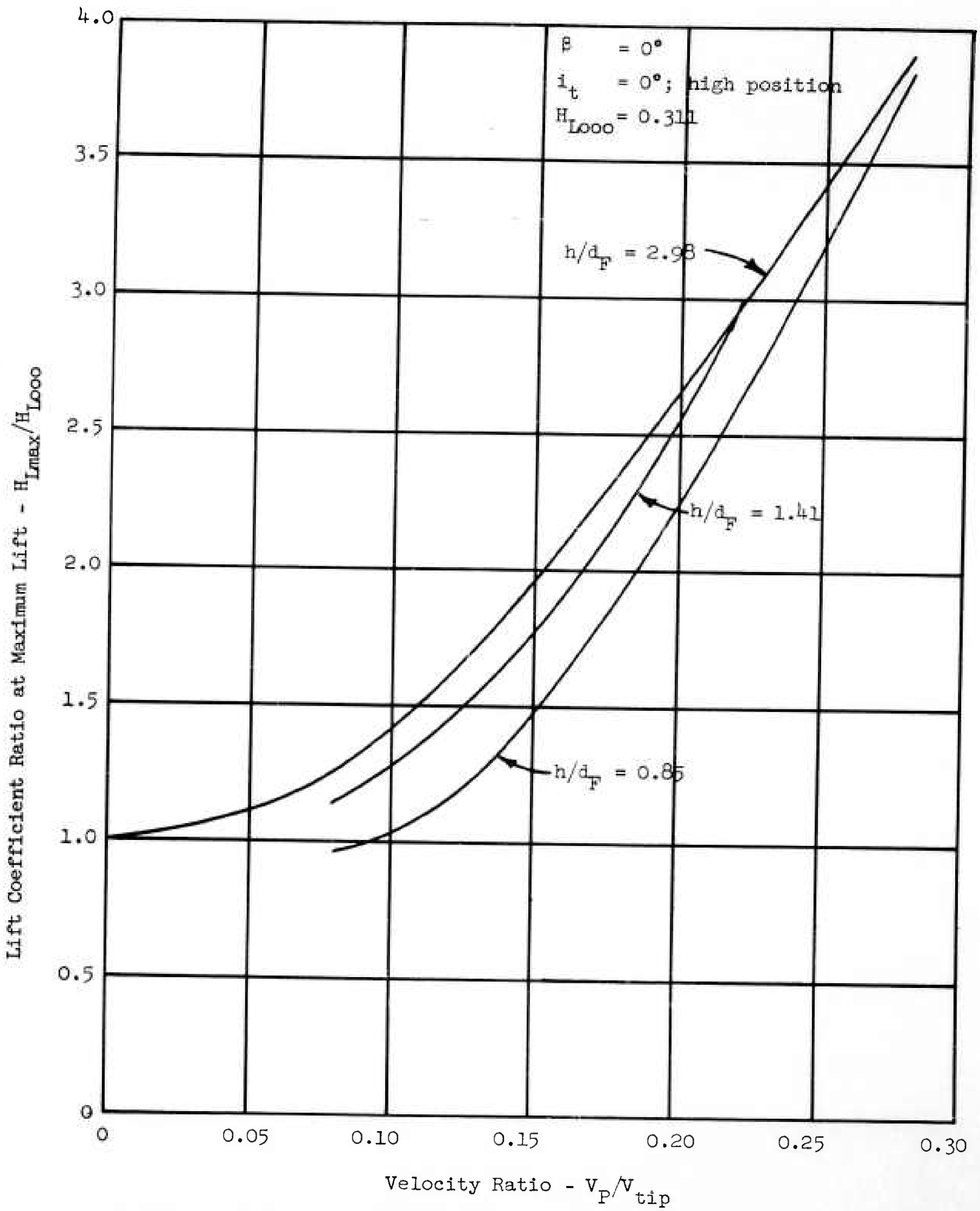

FIGURE 25a - LIFT COEFFICIENT RATIO AT MAXIMUM LIFT VERSUS VELOCITY RATIO

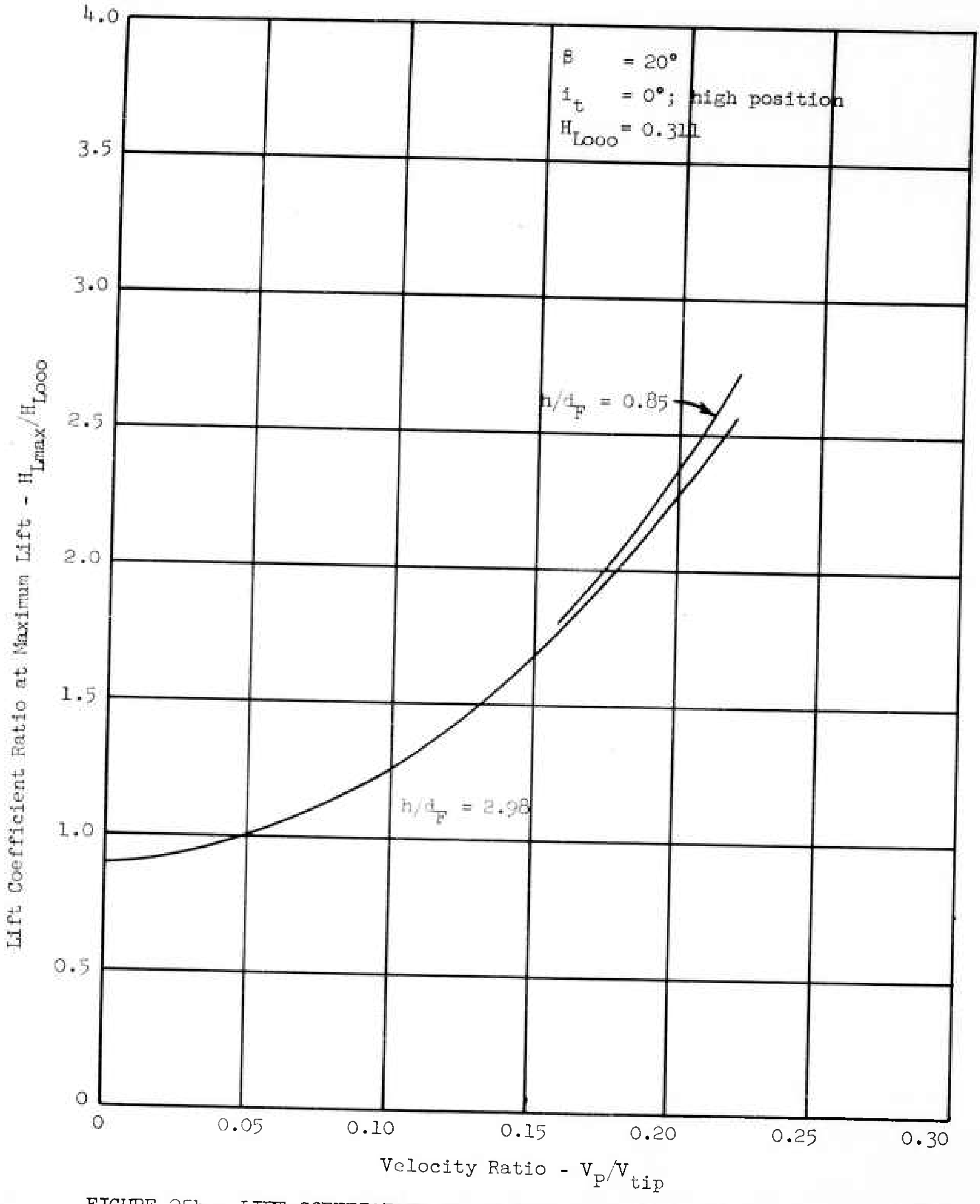

FIGURE 25b - LIFT COEFFICIENT RATIO AT MAXIMUM LIFT VERSUS VELOCITY RATIO

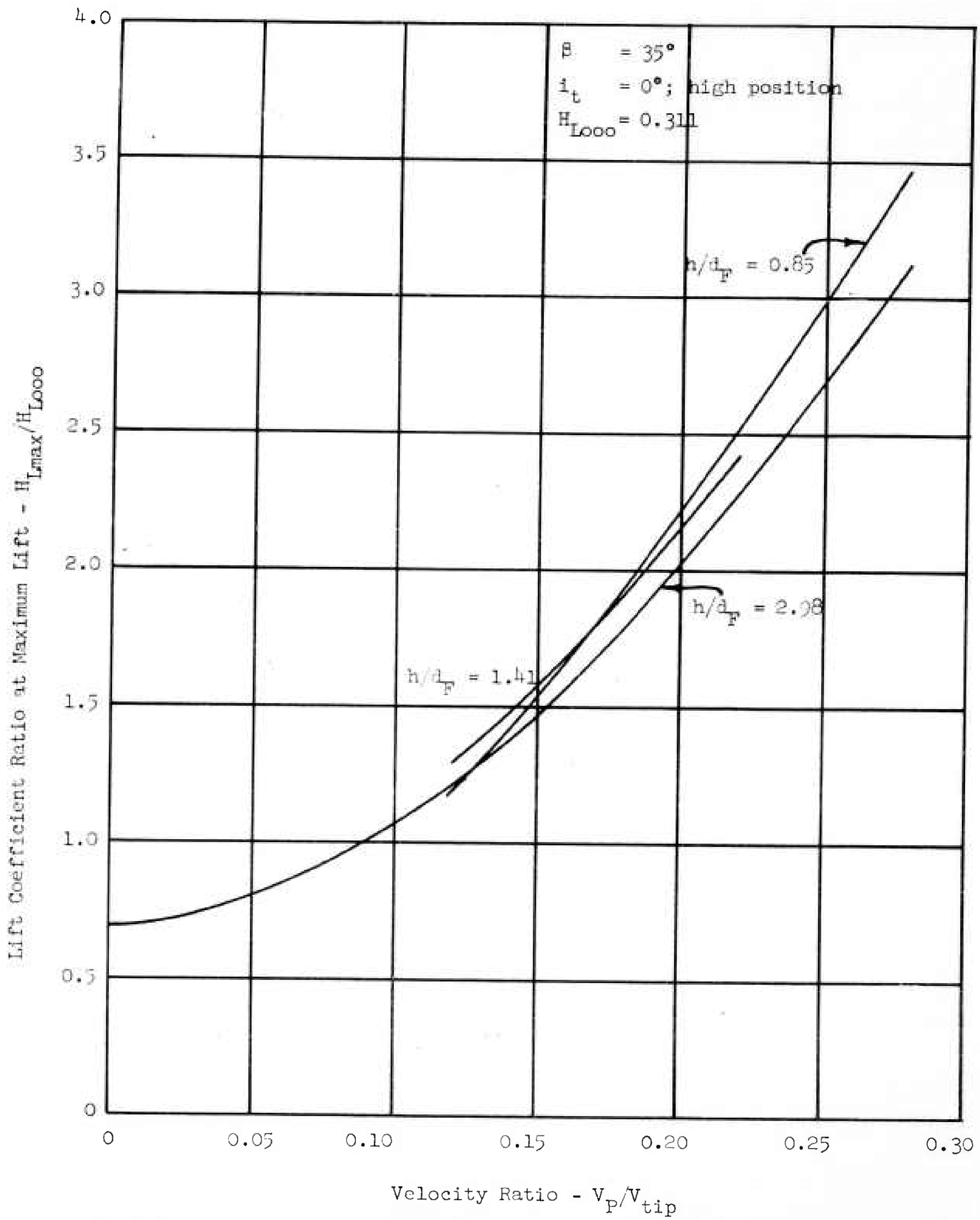

FIGURE 25c - LIFT COEFFICIENT RATIO AT MAXIMUM LIFT VERSUS VELOCITY RATIO

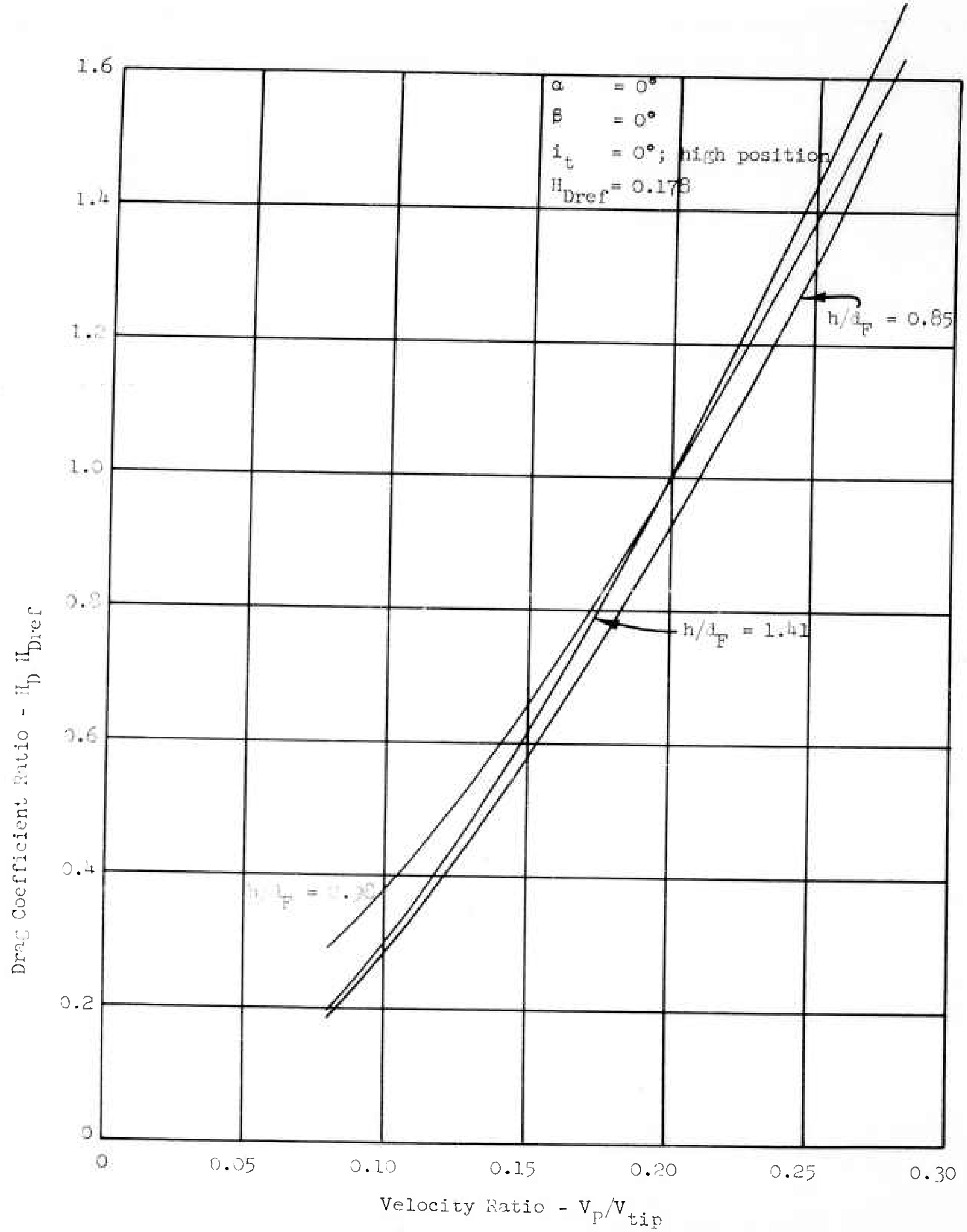

FIGURE 26a - DRAG COEFFICIENT RATIO VERSUS VELOCITY RATIO

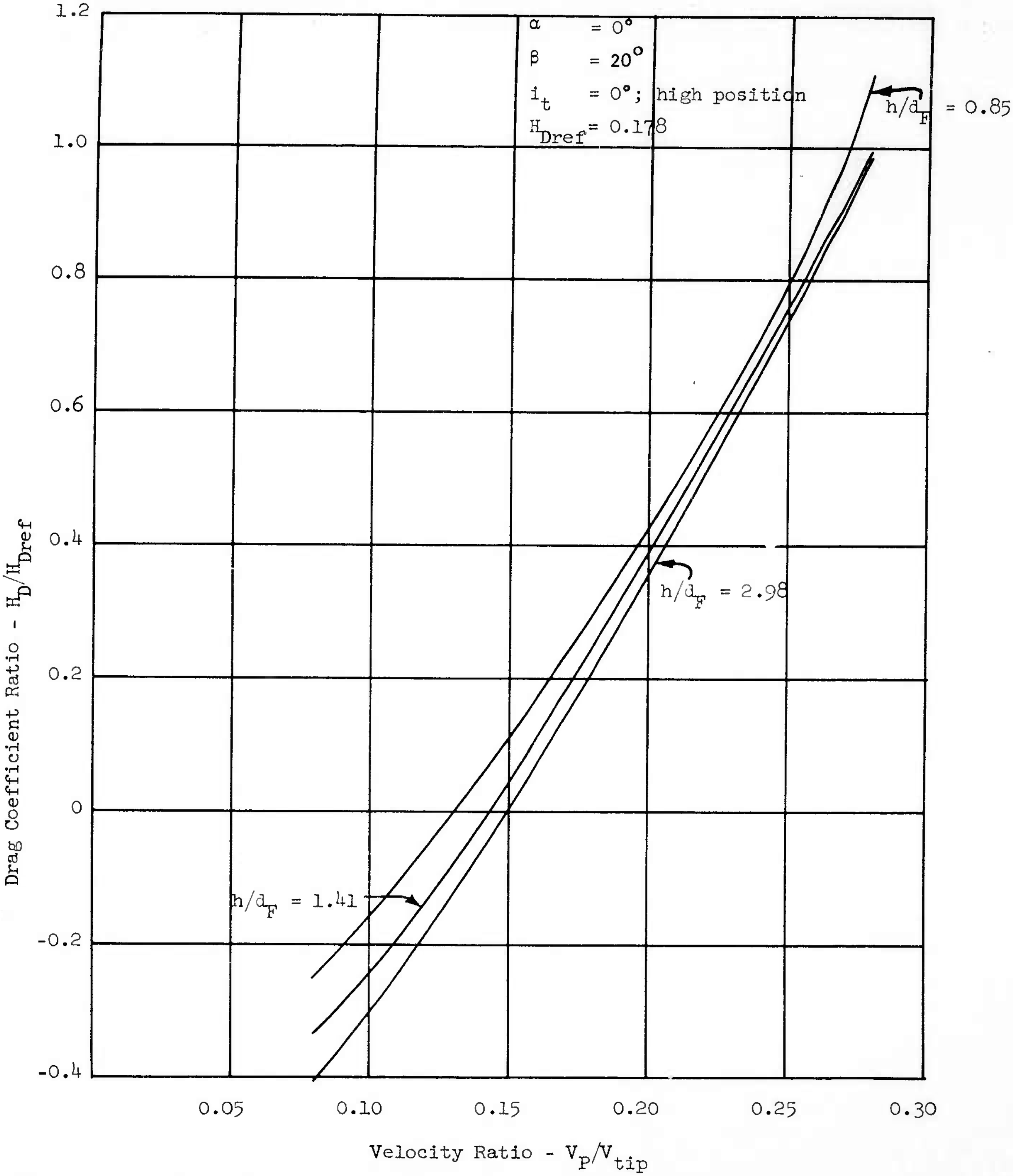

FIGURE 26b - DRAG COEFFICIENT RATIO VERSUS VELOCITY RATIO

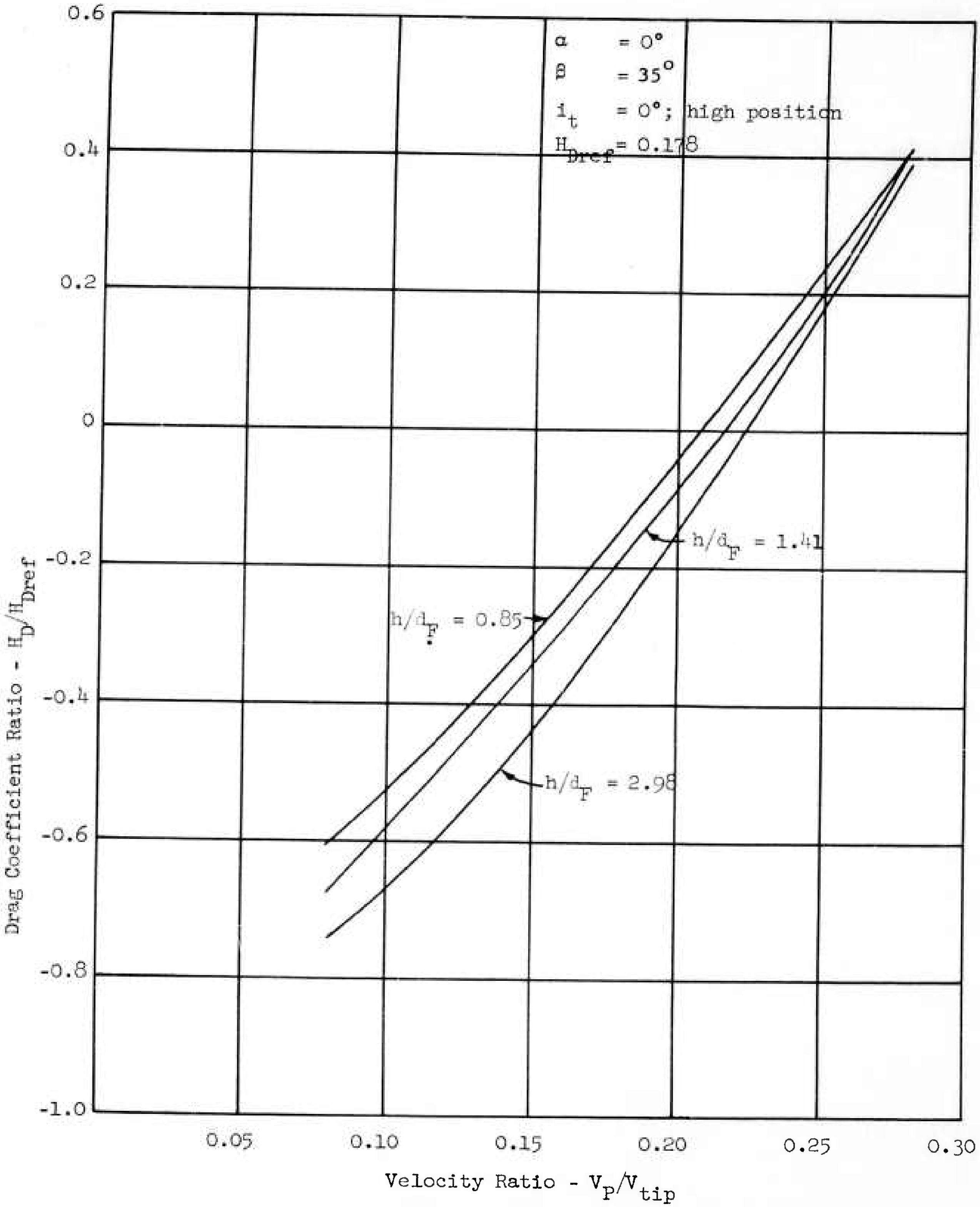

FIGURE 26c - DRAG COEFFICIENT RATIO VERSUS VELOCITY RATIO

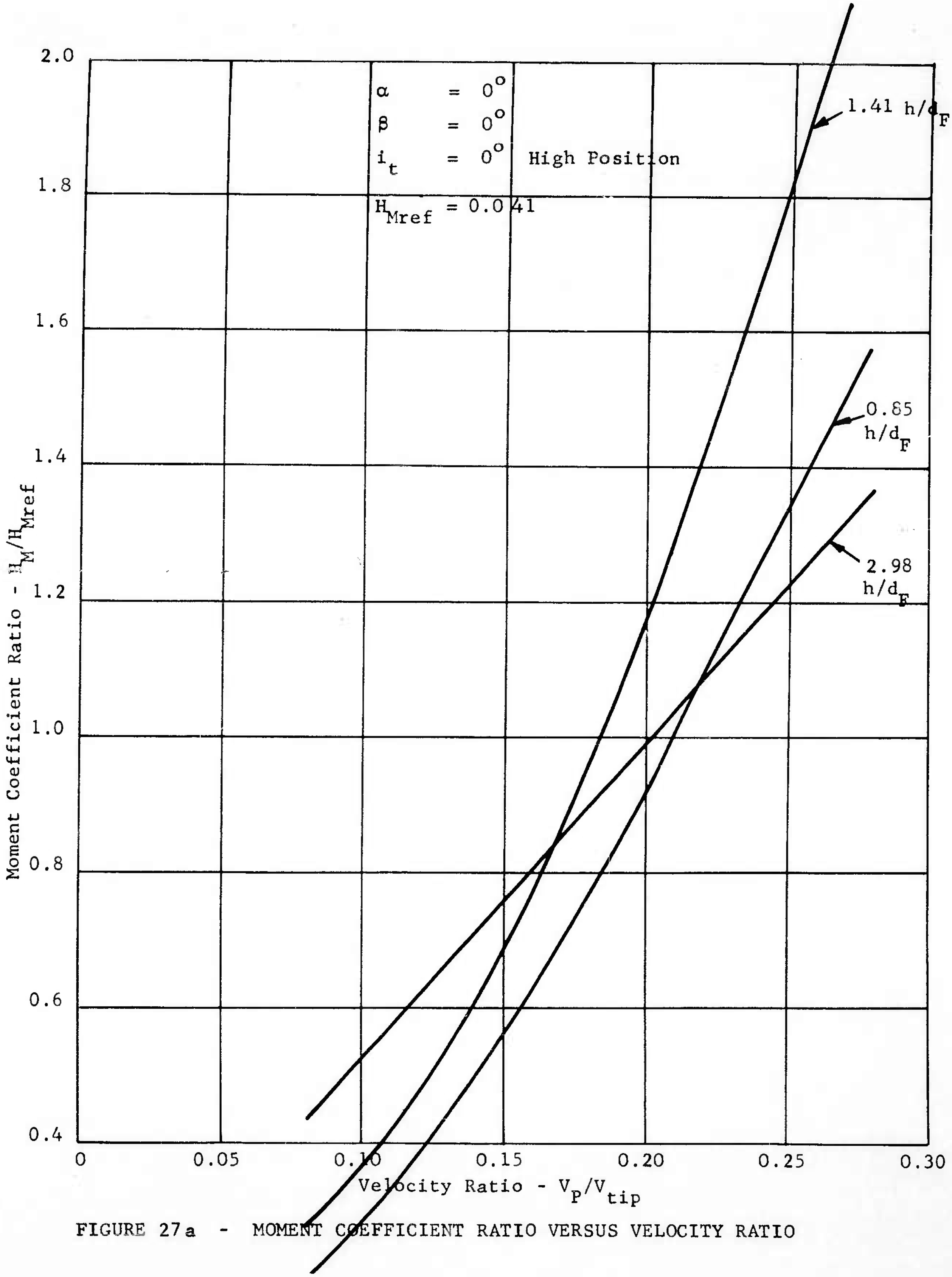

FIGURE 27a - MOMENT COEFFICIENT RATIO VERSUS VELOCITY RATIO

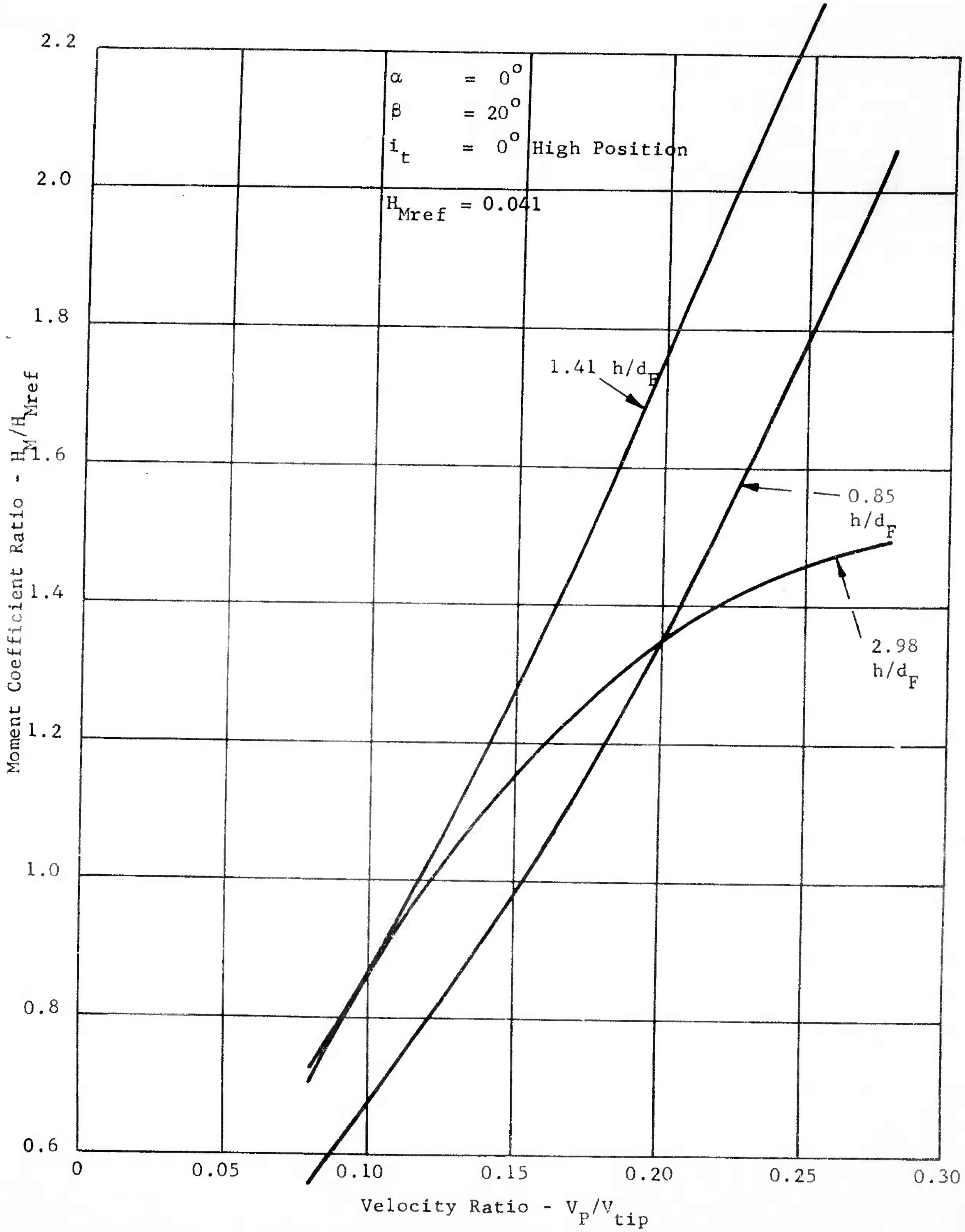

FIGURE 27b - MOMENT COEFFICIENT RATIO VERSUS VELOCITY RATIO

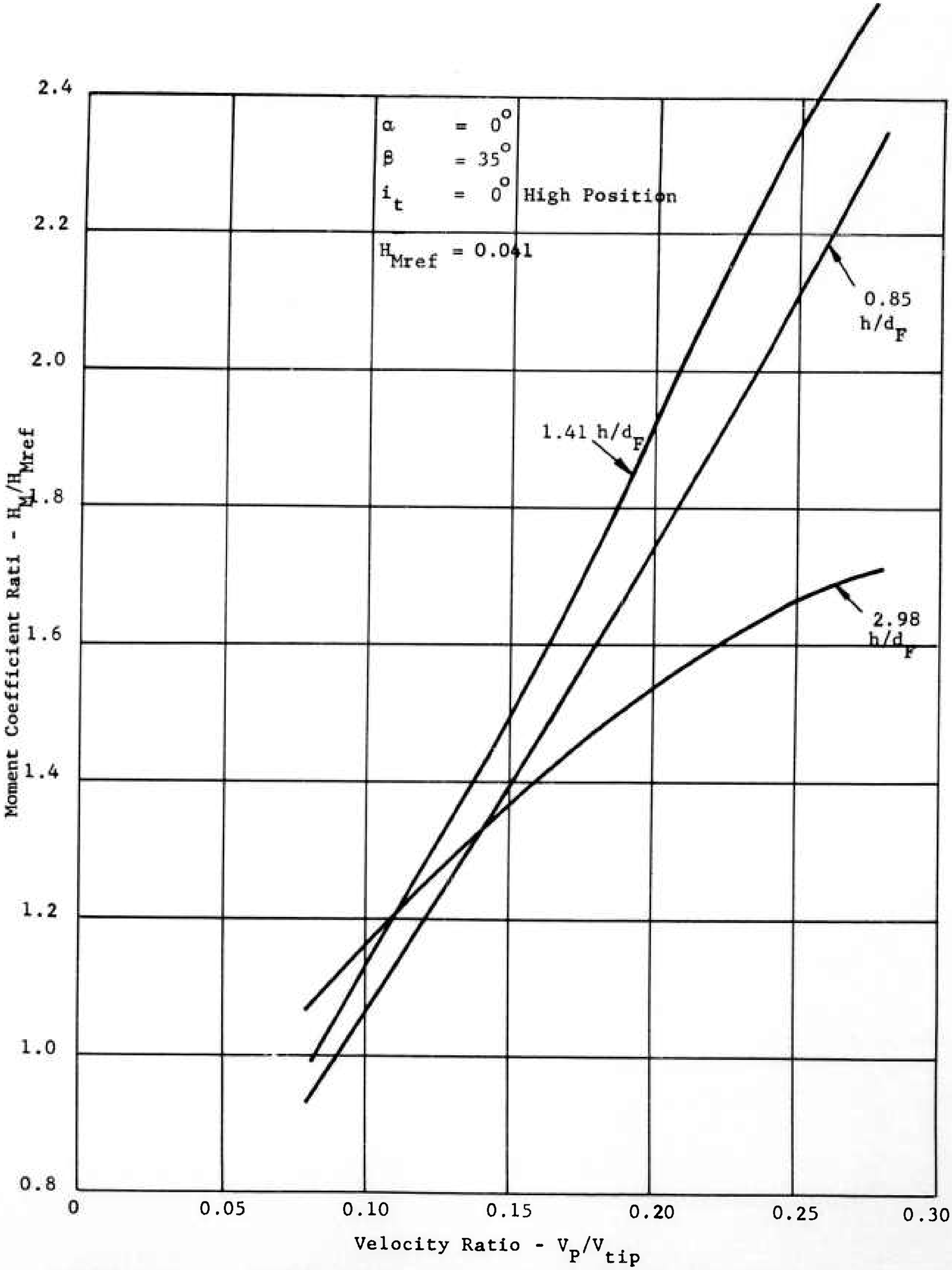

FIGURE 27c - MOMENT COEFFICIENT RATIO VERSUS VELOCITY RATIO

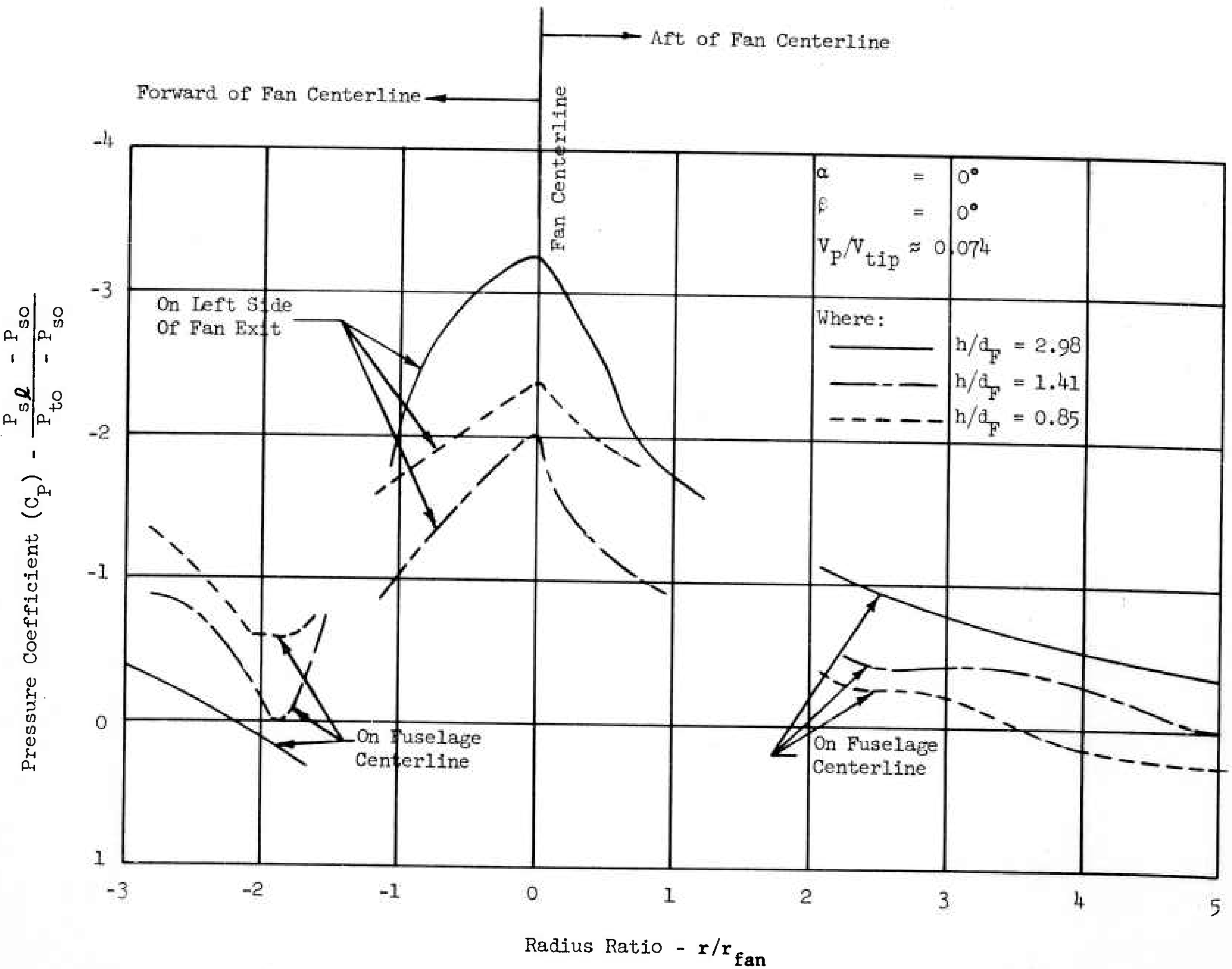

FIGURE 28a - PRESSURE COEFFICIENT ON BOTTOM OF FUSELAGE VERSUS RADIUS RATIO

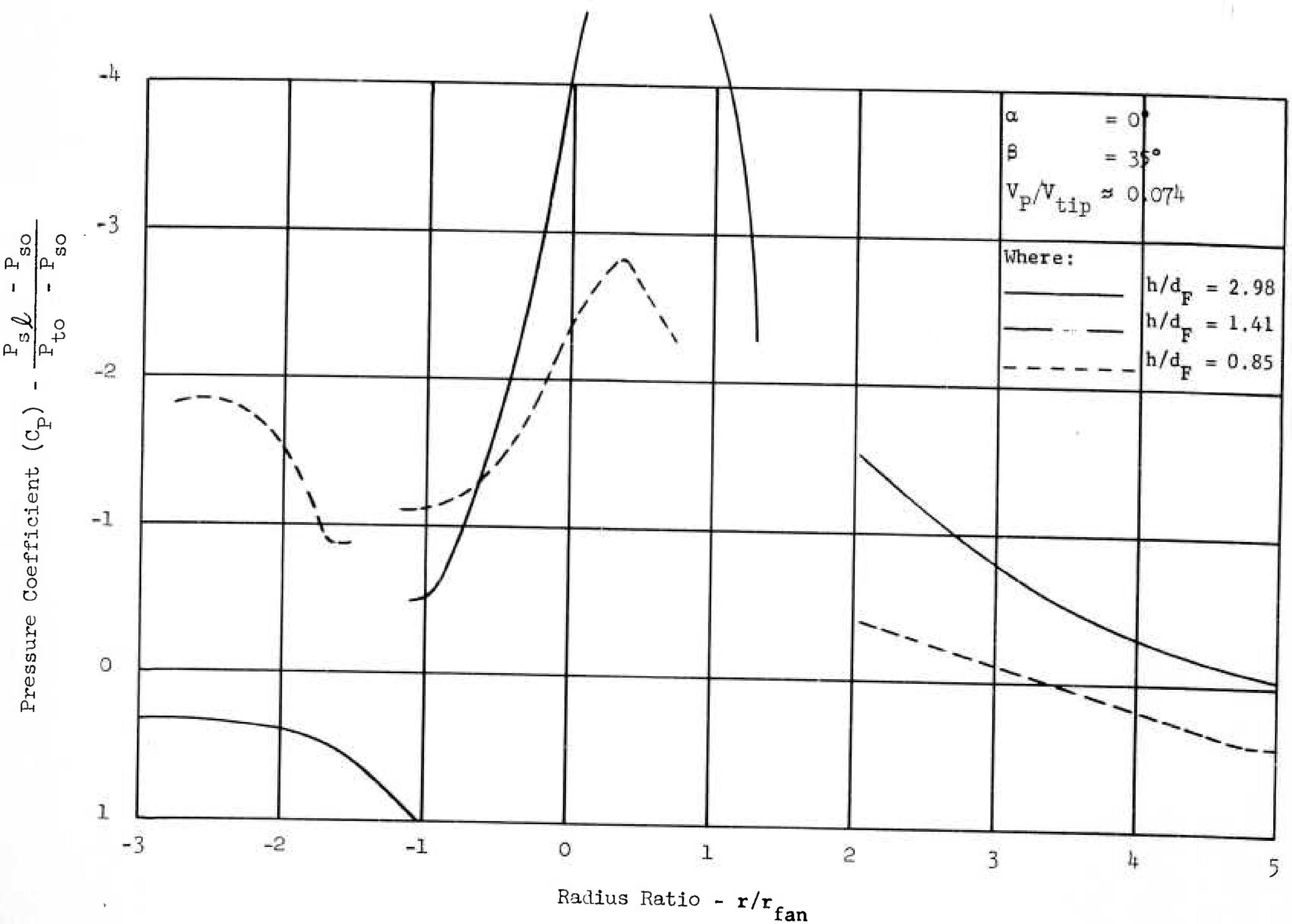

FIGURE 28b - PRESSURE COEFFICIENT ON BOTTOM OF FUSELAGE VERSUS RADIUS RATIO

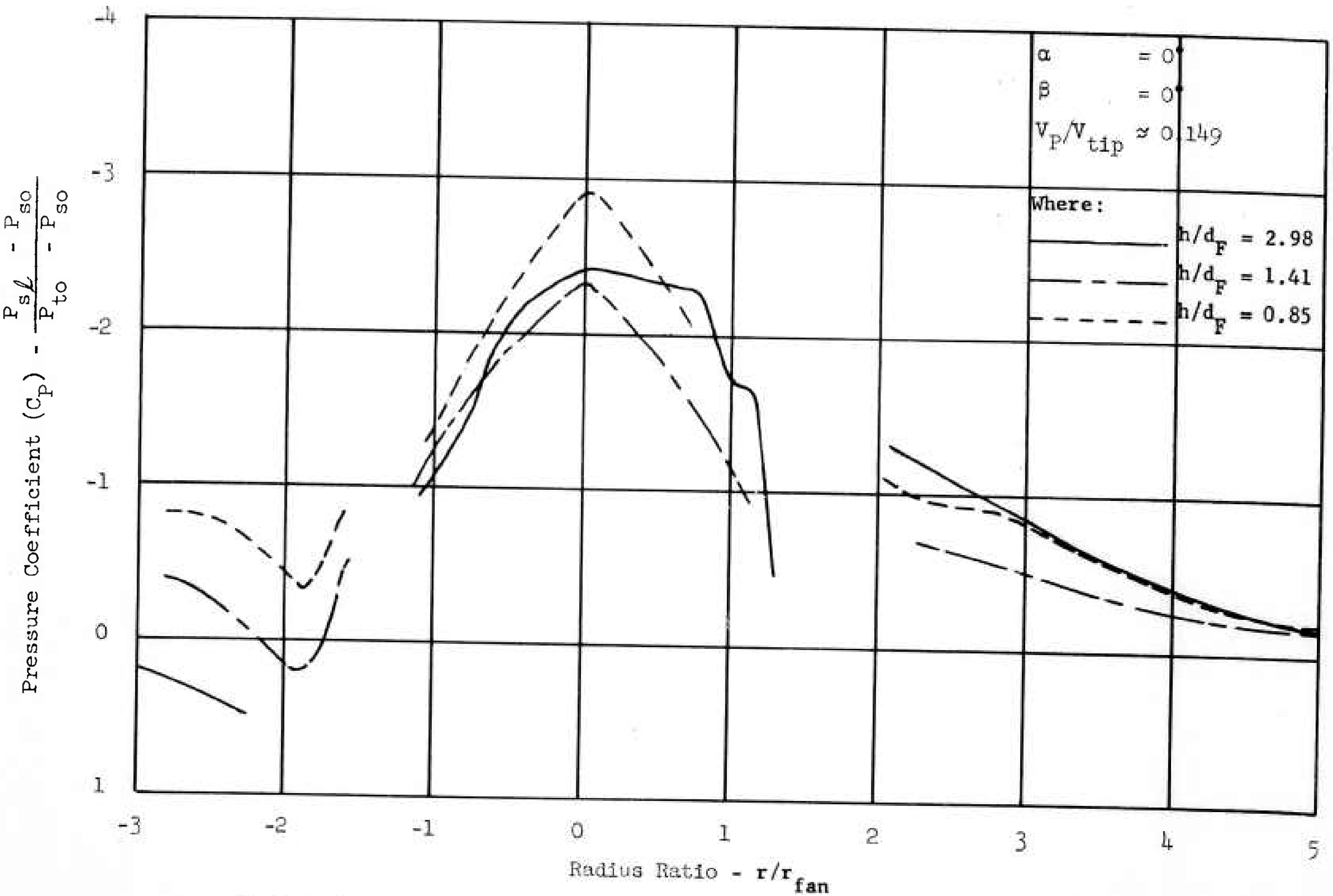

FIGURE 28c - PRESSURE COEFFICIENT ON BOTTOM OF FUSELAGE VERSUS RADIUS RATIO

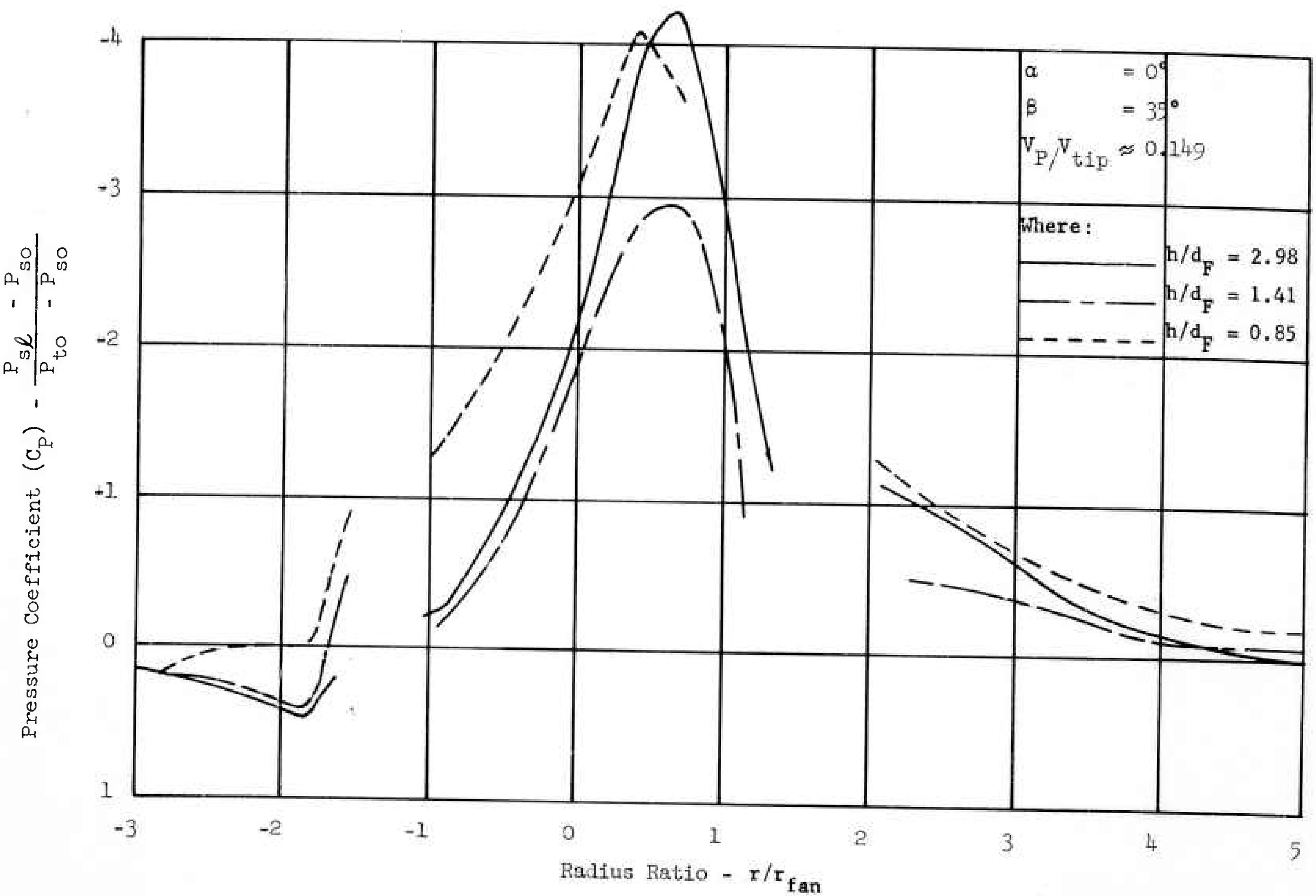

FIGURE 28d - PRESSURE COEFFICIENT ON BOTTOM OF FUSELAGE VERSUS RADIUS RATIO

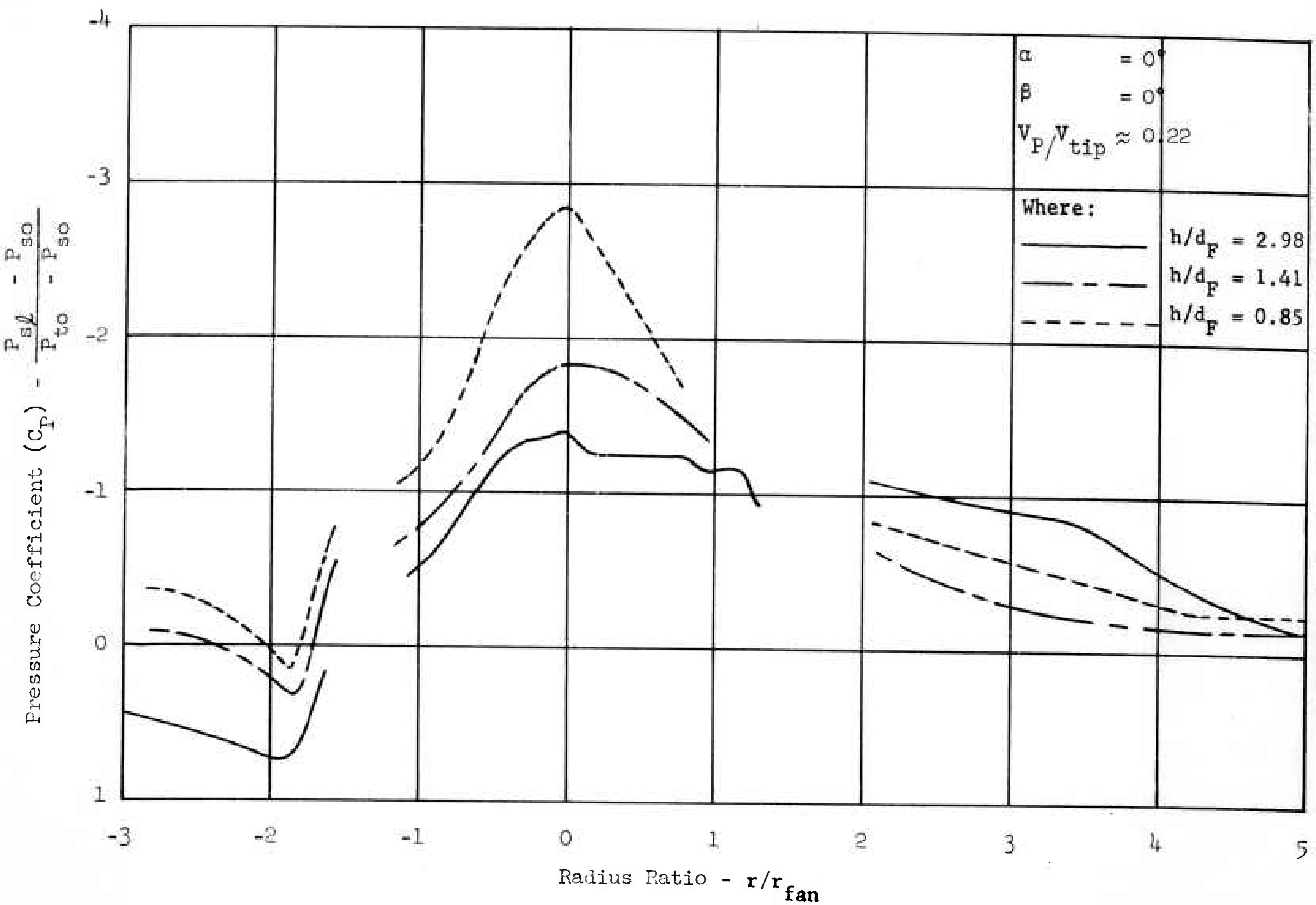

FIGURE 28c - PRESSURE COEFFICIENT ON BOTTOM OF FUSELAGE VERSUS RADIUS RATIO

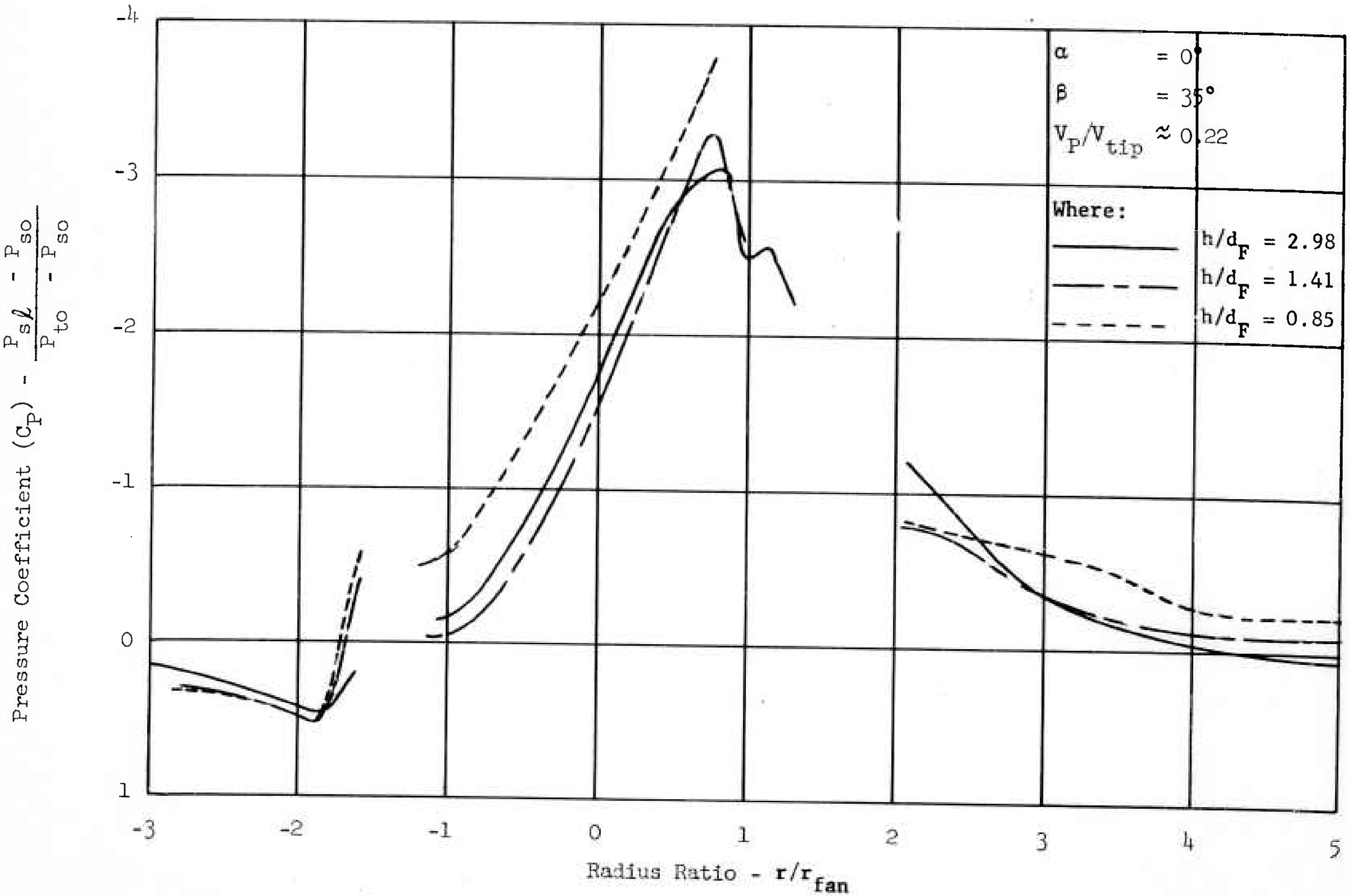

FIGURE 28f - PRESSURE COEFFICIENT ON BOTTOM OF FUSELAGE VERSUS RADIUS RATIO

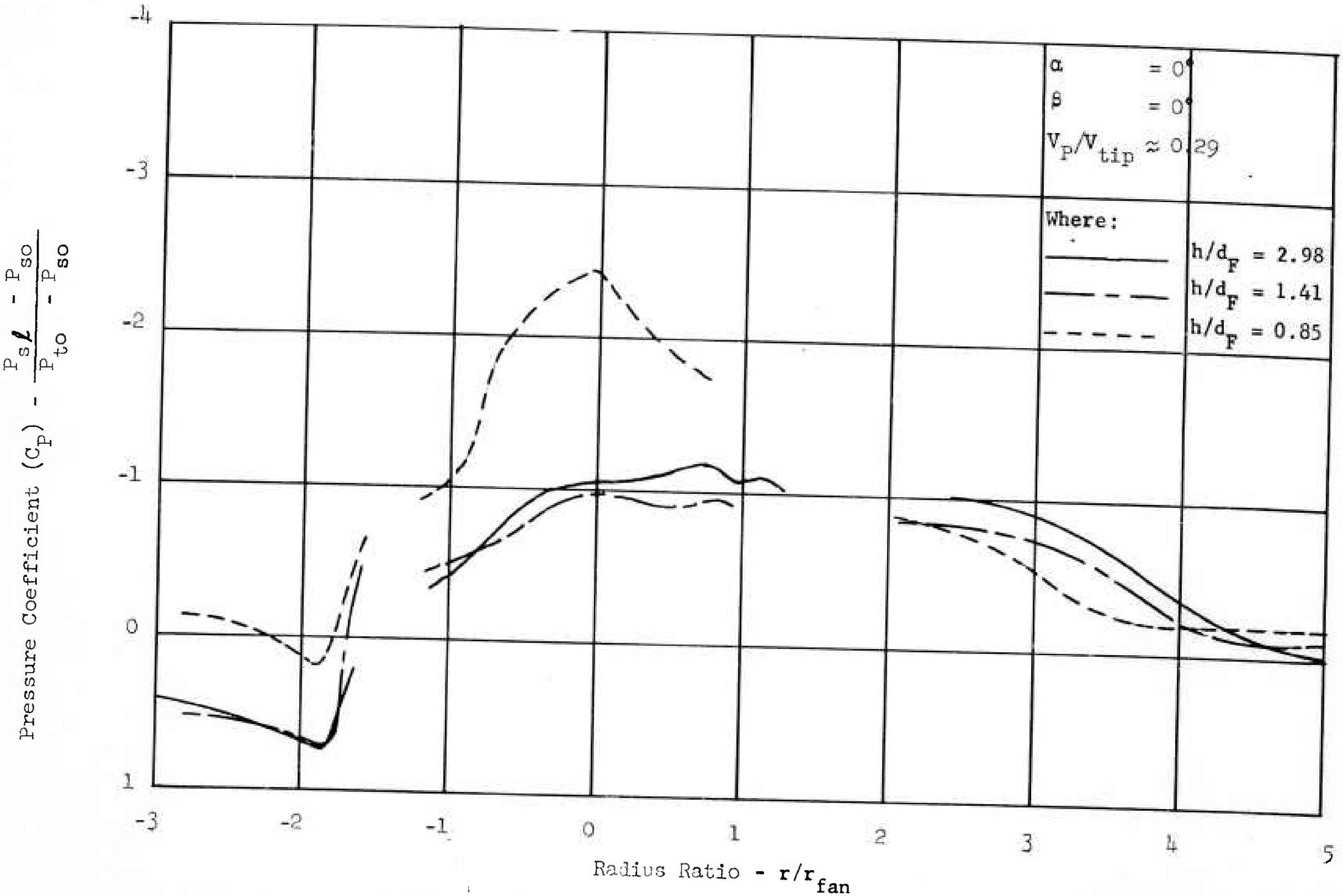

FIGURE 28g - PRESSURE COEFFICIENT ON BOTTOM OF FUSELAGE VERSUS RADIUS RATIO

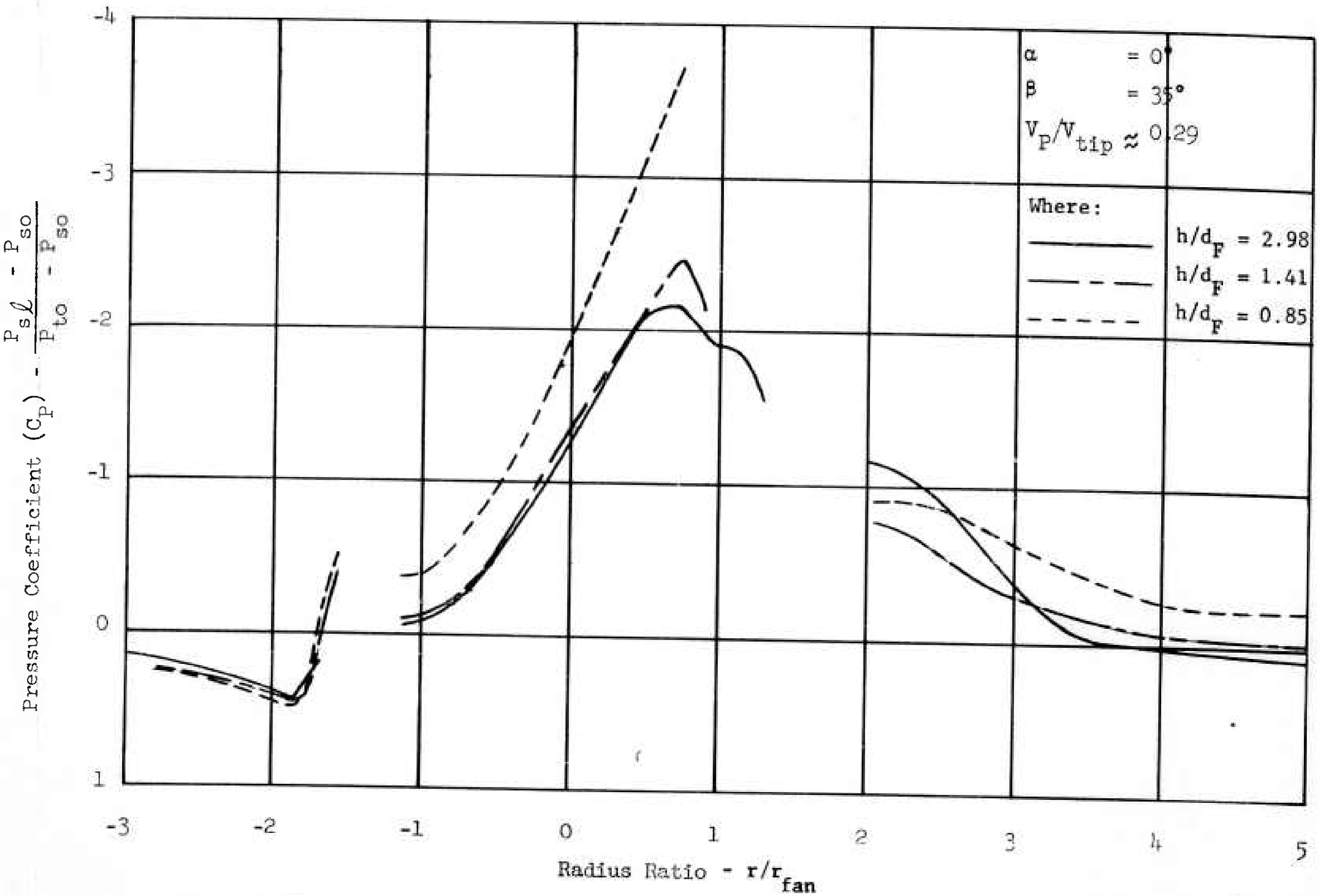

FIGURE 28h - PRESSURE COEFFICIENT ON BOTTOM OF FUSELAGE VERSUS RADIUS RATIO

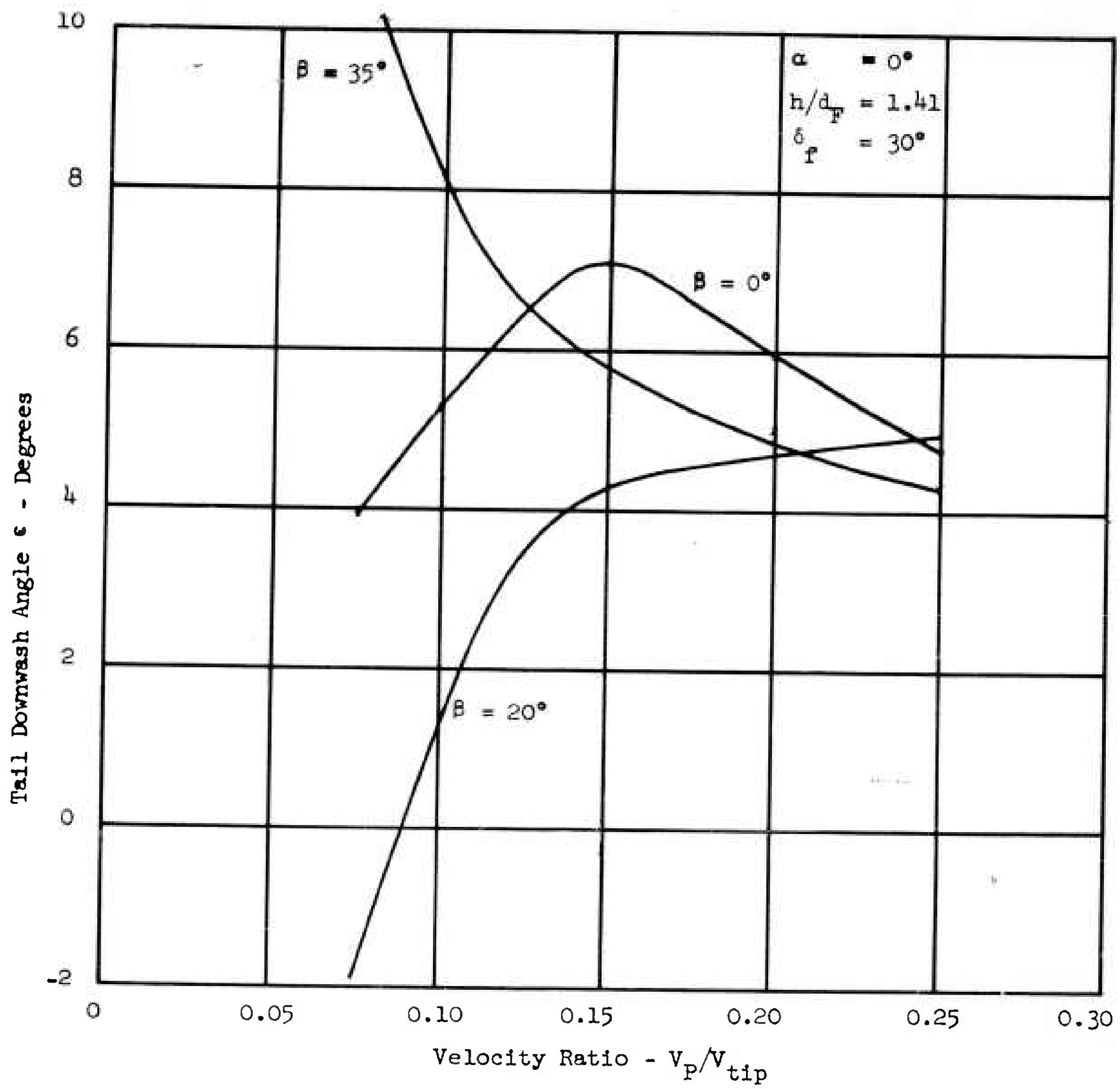

FIGURE 29a - TAIL DOWNWASH ANGLE VERSUS VELOCITY RATIO

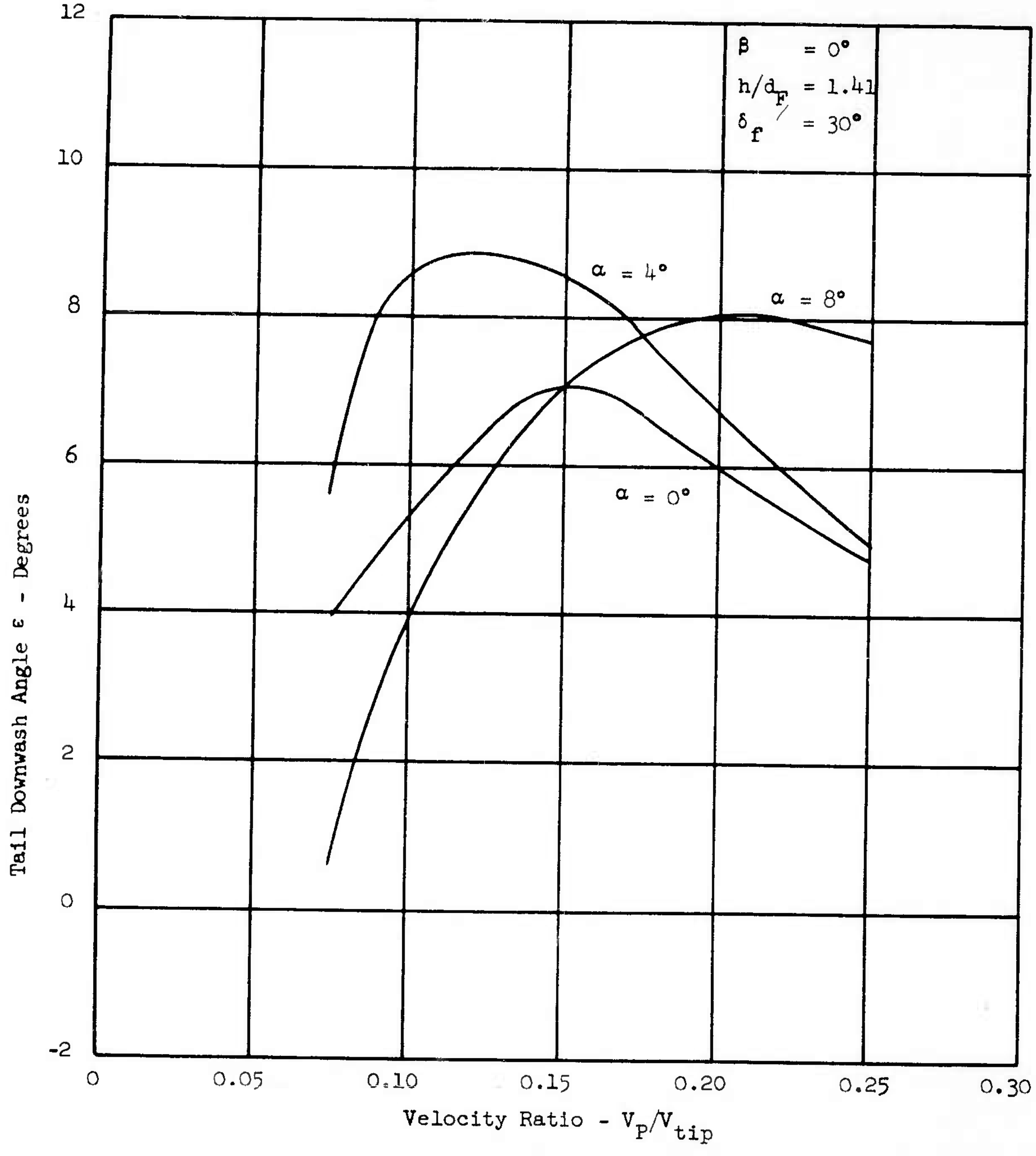

FIGURE 29b - TAIL DOWNWASH ANGLE VERSUS VELOCITY RATIO

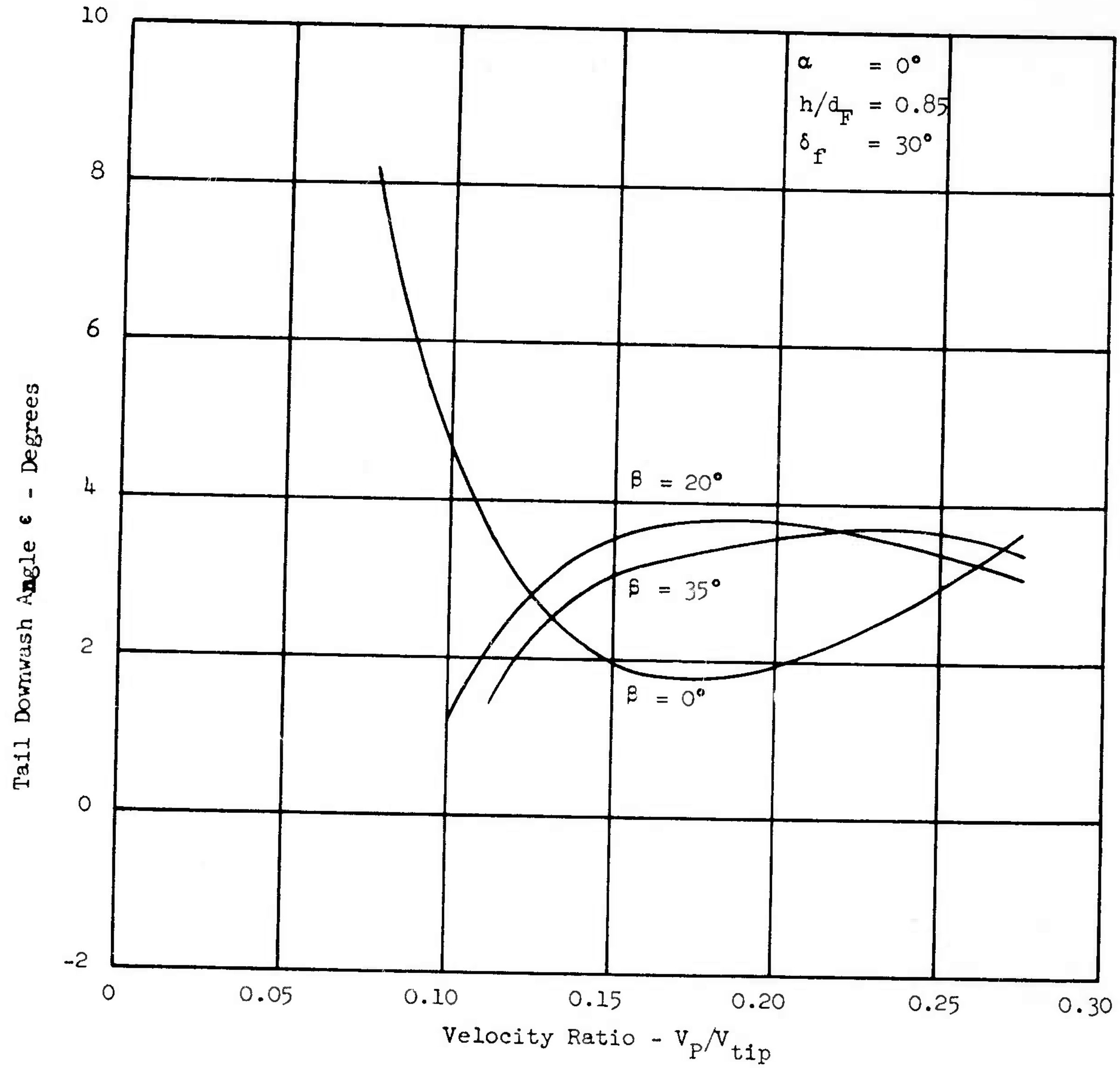

FIGURE 29c - TAIL DOWNWASH ANGLE VERSUS VELOCITY RATIO

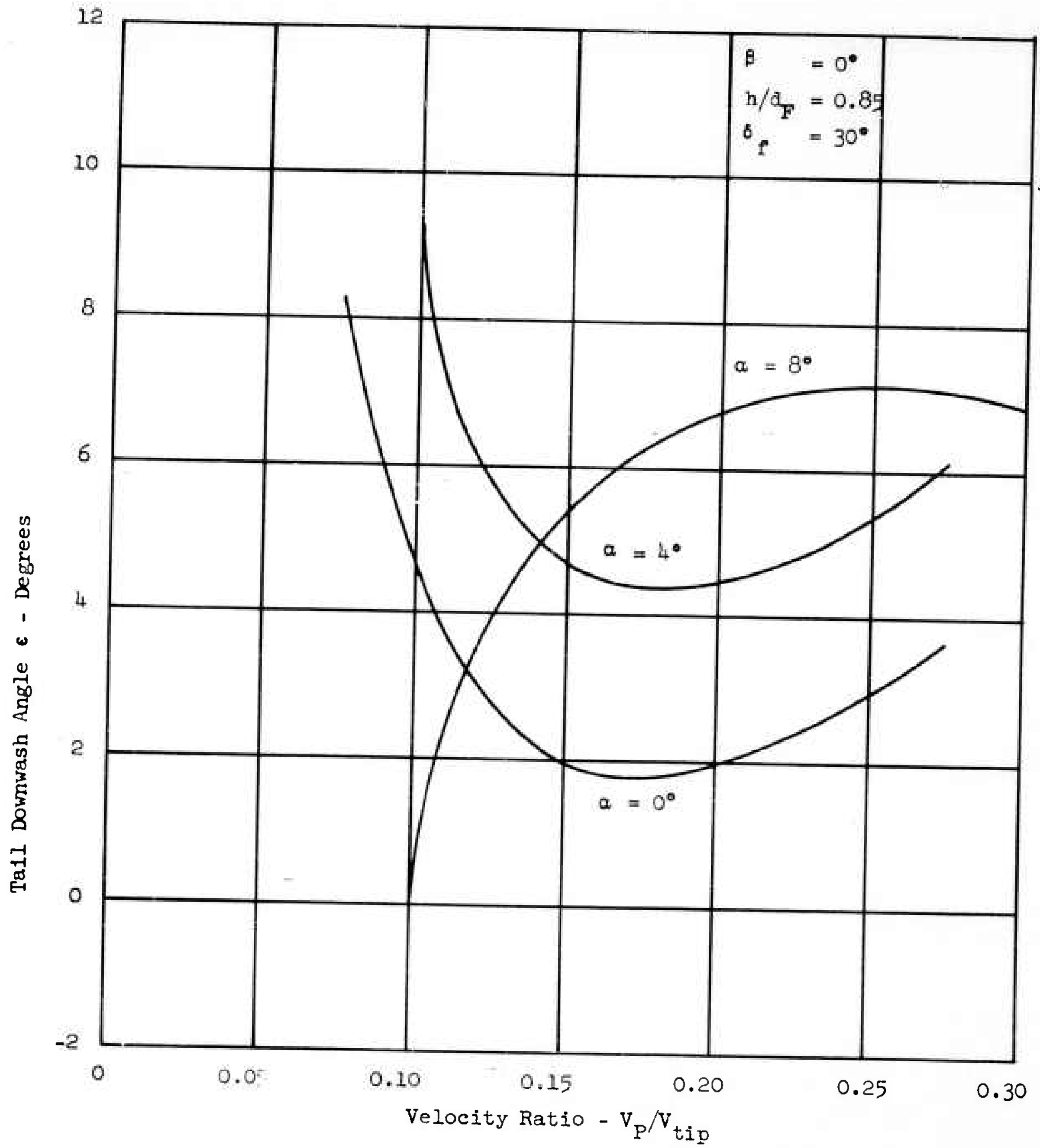

FIGURE 29d - TAIL DOWNWASH ANGLE VERSUS VELOCITY RATIO

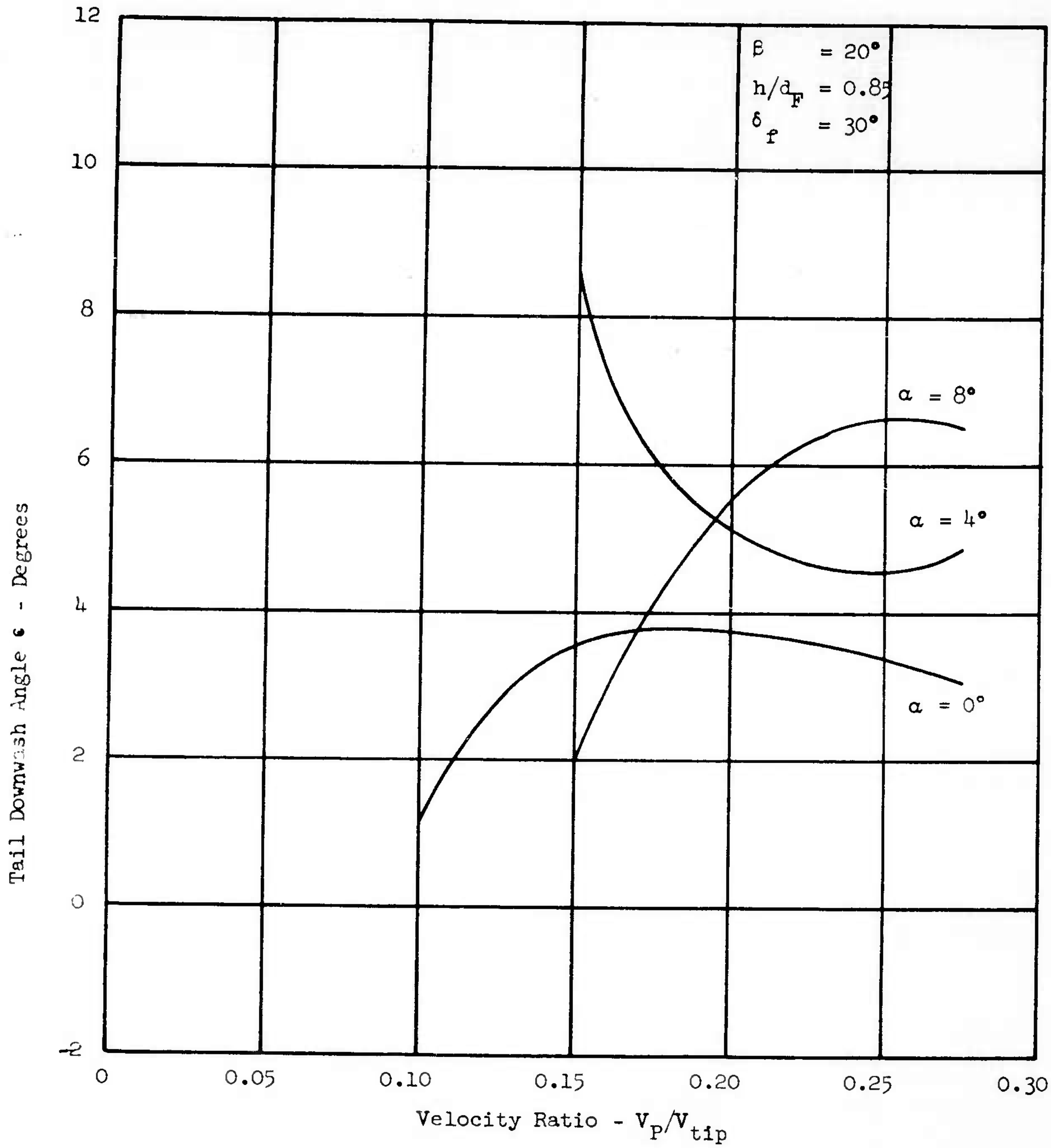

FIGURE 29e - TAIL DOWNWASH ANGLE VERSUS VELOCITY RATIO

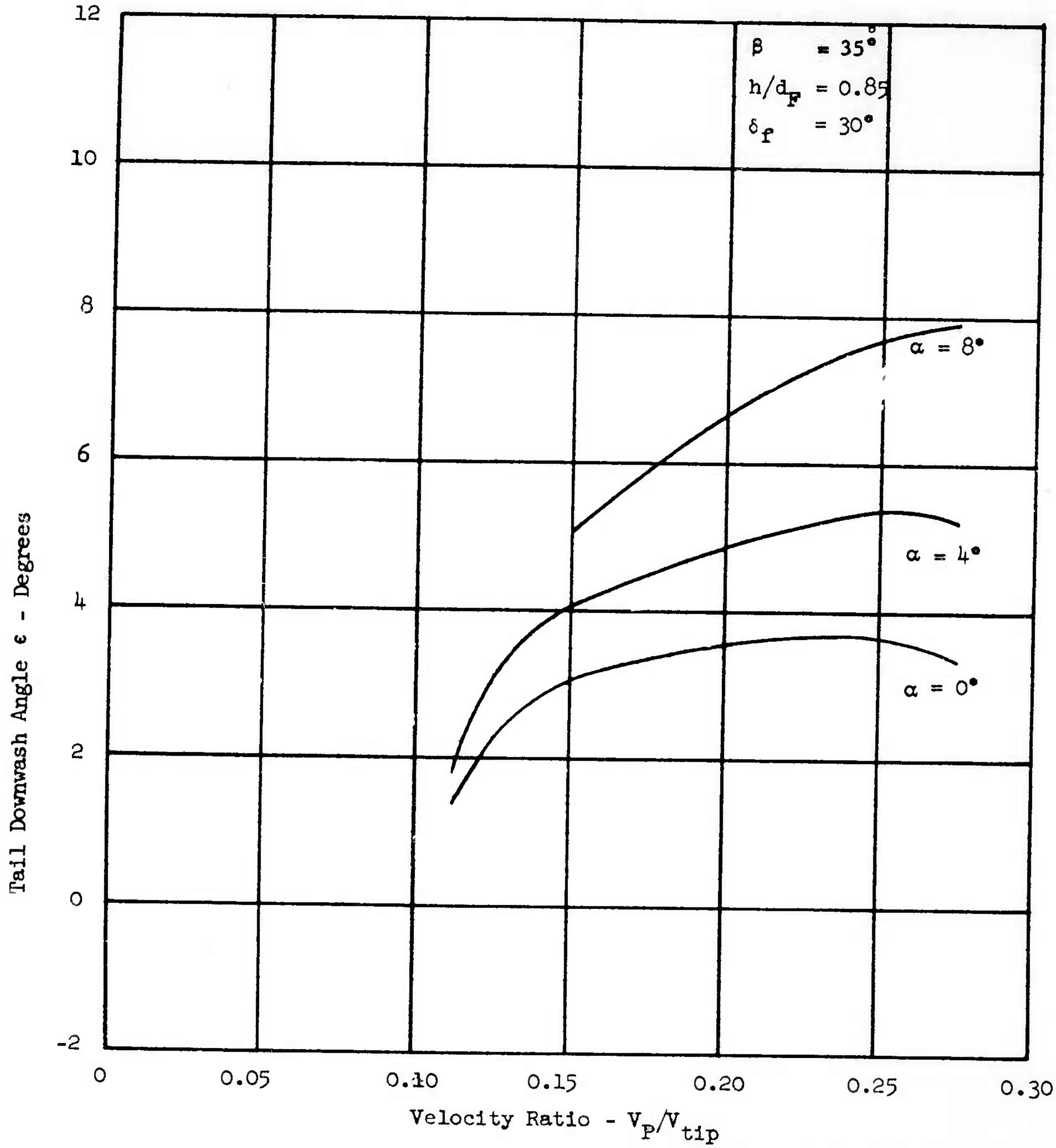

FIGURE 29f - TAIL DOWNWASH ANGLE VERSUS VELOCITY RATIO

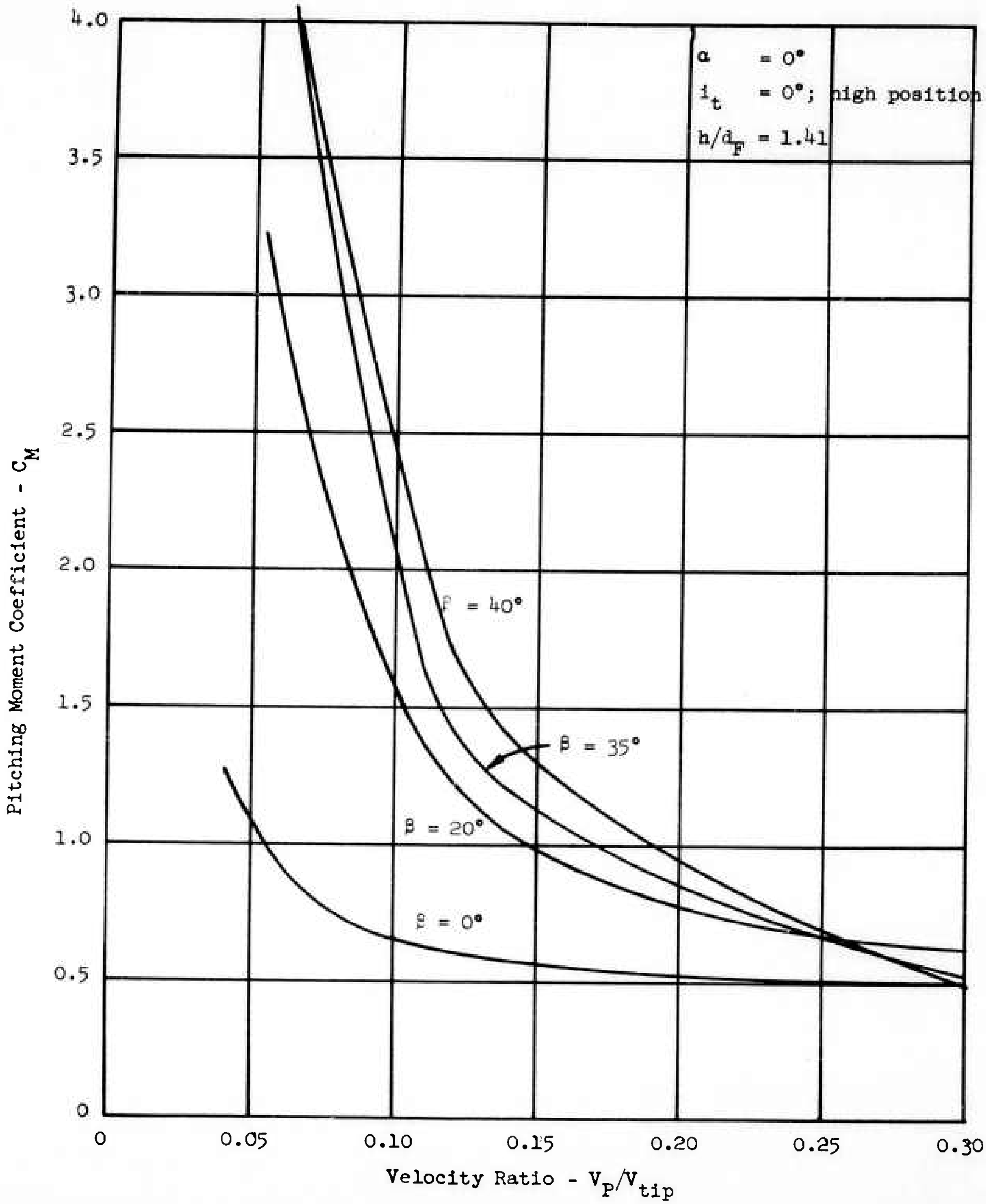

FIGURE 30a - PITCHING MOMENT COEFFICIENT (TAIL ON) VERSUS VELOCITY RATIO

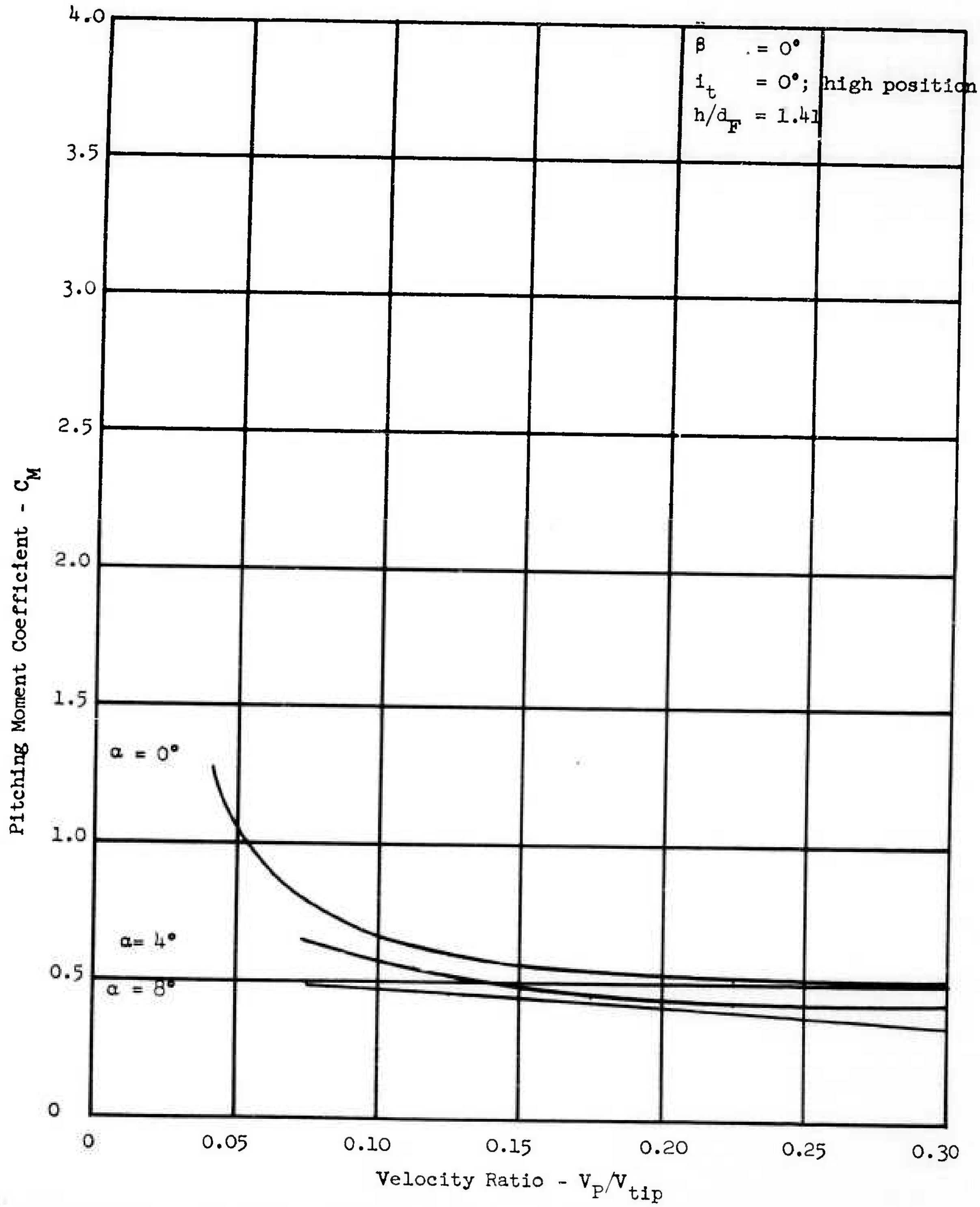

FIGURE 30b - PITCHING MOMENT COEFFICIENT (TAIL ON) VERSUS VELOCITY RATIO

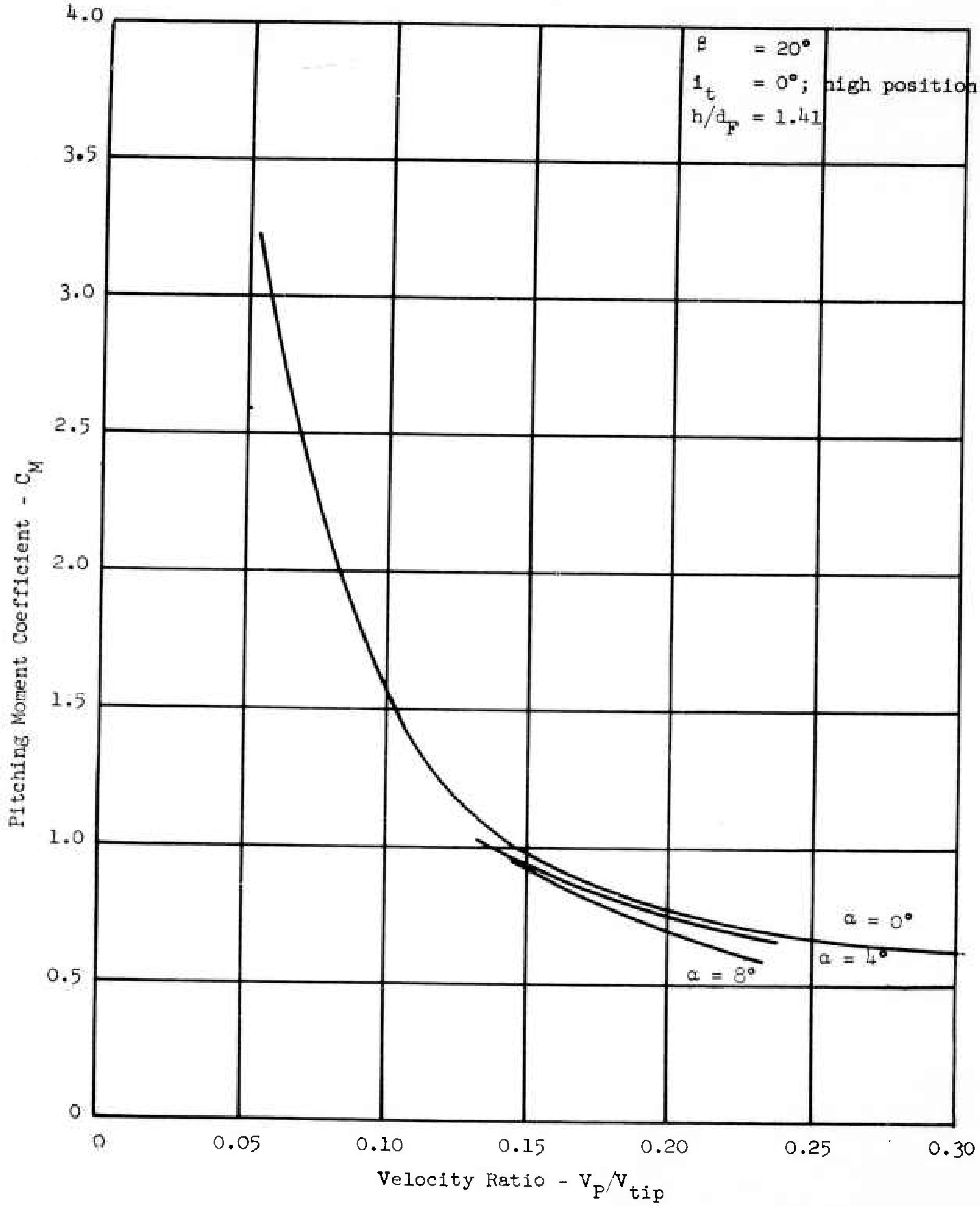

FIGURE 30c - PITCHING MOMENT COEFFICIENT (TAIL ON) VERSUS VELOCITY RATIO

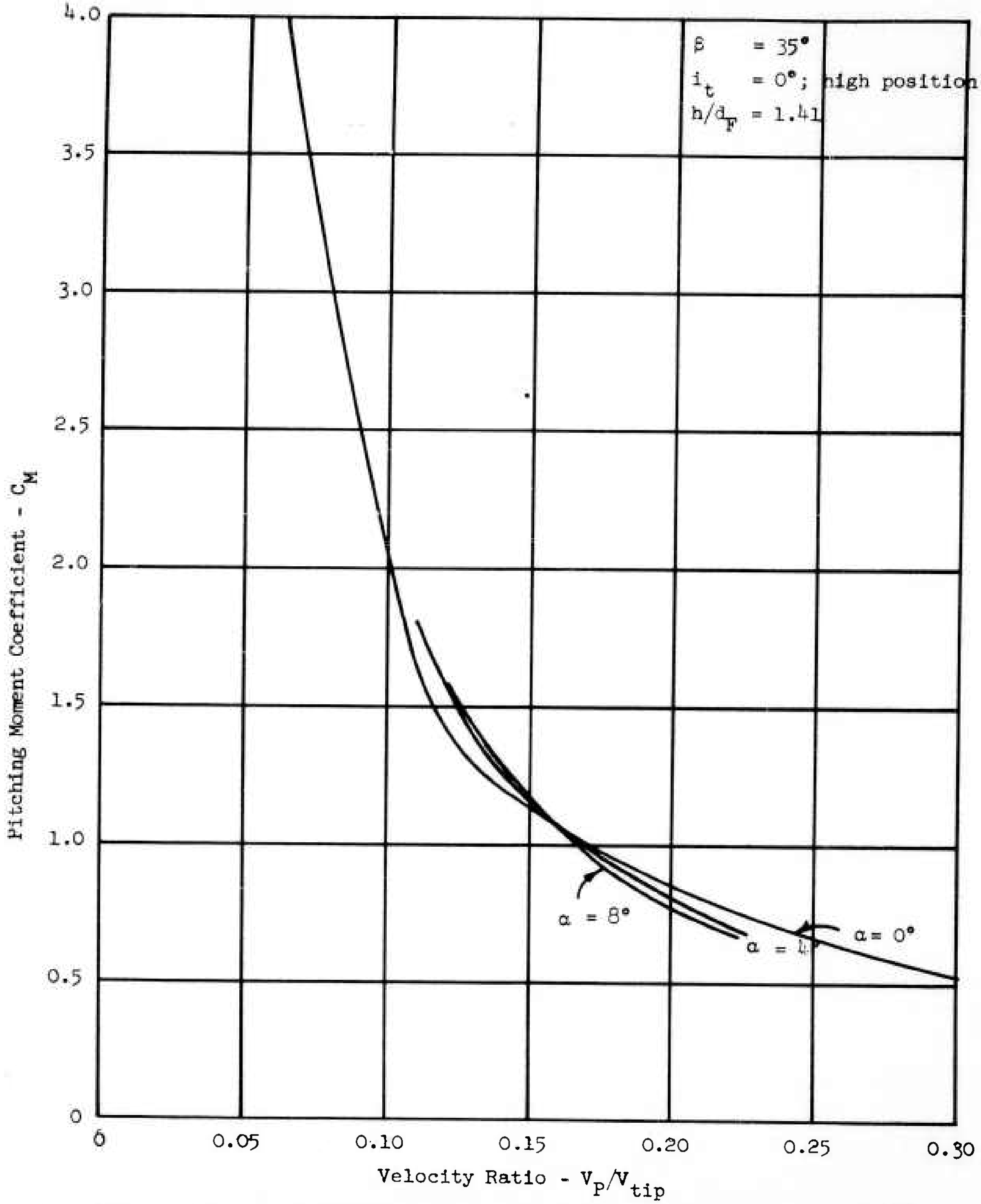

FIGURE 30d - PITCHING MOMENT COEFFICIENT (TAIL ON) VERSUS VELOCITY RATIO

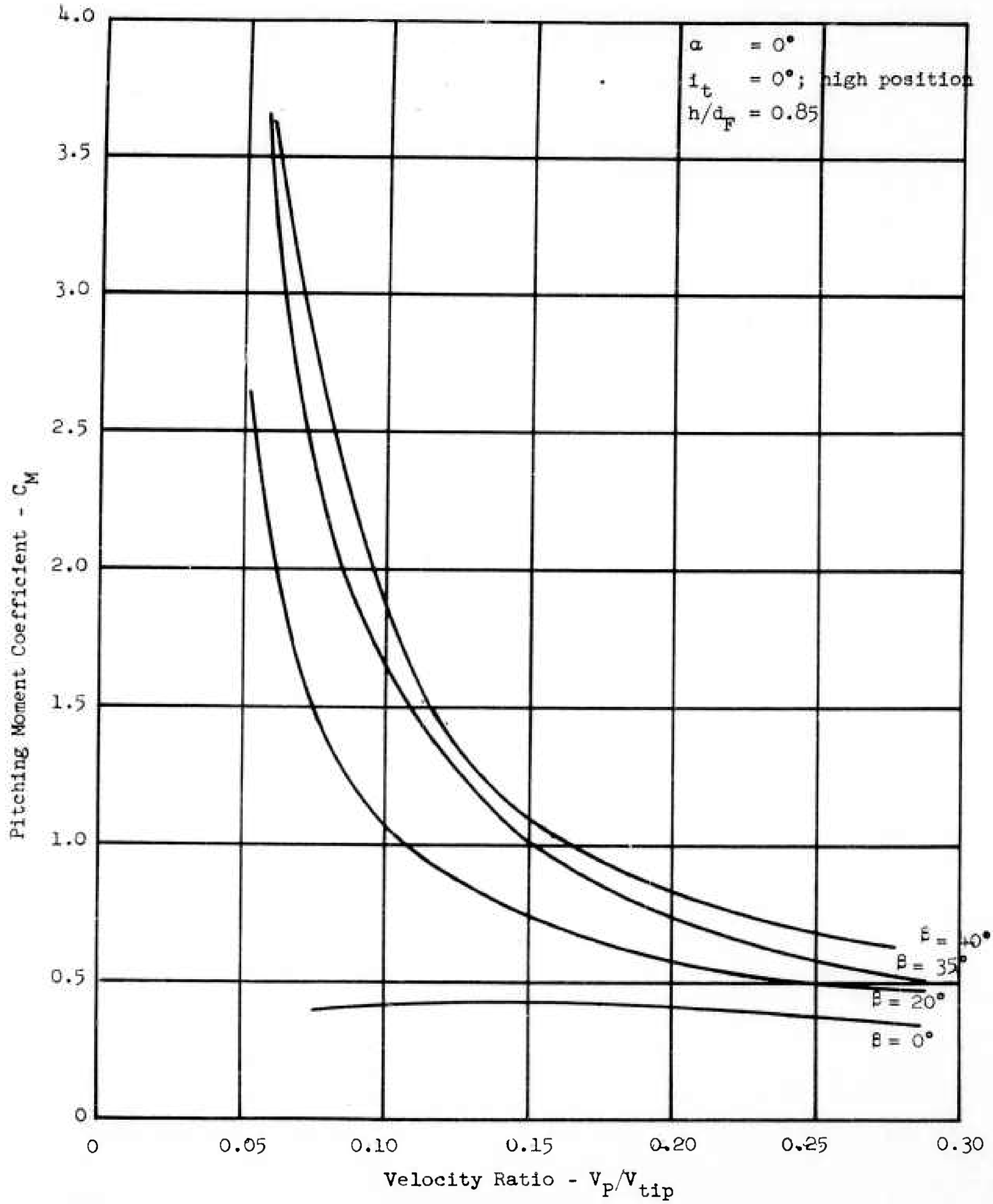

FIGURE 30e - PITCHING MOMENT COEFFICIENT (TAIL ON) VERSUS VELOCITY RATIO

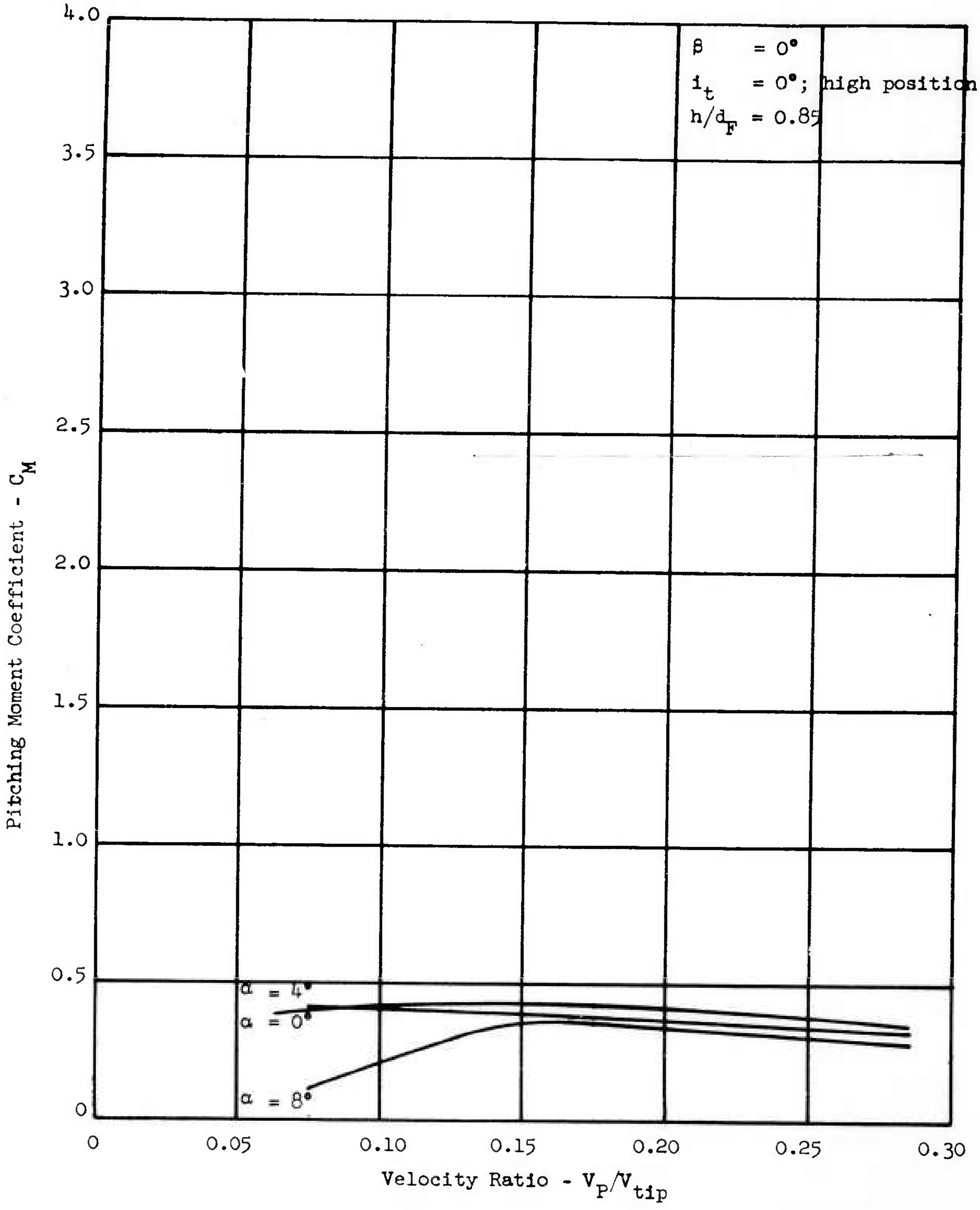

FIGURE 30f - PITCHING MOMENT COEFFICIENT (TAIL ON) VERSUS VELOCITY RATIO

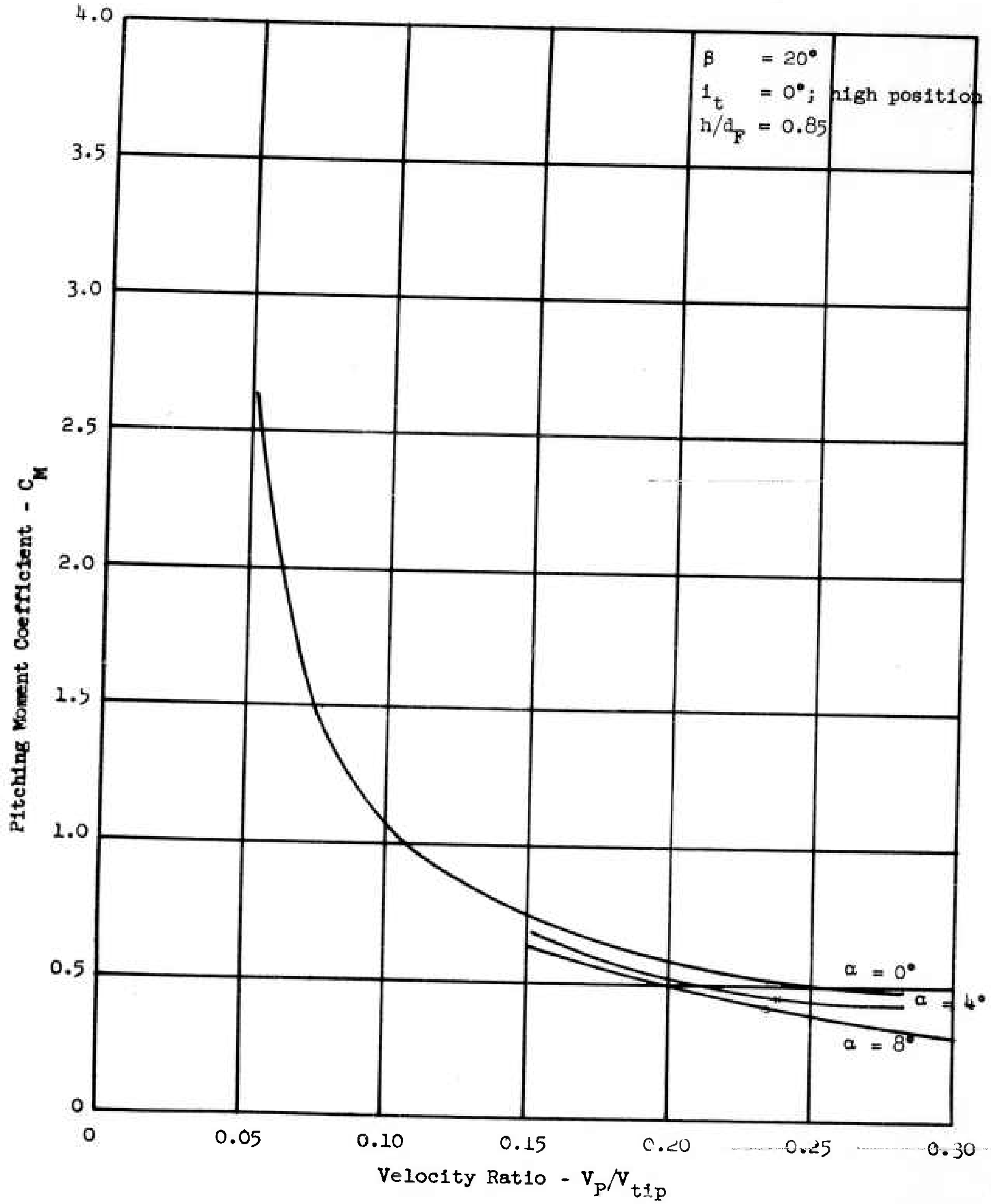

FIGURE 30g - PITCHING MOMENT COEFFICIENT (TAIL ON) VERSUS VELOCITY RATIO

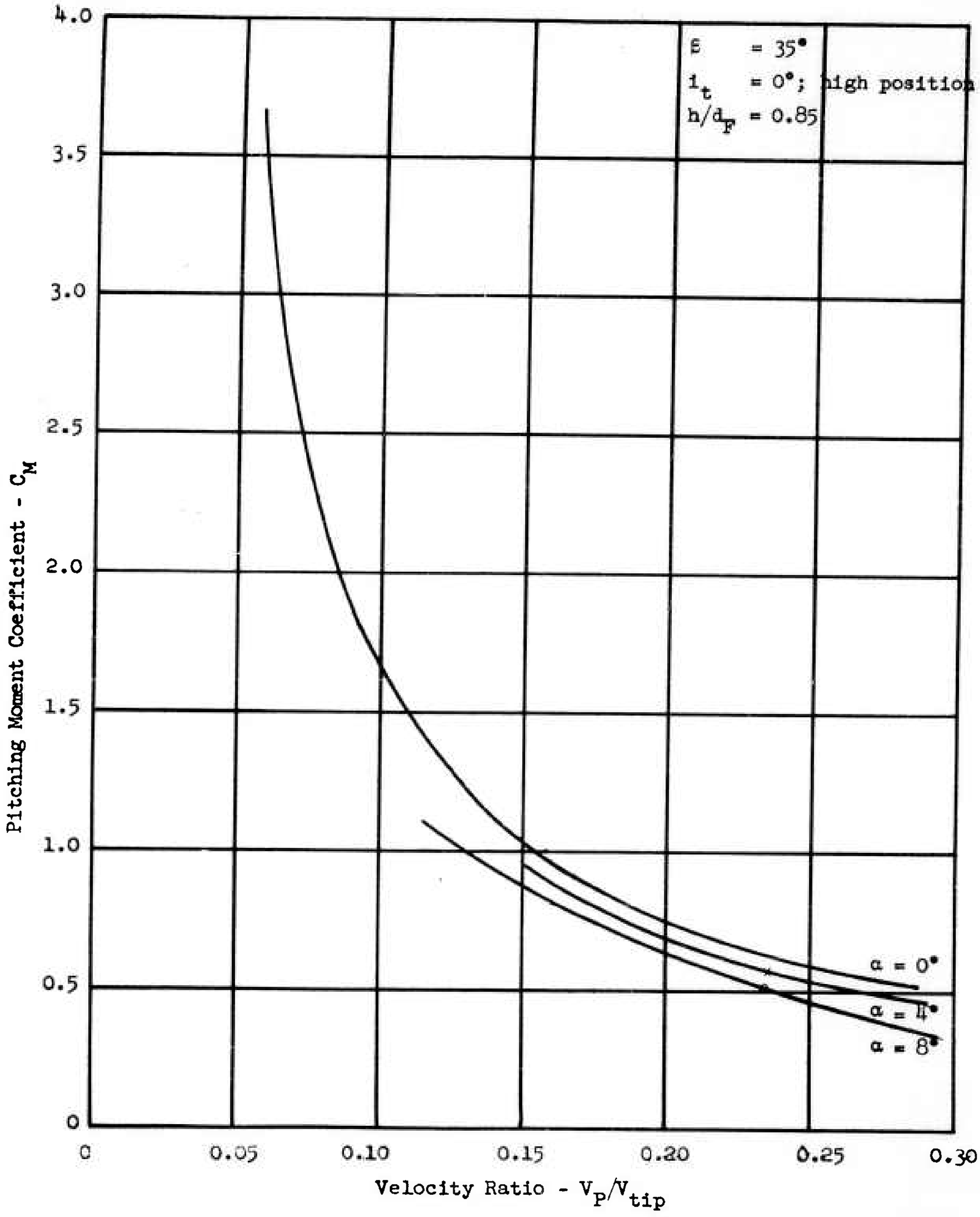

FIGURE 30h - PITCHING MOMENT COEFFICIENT (TAIL ON) VERSUS VELOCITY RATIO

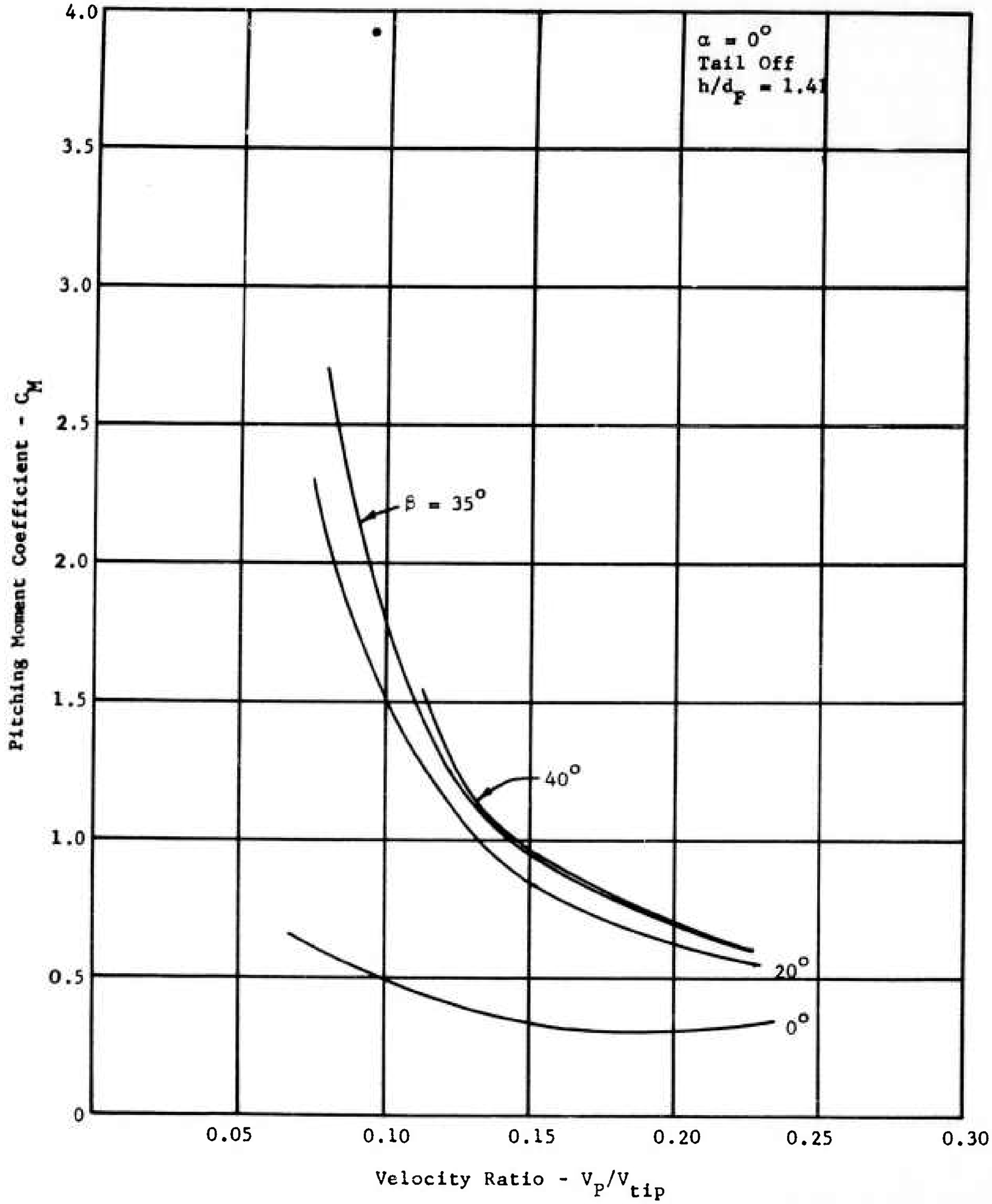

FIGURE 31a - PITCHING MOMENT COEFFICIENT (TAIL OFF) VERSUS VELOCITY RATIO

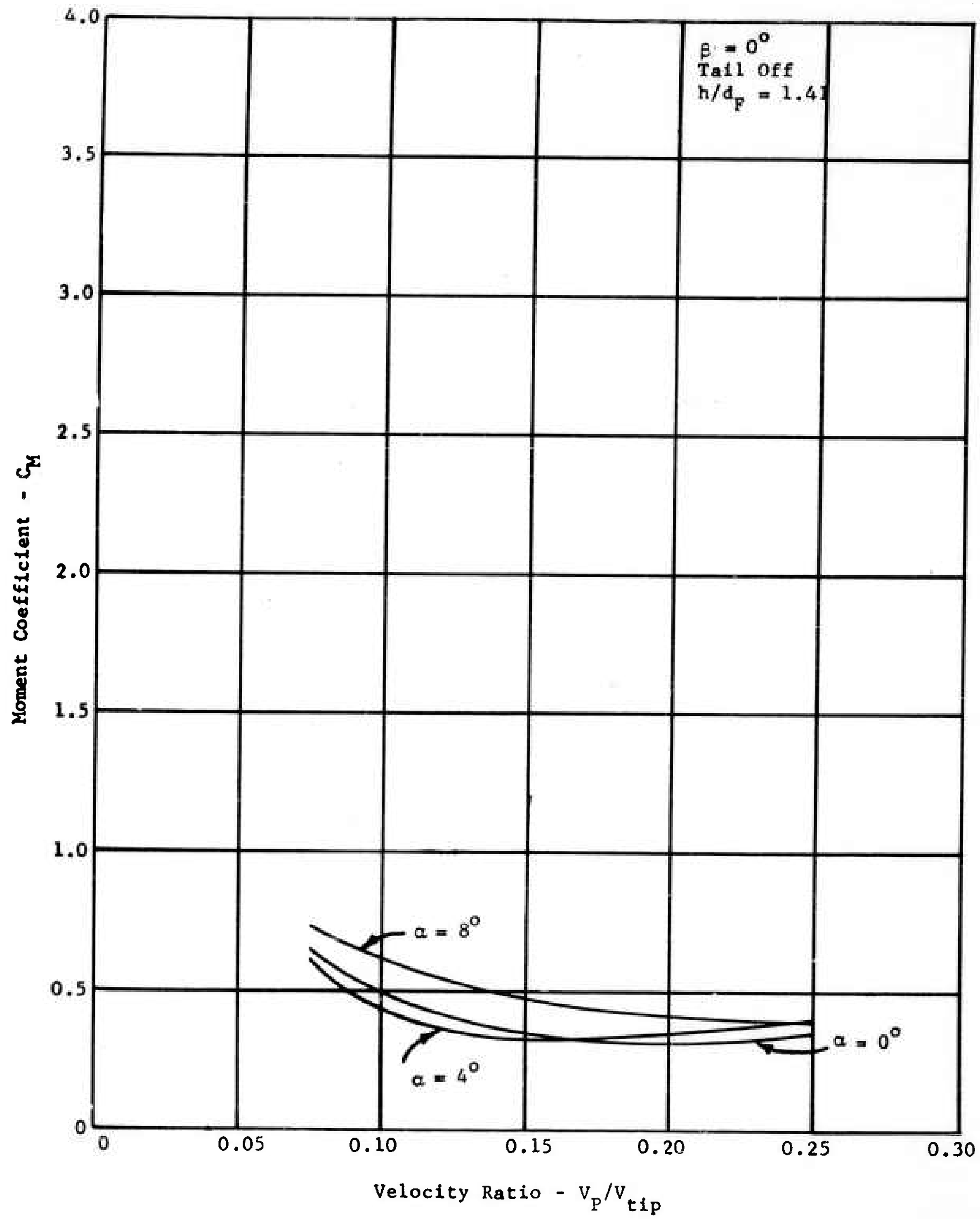

FIGURE 31b - PITCHING MOMENT COEFFICIENT VERSUS VELOCITY RATIO (TAIL OFF)

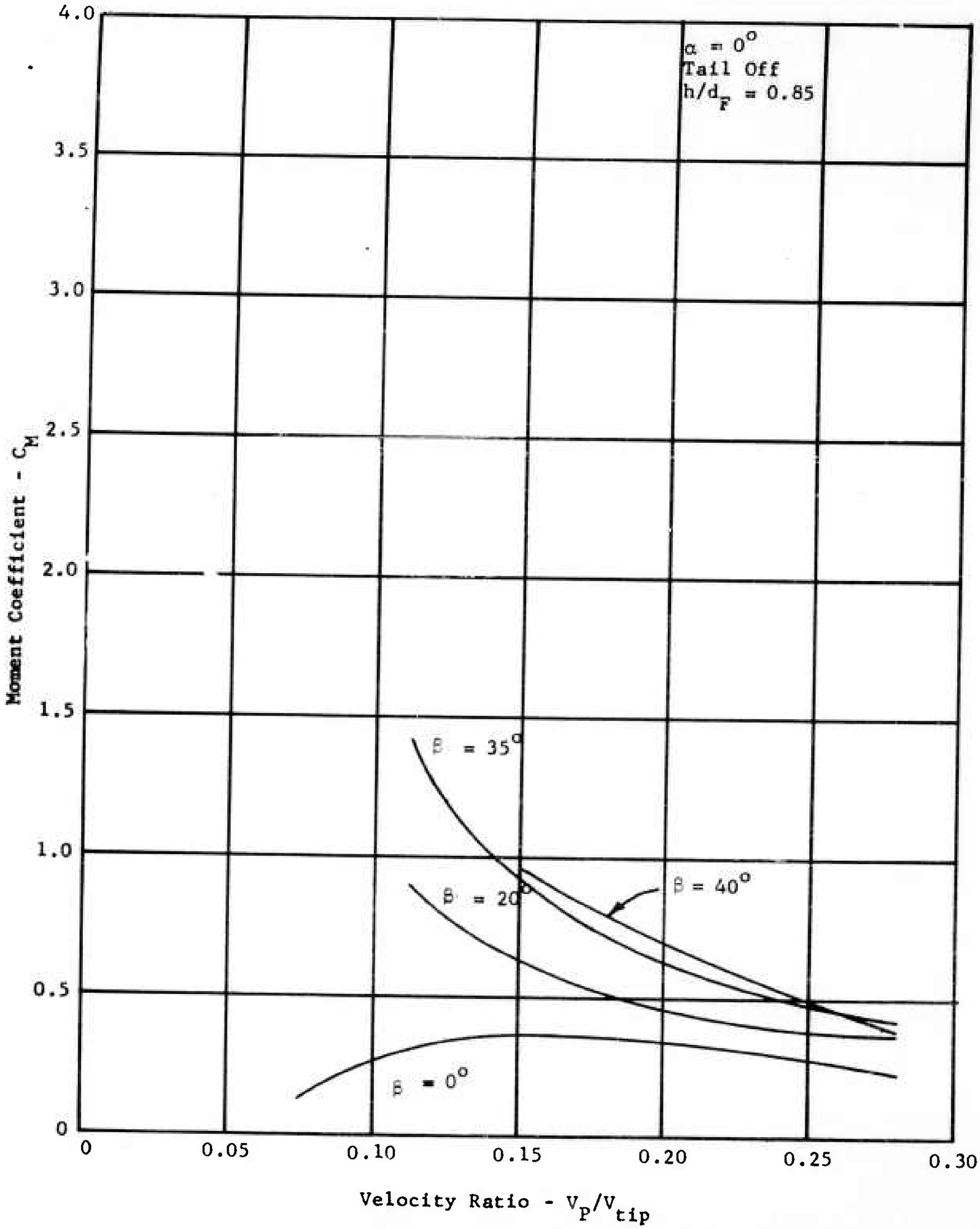

FIGURE 31c - PITCHING MOMENT COEFFICIENT VERSUS VELOCITY RATIO (TAIL OFF)

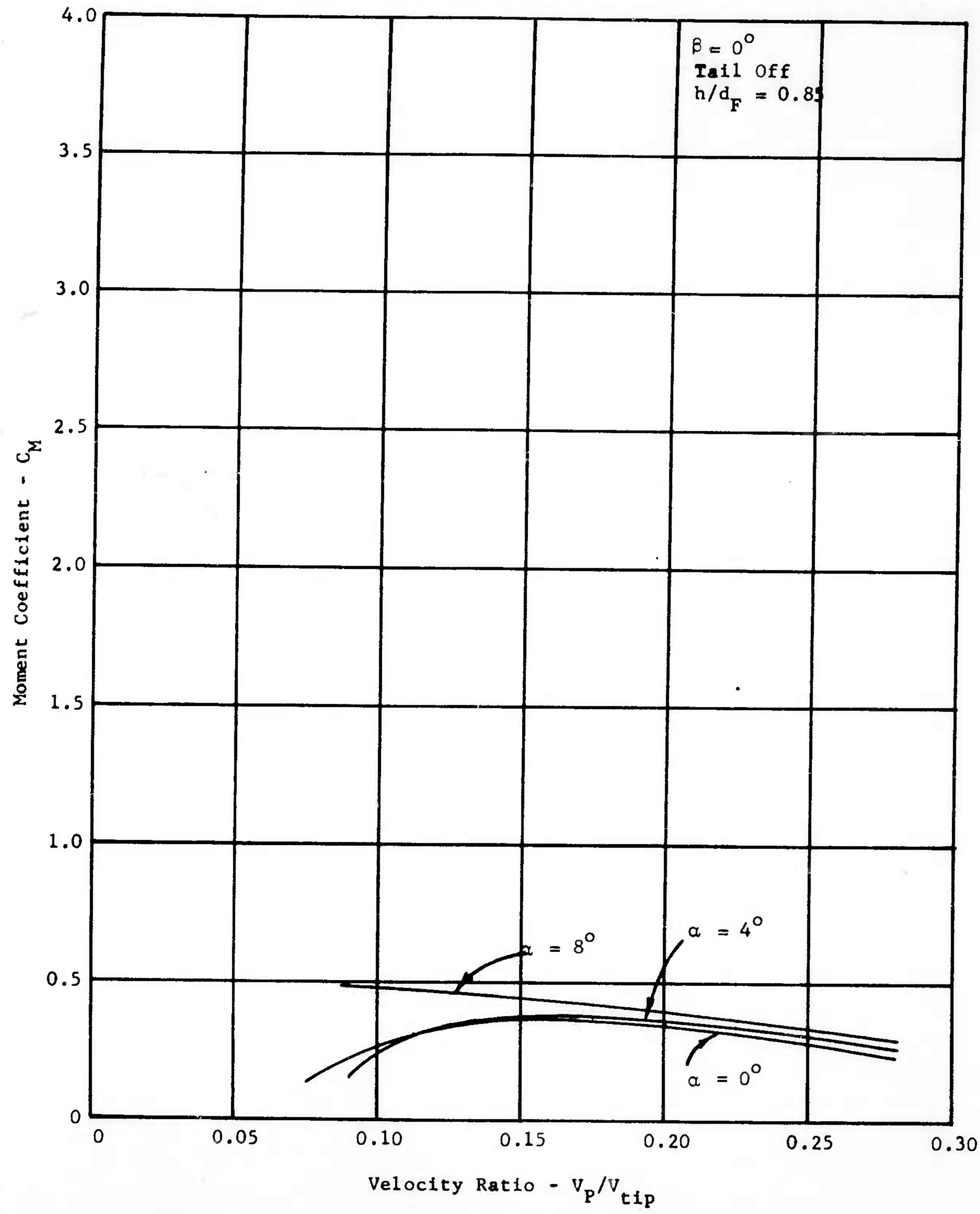

FIGURE 31d - PITCHING MOMENT COEFFICIENT VERSUS VELOCITY RATIO (TAIL OFF)

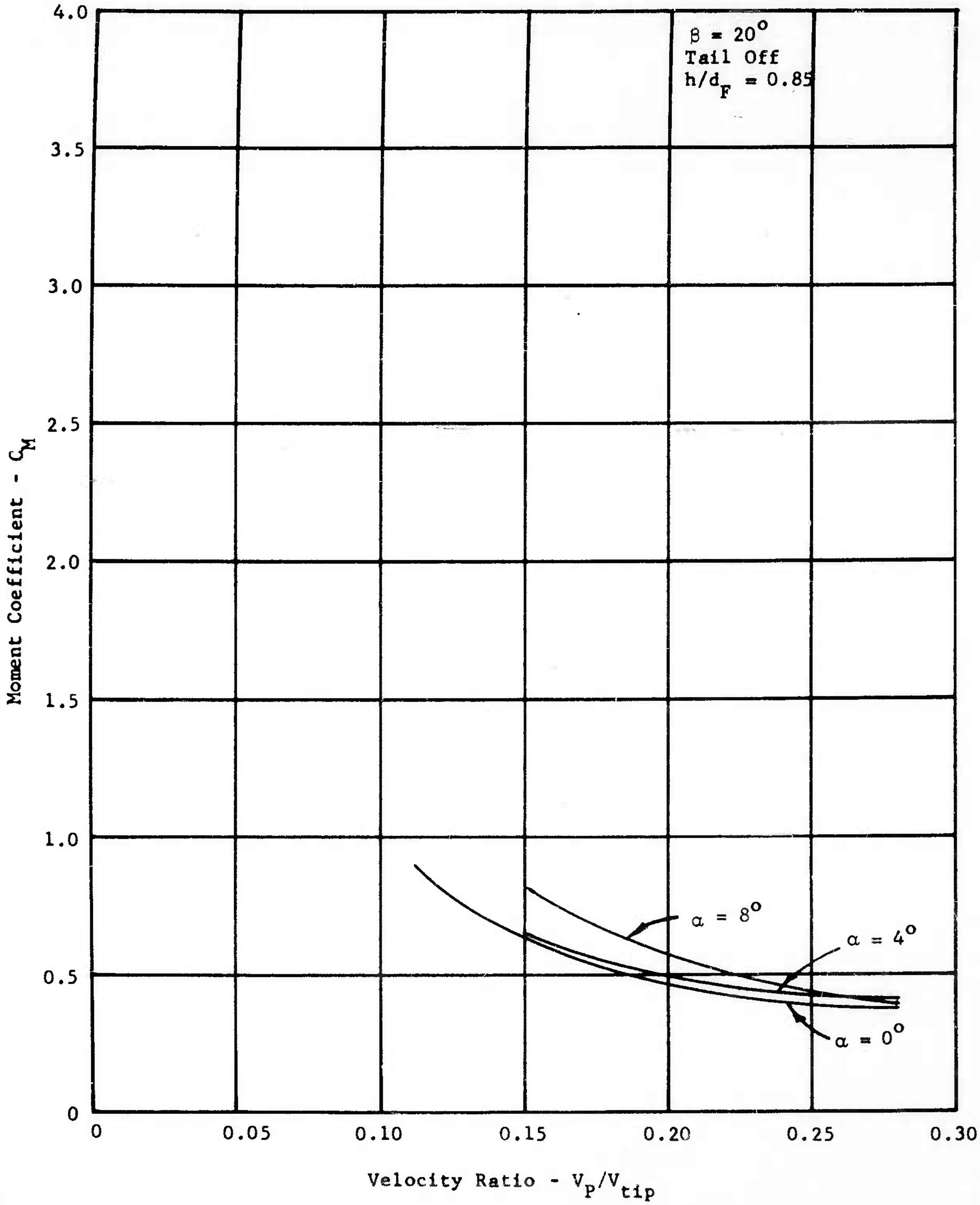

FIGURE 31e - PITCHING MOMENT COEFFICIENT VERSUS VELOCITY RATIO (TAIL OFF)

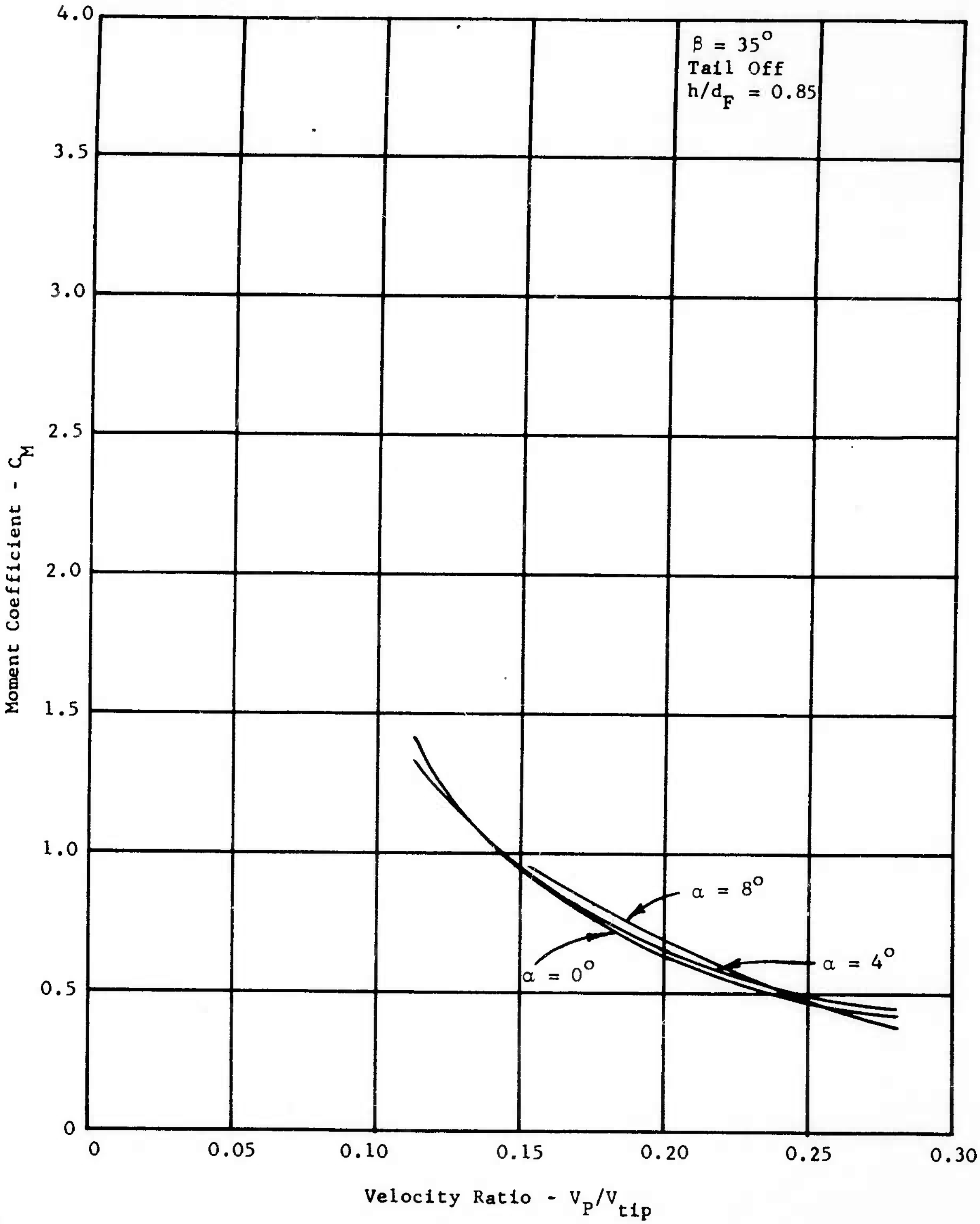

FIGURE 31f - PITCHING MOMENT COEFFICIENT VERSUS VELOCITY RATIO (TAIL OFF)

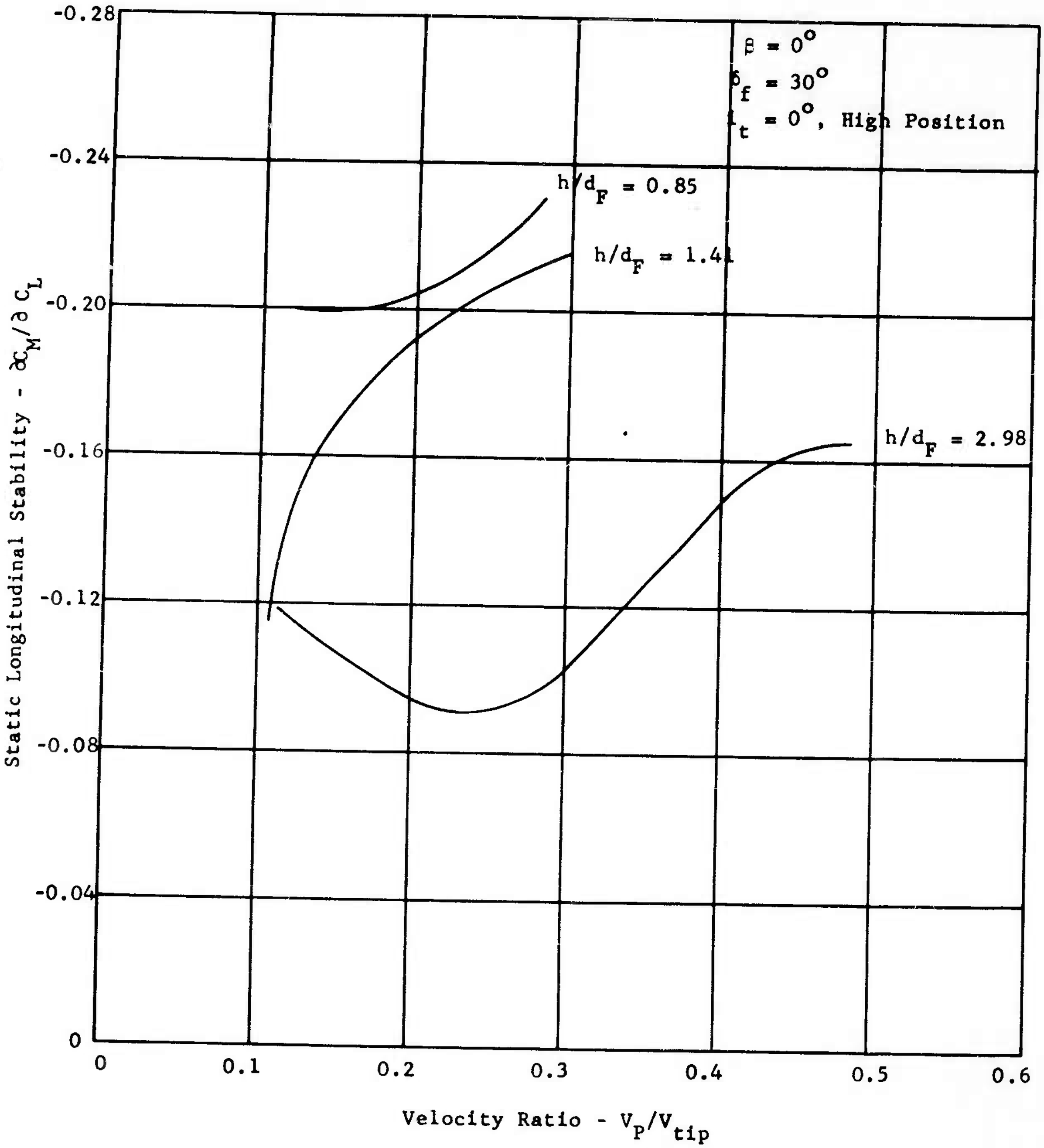

FIGURE 32a - STATIC LONGITUDINAL STABILITY VERSUS VELOCITY RATIO

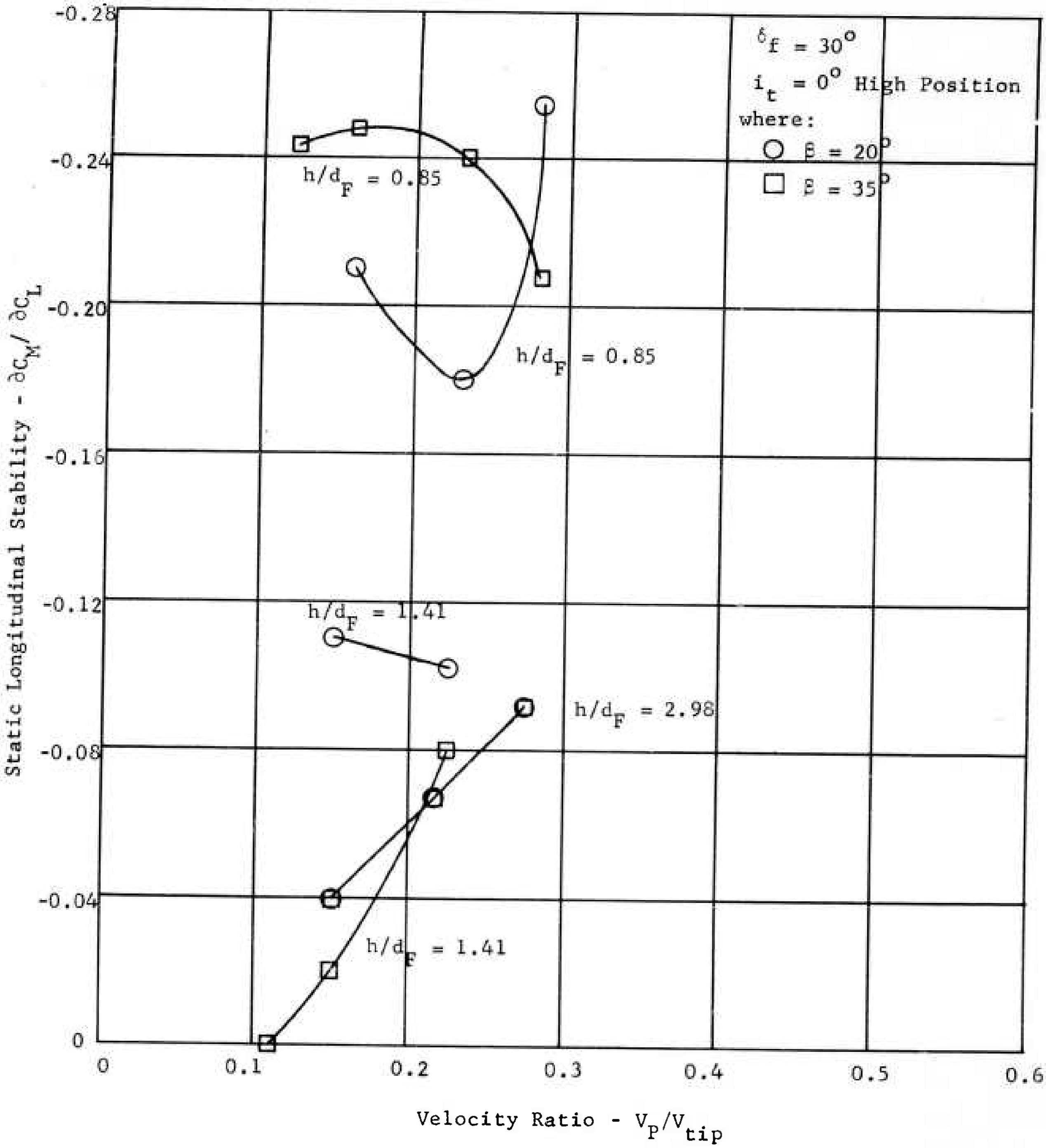

FIGURE 32b - STATIC LONGITUDINAL STABILITY VERSUS VELOCITY RATIO

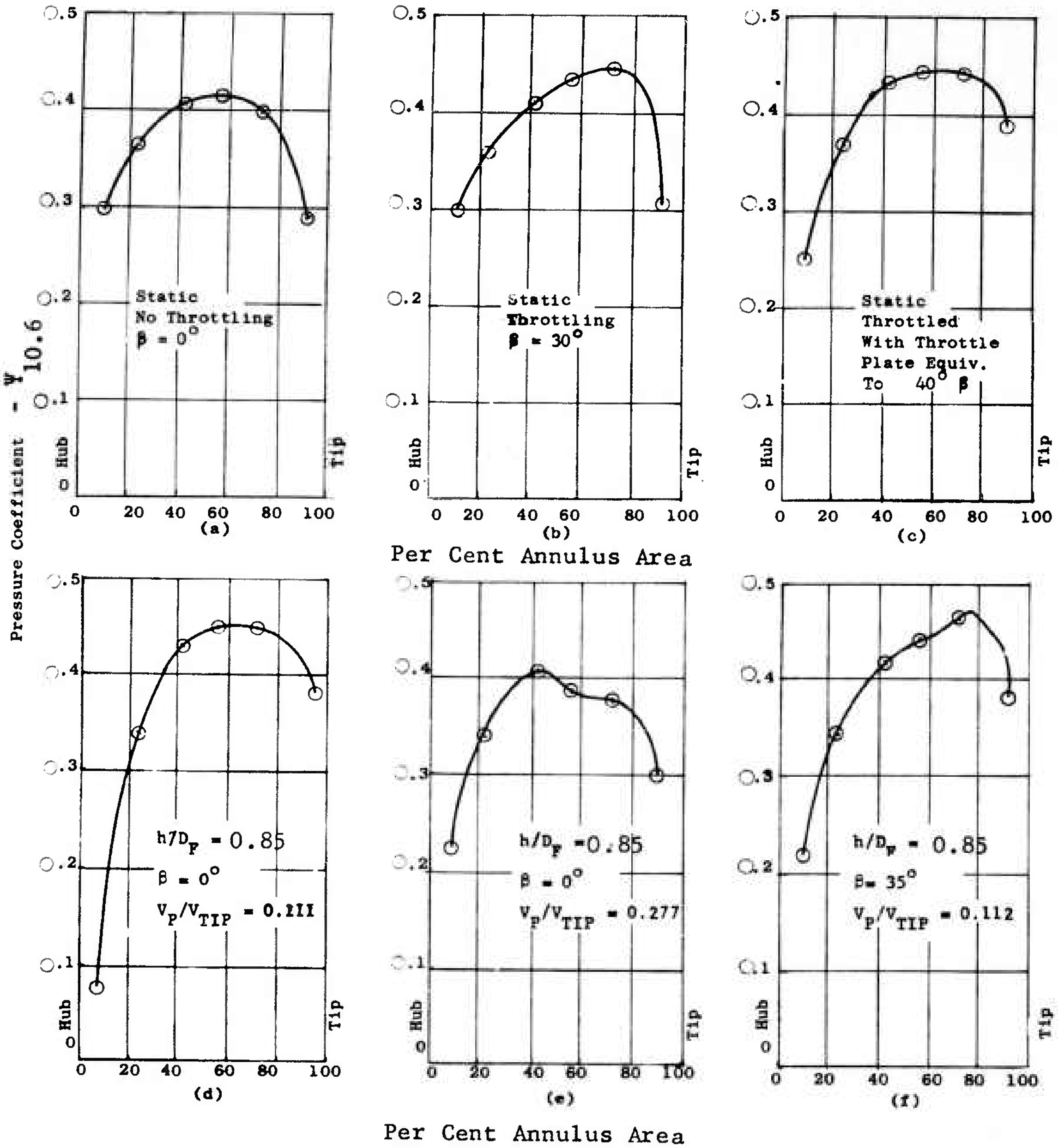

FIGURE 33 - PRESSURE COEFFICIENT VERSUS PER CENT ANNULUS AREA

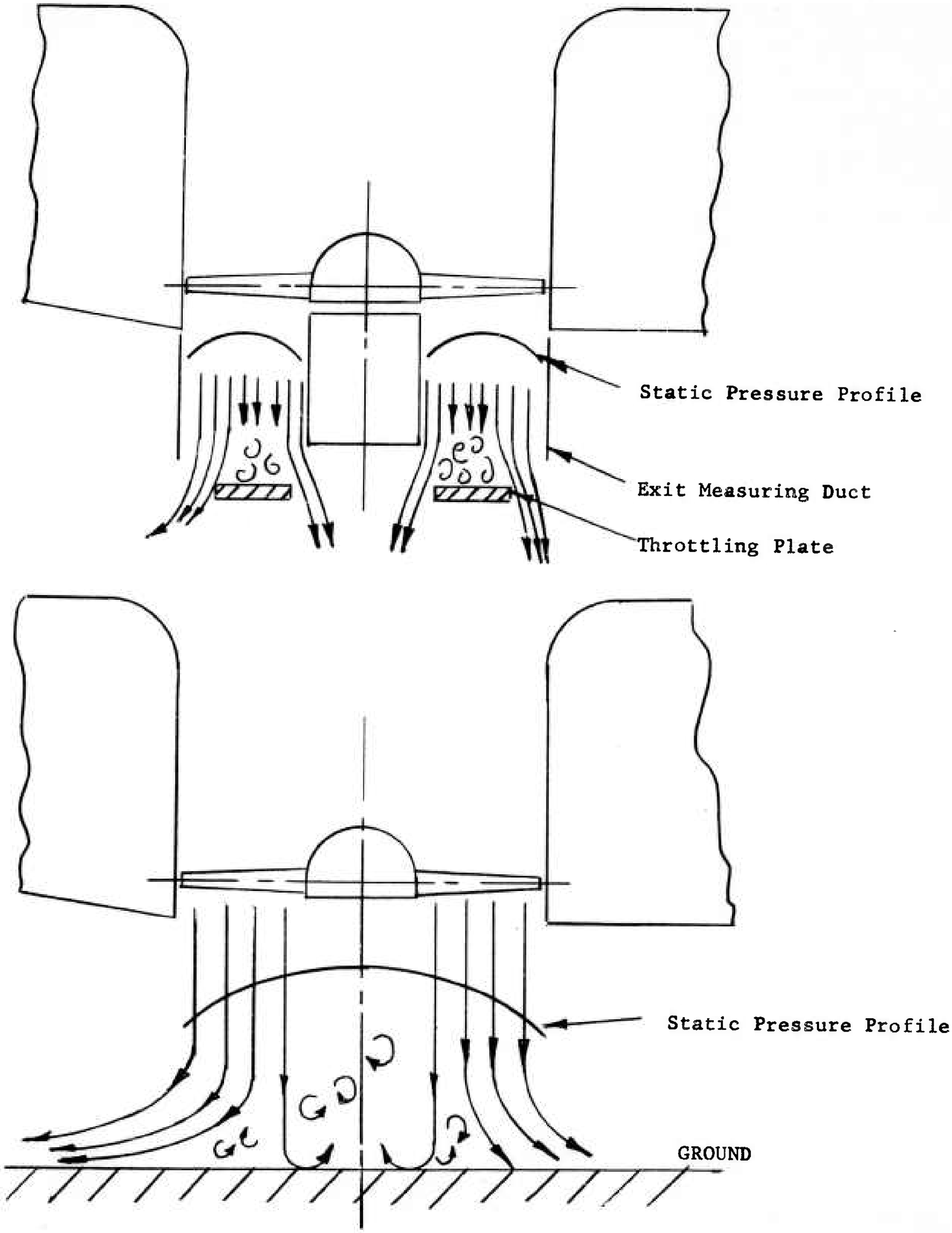

Figure 34 - Comparison of Throttling Methods
(Annular Plate vs "Infinite" Plate)

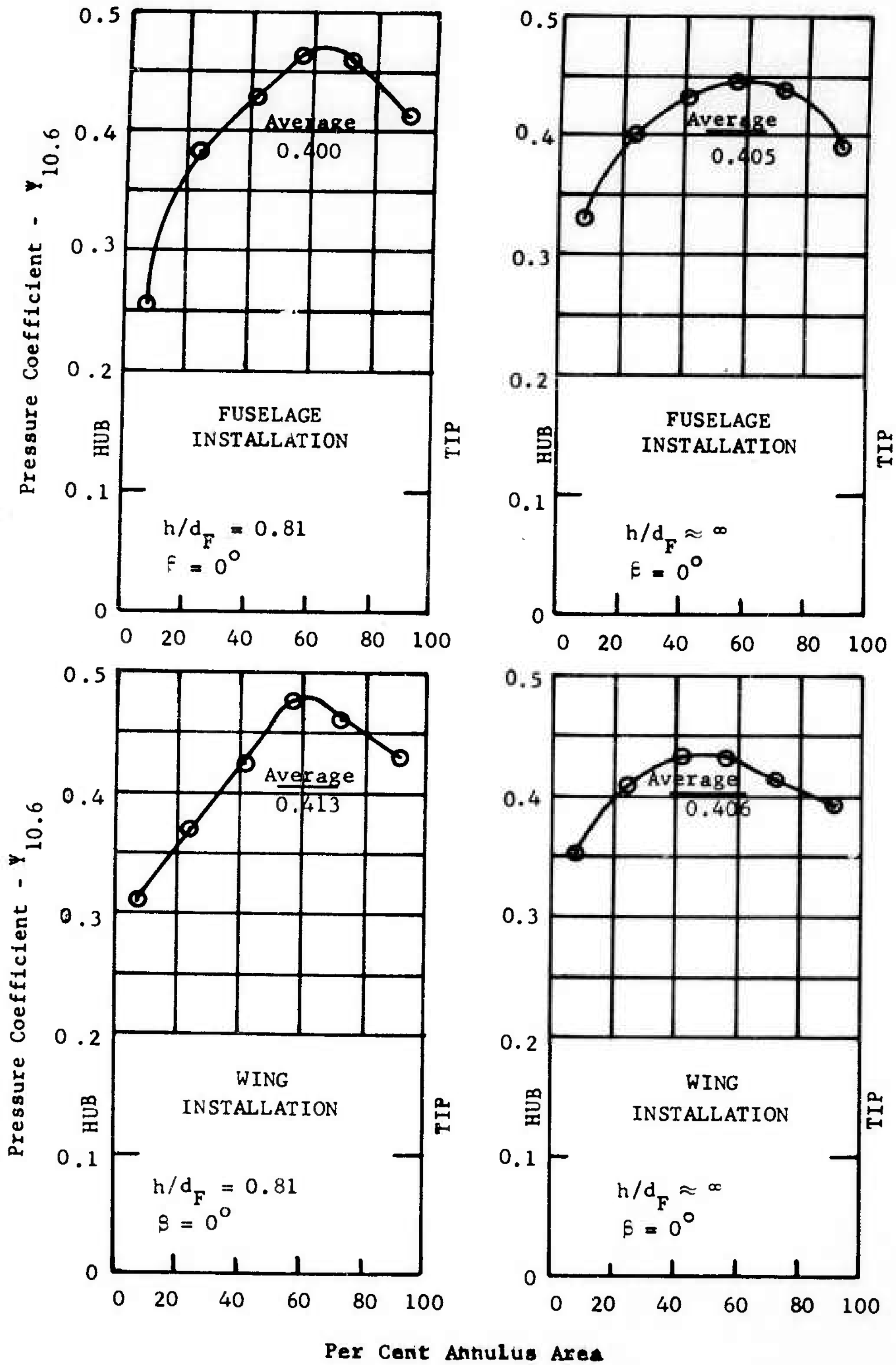

FIGURE 35 - 26 INCH SCALE MODEL FAN PRESSURE COEFFICIENTS VERSUS PER CENT ANNULUS AREA

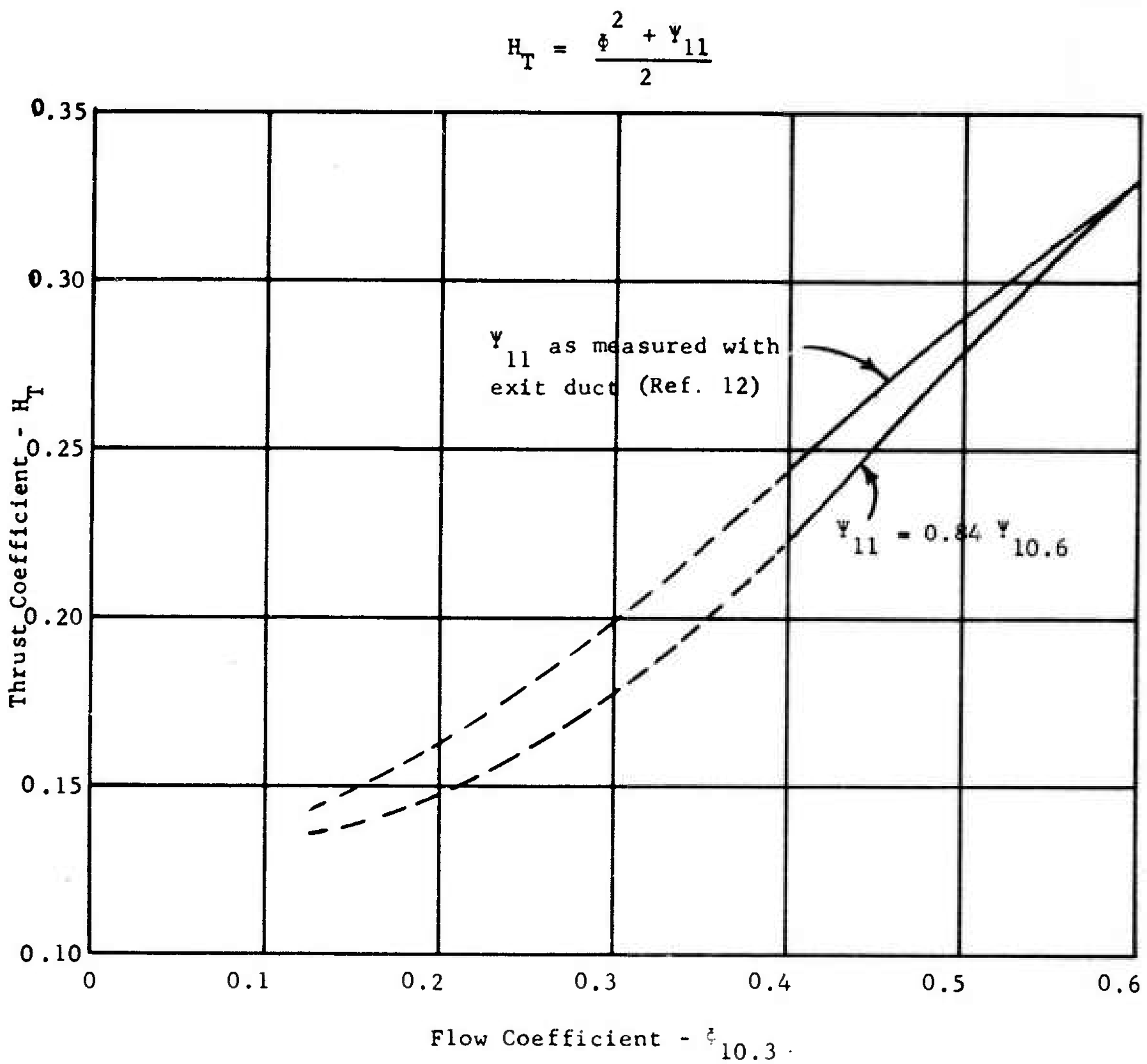

FIGURE 36 - THRUST COEFFICIENT VERSUS FLOW COEFFICIENT

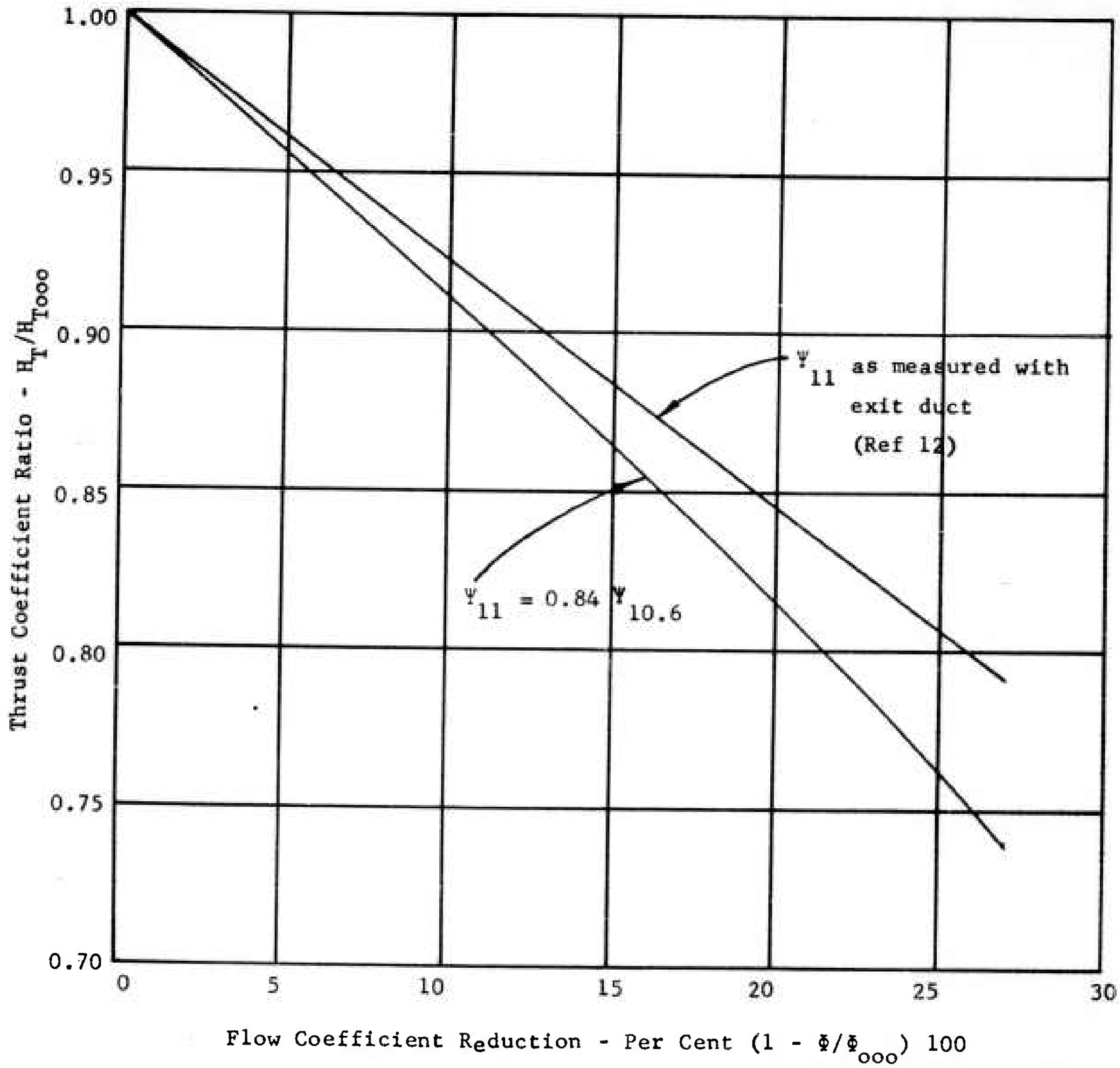

FIGURE 37 - THRUST COEFFICIENT RATIO VERSUS FLOW COEFFICIENT REDUCTION

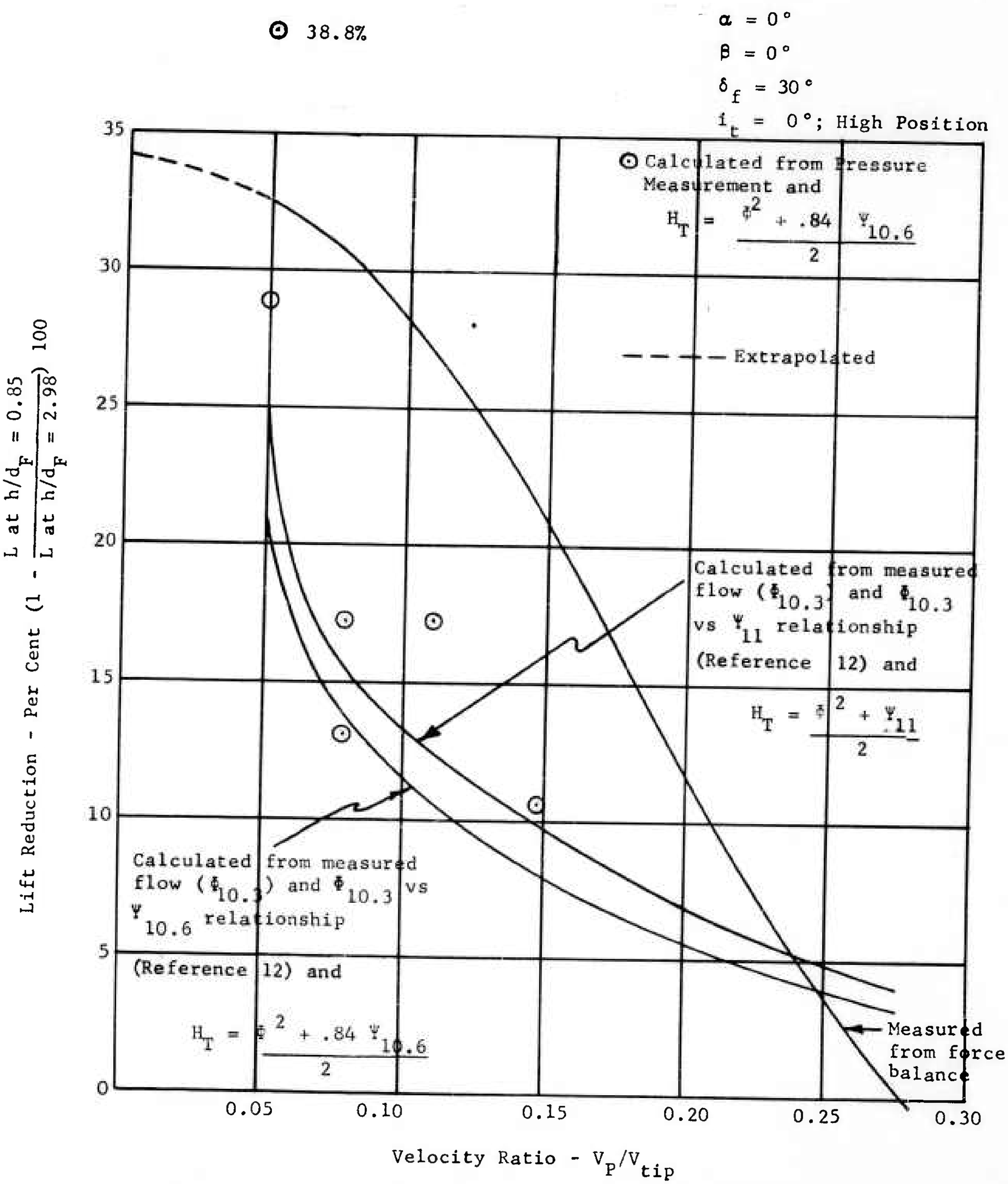

FIGURE 38 - LIFT REDUCTION AT 0.85 h/d_F VERSUS VELOCITY RATIO

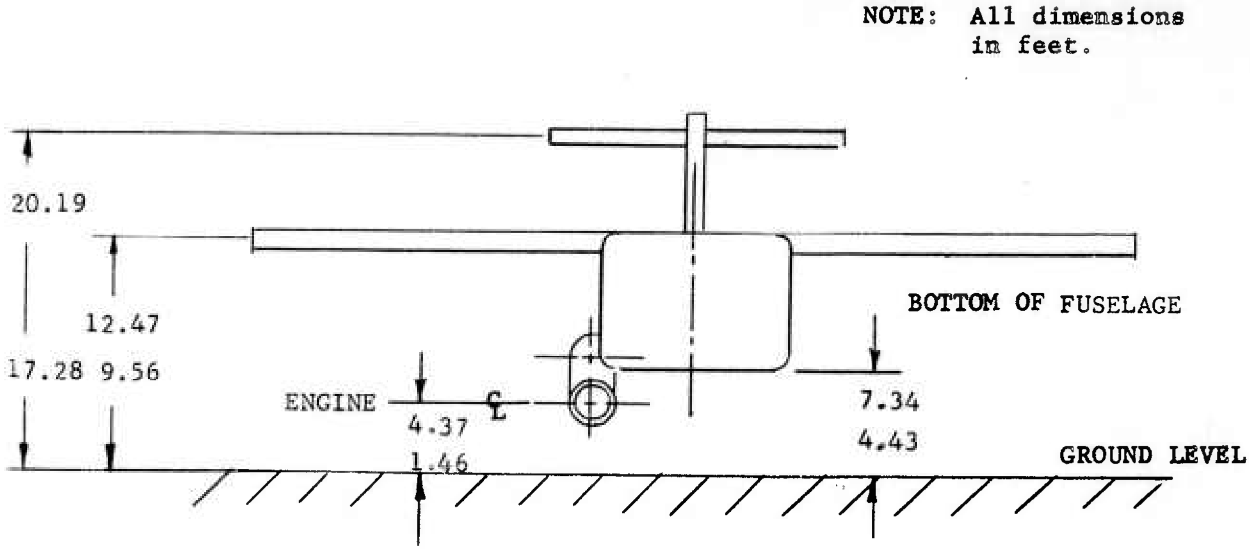

FIGURE 39 - NASA FULL SCALE AIRCRAFT FRONT VIEW SHOWING HEIGHTS ABOVE GROUND FOR 1.41 AND 0.85 h/d_F .

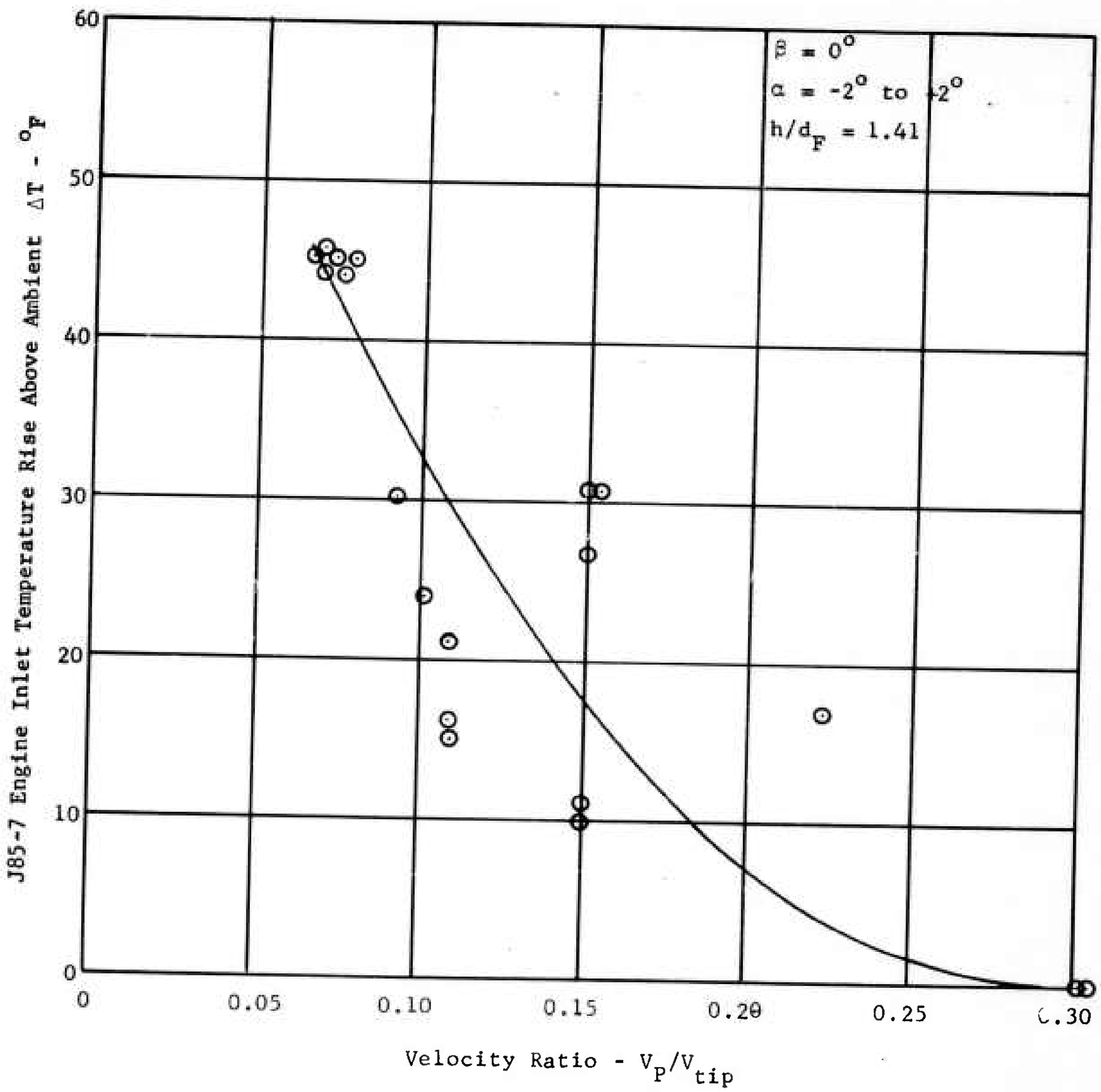

FIGURE 40a - J85-7 ENGINE REINGESTION VERSUS VELOCITY RATIO

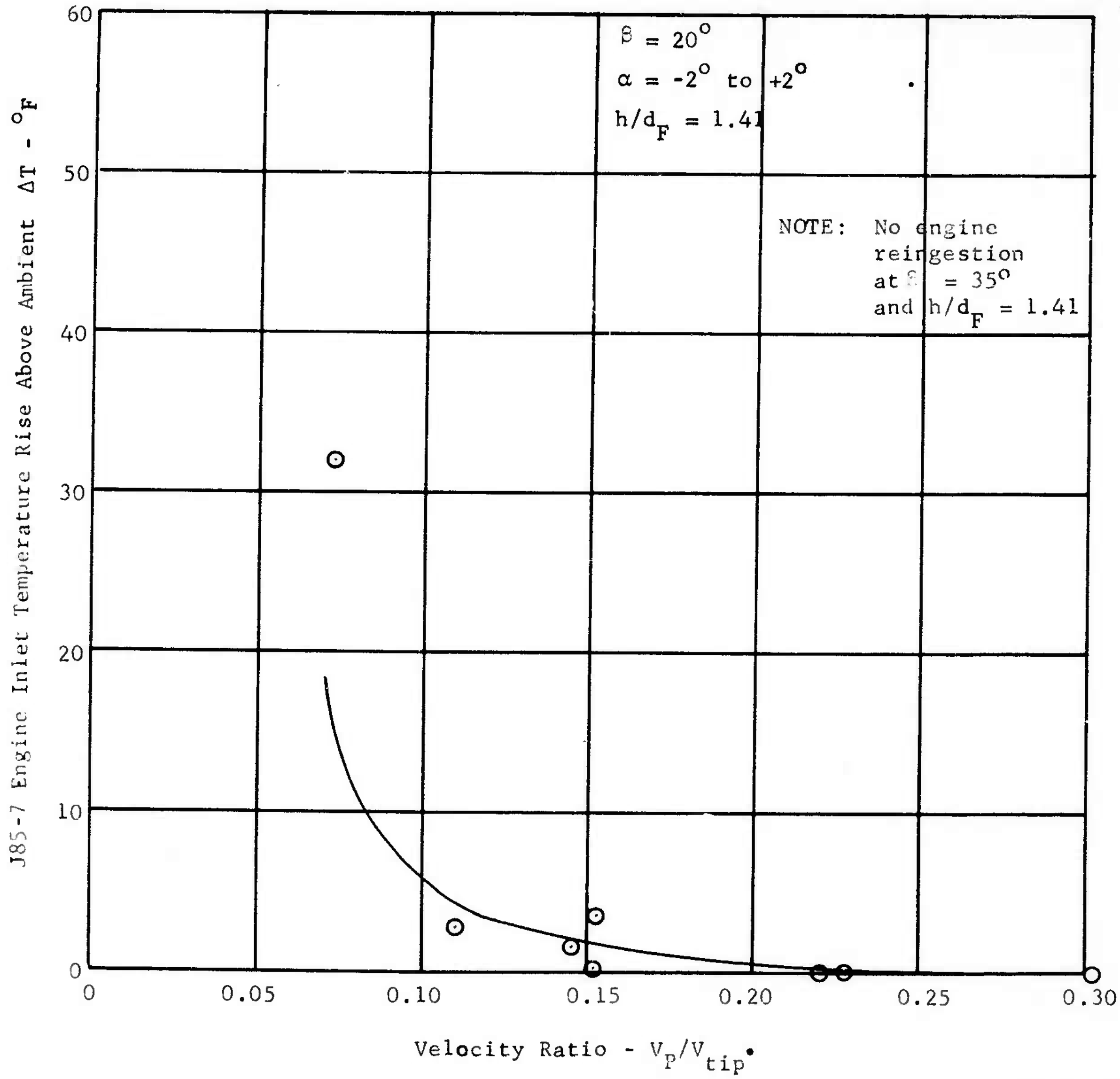

FIGURE 40b - J85-7 ENGINE REINGESTION VERSUS VELOCITY RATIO

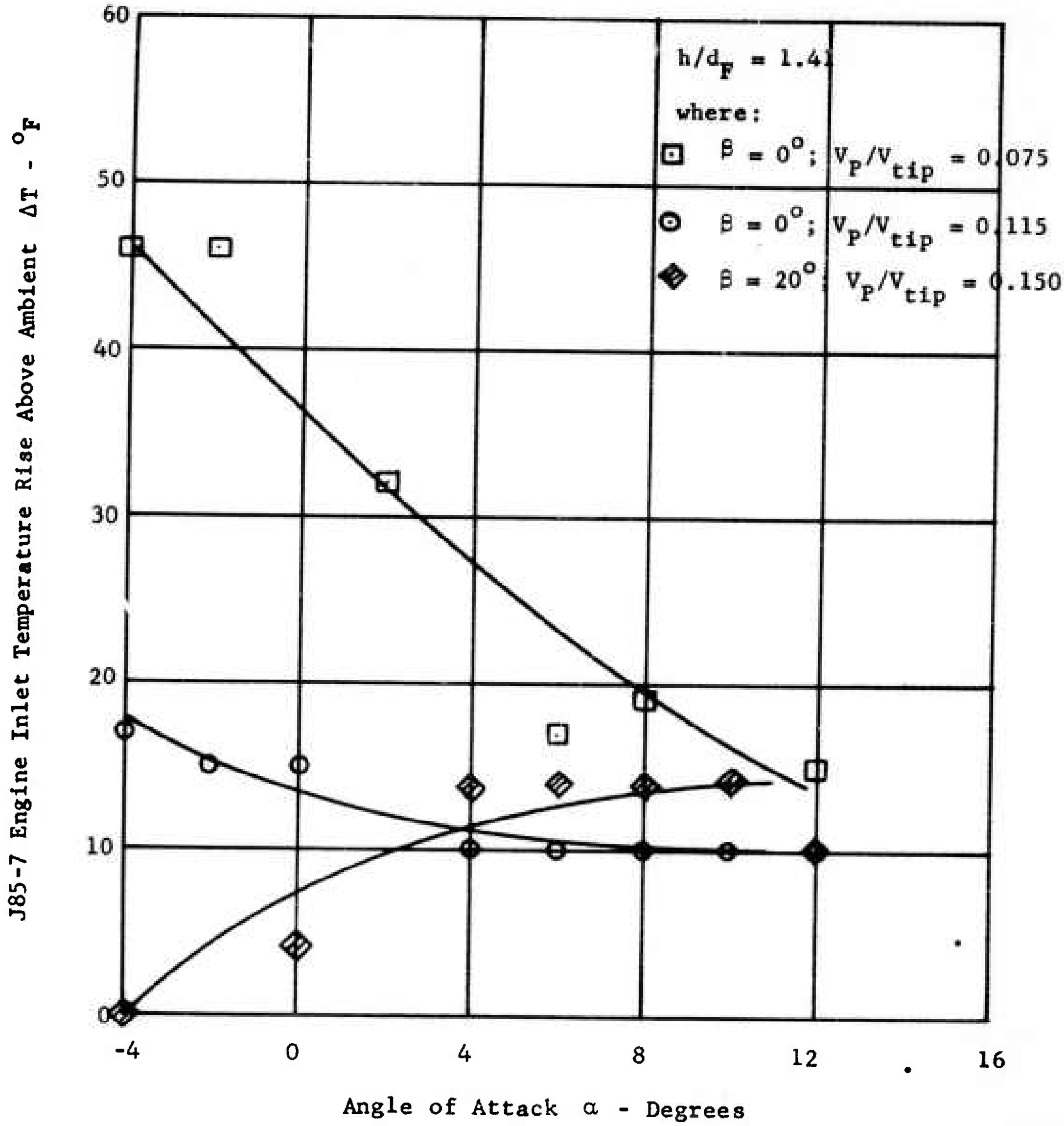

FIGURE 41 - J85-7 ENGINE REINGESTION VERSUS ANGLE OF ATTACK

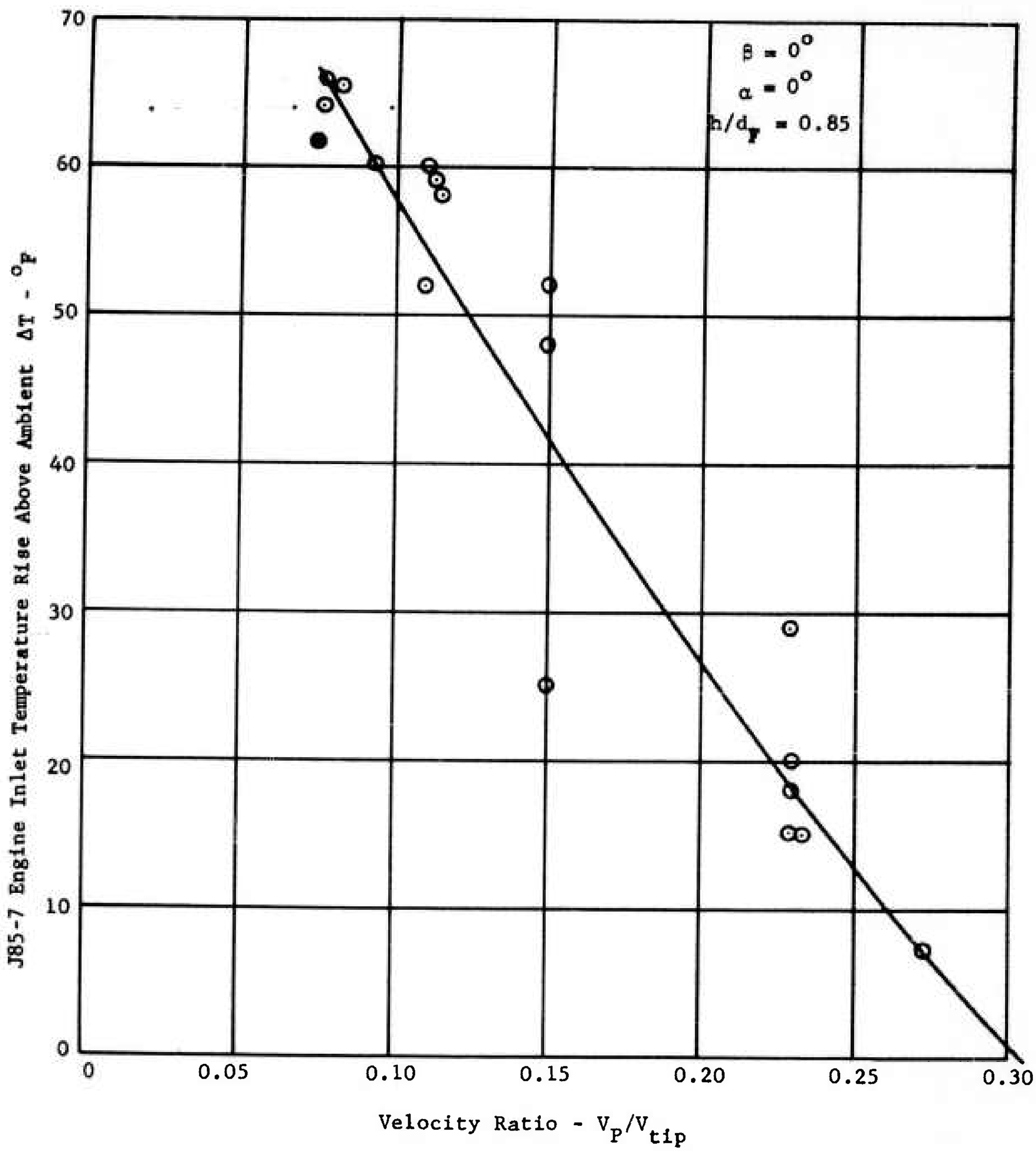

FIGURE 42a - J85-7 ENGINE REINGESTION VERSUS VELOCITY RATIO

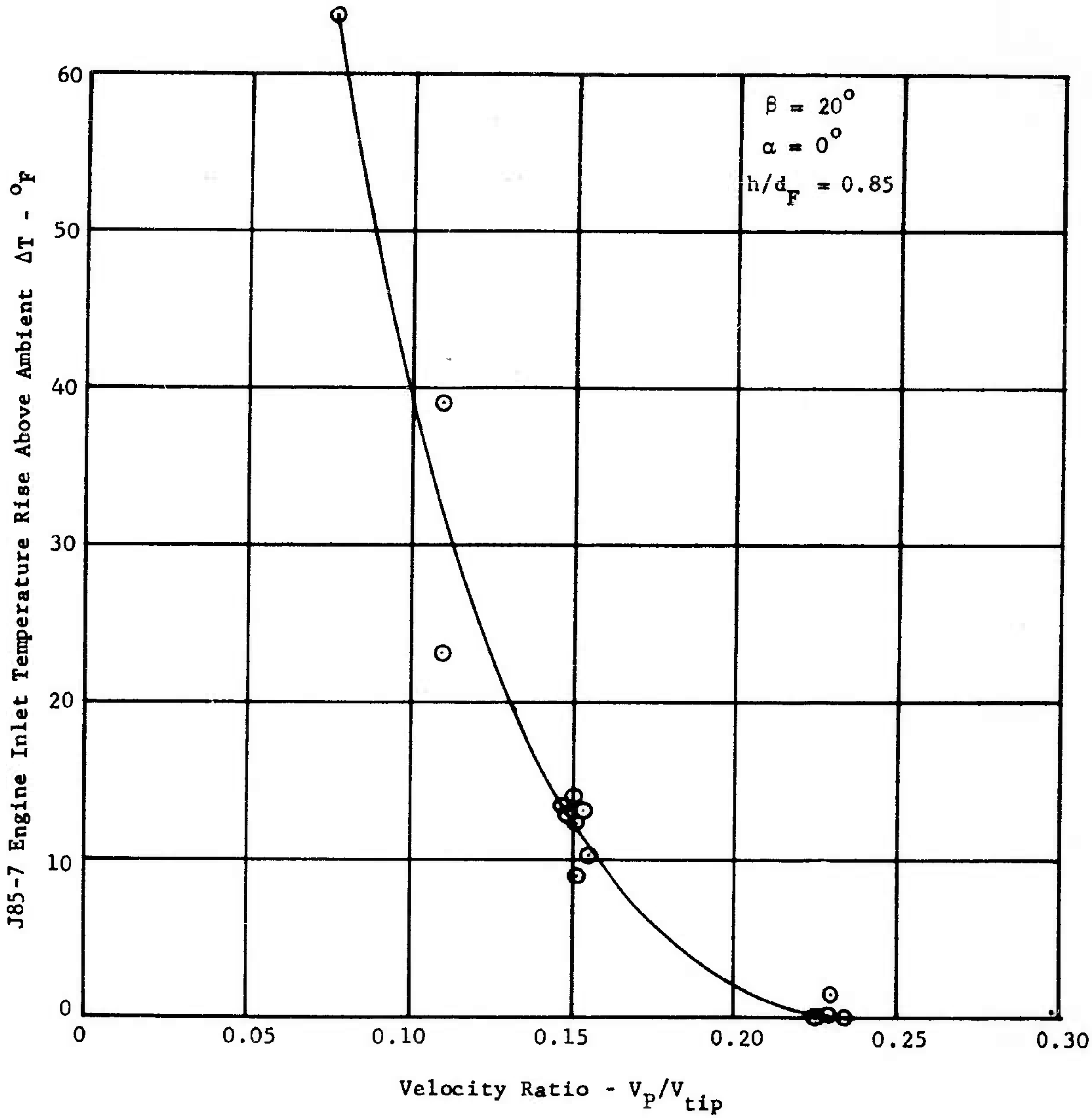

FIGURE 42b - J85-7 ENGINE REINGESTION VERSUS VELOCITY RATIO

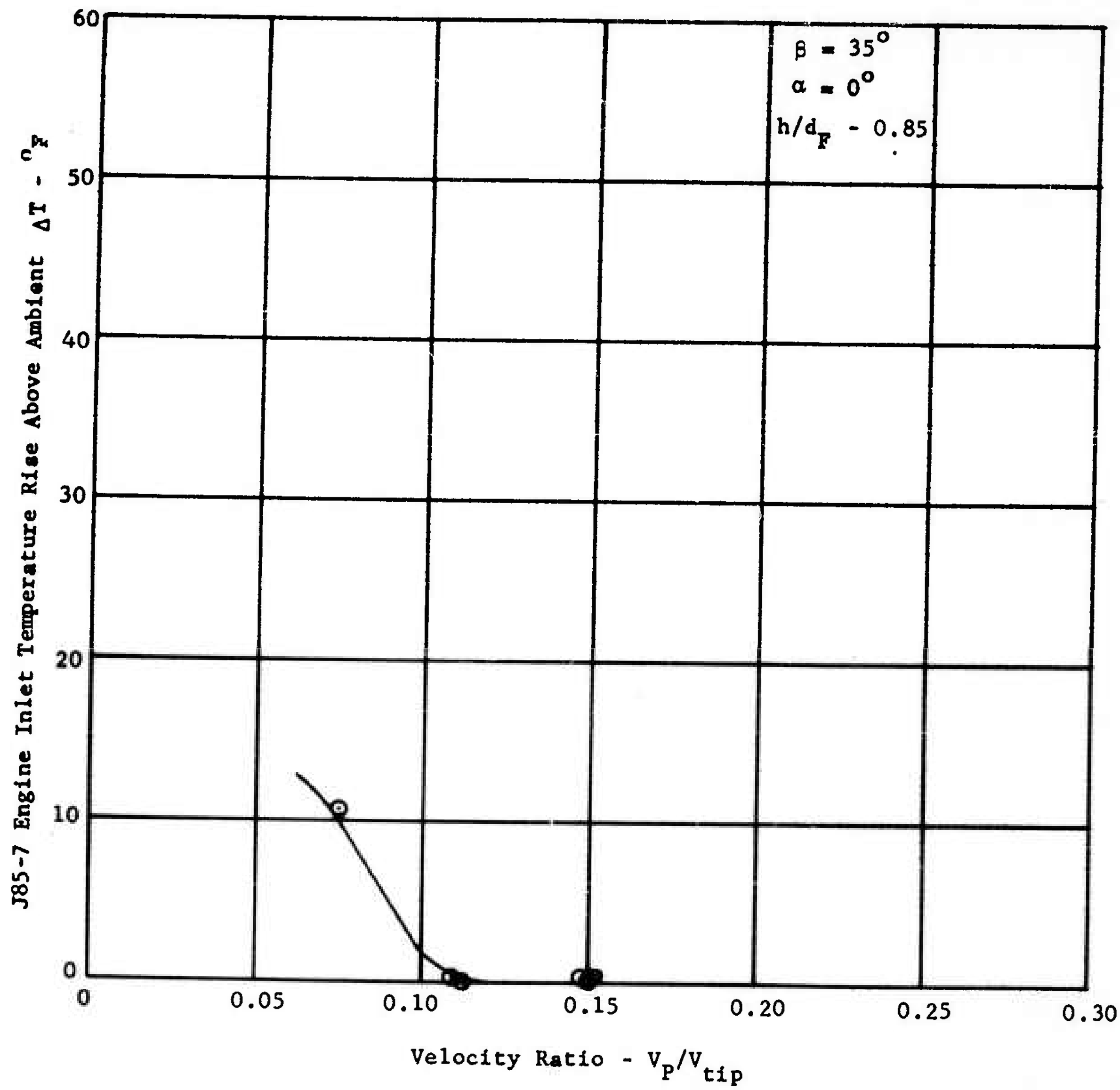

FIGURE 42c - J85-7 ENGINE REINGESTION VERSUS VELOCITY RATIO

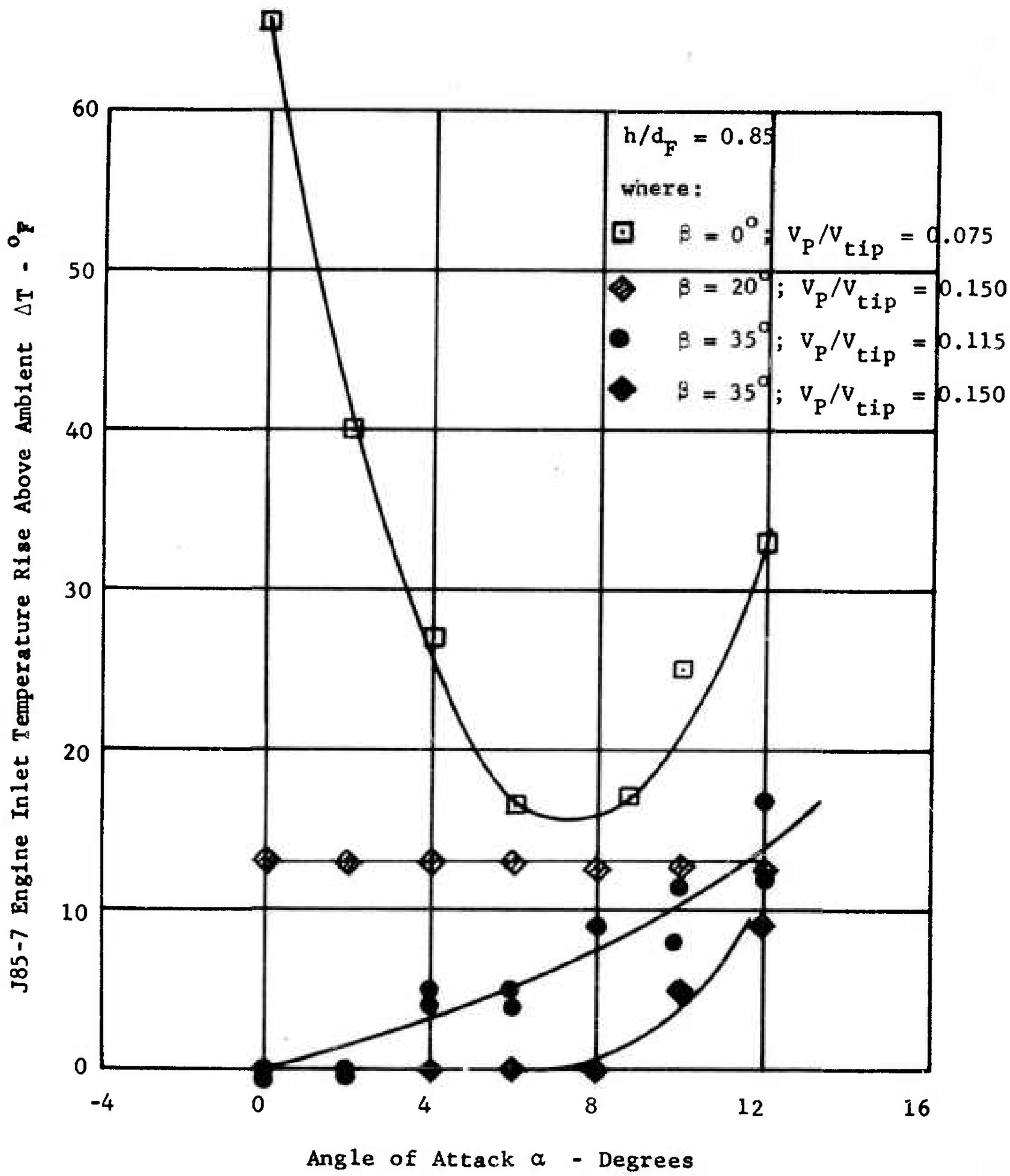

FIGURE 43 - J85-7 ENGINE REINGESTION VERSUS ANGLE OF ATTACK

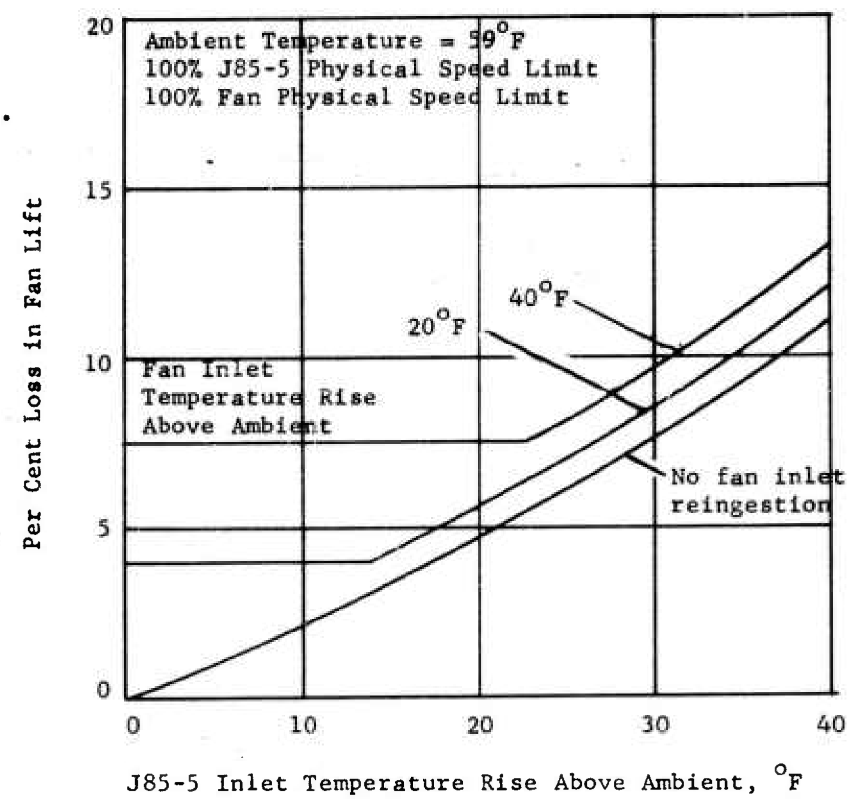

FIGURE 44 - J85-5 AND FAN INLET REINGESTION EFFECTS ON FAN THRUST

Where:

● Thermocouple (T/C) location

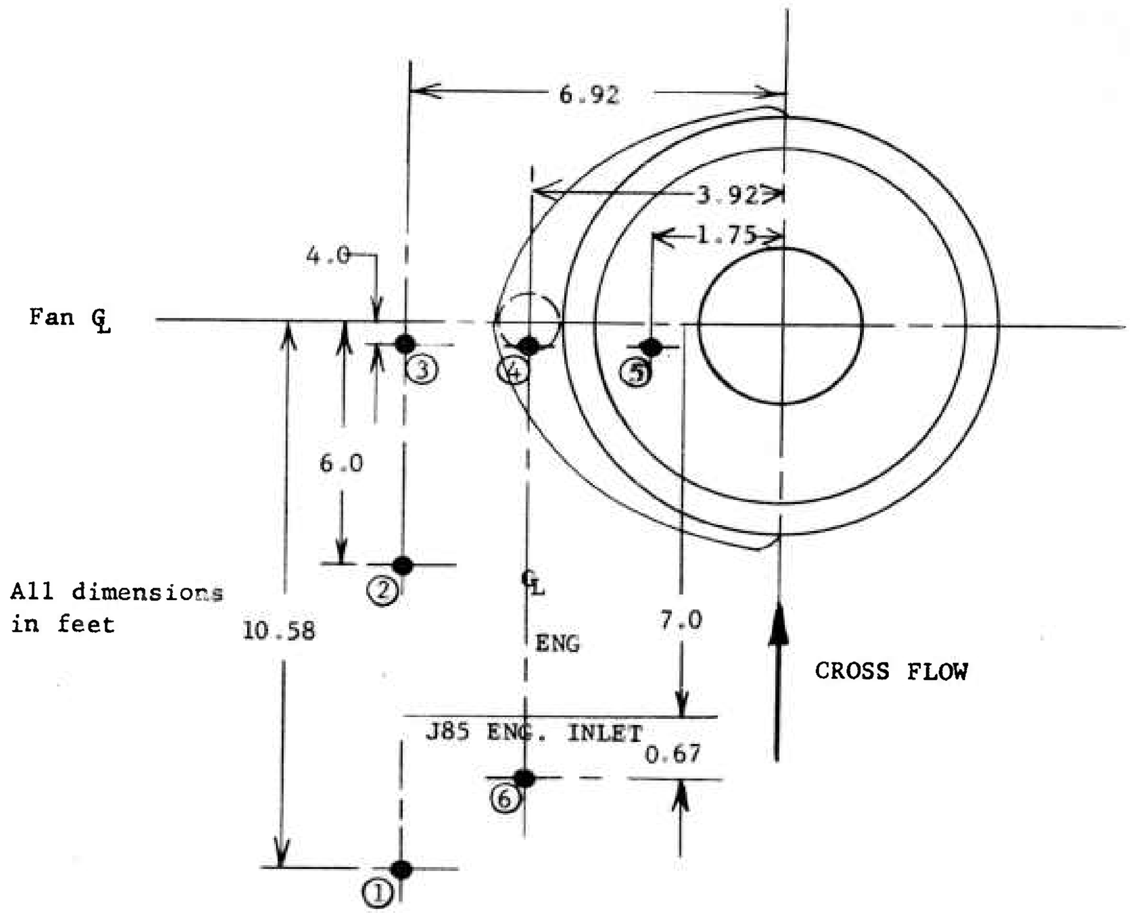

Figure 45 - Thermocouple Layout (Tunnel Floor)

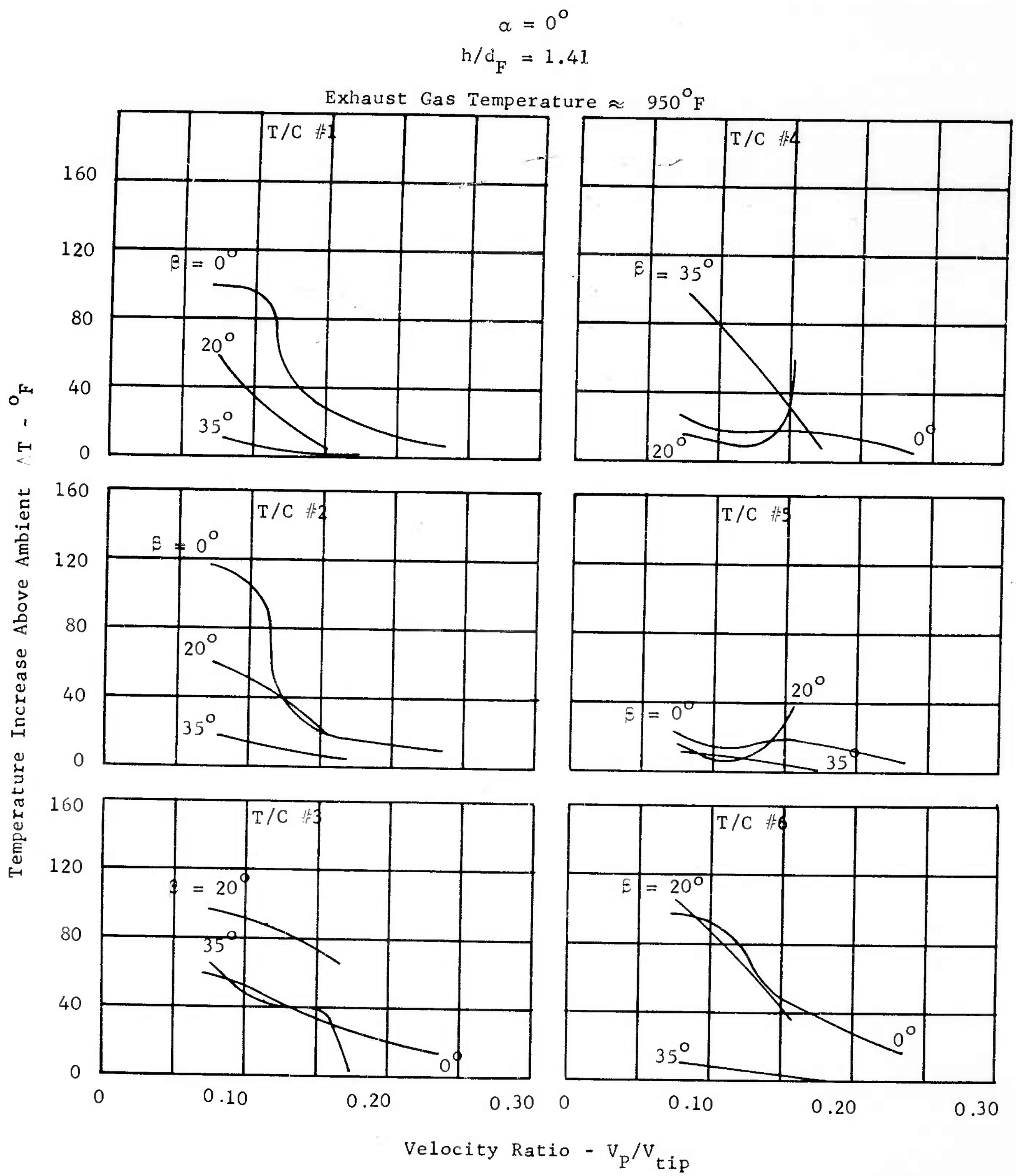

FIGURE 46a - AIR TEMPERATURE INCREASE AT GROUND LEVEL VERSUS VELOCITY RATIO (SEE FIGURE 45 FOR THERMOCOUPLE LOCATION)

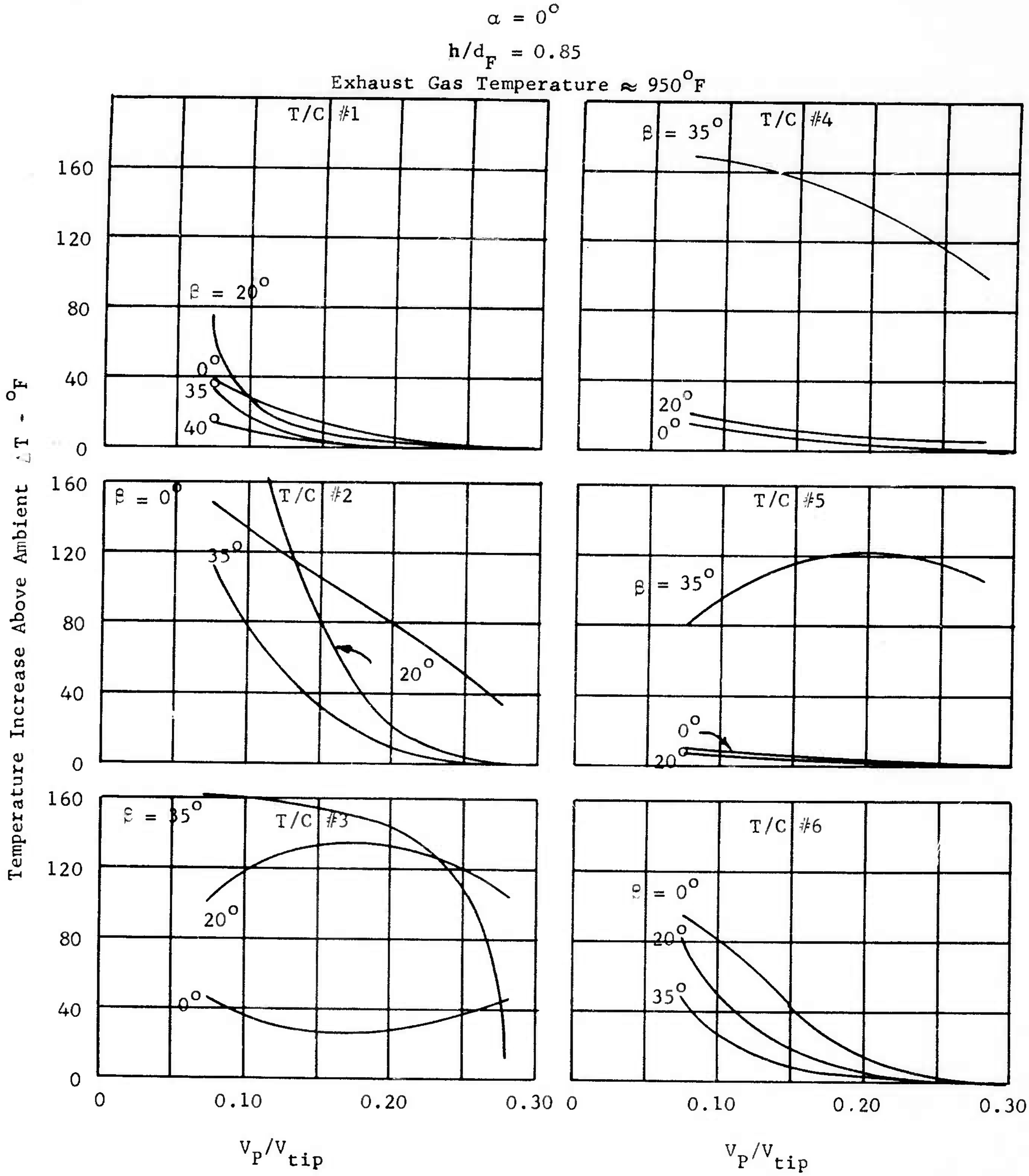

FIGURE 46b - AIR TEMPERATURE INCREASE AT GROUND LEVEL VERSUS VELOCITY RATIO (SEE FIGURE 45 FOR THERMOCOUPLE LOCATION)

$\beta = 0^o$

$h/d_F = 0.85$

Exhaust Gas Temperature $\approx$ 950°F

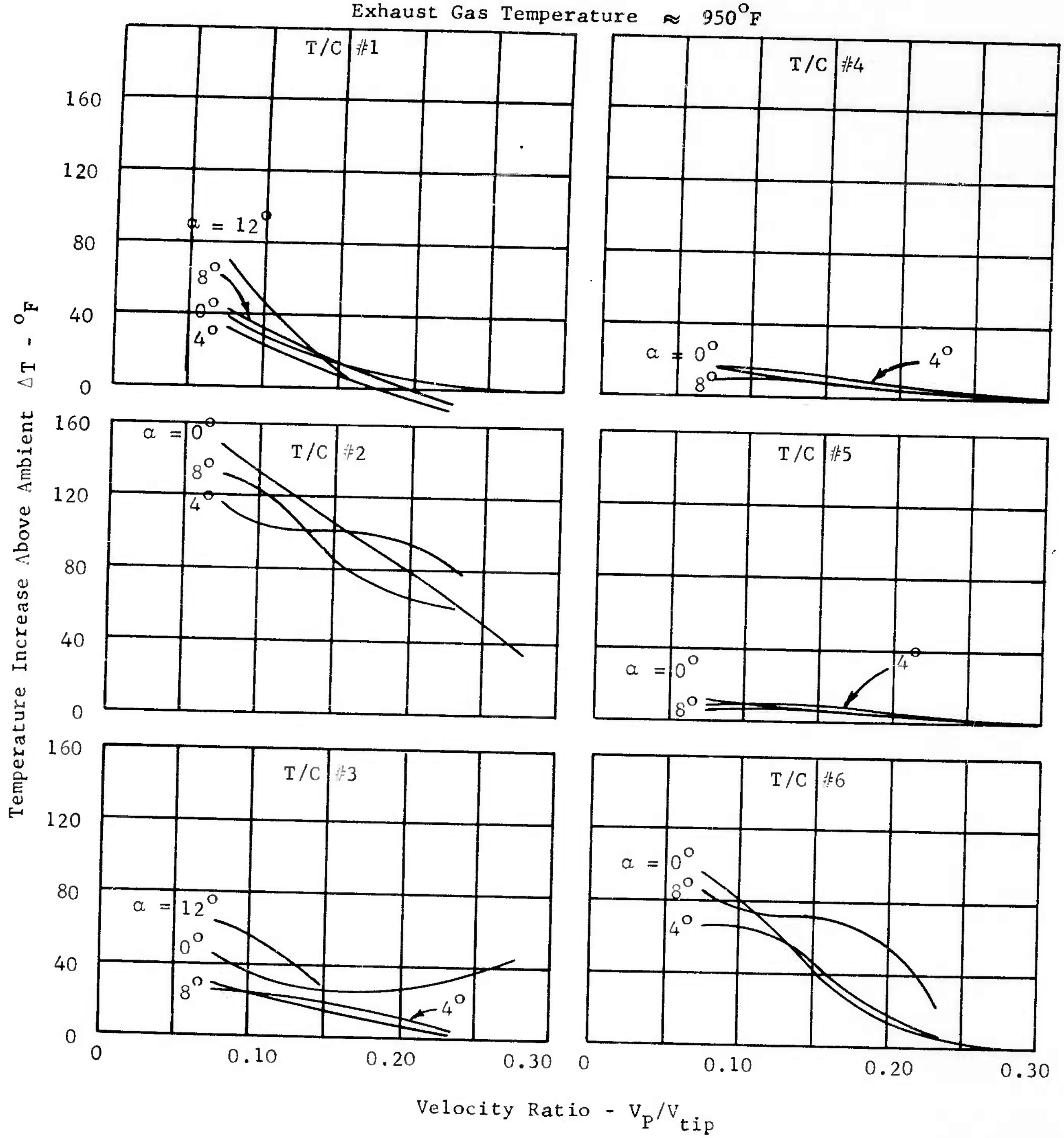

FIGURE 46c - AIR TEMPERATURE INCREASE AT GROUND LEVEL VERSUS VELOCITY RATIO (SEE FIGURE 45 FOR THERMOCOUPLE LOCATION)

β = 20°

h/d_F = 0.85

Exhaust Gas Temperature ≈ 950°F

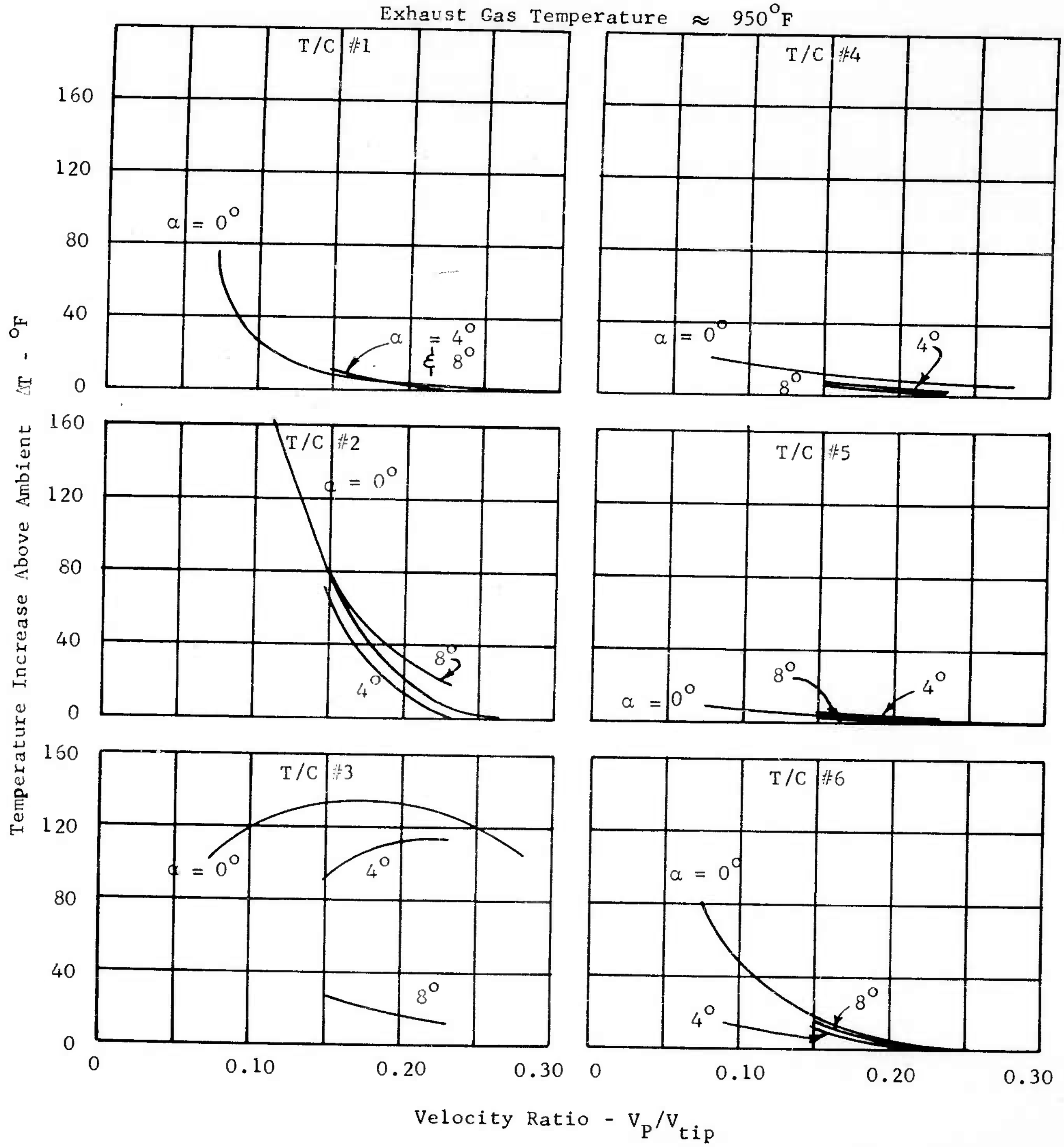

FIGURE 46d - AIR TEMPERATURE INCREASE AT GROUND LEVEL VERSUS VELOCITY RATIO (SEE FIGURE 45 FOR THERMOCOUPLE LOCATION)

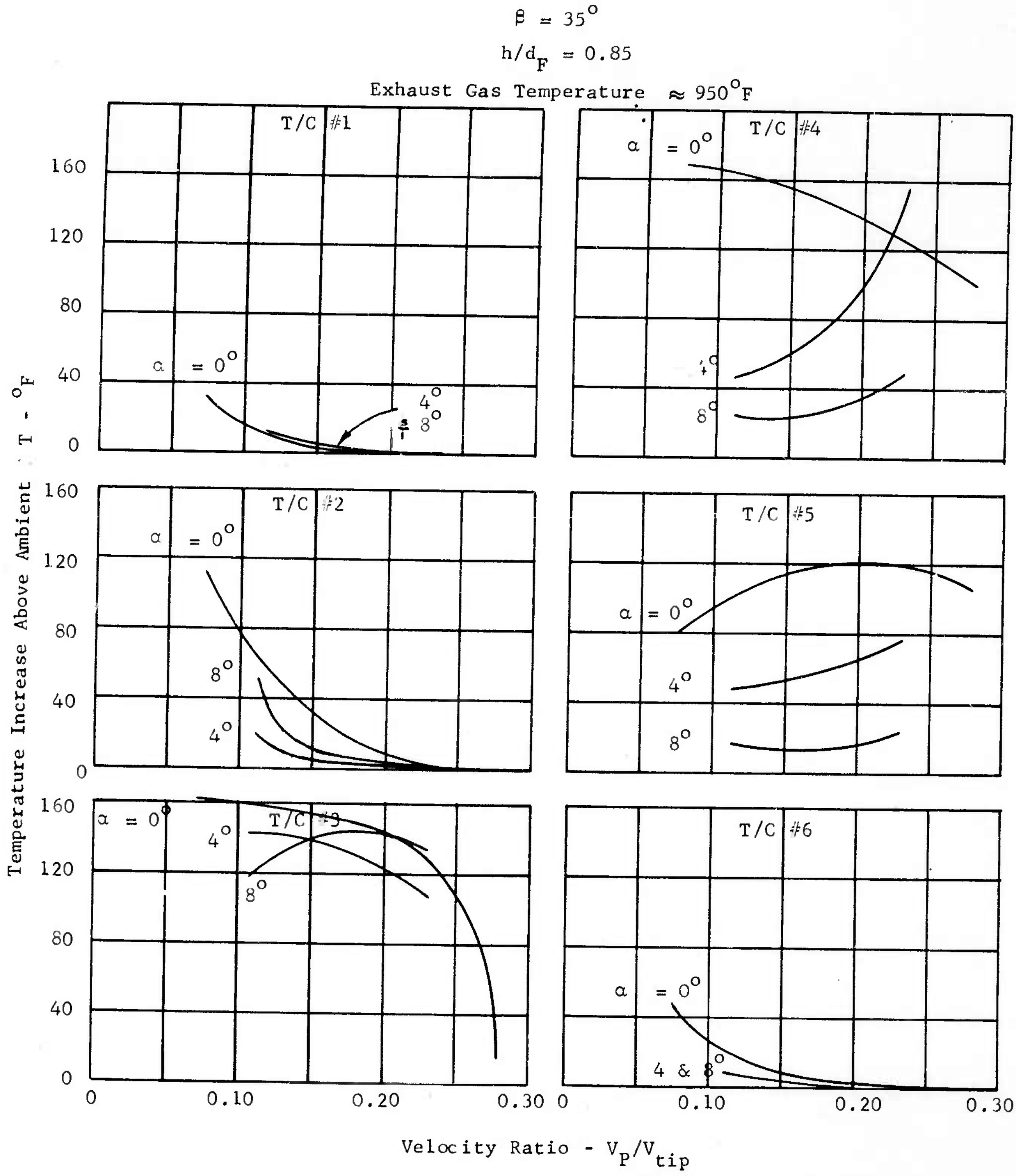

FIGURE 46e - AIR TEMPERATURE INCREASE AT GROUND LEVEL VERSUS VELOCITY RATIO (SEE FIGURE 45 FOR THERMOCOUPLE LOCATION)

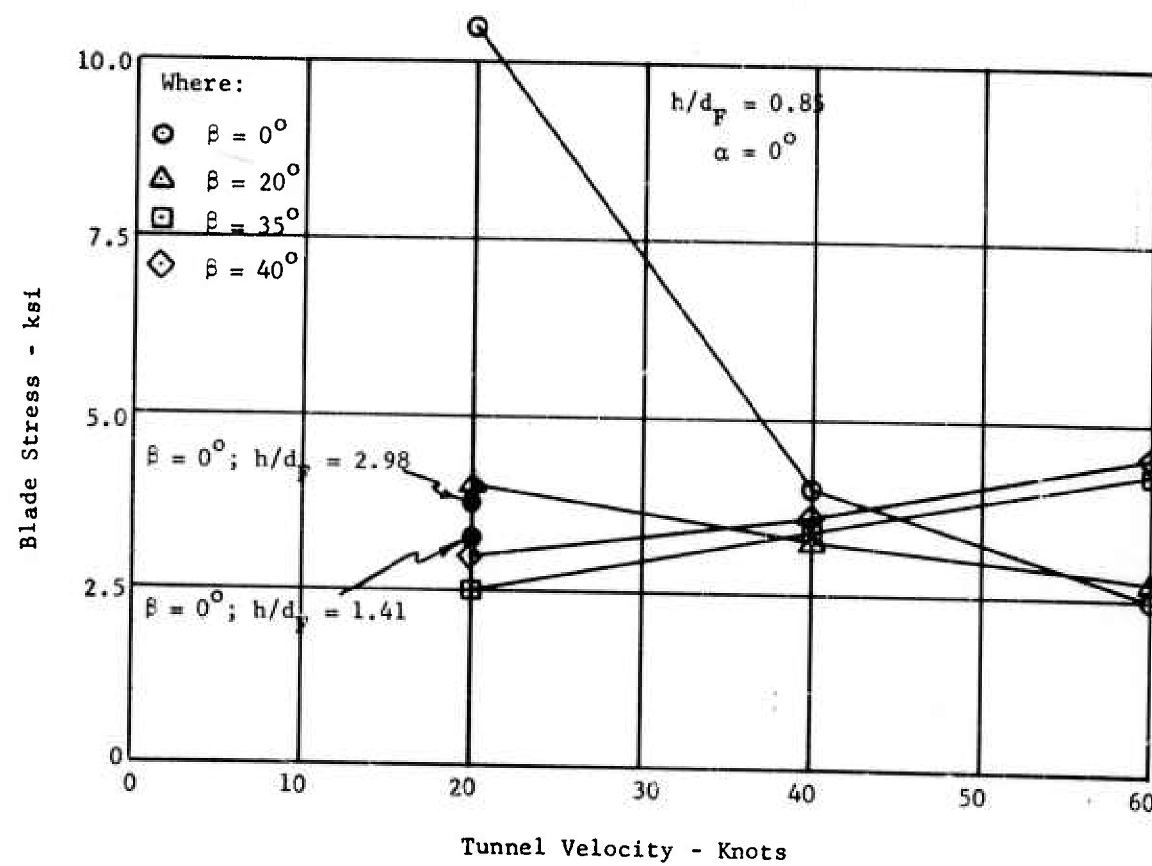

FIGURE 47 - COSINE 2θ MODE BLADE STRESS AT 2250 RPM VERSUS TUNNEL VELOCITY

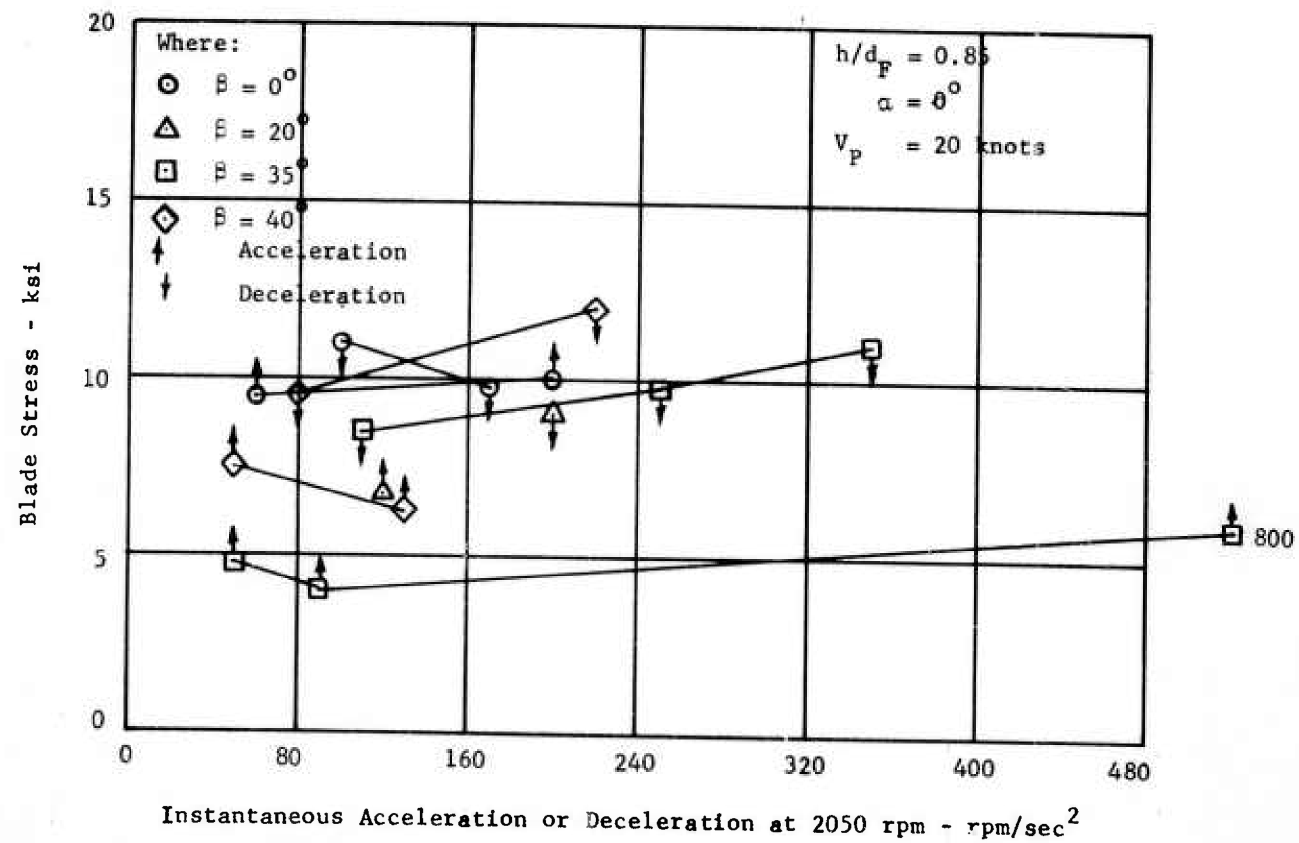

FIGURE 48 - COSINE 2θ MODE BLADE STRESS VERSUS INSTANTANEOUS ACCELERATION OR DECELERATION RATE

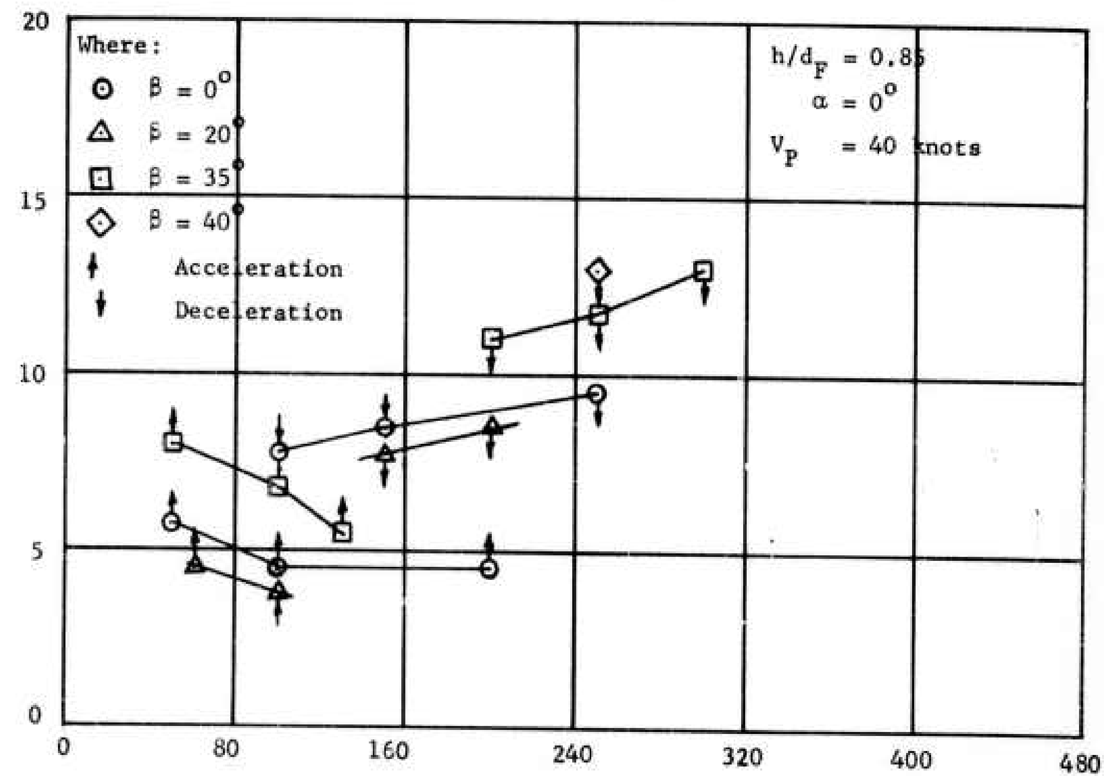

FIGURE 49 - COSINE 2θ MODE BLADE STRESS VERSUS INSTANTANEOUS ACCELERATION OR DECELERATION RATE

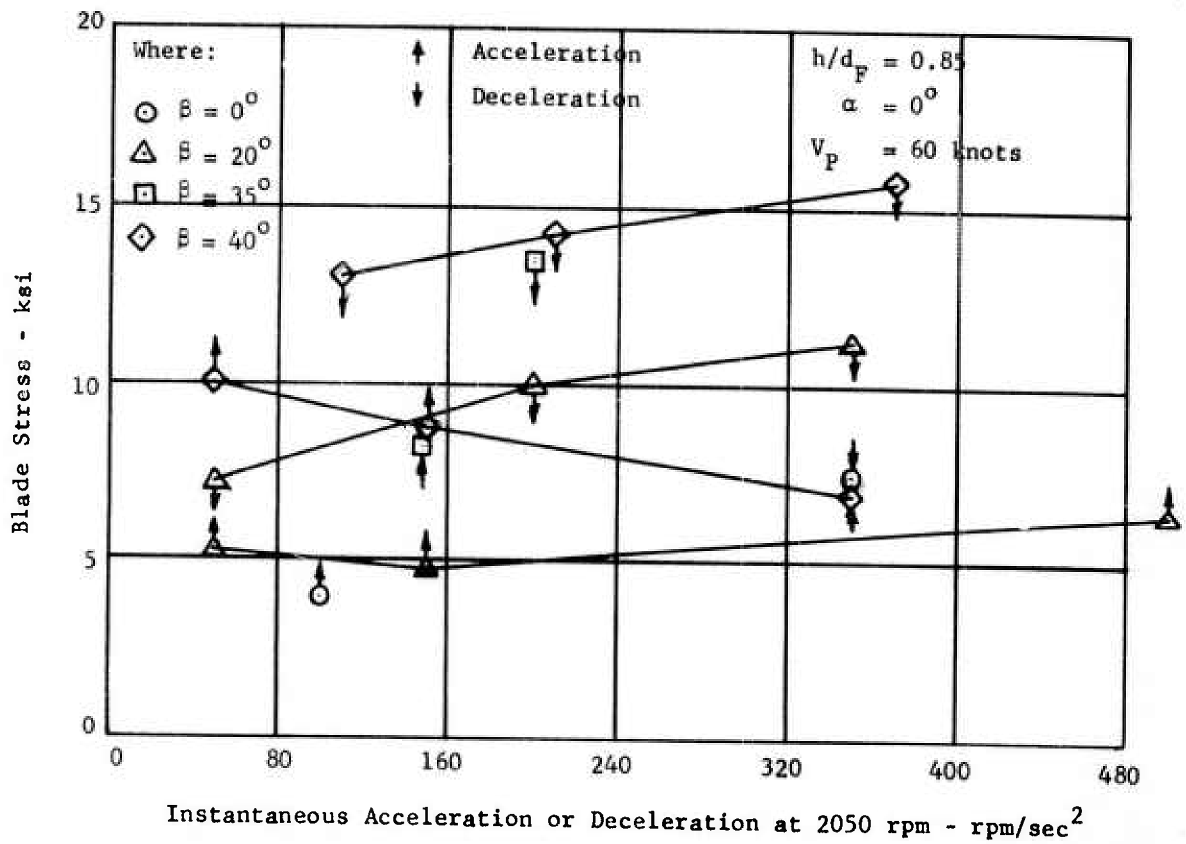

FIGURE 50 - COSINE 2θ MODE BLADE STRESS VERSUS INSTANTANEOUS ACCELERATION OR DECELERATION RATE

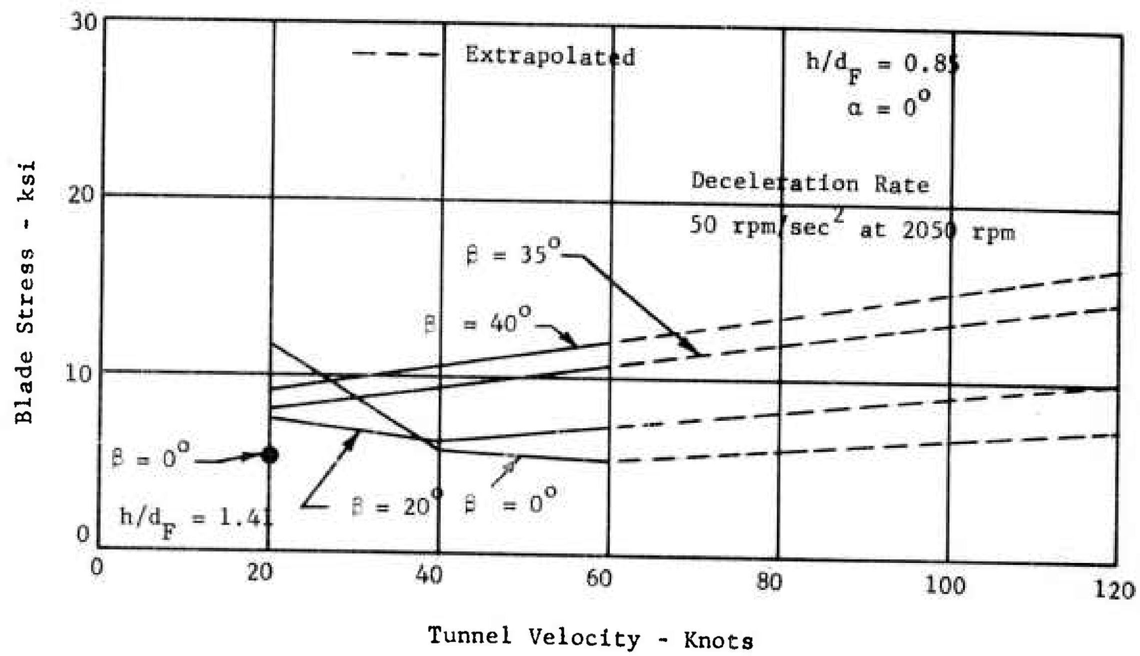

FIGURE 51 - COSINE 2θ MODE BLADE STRESS DURING DECELERATION VERSUS TUNNEL VELOCITY

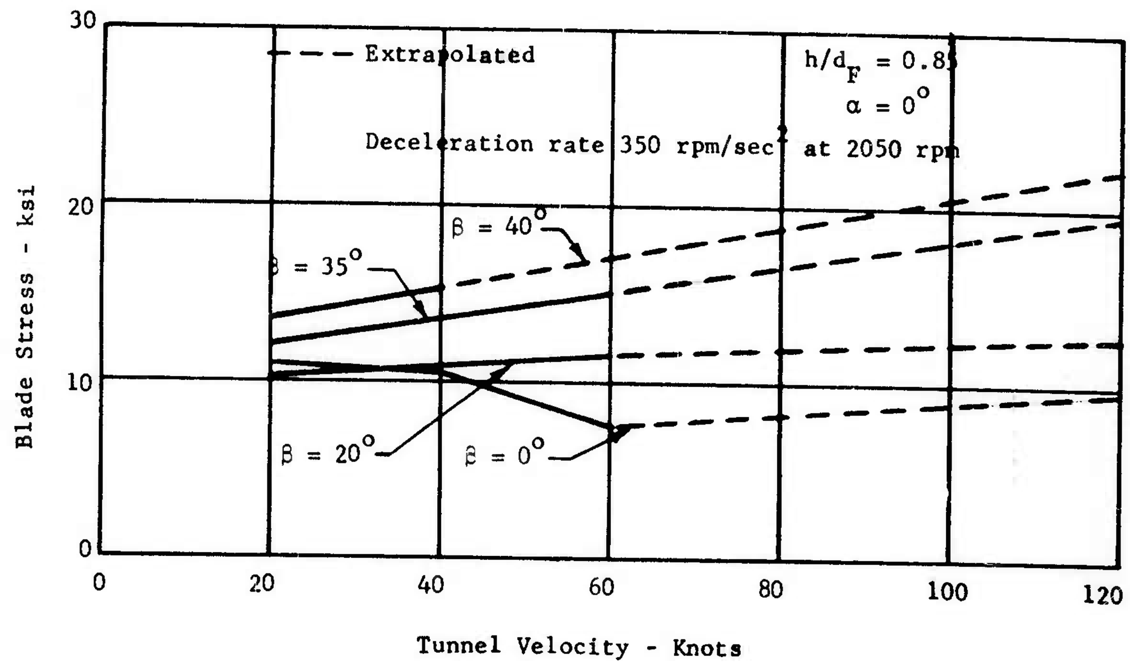

FIGURE 52 - COSINE 2θ MODE BLADE STRESS DURING DECELERATION VERSUS TUNNEL VELOCITY

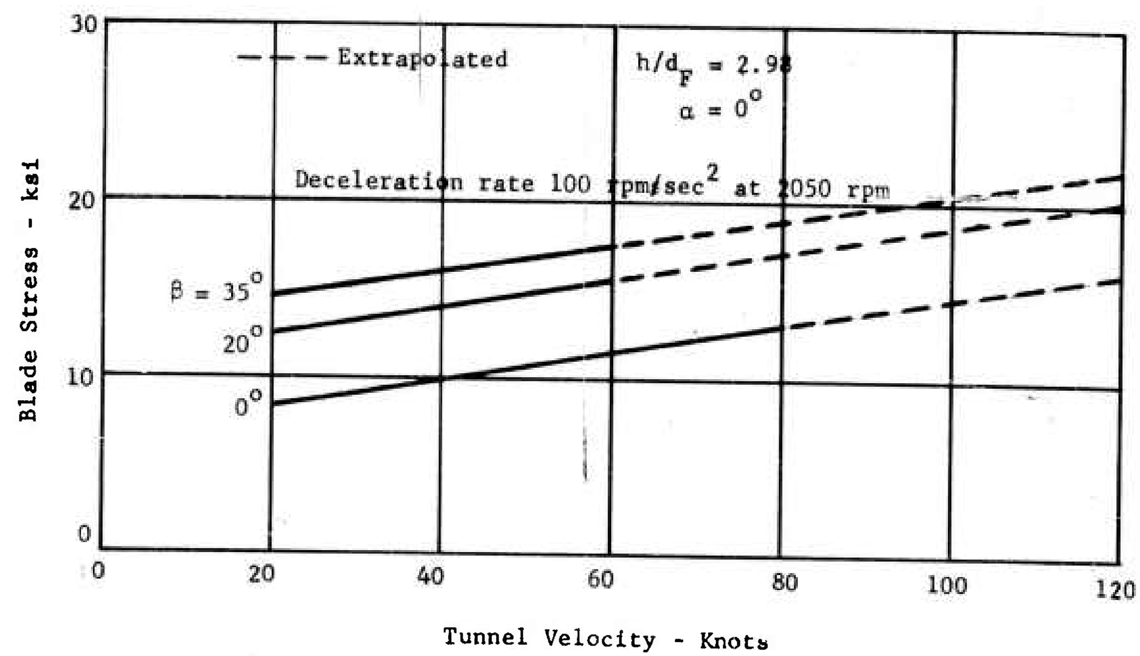

FIGURE 53 - COSINE 2θ MODE BLADE STRESS DURING DECELERATION VERSUS TUNNEL VELOCITY (ONE PIECE TORQUE BAND VOL. 2 RESULTS)

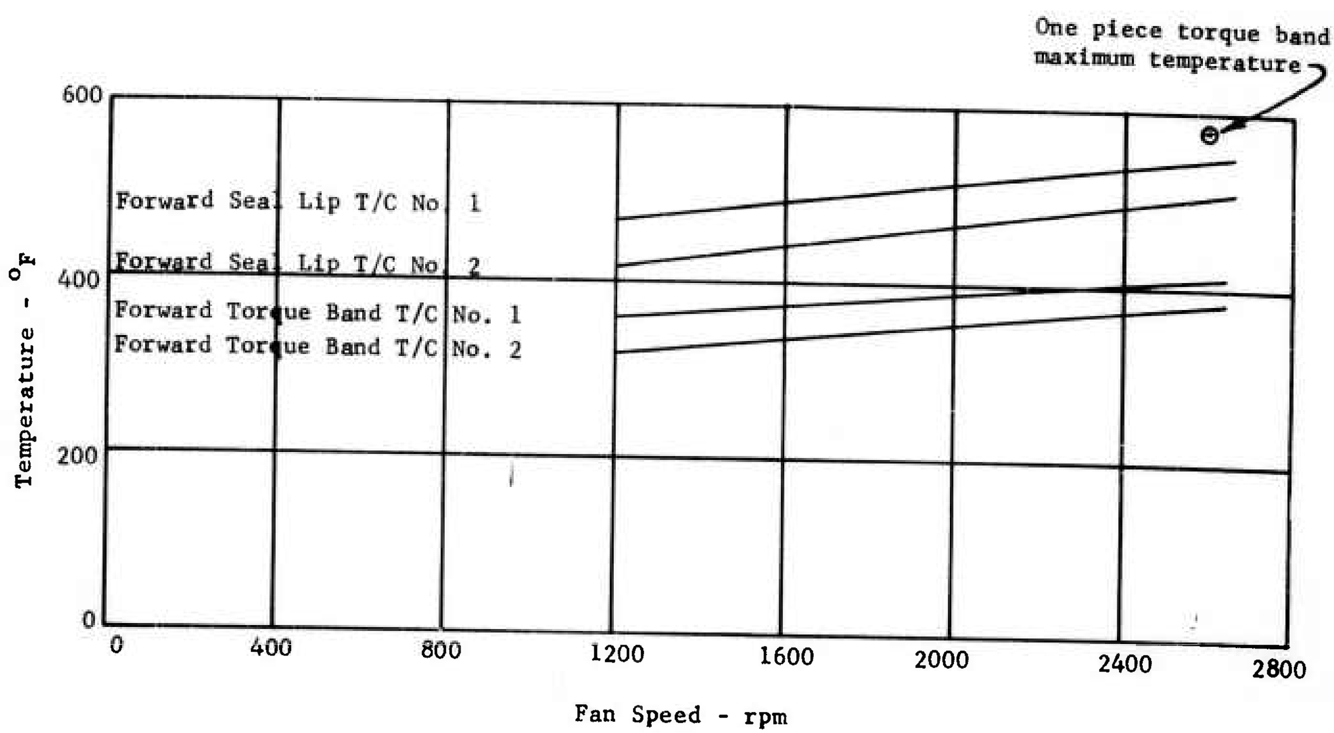

FIGURE 54 - TORQUE BAND AND SEAL LIP TEMPERATURES VERSUS FAN SPEED

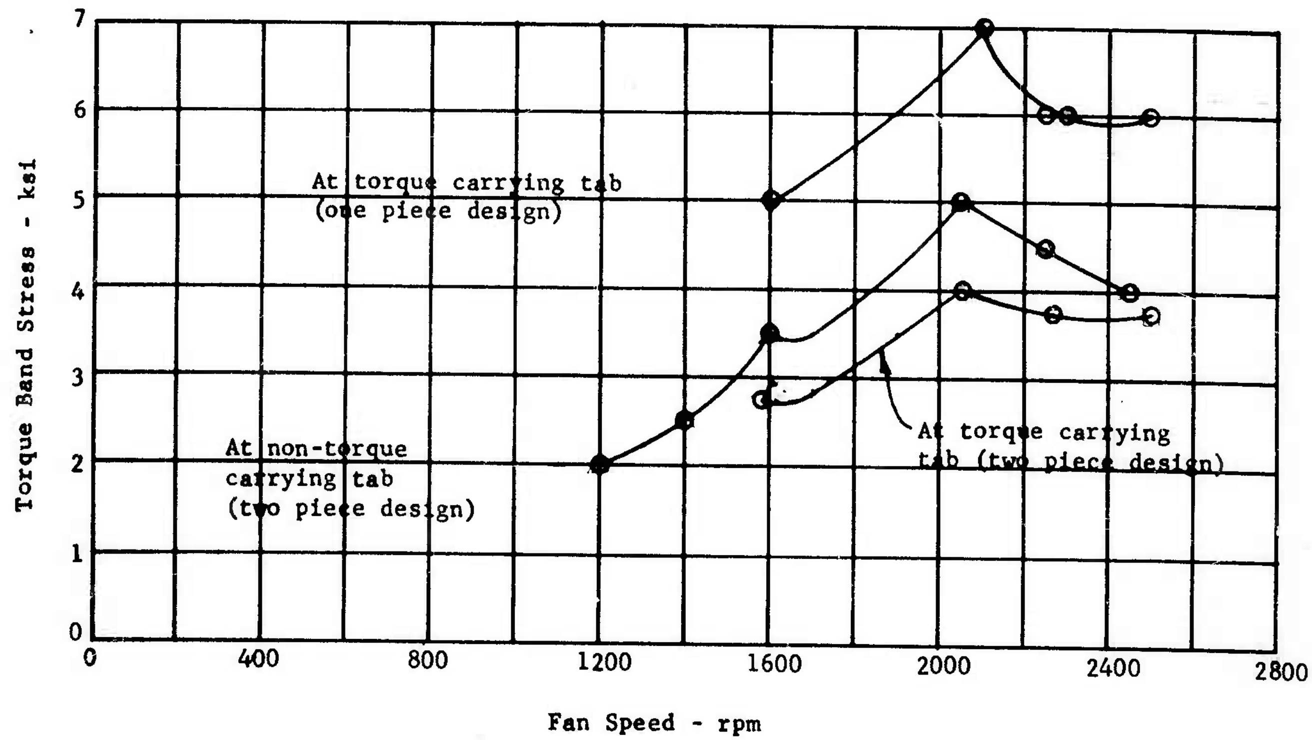

FIGURE 55 - TORQUE BAND AXIAL STRESS VERSUS FAN SPEED

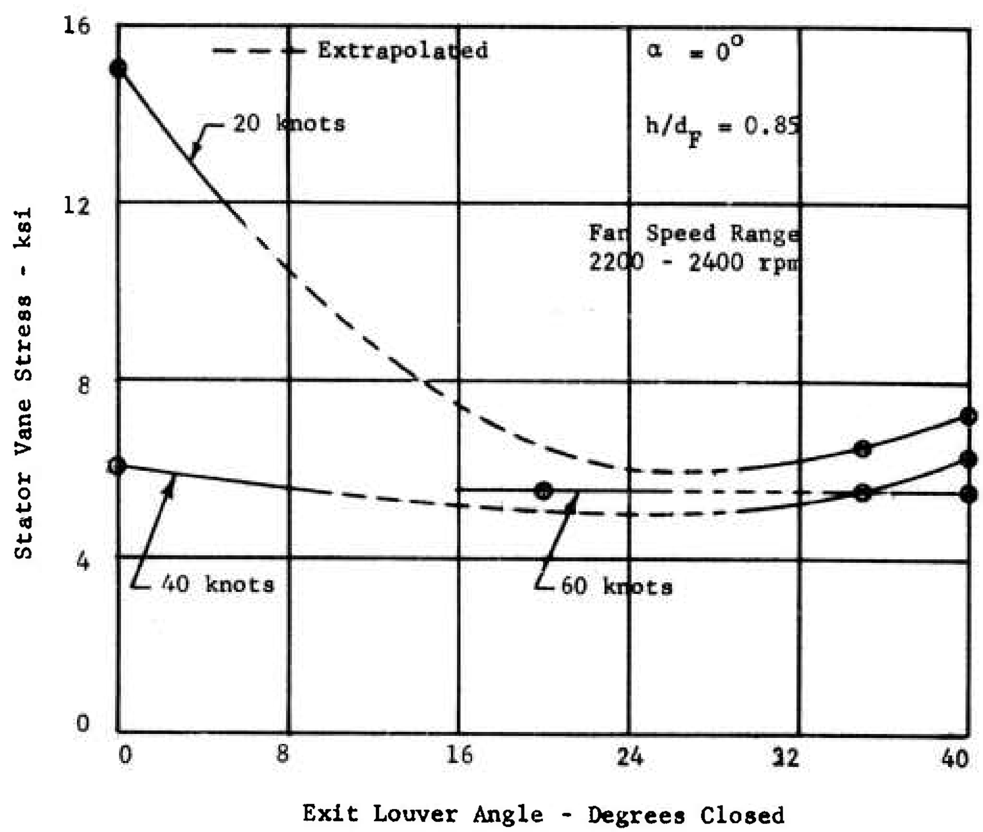

FIGURE 56 - STATOR VANE STRESS VERSUS EXIT LOUVER ANGLE

DISTRIBUTION LIST

Commanding General United States Continental Army Command ATTN: Materiel Developments Fort Monroe, Virginia	(1)
President United States Army Aviation Board ATTN: ATBG-DG Fort Rucker, Alabama	(1)
Chief of Transportation ATTN: TCDRD ATTN: TCAFO-D Department of the Army Washington 25, D.C.	(1) (1)
Commander Aeronautical Systems Division Air Force Systems Command ATTN: WWRMPT Wright-Patterson Air Force Base, Ohio	(2)
Commanding Officer U. S. Army Transportation Research Command ATTN: Research Reference Center ATTN: Aviation Directorate ATTN: Military Liaison and Advisory Office Fort Eustis, Virginia	(4) (1) (1)
U. S. Army Representative Hq. AFSC (SCS-3) Andrews Air Force Base Washington 25, D. C.	(1)
Commanding Officer and Director David Taylor Model Basin Aerodynamics Laboratory Library Washington 7, D. C.	(1)
Chief, Bureau of Naval Weapons (R-38) Department of the Navy ATTN: RAPP-14 ATTN: RAAD-32 Washington 25, D. C.	(1) (1)

Chief of Naval Research
Code 461, Maj. L. C. Robertson (1)
Washington 25, D. C.

Director
The Research Analysis Corporation
ATTN: Library (1)
The Johns Hopkins University
6935 Arlington Road
Bethesda, Maryland

National Aeronautics and Space Administration
ATTN: Bertram A. Mulcahy
Assistant Director for Technical Information (1)
1520 H Street, N. W.
Washington 25, D. C.

Librarian (1)
Langley Research Center
National Aeronautics & Space Administration
Langley Field, Virginia

Ames Research Center
National Aeronautics and Space Administration
ATTN: Library (1)
Moffett Field, California

National Aeronautics and Space Administration
Lewis Research Center
ATTN: Library (1)
21000 Brookpark Road
Cleveland 35, Ohio

Commander
Armed Services Technical Information Agency
ATTN: TIPCR (10)
Arlington Hall Station
Arlington 12, Virginia

Office of Chief of R&D
ATTN: Air Mobility Division (1)
Department of the Army
Washington 25, D. C.

Army Research Office
Office of the Chief of Research and Development
ATTN: Research Support Division (1)
Department of the Army
Washington 25, D. C.

Commanding General
U. S. Army Transportation Materiel Command
ATTN: TCMAC-APU (1)
P. O. Box 209, Main Office
St. Louis 66, Missouri

U.S. Army Standardization Group, U. K. (1)
Box 65, U. S. Navy 100
FPO New York, New York

Office of the Senior Standardization Representative
U. S. Army Standardization Group, Canada
c/o Director of Equipment Policy (1)
Canadian Army Headquarters
Ottawa, Canada

Canadian Army Liaison Officer (3)
Liaison Group, Room 208
U. S. Army Transportation School
Fort Eustis, Virginia

British Joint Services Mission (Army Staff)
ATTN: Lt. Col. R. J. Wade, RE (3)
DAQMG (Mov & Tn)
3100 Massachusetts Avenue, N. W.
Washington 8, D. C.

Convair
Division of General Dynamics Corporation
ATTN: Library (1)
San Diego 12, California

Grumman Aircraft Engineering Corporation
ATTN: Library (1)
Bethpage, Long Island, New York

Hiller Aircraft Corporation
ATTN: Library (1)
Palo Alto, California

North American Aviation, Incorporated (1)
Columbus Division
4300 East Fifth Avenue
Columbus 16, Ohio

Republic Aviation Corporation
ATTN: Library (1)
Farmingdale, Long Island, New York

Ryan Aeronautical Company
ATTN: Library
San Diego, California (1)

Vertol Division
The Boeing Company
ATTN: Library
Morton, Pennsylvania (1)

AP________________ Accession No.__________

General Electric Co., Cincinnati, Ohio

RESULTS OF WIND TUNNEL TESTS OF A FULL SCALE, FUSELAGE MOUNTED, TIP TURBINE DRIVEN LIFT FAN.

Volume 3 of 3, March 1962, 168 page-illustrations-tables (Contract DA 44-177-TC-584) USA TRECOM Project 9R 38-01-020-02, TREC 61-15. Unclassified Report.

This report covers 20 hours of testing in the NASA-AMES 40' x 80' wind tunnel.

Propulsion and aircraft performance and interactions in ground effect are discussed.

Test results indicate that the Lift Fan can proceed to the next phase of the test program.

UNCLASSIFIED

1. VTOL Propulsion System
2. Contract DA 44-177-TC-584

AP________________ Accession No.__________

General Electric Co., Cincinnati, Ohio

RESULTS OF WIND TUNNEL TESTS OF A FULL SCALE, FUSELAGE MOUNTED, TIP TURBINE DRIVEN LIFT FAN.

Volume 3 of 3, March 1962, 168 page-illustrations-tables (Contract DA 44-177-TC-584) USA TRECOM Project 9R 38-01-020-02, TREC 61-15. Unclassified Report.

This report covers 20 hours of testing in the NASA-AMES 40' x 80' wind tunnel.

Propulsion and aircraft performance and interactions in ground effect are discussed.

Test results indicate that the Lift Fan can proceed to the next phase of the test program.

UNCLASSIFIED

1. VTOL Propulsion System
2. Contract DA 44-177-TC-584

AP________________ Accession No.__________

General Electric Co., Cincinnati, Ohio

RESULTS OF WIND TUNNEL TESTS OF A FULL SCALE, FUSELAGE MOUNTED, TIP TURBINE DRIVEN LIFT FAN.

Volume 3 of 3, March 1962, 168 page-illustrations-tables (Contract DA 44-177-TC-584) USA TRECOM Project 9R 38-01-020-02, TREC 61-15. Unclassified Report.

This report covers 20 hours of testing in the NASA-AMES 40' x 80' wind tunnel.

Propulsion and aircraft performance and interactions in ground effect are discussed.

Test results indicate that the Lift Fan can proceed to the next phase of the test program.

UNCLASSIFIED

1. VTOL Propulsion System
2. Contract DA 44-177-TC-584

AP________________ Accession No.__________

General Electric Co., Cincinnati, Ohio

RESULTS OF WIND TUNNEL TESTS OF A FULL SCALE, FUSELAGE MOUNTED, TIP TURBINE DRIVEN LIFT FAN.

Volume 3 of 3, March 1962, 168 page-illustrations-tables (Contract DA 44-177-TC-584) USA TRECOM Project 9R 38-01-020-02, TREC 61-15. Unclassified Report.

This report covers 20 hours of testing in the NASA-AMES 40' x 80' wind tunnel.

Propulsion and aircraft performance and interactions in ground effect are discussed.

Test results indicate that the Lift Fan can proceed to the next phase of the test program.

UNCLASSIFIED

1. VTOL Propulsion System
2. Contract DA 44-177-TC-584

AP________________ Accession No.__________

General Electric Co., Cincinnati, Ohio

RESULTS OF WIND TUNNEL TESTS OF A FULL SCALE, FUSELAGE MOUNTED, TIP TURBINE DRIVEN LIFT FAN.

Volume 3 of 3, March 1962, 168 page-illustrations-tables (Contract DA 44-177-TC-584) USA TRECOM Project 9R 38-01-020-02, TREC 61-15. Unclassified Report.

This report covers 20 hours of testing in the NASA-AMES 40' x 80' wind tunnel.

Propulsion and aircraft performance and interactions in ground effect are discussed.

Test results indicate that the Lift Fan can proceed to the next phase of the test program.

UNCLASSIFIED

1. VTOL Propulsion System
2. Contract DA 44-177-TC-584

AP________________ Accession No.__________

General Electric Co., Cincinnati, Ohio

RESULTS OF WIND TUNNEL TESTS OF A FULL SCALE, FUSELAGE MOUNTED, TIP TURBINE DRIVEN LIFT FAN.

Volume 3 of 3, March 1962, 168 page-illustrations-tables (Contract DA 44-177-TC-584) USA TRECOM Project 9R 38-01-020-02, TREC 61-15. Unclassified Report.

This report covers 20 hours of testing in the NASA-AMES 40' x 80' wind tunnel.

Propulsion and aircraft performance and interactions in ground effect are discussed.

Test results indicate that the Lift Fan can proceed to the next phase of the test program.

UNCLASSIFIED

1. VTOL Propulsion System
2. Contract DA 44-177-TC-584

AP________________ Accession No.__________

General Electric Co., Cincinnati, Ohio

RESULTS OF WIND TUNNEL TESTS OF A FULL SCALE, FUSELAGE MOUNTED, TIP TURBINE DRIVEN LIFT FAN.

Volume 3 of 3, March 1962, 168 page-illustrations-tables (Contract DA 44-177-TC-584) USA TRECOM Project 9R 38-01-020-02, TREC 61-15. Unclassified Report.

This report covers 20 hours of testing in the NASA-AMES 40' x 80' wind tunnel.

Propulsion and aircraft performance and interactions in ground effect are discussed.

Test results indicate that the Lift Fan can proceed to the next phase of the test program.

UNCLASSIFIED

1. VTOL Propulsion System
2. Contract DA 44-177-TC-584

AP________________ Accession No.__________

General Electric Co., Cincinnati, Ohio

RESULTS OF WIND TUNNEL TESTS OF A FULL SCALE, FUSELAGE MOUNTED, TIP TURBINE DRIVEN LIFT FAN.

Volume 3 of 3, March 1962, 168 page-illustrations-tables (Contract DA 44-177-TC-584) USA TRECOM Project 9R 38-01-020-02, TREC 61-15. Unclassified Report.

This report covers 20 hours of testing in the NASA-AMES 40' x 80' wind tunnel.

Propulsion and aircraft performance and interactions in ground effect are discussed.

Test results indicate that the Lift Fan can proceed to the next phase of the test program.

UNCLASSIFIED

1. VTOL Propulsion System
2. Contract DA 44-177-TC-584